Automated Glycan Assembly of Hemicellulosic Oligosaccharides from the Plant Cell Wall

Inaugural-Dissertation
to obtain the academic degree
Doctor rerum naturalium (Dr. rer. nat.)

submitted to the Department of Biology, Chemistry and Pharmacy
of Freie Universität Berlin

by

Pietro Dallabernardina
from Rovereto, Italy

2017

The work in this dissertation was performed between February 2014 and September 2017 in the Department of Biomolecular Systems, Max Planck Institute of Colloids and Interfaces under the supervision of Dr. Fabian Pfrengle.

Date of defense: 05/12/2017

1st Reviewer: Dr. Fabian Pfrengle

2nd Reviewer: Prof. Dr. Philipp Heretsch

Acknowledgements

Foremost, I am deeply grateful to my supervisor Dr. Fabian Pfrengle for his supervision, support, patience, understanding, and constructive suggestions throughout the hard moments in my PhD.

I would like to thank Prof. Dr. Peter Seeberger for giving me the possibility to do my PhD in the Biomolecular Systems department at the Max Planck Institute of Colloids and Interfaces.

I thank Prof. Dr. Philipp Heretsch for kindly agreeing to review this thesis.

I thank all the current and former members of the group, in particular Deborah Senf, Max Bartetzko, and Dr. Colin Ruprecht. They were extremely important during these four years, not only scientifically, but in making a nice atmosphere in the lab and for the friendship built in these years. I would like to thank Dr. Colin Ruprecht for his suggestions during the biological assays, for the availability to reply to all my questions, and for making great use of my compounds.

I´m deeply grateful to all my colleagues and friends in the BMS department; Matthew Plutschack, Dr. Stella Vukelic, Dr. Bopanna M. Ponnappa, Dr. Martina Delbianco, Dr. Richard Fair, Ankita Malik, Silvia Varela, Dr. Bartholomäus Pieber, Dr. Maria Antonietta Carillo, Priya Bharate, Mauro Sella, Monica Guberman, Alonso Pardo, Andreia Marta, Dr. Kathirvel Alagesan, Vittorio Bordoni, Andrew Kononov and Malte Gölden for the fruitful scientific discussions, the time together, and the beers. I would like to express my gratefulness to Matthew Plutschack and Dr. Richard Fair for proofreading parts of my thesis. I want to thank especially Mara, whose presence made the last part of my PhD happier, and for giving me tranquility and support in these last months.

I´m also thankful to the Rovereto community present in Berlin and Dresden; Enrico, Valentina, Michela, Bepi, and Ele; my old friends Pippo, Leandro, En, Wektor, Bano, Uauona, Jimmy, Davide, Ciro, Teddo, Elena, Maria, Adry, Male,

Galli, and all the others in Vienna, Rovereto, Padova, and in the rest of the world for sharing happy and sad moments.

Most importantly I would like to thank my parents and my family, for their patience, for letting me make mistakes which led me to be a better person, and all the support during these 32 years. I am sure; I would not have reached this point without them. A special thought goes to my grandfather which unfortunately was not able to see me achieve this important stage of my life.

Table of Contents

List of Publications

Publications

C. Ruprecht, M. P. Bartetzko, D. Senf, **P. Dallabernadina**, I. Boos, M. C. F. Andersen, T. Kotake., J. P. Knox, M. G. Hahn, M. H. Clausen, F. Pfrengle, *Plant Physiol., in press*. A synthetic glycan microarray enables epitope mapping of plant cell wall glycan-directed antibodies.

P. Dallabernardina, F. Schumacher, P. H. Seeberger, F. Pfrengle, *Chem. Eur. J.,* **2017**, *23*, 3191-3196. Mixed-linkage glucan oligosaccharides produced by automated glycan assembly serve as tools to determine the substrate specificity of lichenase.

M. Wilsdorf, D. Schmidt, M. Bartetzko, **P. Dallabernardina**, F. Schuhmacher, P. Seeberger, F. Pfrengle, *Chem. Comm.*, **2016,** *52*, 10187-10189. A traceless photocleavable linker for the automated glycan assembly of carbohydrates with free reducing ends.

P. Dallabernardina, F. Schumacher, P. H. Seeberger, F. Pfrengle, *Org. Biomol. Chem.* **2016**, *14*, 309-313. Automated glycan assembly of xyloglucan oligosaccharides.

Conference Presentations

P. Dallabernardina, F. Schumacher, P. H. Seeberger, F. Pfrengle. Automated glycan assembly of plant cell wall oligosaccharides. Oral presentation delivered at the Berliner Chemie Symposium, Berlin, Germany, April 2017.

P. Dallabernardina, F. Schumacher, P. H. Seeberger, F. Pfrengle. Automated glycan assembly of plant cell wall oligosaccharides. Poster presentation delivered at the JCF-Frühjahrssymposium, Mainz, Germany, March 2017.

P. Dallabernardina, F. Schumacher, P. H. Seeberger, F. Pfrengle. Automated Glycan Assembly of Mixed-Linkage Glucan Oligosaccharides. Poster presentation delivered at the 1st Biomolecular Systems Conference, Berlin, Germany, November 2016.

P. Dallabernardina, F. Schumacher, P. H. Seeberger, F. Pfrengle. Automated glycan assembly of plant cell wall oligosaccharides. Oral presentation delivered at the XXXVII CDCO, Venezia, Italy, September 2016.

P. Dallabernardina, F. Schumacher, P. H. Seeberger, F. Pfrengle. Automated glycan assembly of xyloglucan oligosaccharides. Poster presentation delivered at the International Carbohydrate Symposium 2016, New Orleans, USA, July 2016.

P. Dallabernardina, F. Schumacher, P. H. Seeberger, F. Pfrengle. Automated glycan assembly of plant cell wall oligosaccharides. Oral presentation delivered at the XV CSCC, Pontignano (Siena), Italy, June 2016.

P. Dallabernardina, F. Schumacher, P. H. Seeberger, F. Pfrengle. Automated glycan assembly of xyloglucan oligosaccharides. Oral presentation delivered at the Berliner Chemie Symposium, Berlin, Germany, April 2016.

P. Dallabernardina, F. Schumacher, P. H. Seeberger, F. Pfrengle. Automated glycan assembly of xyloglucan oligosaccharides. Poster presentation delivered at the JCF-Frühjahrssymposium, Kiel, Germany, March 2016.

Summary

The plant cell wall is the outer-layer of the cell and controls its volume and shape. It plays an important structural role and is involved in the plant's immune response against pathogens. Plant cell walls are composed of a mixture of simple and complex biopolymers that are mainly comprised of highly complex polysaccharides. Well-defined oligosaccharides related to plant cell wall polysaccharides are fundamental molecular tools for studying cell wall structure and biosynthesis, but are difficult to obtain from natural sources. The chemical synthesis of plant oligosaccharide libraries is thus a promising approach for advancing cell wall research.

Automated glycan assembly is a powerful emerging technique for the solid-phase synthesis of oligosaccharides. Through the iterative addition of different building blocks (BB) to a functionalized solid support, glycans of different lengths and branching patterns can be produced. In this work, automated glycan assembly has been used to obtain well-defined oligosaccharide fragments of the cell wall polysaccharides xyloglucan (XG) and mixed-linkage glucan (MLG). These compounds were applied for the characterization of cell wall glycan-directed monoclonal antibodies and cell wall-modifying enzymes.

In Chapter 2, which constitutes the main part of this thesis, the synthesis of XG oligosaccharides is described. XGs are the main hemicellulosic polysaccharides in higher plants. They are made of a cellulosic backbone highly decorated with xylose residues that can be further substituted with galactose and fucose. Initially, we tested the possibility to use exclusively monosaccharide BBs for the assembly of the target oligosaccharides. However, this approach did not provide good α-stereoselectivity when glycosylating backbone glucose residues with xylose. Therefore, a disaccharide BB carrying a pre-installed α-glycosidic linkage between glucose and xylose was synthesized. Using this disaccharide BB a library of XG oligosaccharides was successful prepared. To synthesize galactosylated XG oligosaccharides *p*-methoxybenzyl was used at the C2-position of the xylose. This represents the first example for the use of this temporary protecting group in automated glycan assembly. In collaboration with Dr. Ruprecht, the synthetic XG oligosaccharides were used for the

characterization of monoclonal antibodies (mAbs) that recognize cell wall polysaccharides and for determining the binding specificities of xyloglucan endotransglycosylases (XETs), important enzymes involved in remodeling the cell wall during cell growth.

In chapter 3, a library of MLG oligosaccharides was synthesized by automated glycan assembly. MLGs are an important class of hemicellulose polymers present in grass and cereals. They are constructed from a backbone of cellulosic oligosaccharide stretches randomly connected by β-1,3-glycosidic linkages. Using two differently protected glucose building blocks, a library of MLG oligosaccharides up to an octasaccharide was synthesized. MLGs are degraded by an enzyme named lichenase, which can be used to characterize the composition of MLG polysaccharides and is used in industrial processes such as brewery and animal feed production. The synthetic MLG oligosaccharides represented ideal substrates to investigate the substrate specificity of lichenase, and recent reconsiderations on the specificity of lichenase were confirmed.

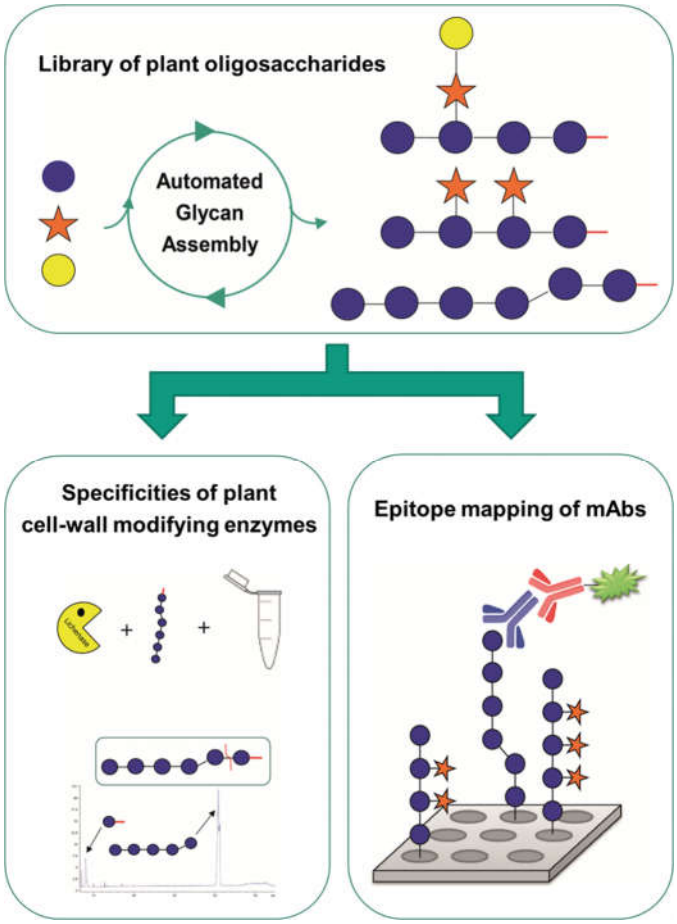

Zusammenfassung

Die Pflanzenzellwand ist die äußere Zellschicht und bestimmt ihr Volumen und ihre Form. Sie hat eine wichtige strukturgebende Rolle und ist in die Immunreaktion gegen Krankheitserreger involviert. Pflanzenzellwände bestehen aus einer Vielzahl einfacher und komplexer Biopolymere, die hauptsächlich hochkomplexe Polysaccharide beinhalten. Kurze Oligosaccharid-Fragmente von Polysacchariden aus der Pflanzenzellwand dienen als fundamentale molekulare Hilfsmittel, um die Struktur und Biosynthese von Pflanzenzellwänden zu untersuchen, wobei strukturell definierte und reine Oligosaccharide nur schwierig aus natürlichen Quellen zu gewinnen sind. Die chemische Synthese von Pflanzenoligosaccharid-Bibliotheken ist deshalb ein vielverspechender Ansatz, um die Forschung an der Pflanzenzellwand voranzubringen.

Automatische Oligosaccharidsynthese ist eine leistungsfähige Technik, um Oligosaccharide an der Festphase zu synthetisieren. Durch die iterative Zugabe von verschiedenen Bausteinen zu einem funktionalisierten festen Trägermaterial können Glykane mit verschiedenen Längen und Verzweigungen synthetisiert werden. In dieser Arbeit wurde automatische Festphasensynthese benutzt, um definierte Oliogosaccharid-Fragmente der Zellwandpolysaccharide Xyloglukan (XG) und Glukane mit gemischten Verknüpfungen (MLG) zu erhalten. Diese Verbindungen fanden Anwendung in der Charakterisierung von monoklonalen Antikörpern, die Zellwandpolysaccharide erkennen, und Enzymen, die die Zellwand modifizieren.

Kapitel 2, welches den Hauptteil dieser Arbeit umfasst, beschreibt die Synthese von XG-Oligosacchariden. XG sind die am häufigsten vorkommenden hemicellulosischen Polysaccharide in vaskulären Pflanzen. Sie bestehen aus einem Celluloserückgrat, welches mit Xyloseeinheiten dekoriert ist, die wiederum mit Galaktose und Fukose substituiert sein können. Zuerst wurde die Möglichkeit getestet, die Zielstrukturen ausschließlich aus Monosaccharid-Bausteinen zu synthetisieren. Bei diesem Ansatz wurde allerdings keine gute α-Stereoselektivität in der Glykosylierung von Glukoseeinheiten des Rückgrats mit Xylose erzielt. Deshalb wurde ein Disaccharid-Baustein genutzt, in dem die α-glykosidische Bindung zwischen Glukose und Xylose bereits vorinstalliert war.

Durch die Verwendung dieses Disaccharid-Bausteins wurde eine Bibliothek von XG-Oligosacchariden erfolgreich synthetisiert. Um Galaktose-substituierten XG Oligosaccharide zu synthetisieren, wurde *p*-Methoxybenzyl in der C2-Position von Xylose genutzt. Dies ist das erste Beispiel für die Verwendung dieser temporären Schutzgruppe in der automatischen Oligosaccharid-Festphasensynthese. In einer Kollaboration mit Dr. Ruprecht wurden die synthetisierten XG-Oligosaccharide für die Charakterisierung von monoklonalen Antikörpern (mAbs), die Zellwandpolysaccharide erkennen, genutzt. Außerdem die wurden die Bindungsspezifitäten von Xyloglucan-Endotransglycosylasen (XET) bestimmt, die wichtige Enzyme, der Zellwand während des Zellwachstums sind in der Reorganisation.

In Kapitel 3 wird die Festphasensynthese einer Bibliothek von MLG-Oligosacchariden beschrieben. MLG sind eine wichtige Klasse von Hemicellulosepolymeren in Gräsern und Getreide. Sie bestehen aus einem Rückgrat von Cellulose-Oligosaccharidabschnitten, die unregelmäßig durch β-1,3-glykosidische Bindungen verknüpft sind. Indem zwei unterschiedlich geschützte Glukosebausteine verwendet wurden, konnte eine Bibliothek von MLG-Oligosacchariden bis zur Länge eines Oktasaccharids synthetisiert werden. MLG werden durch das Enzym Lichenase abgebaut, welches für die Charakterisierung der strukturellen Zusammensetzung von MLG-Polysacchariden genutzt werden kann, und in industriellen Prozessen wie dem Brauwesen und in der Futtermittelproduktion genutzt wird. Die synthetischen MLG-Oligosaccharide stellten ideale Substrate dar, um die Substratspezifitäten von Lichenase zu untersuchen und um jüngste Neubewertungen der Spezifität von Lichenase zu bestätigen.

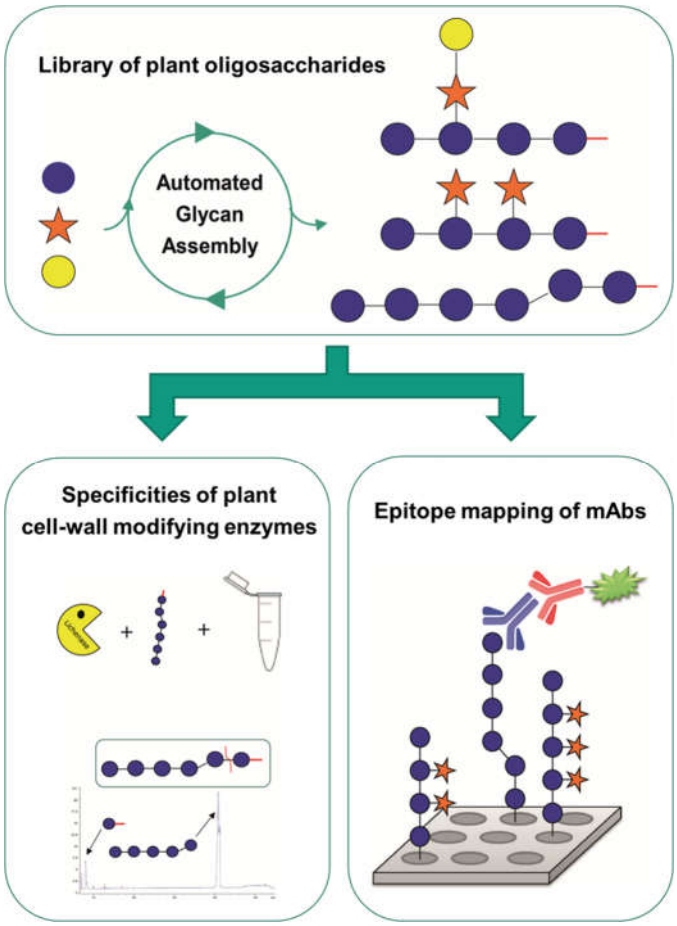
Library of plant oligosaccharides
Automated
Glycan
Assembly
Specificities of plant
cell-wall modifying enzymes
Epitope mapping of mAbs

Abbreviations

Ac: acetyl

ACN: acetonitrile

Ar: aryl

Azmb: 2-(azidomethyl)benzoyl

BB: building block

Bn: benzyl

Bu: butyl

Bz: benzoyl

Cbz: Carboxylbenzyl

CESA: cellulose synthase catalytic subunits

CIP: contact ion pair

CMPI: 2-chloro-1-methylpyridinium iodide

CSC: cellulose synthase complex

CSL: cellulose-synthase like

DABCO: 1,4-diazabicyclo[2.2.2]octane

DCE: 1,2-dichloroethane

DCM: dichloromethane

DDQ: 2,3-dichloro-5,6-dicyano-1,4-benzoquinone

DIC: *N,N'*-diisopropylcarbodiimide

DMAP: dimethylaminopyridine

DMF: dimethylformamide

DBU: 1,8-diazabicyclo[5.4.0]undec-7-ene

ELISA: enzyme-linked immunosorbent assay

ELSD: evaporative light scattering detector

ESI: electronspray ionization

Et: ethyl

EtOAc: ethyl acetate

FEP: fluorinated ethylene propylene

FID: flame ionization detector

FITC: fluorescein isothiocyanate

Fmoc: fluorenylmethyloxycarbonyl

FTIR: fourier transform infrared

GC: gas chromatography

GH: glycosyl hydrolase

GT: glycosyltransferase

HBMAD: hydrogen bond mediated aglycone delivery

Hex: hexane

HPLC: high performance liquid chromatography

HRMS: high resolution mass spectrometry

HSQC: heteronuclear single quantum coherence spectroscopy

HTP: high-throughput

LC: liquid chromatography

Lev: levulinoyl

LevOH: levulinic acid

LG: leaving group

mAb: monoclonal antibody

MALDI-TOF: matrix-assisted laser desorption/ionization-time of flight

Me: methyl

MLG: mixed-linkage glucan

MPIKG: Max-Planck-Institute for Colloids and Interfaces

MS: mass spectrometry

Nap: naphtyl

NHS: *N*-hydroxysuccinimide

NIS: *N*-iodosuccinimide

NMR: nuclear magnetic resonance

PG: protecting group

Ph: phenyl

PMB: *p*-methoxybenzyl

RG: rhamnogalacturan

rt: room temperature

SSIP: solvent separated ion pair

TFA: trifluoroacetic acid

TFAA: trifluoroacetic anhydride

TfOH: triflic acid

THF: tetrahydrofuran

TMSOTf: trimethylsilyl triflate

Tol: tolyl

UDP: uridine diphosphate

UV: ultraviolet

XET: xyloglucan endotransglycosylase

XG: xyloglucan

Symbols

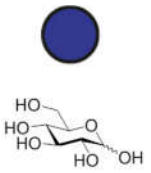

D-Glucose
(Glc)

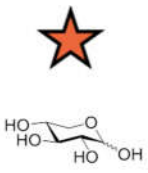

D-Xylose
(Xyl)

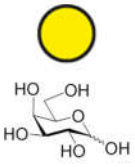

D-Galactose
(Gal)

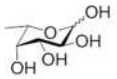

L-Fucose
(Fuc)

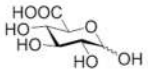

D-Glucuronic acid
(GlcA)

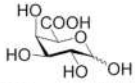

D-Galacturonic acid
(GalA)

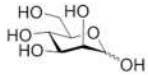

D-Mannose
(Man)

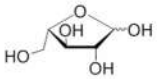

L-Arabinose
(Ara)

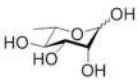

L-Rhamnose
(Rha)

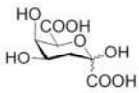

3-deoxy-D-lyxo-heptulosaric acid
(DHA)

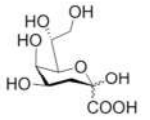

3-Deoxy-D-manno-oct-2-ulosonic acid
(Kdo)

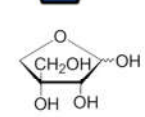

D-Apiose
(Api)

Monoclonal antibody

Fluorescent dye

Solid support

1. Introduction

1.1 Plant Cell Wall Structure

The plant cell wall is composed of a mixture of simple and complex biopolymers. Polysaccharides are the major components and are linked in a highly organized network to give the plant cell wall its characteristic properties. The cell wall is composed of a relatively unspecialized primary cell wall (Figure 1) and a more specialized secondary cell wall, which is strengthened by a phenolic polymer called lignin. Cell wall polysaccharides fall into three categories: cellulose, hemicellulose, and pectin.[1]

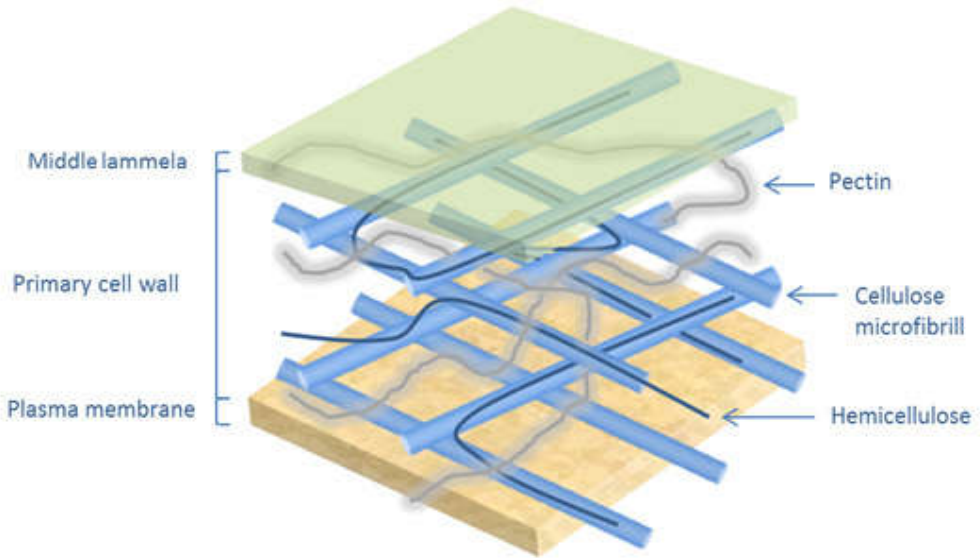

Figure 1: Schematic representation of the primary cell wall

The cell wall controls the volume and shape of the cell, and its flexibility and elasticity allows for growth during cell differentiation.[2] Furthermore, cell wall polysaccharides may act as important signaling molecules during cell differentiation and in the activation of the immune response of the plant.[1-7] Plant cell walls are relevant to economics, since they are raw material for a large number of industrial products such as paper, food ingredients, and biofuels.[3,8] Also, cell wall polysaccharides play an important role in the human diet, for

example as components of fruits and cereals.[9] Dietary fibers have beneficial physiological effects including laxation and blood cholesterol and/or glucose attenuation.[10] Plant polysaccharides provide therapeutic benefits including immuno-stimulatory[11-13] and anti-tumor[12,14] effects as well.

1.1.1 Cellulose

The term cellulose was mentioned for the first time in 1839 by the French academy, referring to the work of the French chemist Payen,[15] who obtained a fibrous solid isomer of starch after treating plant tissues with acids and ammonia, and then extracting it with water, alcohol, and ether.[16] Even before the discovery of its structure and the attribution of a name, the properties of cellulose were exploited by humans for centuries. It is currently considered the most common organic polymer[17] and is particularly important as a raw source of biocompatible and environmentally friendly products.[18,19]

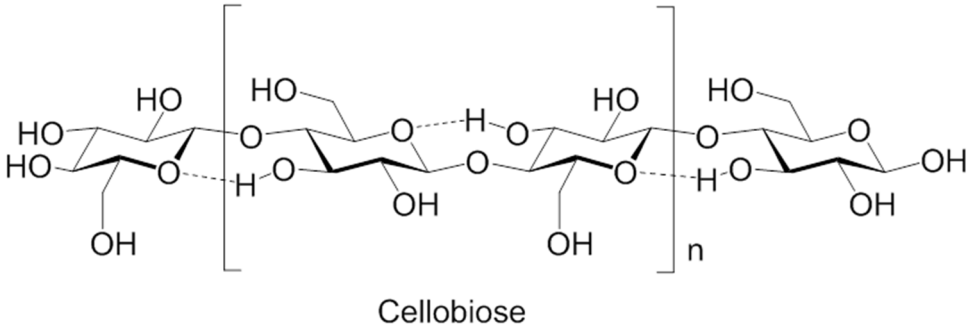

Figure 2: Structural model of cellulose. Cellobiose repeating units form long polymer chains with a linear conformation due to the strong H-bond between O3–H - - -O5.

Cellulose is a β-1,4-glucan composed of 2,000 to more than 25,000 glucose residues.[20] The minimum repeating unit is the disaccharide cellobiose (Figure 2). Cellulose chains have a linear conformation due to intra-chain hydrogen bonding between the hydroxyl groups and the ring oxygen of the glucose monosaccharides. Moreover, intermolecular hydrogen bonds and van der Waals forces promote the formation of elementary fibrils which can further aggregate to form larger microfibrils. Depending on the source those microfibrils are quite different in length, width and degree of order. This depends on the number of singular chains that compose the microfibrils, which have been estimated to contain about 20-40 chains in the thinner elementary fibrils.[2] Those microfibrils

have diameters of 5-50 nms.[21] The elementary fibrils have two distinct regions: a more crystalline and organized region and an amorphous region which is more disordered. The structure and distribution of those domains has not been determined yet.[22] The non-covalent interactions create the characteristic properties of cellulose: high tensile strength, insolubility, chemical stability, and enzymatic stability.[2]

Cellulose is synthesized by the most prolific bio-machines in nature,[23] membrane-bound cellulose synthase complexes (CSCs), which are complexes of glycosyltransferases. Those complexes have a unique hexagonal structure known as a particle rosette. A particle rosette is composed of six rosette subunits containing cellulose synthase catalytic subunits (CESAs) that synthesize cellulose chains. CESAs face the cytoplasm and use uridine diphosphate (UDP) glucose to extend the chain while pushing the growing chain through a channel in the cell wall.

1.1.2 Hemicellulose

Hemicellulose was the name given to a heterogeneous class of polysaccharides, which was extractable with alkaline solutions.[24] Initially the structure and biosynthesis of this polysaccharide class was not known, and hemicellulose was wrongly thought to be the precursor of cellulose.[25] Despite this hypothesis being incorrect and a definition based on extractability potentially leading to erroneous identifications, the name hemicellulose is still commonly used. However, now it is used to indicate a heterogeneous group of polysaccharides with β-(1,4)-linked backbones[26] that bind cellulose and prevent contacts between the microfibrils. Based on this definition hemicellulose can be divided in four classes of polysaccharides: xyloglucans (XGs), mixed-linkage glucans (MLGs), xylans and mannans (Figure 3). XGs are composed of a cellulosic backbone, highly decorated with xylose residues that can be further extended with galactose and other monosaccharides. MLGs are homopolymers composed of cellulose subunits randomly connected by β-1,3-linkages. Xylans have a backbone composed of β-1,4-linked xylose units, usually decorated with single monosaccharides such as glucuronic acid and arabinose. Mannans can be

found as homopolymer of β-1,4-linked mannose residues or substituted with galactose.

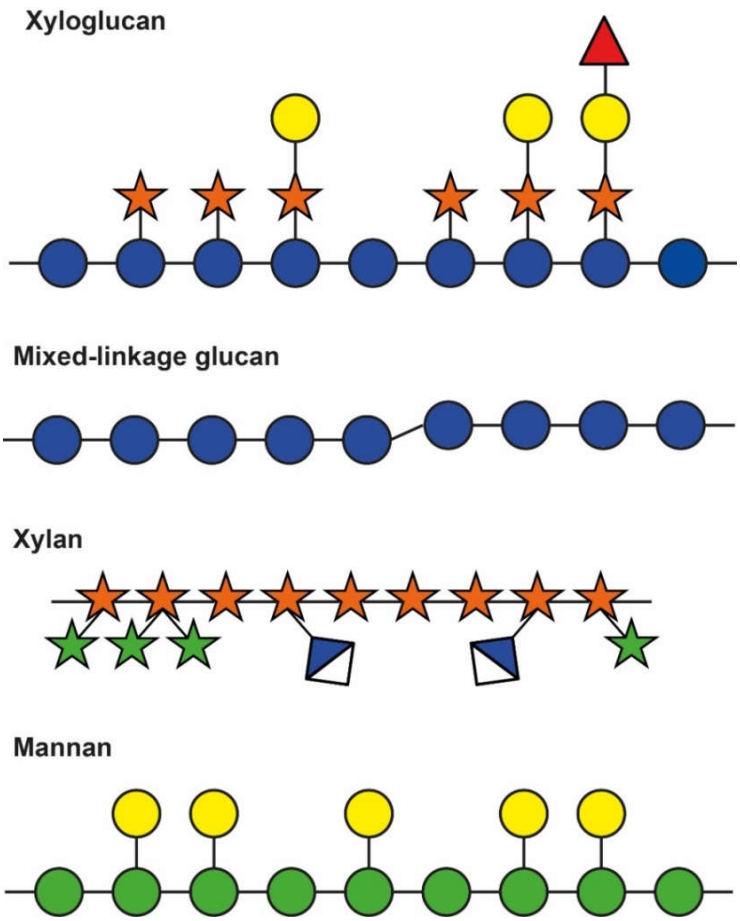

Figure 3: Main classes of hemicellulosic polysaccharides.

Hemicellulose represents 50% of the biomass in perennial and annual plants and, due to their abundance, the importance of this class of polysaccharides as a possible source of raw material is increasingly recognized. Hemicelluloses are considered as a sustainable source of energy and include diverse molecular structures that can be used as natural or functionalized bio-inspired materials.[25] Hemicellulose is synthesized intracellularly in the Golgi apparatus and transported via vesicles through the cytoplasm to be released in the cell wall. Since the similitude with the cellulose backbone, hemicellulose synthesis has been proposed to be performed by proteins similar to the CESA called cellulose synthase-like (CSL) proteins which synthesize the backbone before other glycosyltransferases (GTs) add branches. This hypothesis was found to be true for mannans,[27,28] MLGs[29] and XGs.[30]

1.1.3 Pectin

Pectin was first described by Bracconot in 1825[31] and is a heterogeneous group of polysaccharides mainly consisting of galacturonic acid residues, but also containing neutral monosaccharides such as galactose and rhamnose (Figure 4). Structures range from simple homogalacturans to the highly branched rhamnogalacturans (RGs) of type I and type II (Figure 4).

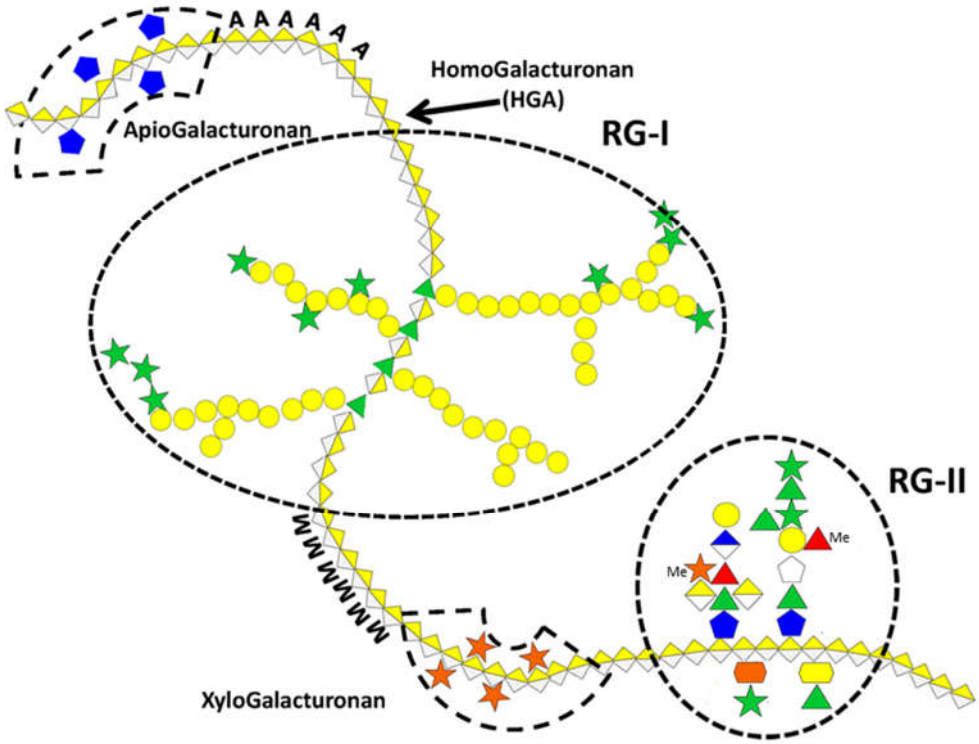

Figure 4: Schematic representation of pectin.[32]

The galacturonic acid can be acetylated in position 2 or 3 and the carboxylic acid may be methylated, masking the negative charge. Pectin is the most water soluble class of polysaccharides in plants due to the presence of multiple negative charges. Pectin is extractable with acidic solutions or with chelator agents. It is present in the primary cell wall but completely absent in the secondary cell wall. Pectin plays a key role during cell expansion and has gelling properties due to the carboxylic acid groups forming complexes with divalent cations, in particular calcium.[33] Pectin is synthesized in the Golgi apparatus

where the carboxylic acid of the galacturonic acid is found methylated. After transport to the cell wall, the removal of some of the methyl groups by methylesterases might help in cell adhesion processes.[34]

1.2 Plant Cell Wall Analysis

1.2.1 Monosaccharide Composition and Linkage Analysis

Plant cell wall composition can be analyzed using different methods. The monosaccharide composition can be determined both quantitatively and qualitatively using the alditol acetates approach.[35,36] After extraction, the polysaccharides are hydrolyzed to give monosaccharide units, then reduced by $NaBH_4$ to the alditol, and finally peracetylated. The acetylated alditols are analyzed by gas chromatography (GC) using a mass spectrometer (MS) or flame ionization detector (FID) by comparing the retention time with internal standards.[37] The alditols are peracetylated because acetylated glycan are easier to separate compared to other derivatives.[36] The alditol acetate approach only identifies the monosaccharide composition without providing any information on the stereochemistry and regiochemistry of the linkages. The position of the linkages can be elucidated by methylation analysis as shown in Scheme 1.

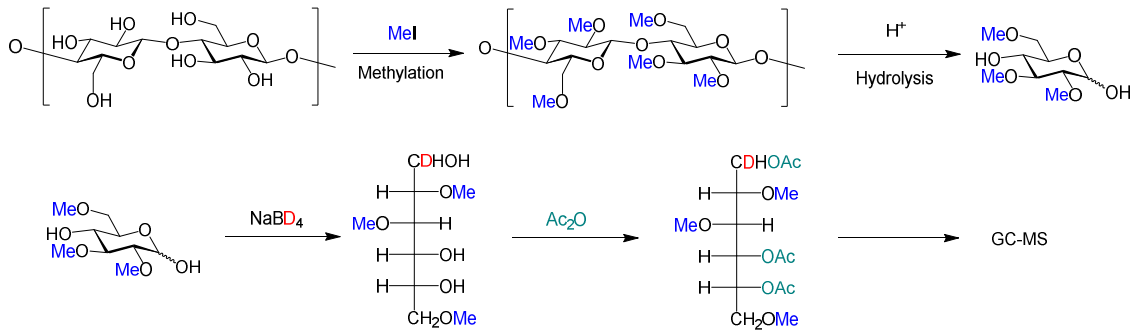

Scheme 1: Example of methylation analysis.

For methylation analysis the polymer is initially methylated by MeI and then hydrolyzed. The positions methylated on the monosaccharides are those not involved in any linkages. The resulting partially methylated sugars are reduced to alditols, followed by peracetylation. Analysis by GC-MS in addition to separating and quantifying the alditols provides fragmentation patterns that allow to

determine where the glycosidic linkages were located before hydrolysis.[37] Unfortunately, with this technique, all information on the stereochemistry is lost during the reductive opening of the pyranose ring. Therefore, nuclear magnetic resonance (NMR) techniques are required to analyze the stereochemistry.[38]

1.2.2 Monoclonal Antibodies

In situ analysis of the structures and the occurrence of plant cell wall polymers can be performed by immunohistochemical techniques which give high resolution images of cell wall microstructures.[39] Monoclonal antibodies (mAbs) and carbohydrate-binding modules developed against plant polysaccharides are used as powerful molecular probes to detect the structural elements of glycans in the cell wall (Figure 5).[39-41] The mAbs are usually produced using a hybridoma technique,[42] where myeloma cells are fused with a spleen cell from an animal previously immunized with either extracted oligosaccharides or well-defined polysaccharides. The resulting hybridoma cells release the antibodies into the supernatant which are screened for binding of the antigen. Another possibility is

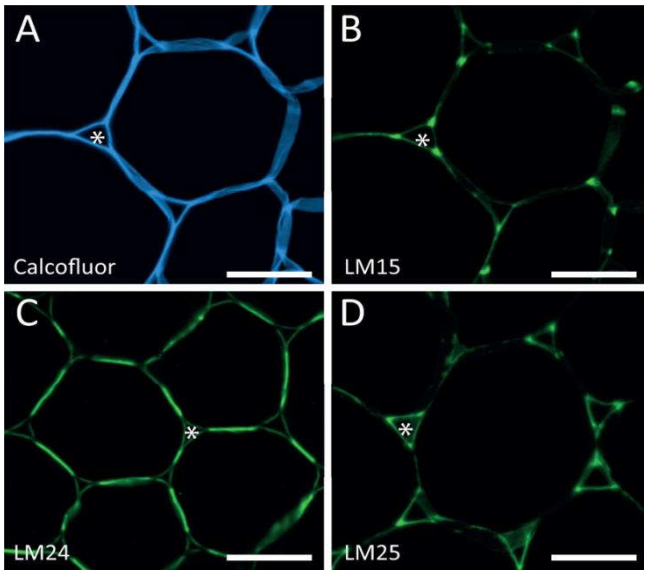

Figure 5: Immunofluorescence imagining of tobacco stem pith parenchyma cell walls with different mAbs directed at xyloglucan polysaccharides (B, C, D) and calcofluor (A).[43]

shotgun immunization, where multiple antigens are injected into the mouse.[44] Once the mAbs are generated, they are purified and screened against different polysaccharides for example by enzyme-linked immunosorbent assay (ELISA). Besides ELISA, carbohydrate microarrays can be used to investigate the binding

epitopes of the mAbs. Carbohydrate microarrays were introduced in 2002[45-50] and are now routinely used to screen carbohydrate-mAb interactions. Microarrays have been a breakthrough in the high-throughput (HTP) screening of biologically relevant molecules. Carbohydrate microarrays permit the study of a large number of combinations of antigens and antibodies at the same time and require only very small amounts of glycan. The compound is printed on a plate using different covalent or non-covalent immobilization methods. Once the molecules are immobilized on the microarray they can be detected using mAbs that are labelled with fluorescent dyes (direct method) or by incubating them with the mAbs of interest and subsequently introducing a fluorescently-labelled secondary mAb to bind the primary mAb (indirect method, Figure 6).

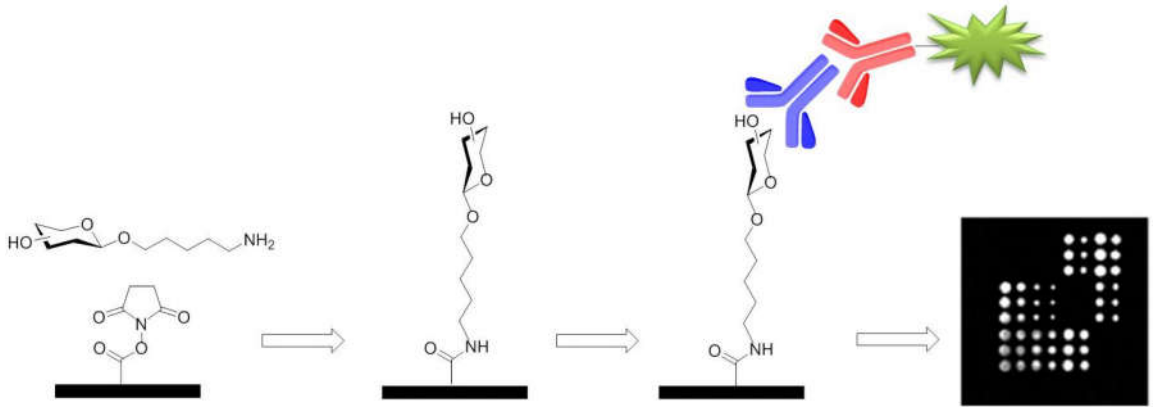

Figure 6: Indirect recognition of a glycan covalently immobilized on a *N*-hydroxysuccinimide (NHS) ester coated slide. The oligosaccharide is then recognized by an mAb to give a fluorescent signal, that is visualized using a fluorescence microarray reader.[51]

So far mostly isolated plant polysaccharides have been used to screen the binding specificities of the mAbs in ELISA or glycan microarray experiments. However, they do not permit to determine the precise molecular structure bound. For this purpose structurally well-defined oligosaccharides are required. However, they are difficult to obtain by extraction from natural sources.[43] The availability of libraries of well-defined synthetic oligosaccharides would greatly facilitate the characterization of mAbs directed at cell wall polysaccharides.

1.3 Oligosaccharide Synthesis

Interest in glycosciences increases as biologists continually elucidate carbohydrate roles in biological processes such as immune defence as well as roles in many diseases such as cancer, infectious diseases, and autoimmune disorders.[52]

However, despite the importance of carbohydrate interactions with other biomolecules in nature, for carbohydrates, structure-activity relationships are not as well studied as for peptides and nucleotides. This is mainly due to difficulties in the extraction, purification, and isolation of pure carbohydrate samples for systematic studies. Chemical synthesis is a powerful method to generate well defined oligosaccharides for therapeutic use, but one limiting factor is the complexity of carbohydrate structures that makes their synthesis very challenging. In contrast to linear oligonucleotides and peptides, oligosaccharides are usually highly branched. The need to produce branched structures with the required stereocontrol requires careful differentiation of the protecting groups (PGs) used in their synthesis.[53]

Nevertheless, synthetic oligosaccharides have already been used to treat vein thrombosis. They also show potential to treat cancer, neurological diseases, infections, and in the development of vaccines.[52] A milestone in the synthesis of large glycans was recently achieved by Ye *et al.,*[54] who synthesized the largest fully synthetic carbohydrate to date. A glycan containing 92 monosaccharides was synthesized using a highly convergent [31+31+30] coupling strategy. Despite this success the chemical synthesis of glycans is still challenging, and there have not been many examples of fully synthetic, very large oligosaccharides reported.[55-63] This is due to several synthetic difficulties such as the selective formation of single stereoisomers during glycosylation reactions.[64]

1.3.1 Glycosylation Reactions

A chemical glycosylation is a condensation reaction between the hemiacetal moiety of a monosaccharide (donor) and the hydroxyl group of an organic compound (acceptor), to form an acetal called glycosidic bond. The first reported example was the Fischer glycosylation[65] where an unprotected monosaccharide and an alcohol react under acidic conditions. In most cases, however, there is the

need to activate the donor through the use of a leaving group to form the glycosidic bond.

The first example in this direction was described by Königs and Knorr in 1901, who used a glycosyl bromide as a donor and Ag_2CO_3 as a promoter.[66] Later, imidate based donors represented a breakthrough in carbohydrate chemistry. Introduced in 1980 by Schmidt,[67] these donors are activated by catalytic amounts of trimethylsilyl triflate (TMSOTf) or $BF_3 \cdot OEt_2$. Most commonly used are trichloroacetimidates, which have become one of the most routinely used leaving groups in glycosylation reactions.[68] The continued need to improve glycosylation selectivity and the introduction of new PGs has led to the development of a wide range of additional leaving groups. Among them, thioethers are the most successful class. Thioglycosides can be activated using a wide range of electrophiles including the Ph_2SO/Tf_2O[69,70] and NIS/TfOH[71,72] systems. Thioethers are used not only as a leaving group but also to mask the anomeric center during protection and deprotection steps owing to their chemical stability.[73] Another class of leaving groups that are commonly used are phosphates. They are activated using stoichiometric amounts of TMSOTf and have proven to be powerful leaving groups in automated solid-phase synthesis.[74,75]

1.3.2 Glycosylation Mechanism and Stereoselectivity

Despite being a simple reaction between an alcohol and a hemiacetal, great efforts to control the reaction conditions of glycosylations are required to obtain the desired product. Hydrolyzed glycosyl donor and products resulting from migration/cleavage of PGs are just some examples of the possible side products formed during a glycosylation reaction. In addition, two stereoisomers may be formed. They are called 1,2-*cis* and 1,2-*trans* when referring to the orientation of the glycosidic linkage with respect to the substituent at the C2 position, and α or β when referring to the orientation of the substituent at the anomeric center compared to the stereocenter that determines the absolute configuration. The mechanism of the glycosylation reaction is still not fully understood but it is generally described as an S_N1 mechanism.[76] The activation and departure of the

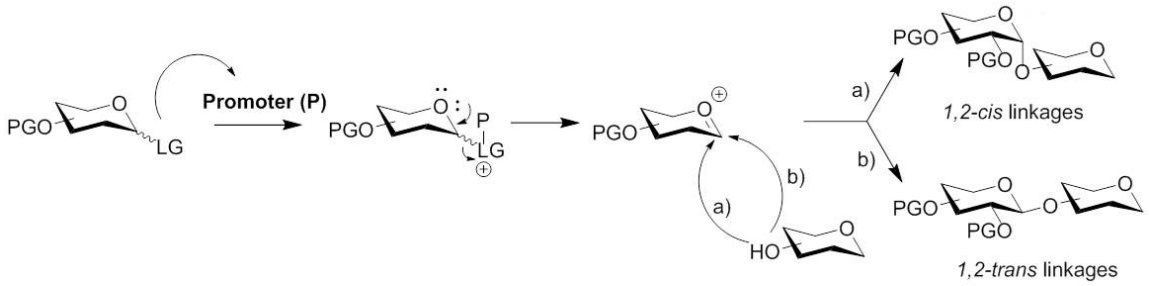

Scheme 2: Glycosylation mechanism.

leaving group upon activation leads to the formation of an oxocarbenium ion, which subsequently reacts with a nucleophilic alcohol to form the glycosidic bond (Scheme 2). The presence of an isolated oxocarbenium ion alone, however, is thermodynamically unfavorable.[77] Therefore it interacts with the activator counter ion and the solvent, forming an array of different oxocarbenium ion intermediates. They range from covalent species to more reactive contact ion pair (CIP) species to solvent separated ion pair (SSIP) species.[78] The presence of these species impact the mechanism: the presence of a covalent bond leads to a S_N2 mechanism, with displacement of the counter ion by the nucleophile, gradually switching to an S_N1 character for the SSIP (Scheme 3).

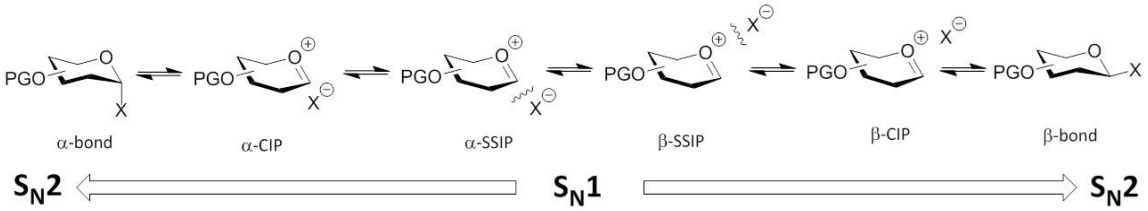

Scheme 3: Different oxocarbenium intermediates during glycosylation.

In carbohydrate chemistry, a lot of effort was spent to control the stereoselectivity of glycosylation reactions. The most important approach to control the stereoselectivity is to use an ester PG at the C2-position of the glycosyl donor, which leads to a so called participating mechanism. Once the donor is activated upon addition of the promoter, the carbonyl group of the ester attacks the resulting oxocarbenium ion, forming an acyloxonium ion. The acyloxonium ion masks one of the diastereotopic faces, leading to a nucleophilic attack from the other face, thus forming a *trans*-linkage (Scheme 4). The formation of 1,2-*cis*-linkages is rare in these cases, but still possible when using poor nucleophiles or a weak participating group at the C2-position.[68]

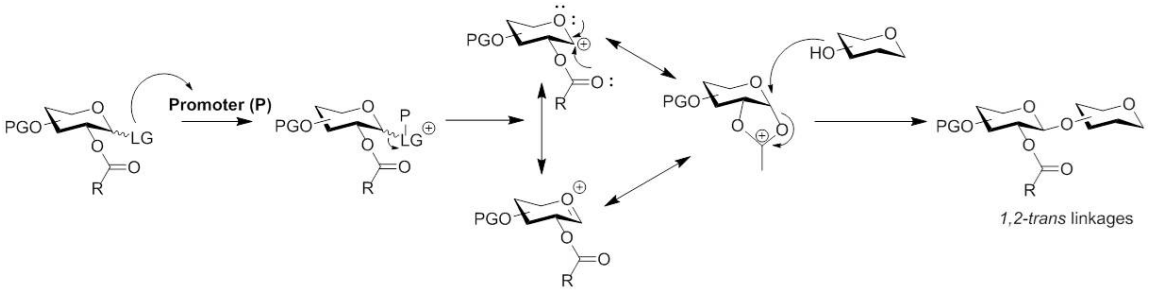

Scheme 4: Glycosylation mechanism with participating group at the C2-position of the glycosyl donor.

One way to control the stereoselectivity is through temperature. Since the formation of the β-anomer is kinetically favored, it is possible to increase the formation of this product by operating at low temperature. The α-anomer is thermodynamically favored, so increasing the temperature favors formation of the α-anomer. Another well-studied effect is the solvent effect (Scheme 5). The most

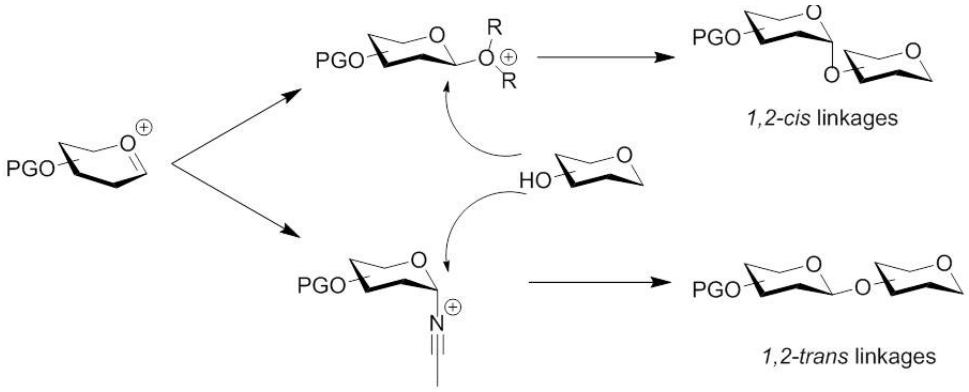

Scheme 5: Solvent effects in glycosylation.

commonly used solvents for improving stereoselectivity are acetonitrile and ethereal solvents. Acetonitrile as solvent leads to the formation of a 1,2-*cis*-nitrilium intermediate shielding one face. The nucleophile attacks from the other face, resulting in the formation of the 1,2-*trans*-product.[79,80] Conversely, ethers form an equatorial intermediate and increase the 1,2-*cis*-selectivity.[81,82] In the past several decades, various methods to promote the formation of 1,2-*cis*-linkages in a controlled manner were developed: installing a *cis*-directing participating group at C2,[83-87] the use of remote PGs,[88-91] the hydrogen bond mediated aglycone delivery (HBMAD)[92,93] and conformation restraining PGs[94,95] are just some examples (Scheme 6).

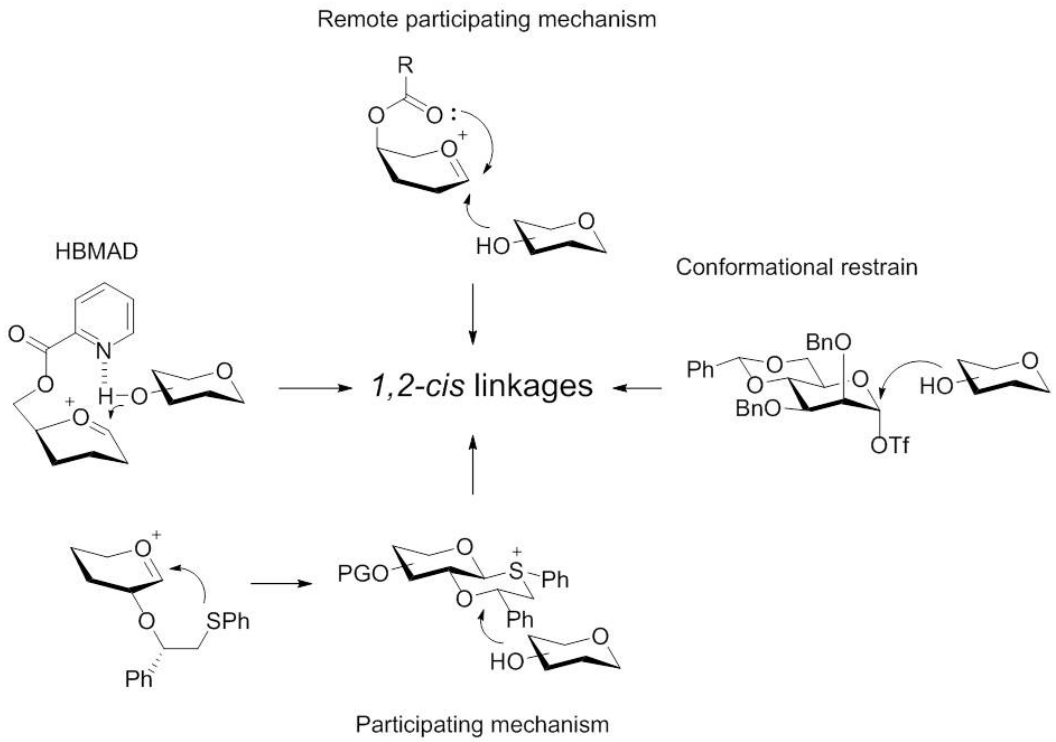

Scheme 6: Exemplary strategies to promote the formation of 1,2-*cis*-linkages in glycosylation reactions.

The role of the acceptor in controlling the stereochemistry is comparatively poorly understood. Few systematic studies were performed, such as the work of Woerpel at al.[96] and recently Codée et al.[78] Both report how increasing the nucleophilicity of the acceptor decreases the α-selectivity in the reaction. Despite the progress in developing new glycosylation strategies and in understanding glycosylation mechanisms, there is still no universally applicable strategy to selectively access 1,2-*cis*-glycosides. Thus, more research is needed to develop new coupling methods and technologies for the synthesis of oligosaccharides.[64]

1.3.3 Automated Glycan Assembly

In the 1960s, Merrifield reported the first solid-phase synthesis of a tetrapeptide,[97] for which he received the Nobel prize in 1984.[98] This was a breakthrough in the field that led to the development of fully-automated solid-phase peptide synthesis. Later, in 1985, Caruthers introduced solid-phase DNA synthesis.[99] Presently, automated solid-phase synthesis is routinely used for the synthesis of oligopeptides and oligonucleotides, providing access to tailor-made oligomers that allow researchers to explore new diagnostic and therapeutic

opportunities.[99,100] Even non-experienced workers can easily synthesize a wide range of structures. The first solid-phase synthesis of carbohydrates was reported in the 1970s,[101] but only in 2001 Seeberger`s group reported the first automated solid-phase synthesis of an oligosaccharide.[102] Recently, many groups have begun tackling this challenge.[103-105] Currently though, Seeberger's automated glycan assembly approach has been the only one to show great potential for the preparation of large glycans.[61,63,102,106-109] Solid-phase synthesis (Scheme 7) is based on the use of a solid support functionalized with a cleavable

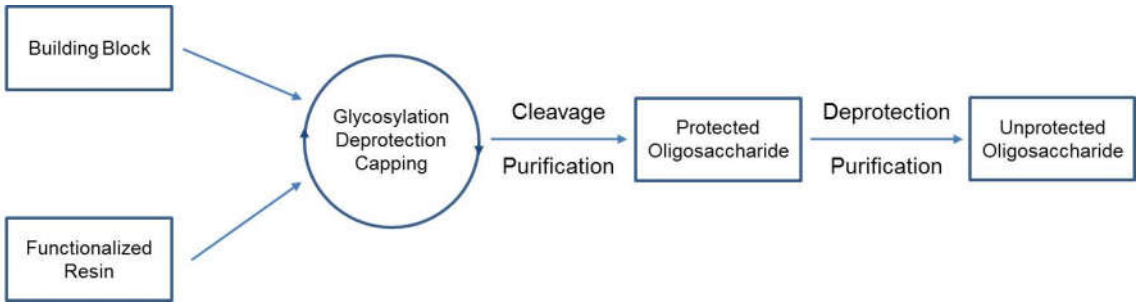

Scheme 7: Schematic representation of automated glycan assembly.

linker to which the monosaccharide building blocks (BBs) are coupled. The linker must not take part in the reactions during the elongation process and is cleaved from the solid support at the end of the process.[53] The synthetic cycles are based on glycosylation and deprotection steps: the BB is coupled to the resin in a glycosylation reaction, followed by the removal of a temporary PG which will free the required hydroxyl for the next glycosylation. The solid support allows the use of excess reagents to drive the reaction to completion and it facilitates the purification of intermediates by simple filtration. A capping step can block all unreacted hydroxyls after the glycosylation step, preventing any deletion sequences from elongating and thus from consuming BB in the next steps. Once the synthesis is completed, the resin is removed from the reaction vessel, and the oligosaccharide is cleaved from the solid support and eventually purified by high performance liquid chromatography (HPLC). Final deprotection steps afford the unprotected oligosaccharide with or without a linker for conjugation to proteins or surfaces.

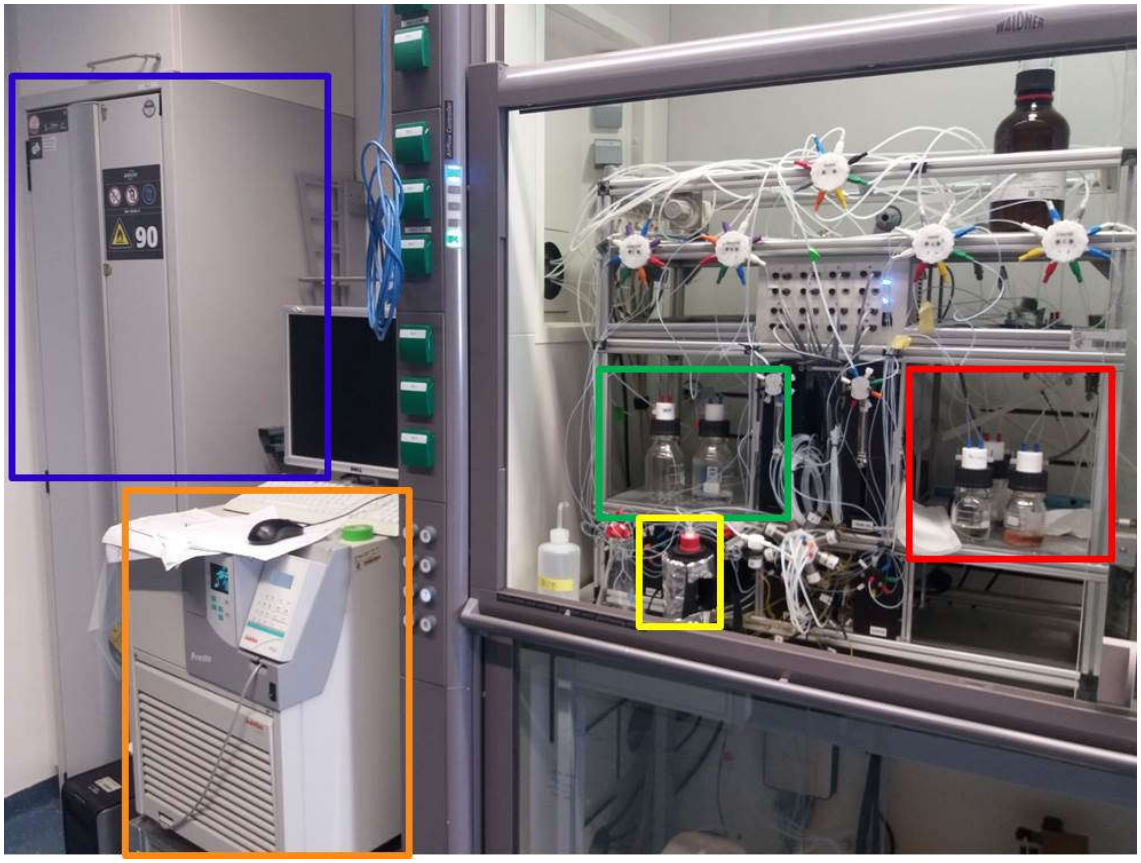

Figure 7: Automated oligosaccharide synthesizer used for automated glycan assembly.

Figure 7 shows a picture of a homemade automated oligosaccharide synthesizer available at the Max Planck Institute of Colloids and Interfaces (MPIKG). In the left cabinet (blue box) different solvents including dichloromethane (DCM), dimethylformamide (DMF) and tetrahydrofuran (THF) for washing the resin are stored. Next to it there is the chiller (orange box) to control the temperature in the reaction vessel (yellow box). The resin is located in the reaction vessel where the different reaction steps take place. The reaction vessel is equipped with a filter to drain the different solutions. Mixing of the reaction mixture is performed by bubbling argon through the reaction vessel. In the metal frame in the fume hood are located the different solutions for deprotection (green box), activation of the donor and capping (red box). The most commonly used temporary PGs are levulinoyl (Lev), fluorenylmethyloxycarbonyl (Fmoc), naphthylmethyl (Nap)[51] and 2-(azidomethyl)benzoyl (Azmb)[110] which are either used to elongate the backbone chain or to introduce side branches. Permanent PGs such as benzyl (Bn) or benzoyl (Bz) are removed in solution-phase reactions after cleavage of the oligosaccharide from the solid support in the final steps of

the synthesis. Glycosyl trichloroacetimidates,[102] glycosyl phosphates,[102,111] and thioglycosides[109] have been used as glycosyl donors in the synthesizer. The most

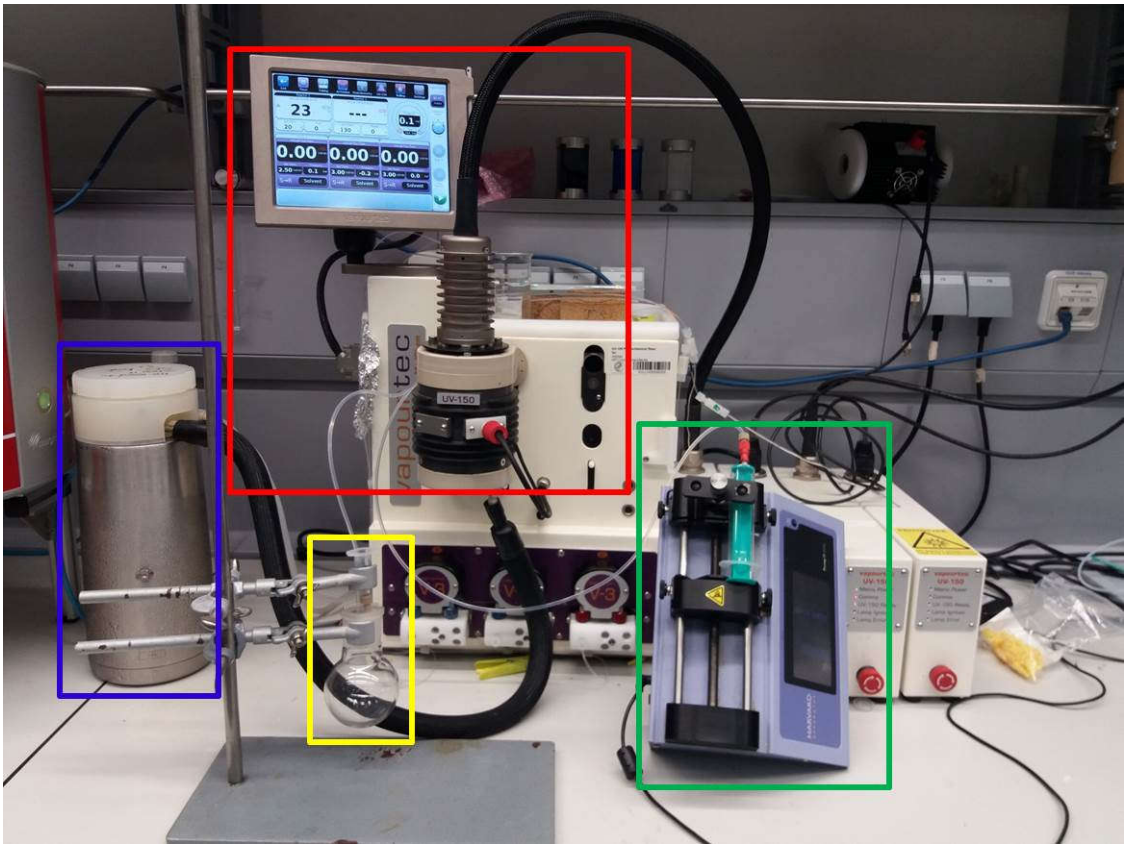

Figure 8: Continuos flow reactor for the cleavage of the photocleavable linker. The cleavage of the oligosaccharide is performed using a Vapourtec photoreactor Flow Chemistry System (red box). The resin, suspended in DCM, is loaded into a plastic syringe. The suspension is then pumped using a syringe pump (green box) through fluorinated ethylene propylene tubing in the photoreactor to finally accumulate in a filter (yellow box) which separates the resin from the DCM containing the oligosaccharide. The temperature in the photoreactor is maintained low by cooled nitrogen, which passes though a Dewar (blue box) containing dry ice.

commonly used linker in automated glycan assembly is a photocleavable linker[111] that is cleaved from the solid support in a continuous-flow photoreactor (Figure 8) by ultraviolet (UV) light (305 nm), providing a terminal free amine for conjugation to proteins and surfaces. An example for the automated glycan assembly of a fungal oligosaccharide library is shown in Scheme 8.[112] In the synthesis of branched β(1,3)glucans two different glucose BBs were employed. The first BB carries as temporary PG an Fmoc group in the C3-position to build the backbone. The second BB is equipped with an additional Lev PG at the C6 position. Lev is orthogonal to Fmoc and required to introduce branching. Iterative addition of BB **1** and **2** to the linker-functionalized resin have led to the construction of the

backbone.Subsequently, to branch the oligosaccharide, Lev was deprotected using hydrazine and BB **1** was coupled to the resulting free primary alcohol. Once

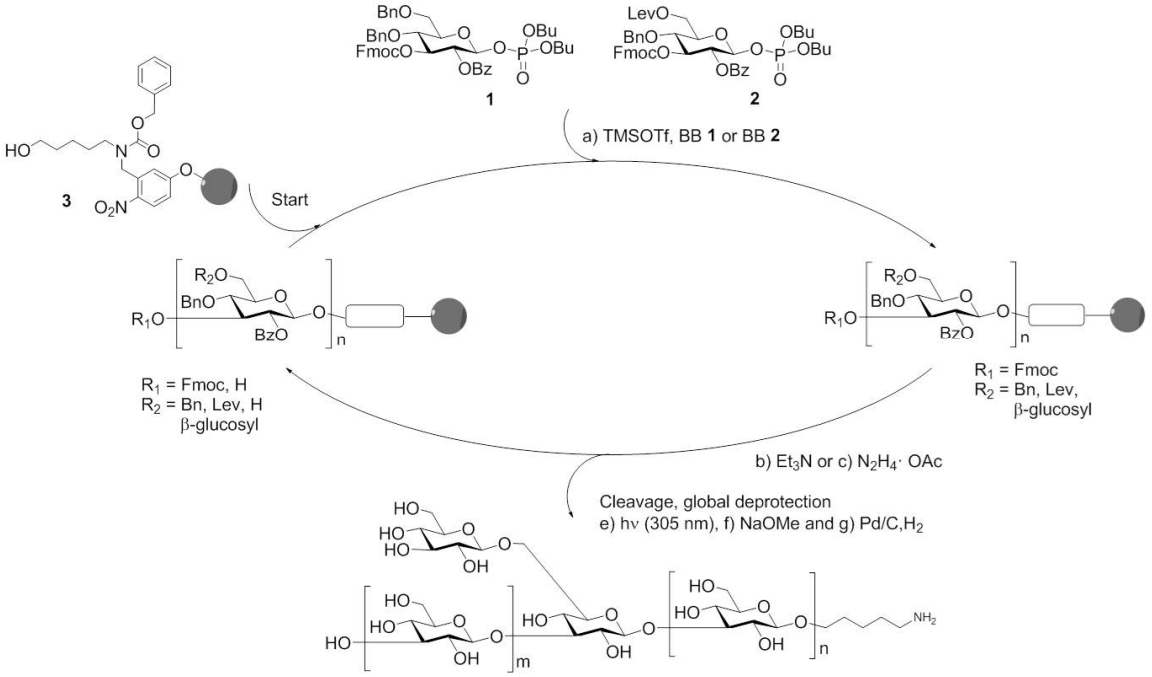

Scheme 8: Automated glycan assembly of fungal glucan oligosaccharides.[112]

the synthesis was completed, the resin was passed through the photoreactor (Figure 8) to cleave the oligosaccharide from the resin, and all remaining permanent PGs were removed by methanolysis and hydrogenolysis to obtain the fully deprotected oligosaccharide.

1.5 Aims of this Thesis

The overall goal of this thesis was to contribute to solving one of the major drawbacks in the study of plant carbohydrates that is the lack of synthetic pure well-defined oligosaccharide samples. In particular, this work aimed at the synthesis of oligosaccharide fragments of xyloglucan (XG) and mixed-linkage glucan (MLG) which are abundant classes of hemicellulosic polysaccharides in plants. Automated glycan assembly was chosen as the key technology to enable the rapid synthesis of large collections of oligosaccharides.

In the synthesis of XGs the construction of the α-bond between xylose and glucose is particularly challenging. Therefore, a suitable strategy for the automated synthesis of multiple of these 1,2-*cis*-glycosidic bonds had to be developed. Different BBs were to be designed and tested in order to determine the optimal strategy for the assembly of complex XG oligosaccharides. Once the synthetic oligosaccharides are prepared, they can be used for the characterization of mAbs and for studying the specificity of cell wall-remodeling enzymes.

Compared to the synthesis of the XG oligosaccharide library the synthesis of MLG oligosaccharides appeared to be relatively straightforward. Two glucose BBs are required, one with a temporary protecting group at the C4-postion for producing stretches of cellulosic oligosaccharides and one with a temporary protecting group at C-3 to introduce occasional β-1,3-linkages. The synthetic MLG oligosaccharides represent ideal samples for investigating the substrate specificities of MLG-degrading enzymes. These studies were aimed to be performed within the scope of this thesis as well.

2. Automated Glycan Assembly of Xyloglucan Oligosaccharides

This chapter has been modified in part from the following articles:

M. Wilsdorf, D. Schmidt, M. Bartetzko, **P. Dallabernardina**, F. Schuhmacher, P. Seeberger, F. Pfrengle, *Chem. Comm.*, **2016,** *52*, 10187-10189. A traceless photocleavable linker for the automated glycan assembly of carbohydrates with free reducing ends. DOI: http://dx.doi.org/10.1039/C6CC04954K

P. Dallabernardina, F. Schumacher, P. H. Seeberger, F. Pfrengle, *Org. Biomol. Chem.* **2016**, *14*, 309-313. Automated glycan assembly of xyloglucan oligosaccharides. DOI: http://dx.doi.org/10.1039/C5OB02226F

2.1 Xyloglucan and Xyloglucan Endotransglycosylases

2.1.1 Xyloglucan

Xyloglucans (XGs) are the most prevalent class of hemicelluloses in the cell walls of higher plants.[25] XGs are comprised of a β-(1,4)-D-glucan backbone decorated with α-D-xylopyranosyl residues at *O*-6, and are often further extended by addition of galactosyl and fucosyl substituents (Figure 9a). To date, 24 different naturally occurring xyloglucan side-chain structures have been identified.[113] Despite this diversity, galactose substitution at *O*-2 of the xylose residue is present in all plant species, suggesting that this modification plays an important structural or functional role in the plant cell wall.[114] XGs occur in two major forms: the XXGG-type consists of two xylose-substituted glucose moieties alternating with two unsubstituted glucose residues, and the XXXG-type has three xylose-substituted residues separated by only one unsubstituted glucose (Figure 9b).[25,115]

Despite the structural diversity of XGs across species, the functions of XGs in plant growth and development are conserved for all flowering plants.[116] XGs are strongly bonded through non-covalent interactions to the cellulose microfibrils

in the cell wall (Figure 9a).[117] These interactions are not only essential for the structural viability of the cell wall but also its flexibility during synthesis.[116-120] XGs are also important for energy storage [119] and can act as signaling molecules.[116]

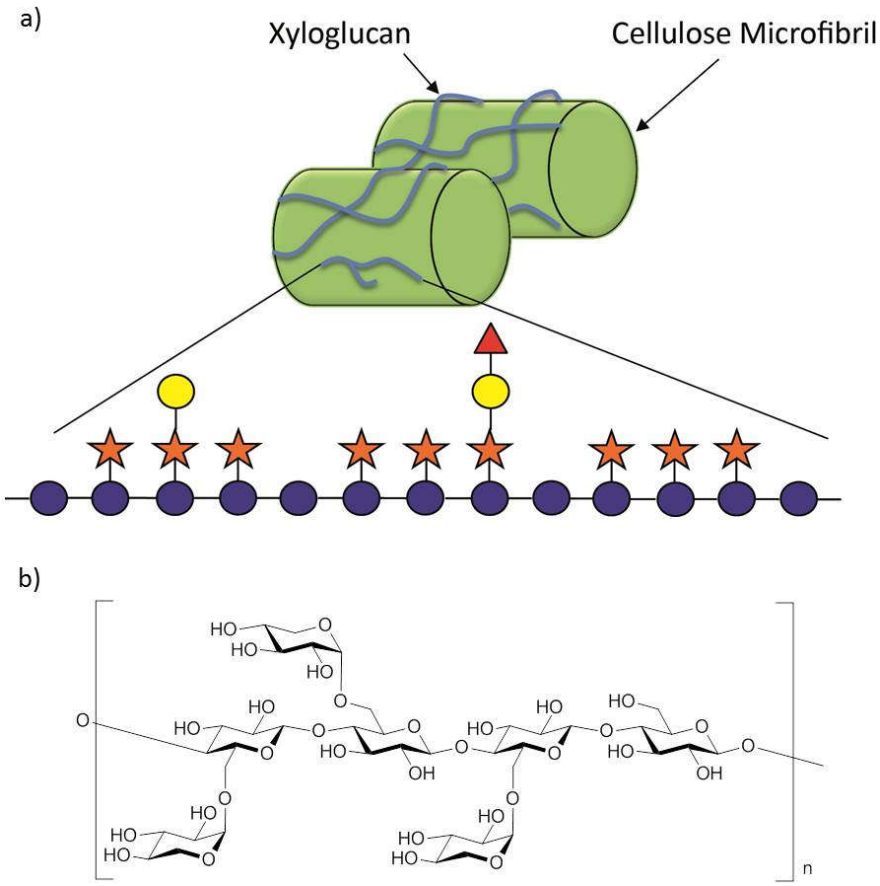

Figure 9: a) The hemicellulose xyloglucan interconnects cellulose microfibrils through hydrogen bonding interactions; b) XXXG-type of XG oligosaccharides

2.1.2 Xyloglucan Endotransglycosylases

Xyloglucan Endotransglycosylases (XET) are enzymes involved in the morphogenesis of the cell wall by loosening the XG-cellulose network and incorporating new freshly synthesized XGs, thus remodeling the cell wall.[121-123] XETs cleave existing XG polysaccharides and recombine them with other XG chains to generate new XG polysaccharides (Figure 10a). Despite their importance, the substrate requirements for XET activity are still not fully resolved. The substrate determinants for activity in the positive subsite are contested with two opposing viewpoints present in the literature (Figure 10b).

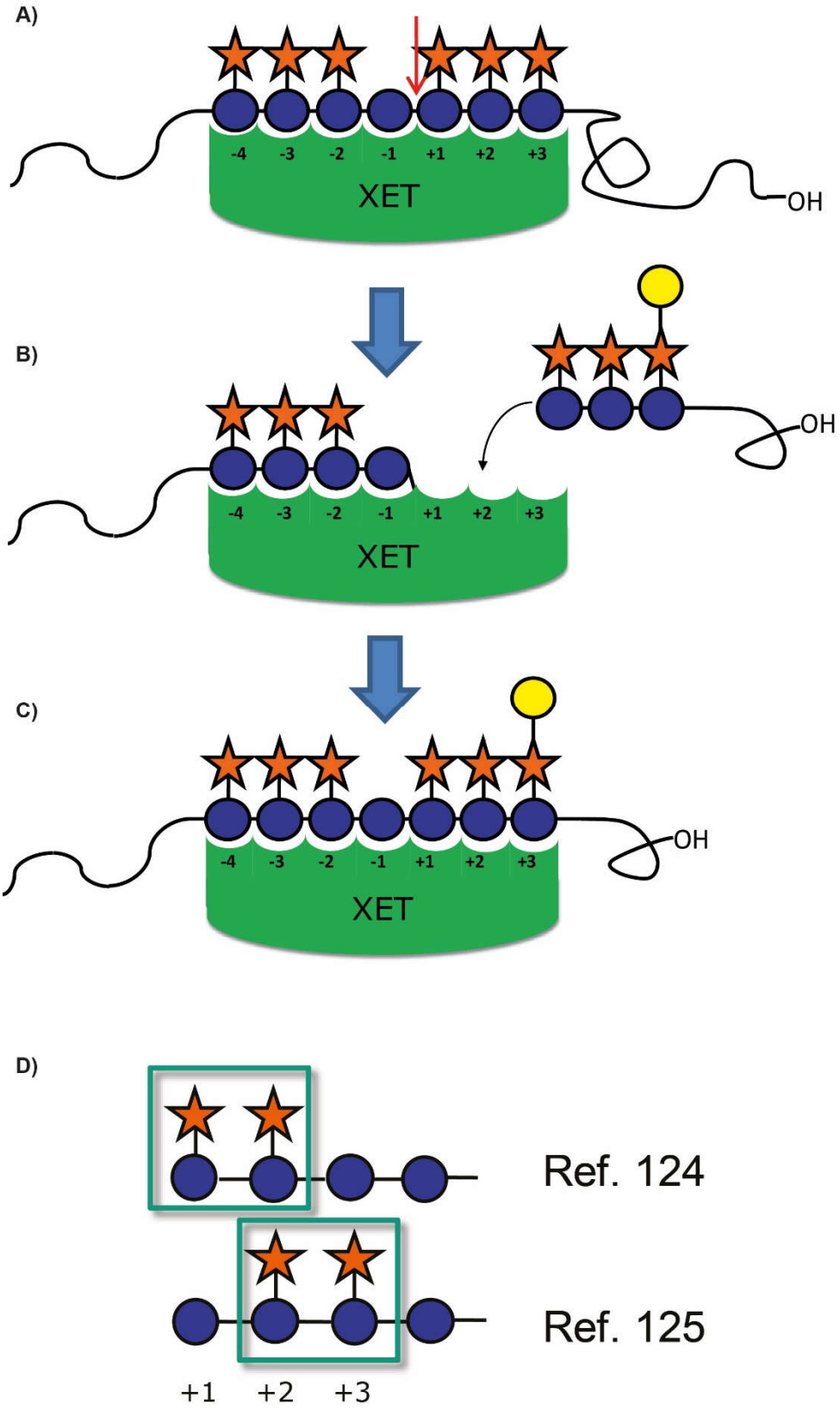

Figure 10: Graphical representation of XET activity. A) The XET hydrolyses the XG polymer between positions -1 and + 1 (red arrow). B) Once the glycosyl-enzyme intermediate is formed a new XG polymer acts as an acceptor and C) a new XG is formed. D) Two hypotheses regarding the importance of xylose-substitutions of the acceptor are reported in the literature: Fry *et al*[124] suggested that position +1 and +2 positions need to be occupied by xylose substituted glucoses. Alternatively, Saura-Varell *et al*[125] claimed that the posititions +2 and +3 must be xylosylated.

XET is an enzyme of the glycoside hydrolase (GH) family GH16[126] that works with a stereochemistry-retaining double displacement mechanism under acid-base catalysis (Scheme 9).[127] The reaction is catalyzed by two glutamic acid residues (Glu_{85} and Glu_{89}) (Scheme 9a). When bound to the XET, a glucose residue of the XG chain potentially assumes a twist-boat conformation[128] that allows a glutamic acid to transfer a proton to the pseudo glycosidic oxygen, inducing a displacement by another glutamic acid which forms a strong hydrogen

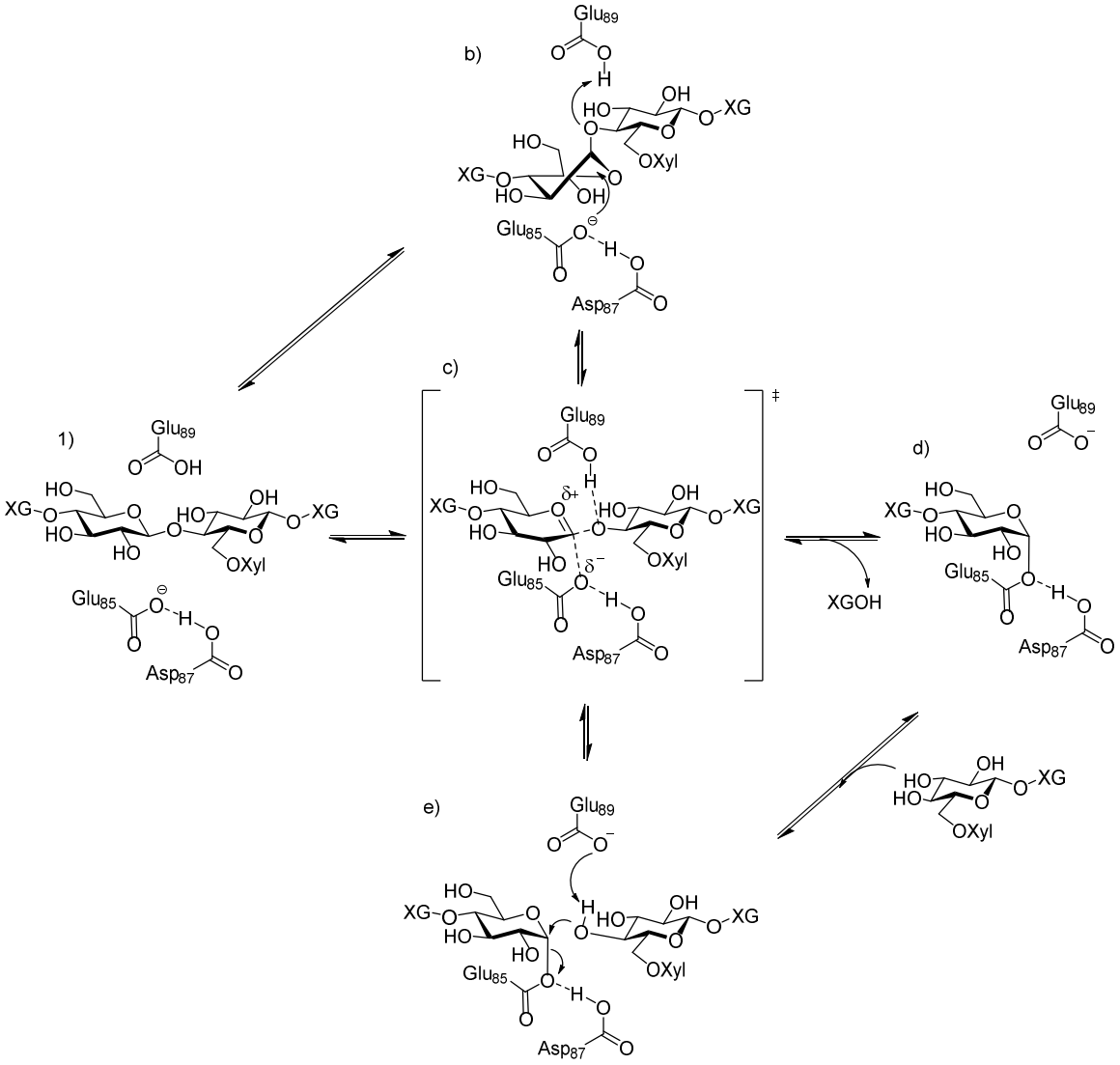

Scheme 9: Schematic representation of the acid/base catalysis of XETs following a stereochemistry-retaining double displacement mechanism.

bond with an aspartic acid (Asp_{87}) next to it (Scheme 9b).[129] The reaction proceeds through an oxocarbenium-like transition state, with inversion of configuration (Scheme 9b). The enzyme-glycosyl (Scheme 9d) intermediate is

then attacked by a different XG polysaccharide under catalysis of the conjugate base of glutamic acid 89 (Scheme 9e). The second displacement inverts the configuration again (Scheme 9c), leading to an overall retention of configuration (Scheme 9a).

2.2 Results and Discussion

2.2.1 Automated Glycan Assembly of Xyloglucan Oligosaccharides Exclusively from Monosaccharide BBs

To date, few chemical syntheses of XG oligosaccharides have been reported.[130-133] The multi-step total synthesis of a XG-derived nonasaccharide[131] relied on a late-stage introduction of a fucose-galactose-xylose trisaccharide side chain using glycosyl imidate donors. Large defined XG fragments have also been prepared by enzymatic coupling of XG oligosaccharides obtained from the enzymatic degradation of XG polymers.[134] This approach is limited only in the diversity of potential products due to the limited accessibility of oligosaccharide building blocks. The main synthetic challenge in the chemical synthesis of XG oligosaccharides is the formation of the α–glycosidic bond between the xylose and the glucose.

Initially we investigated the possibility to assemble XG oligosaccharides exclusively from monosaccharide BBs. Two glucose BBs (**1** and **2**) and a xylose BB (**3**) were designed for automated synthesis (Figure 11). Glucose BBs **1** and **2** were equipped with Bz esters in the C2-position as participating protecting groups to favor the formation of β-linkages. Fmoc and Lev were used as temporary protecting groups to enable either elongation of the β-1,4-glucan backbone or introduction of xylose at the C6-position. All remaining positions were permanently protected with Bn ethers. Both BBs contained phosphate leaving groups to enable smooth chain elongation.[74,75] There are no effective methods for the generation of α-xylosidic bonds in automated glycan assembly reported. Xylose lacks the C6-position and therefore remote participating protecting groups, previously used for the generation of consecutive 1,2-*cis*-linkages, are not applicable.[91] For these reasons, the easily accessible xylose BB

3 (Figure 11) was chosen as the first option. Xylose BB **3** was protected in all positions with Bn groups and used as the thioglycoside.

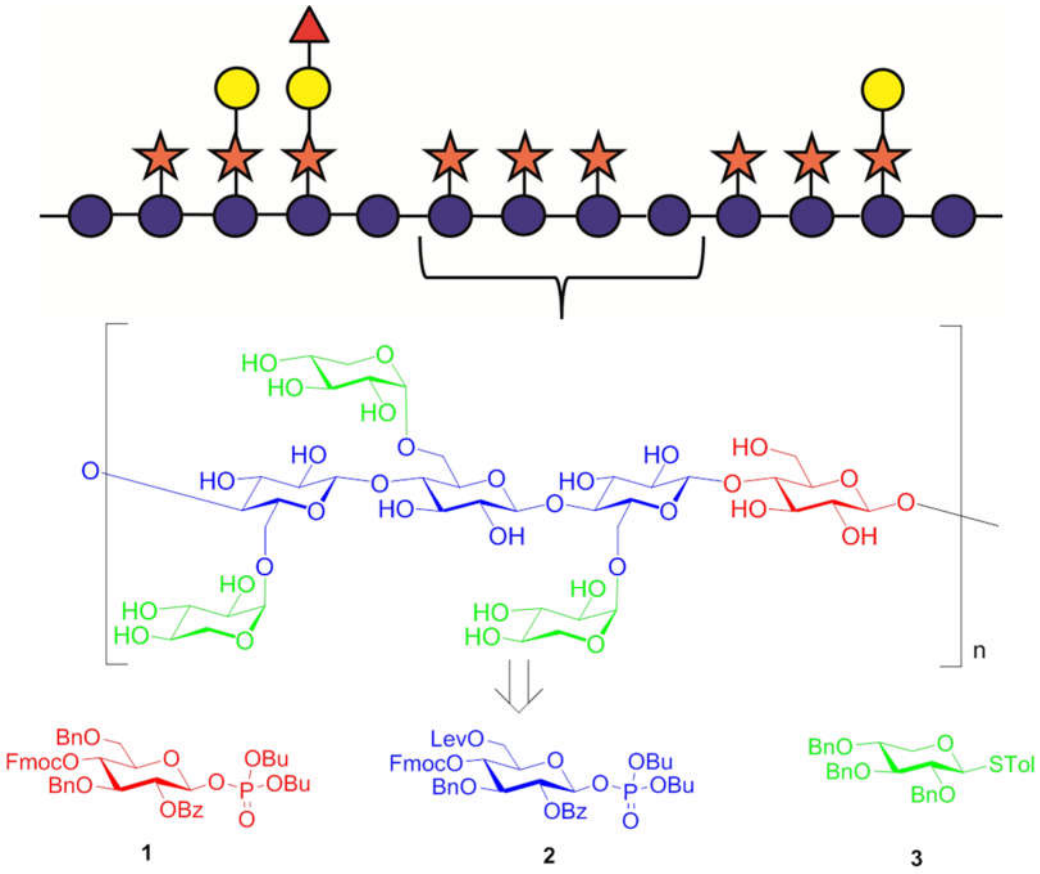

Figure 11: Retrosynthetic approach for the automated glycan assembly of a XG oligosaccharide library using exclusively monosaccharide BBs.

The synthesis of BBs **1** and **2** started from common intermediate **5** (Scheme 10) which was prepared from glucose diacetonide in seven steps following established procedures.[135,136] To achieve the synthesis of **1**, the 4,6-benzylidene group was reductively opened in a regioselective manner using Et_3SiH and trifluoroacetic acid (TFA)[137] to give the 6-OBn protected compound **6**. The free 4-hydroxyl in **5** was protected with an Fmoc group followed by the transformation of the thioglycoside into the corresponding glycosyl phosphate **1**. BB **2** was obtained by acidic hydrolysis of the benzylidene acetal in **5** to give diol **8**,[136] which was selectively protected at the primary hydroxyl group at the C6-position using levulinic acid (LevOH) in the presence of 2-chloro-1-methylpyridinium iodide (CMPI) and 1,4-diazabicyclo[2.2.2]octane (DABCO)[138,139] to provide **9.** The low yield is due to some over-acylation resulting in the double-protected compound. The synthesis of BB **2** was completed following a similar procedure as described

for BB **1**. The presence of the Lev group led to the formation of many side-products in the preparation of glycosyl phosphate **2** from thioglycoside **10** when performing the reaction at 0 °C. Therefore, the reaction temperature needed to be decreased to -15 °C. BB **3** was synthesized in four steps as reported in the literature by Lüning *et al*.[140]

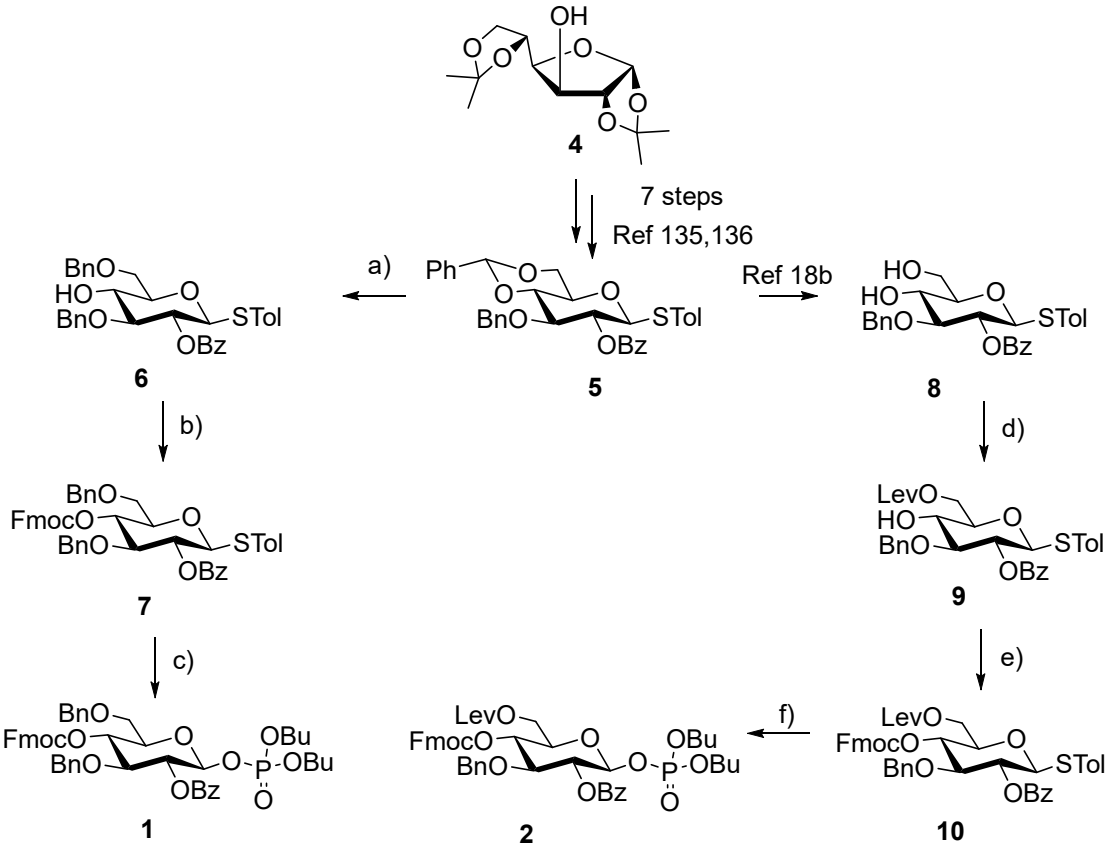

Scheme 10: Synthesis of BBs **1** and **2.** Reagents and conditions: a) Et_3SiH, TFA, TFAA, CH_2Cl_2, 0 °C to rt, 70%; b) FmocCl, pyridine, CH_2Cl_2, 0 °C to rt, 90%; c) $HOP(O)(OBu)_2$, NIS, TfOH, CH_2Cl_2, 0 °C, 92%; d) LevOH, CMPI, DABCO, CH_2Cl_2, -15 °C, 77%; e) FmocCl, pyridine, CH_2Cl_2, 0 °C to rt, 74%; f) $HOP(O)(OBu)_2$, NIS, TfOH, CH_2Cl_2, -15°C, 75%.

With BBs **1-3** in hand, we explored their potential for the automated glycan assembly of trisaccharide **12** (Scheme 11a). BB **1** was installed on the photo-labile linker-functionalized resin **11**[74] by TMSOTf-promoted glycosylation using two cycles of 3.7 equivalents BB. Fmoc-deprotection and another glycosylation with BB **2** provided the disaccharide ready for installation of the α-xyloside. After removal of the Lev-group, we investigated the glycosylation of the second glucose unit of the resin-bound disaccharide with BB **3** promoted by *N*-iodosuccinimide (NIS) and a catalytic amount of triflic acid (TfOH). At temperatures as low as -35 °C, full conversion was achieved and the desired

trisaccharide was obtained in 29% yield after cleavage of the linker in a commercial continuous flow photoreactor.[141] Unfortunately, the reaction resulted

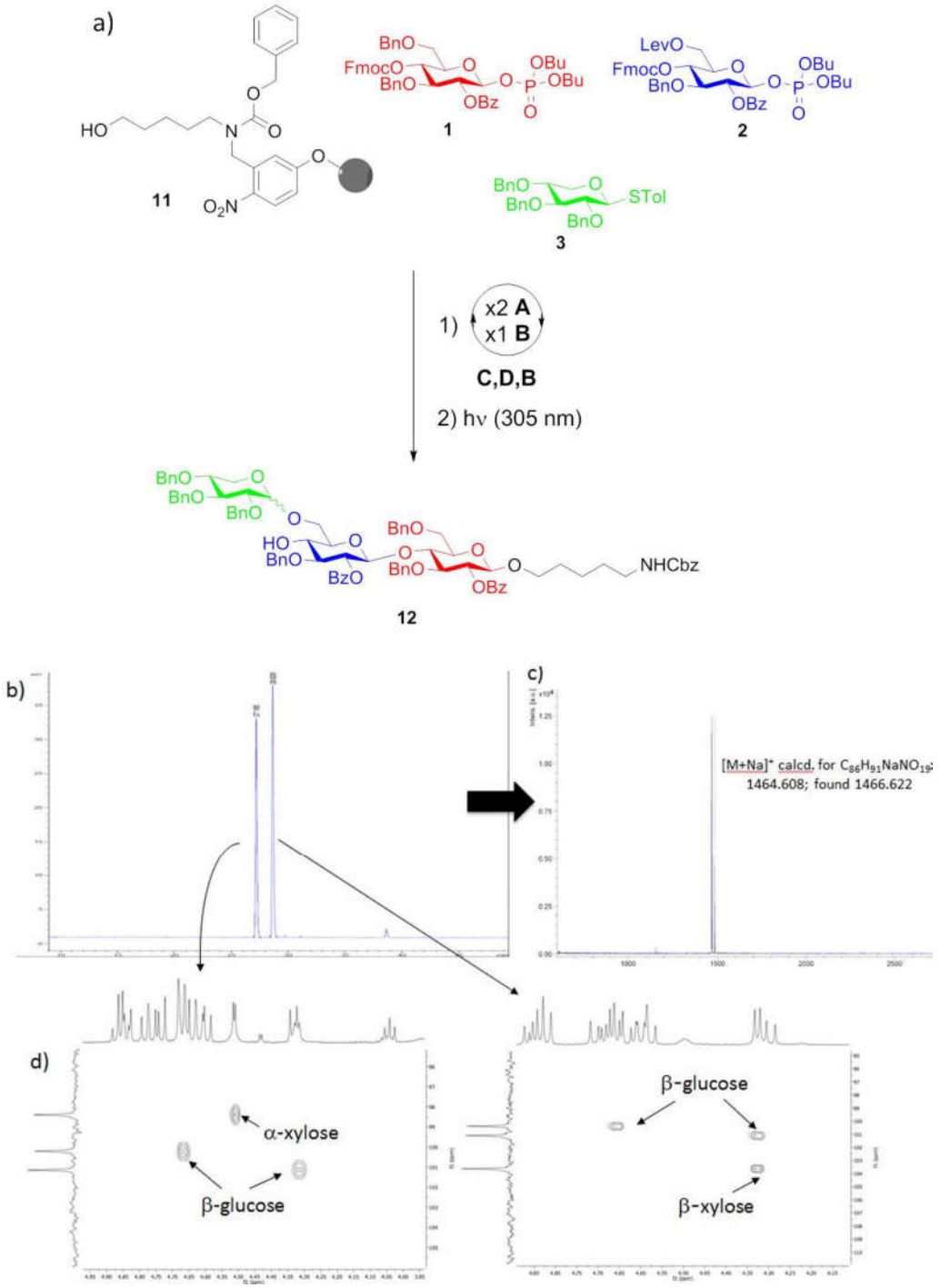

Scheme 11: a) Automated glycan assembly of trisaccharide **12**. Reagents and conditions: 2 x 3.7 equiv of BB **1** or **2**, TMSOTf, CH_2Cl_2, -30 °C (5 min) or -35 °C (5 min) → -15 °C (30 min) (module A); 3 cycles of 20% Et_3N in DMF, 25 °C (5 min) (Module B); N_2H_4·OAc (155 mM) in pyridine/AcOH/H_2O 4:1:0.25, 25 °C (30 min) (Module C);2 x 3.7 equiv BB 3 NIS/TfOH, CH_2Cl_2/dioxane 2:1, -55 °C (5 min) → -35 °C (40 min) (Module D); b) HPLC-chromatogram of the crude product; c) MALDI-TOF analysis; d) HSQC of the anomeric region of the two stereoisomers after separation of the diastereomers by preparative HPLC.

in the formation of a mixture of α/β-isomers with a relative ratio of 1:1 (Scheme 11b). The two stereoisomers were unambiguously assigned by matrix-assisted laser desorption/ionization-time of flight (MALDI-TOF) mass spectrometry and heteronuclear single quantum coherence NMR spectroscopy (HSQC) (Scheme 11c/d). Since less of the desired α-isomer was obtained by this method than in similar solution-phase reactions,[134] and since multiple α-xylosides have to be installed in the synthesis of larger XG oligosaccharides, BB **3** was deemed unsatisfactory for our purposes.

2.2.2 Automated Glycan Assembly of Xyloglucan Oligosaccharides using Disaccharide Building Blocks

Due to the lack of stereoselectivity provided by BB **3**, a different approach was necessary. A disaccharide BB containing a preinstalled α-xylosidic linkage

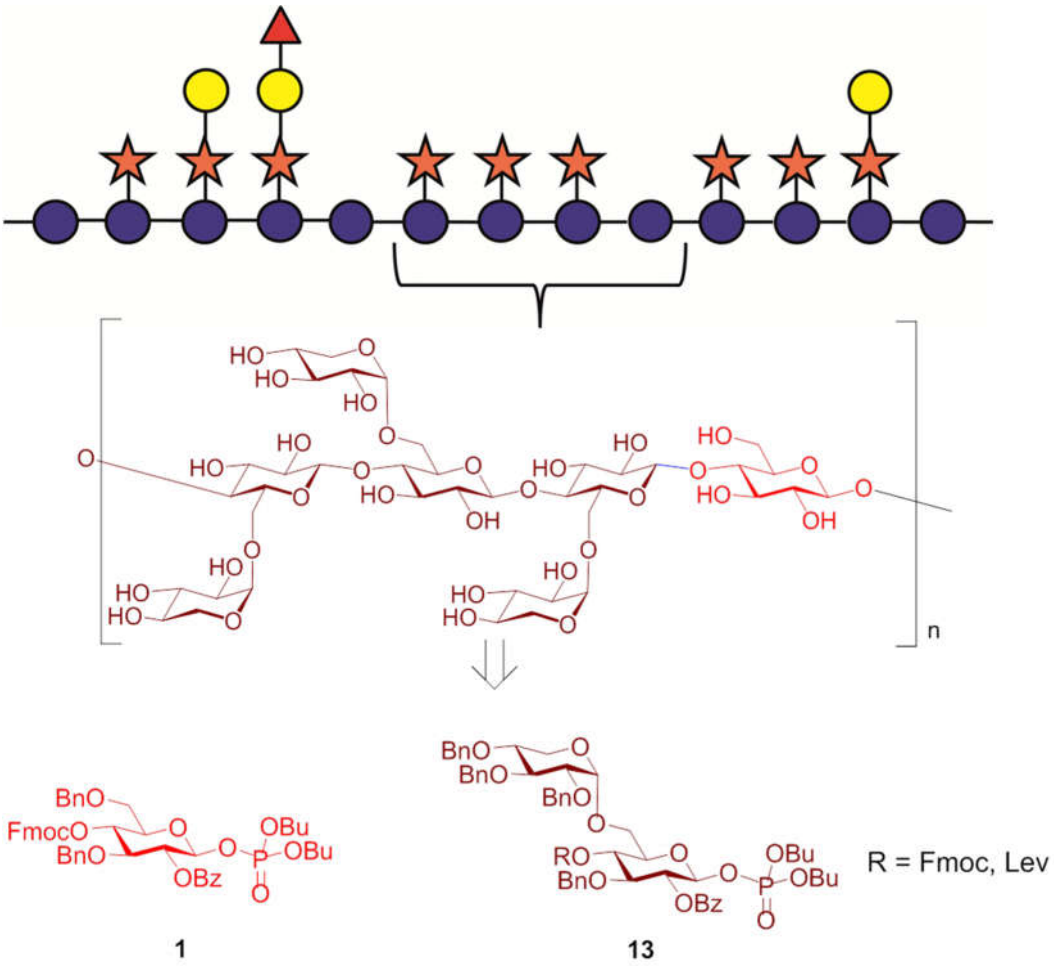

Figure 12: Retrosynthetic approach for the generation of a XG oligosaccharide library using a disaccharide BB.

seemed to be a suitable option since it would avoid the problem of forming this challenging bond in automation. Fortunately, the synthesis of disaccharide BB **13** (Figure 12) does not require more steps than the synthesis of BB **2** (Scheme 12). Key to the synthesis of disaccharide BB **13** was the selective xylosylation of diol **8**. Since both glucose **8** and xylose **3** were thioglycosides, there was the need to exchange the leaving group at the xylose for selective activation first. To prepare glycosyl imidate **15**, **3** was hydrolized with NIS in presence of water, and then the

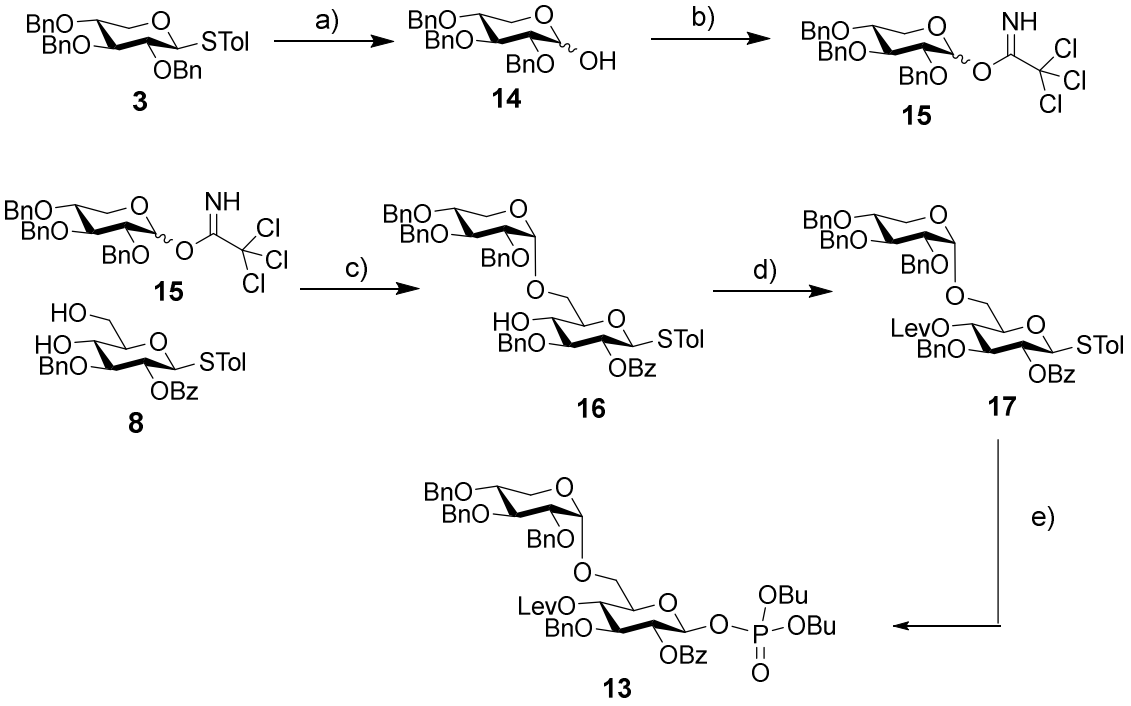

Scheme 12: Synthesis of disaccharide BB **13**. Reagents and conditions: a) NIS, acetone/H_2O 9:1, 81%; b) CCl_3CN, DBU, CH_2Cl_2, 96%; c) TMSOTf, CH_2Cl_2, -78 °C → -10 °C, 39%; d) LevOH, DIC, DMAP, CH_2Cl_2, 84%; e) $HOP(O)(OBu)_2$, NIS, TMSOH, CH_2Cl_2, 0 °C, 57%.

free hydroxyl was reacted with trichloroacetonitrile using 1,8-diazabicyclo[5.4.0]undec-7-ene (DBU) as a base. Subsequently, the primary alcohol of **8** was regioselectively glycosylated with the xylopyranose imidate **15** to provide disaccharide **16** as the major product. The transformation proceeded in rather low yield due to the formation of the β–isomer and the bis-glycosylated compound as side products.[134] Next, the C4-hydroxyl of glucose was protected as the Lev-ester (**17**) and thioglycoside **17** was converted subsequently into corresponding phosphate **13**. Installation of an Fmoc-group at position C4 of **16** failed likely due to steric hinderance.

With the required BBs in hand, three cellulose fragments (**19**, **20** and **21**) were prepared first. Coupling reactions with only one cycle of 3.7 equivalents of BB **1** were sufficient to ensure complete conversion in the glycosylation reactions. For the synthesis of XG oligosaccharides, disaccharide BB **13** was employed. Disaccharides have been successfully used in automated glycan assembly previously, and the iterative addition of BBs **1** and **13** to the linker-functionalized

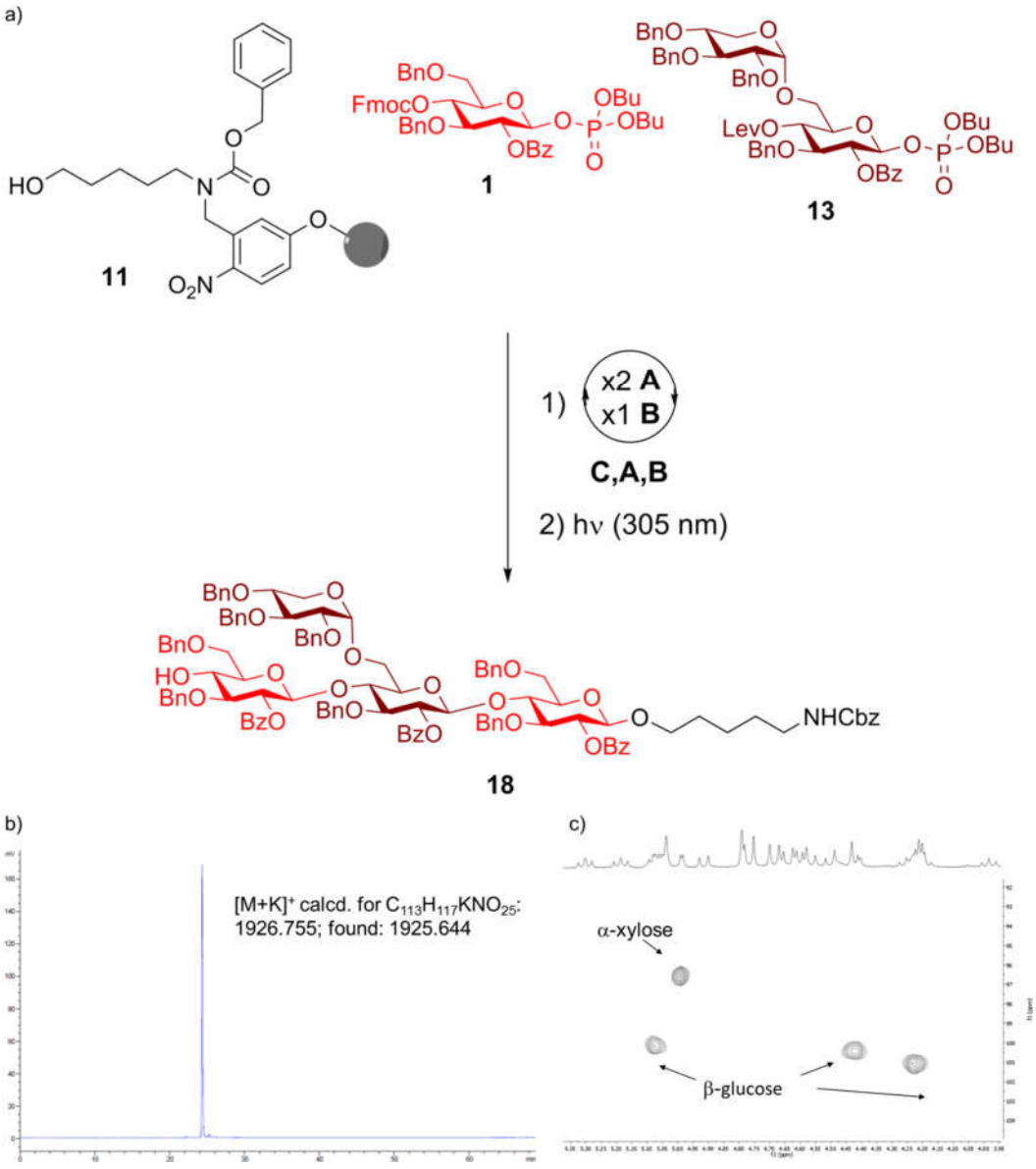

Scheme 13: a) Automated glycan assembly of tetrasaccharide **18**. Reagents and conditions: 2 x 3.7 equiv BB **1** or BB **13**, TMSOTf, CH_2Cl_2, -30 °C (5 min) or -35 °C (5 min) → -15 °C (30 min or 35 min) (Module A); 3 cycles of 20% Et_3N in DMF, 25 °C (5 min) (Module B); N_2H_4·OAc (155 mM) in pyridine/AcOH/H_2O 4:1:0.25, 25 °C (30 min) (Module C); b) HPLC-chromatogram of the crude product; d) HSQC of the anomeric region.

resin **11** provided successfully the protected tetrasaccharide **18** after cleavage of the oligosaccharide from the solid support (Scheme 13). Using this strategy the desired tetrasaccharide was obtained as a single product as observed in the crude HPLC chromatogram (Scheme 13b). The stereochemistry at the four anomeric carbon atoms was assigned by 2D-NMR spectroscopy. Once BB **13** proved to be effective for our purposes, various xyloglucan fragments were produced using the automated oligosaccharide synthesizer (Scheme 14). After cleavage from the solid support, the protected compounds were deprotected via methanolysis and hydrogenolysis. The fully deprotected compounds **22-28** were isolated in overall yields of 9-42%. Oligosaccharides containing two α-xyloside substituents were formed with reduced efficiency and the desired products were accompanied by deletion sequences missing one of the disaccharide units. Octasaccharide **29**, containing three disaccharide units, was assembled in only 2% overall yield even when using three cycles instead of two cycles of 3.7 equivalents BB **13** for the two key glycosylations. Due to the low yield likely caused by steric hindrance, the assembly of chains containing more than three disaccharide units was not practical.

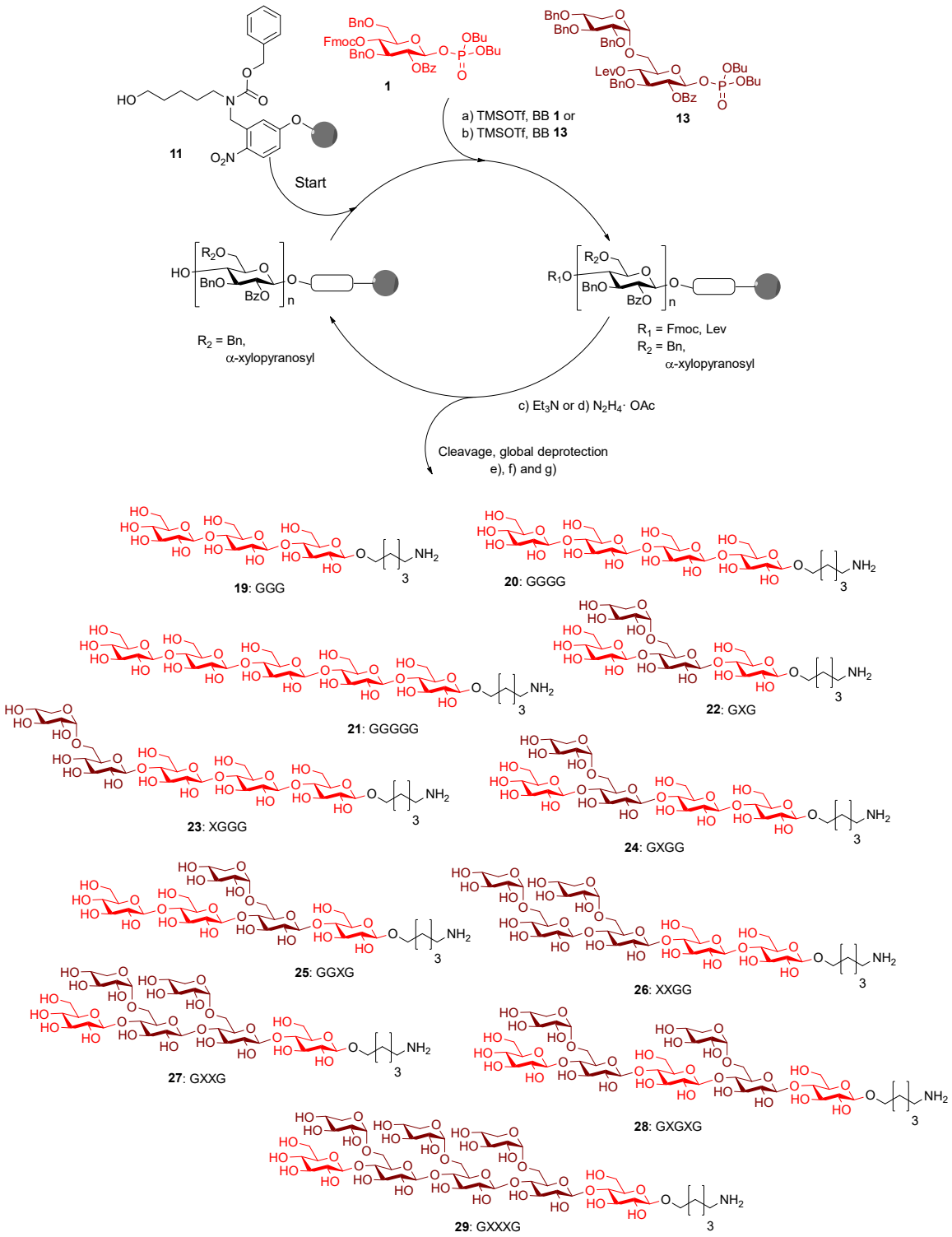

Scheme 14: Automated glycan assembly of a collection of XG oligosaccharides. Reagents and conditions: a) 1 or 2 x 3.7 equiv BB **1**, TMSOTf, CH_2Cl_2, -30 °C (5 min) → -15 °C (30 min) (Module A); b) 2 or 3 x 3.7 equiv BB **13**, TMSOTf, CH_2Cl_2, -35 °C (5 min) → -15 °C (35 min) (Module A); c) 3 cycles of 20% NEt_3 in DMF, 25 °C (5 min) (Module B); d) N_2H_4·OAc (155 mM) in pyridine/AcOH/H_2O 4:1:0.25, 25 °C (30 min) (Module C); e) CH_2Cl_2, hν (305 nm); f) NaOMe, THF/MeOH, 12 h; g) H_2, Pd/C, EtOAc/MeOH/H_2O/HOAc, 12 h. **19**: 28%; **20**: 14%; **21**: 23%; **22**: 15%; **23**: 10%; **24**: 36%; **25**: 42% **26**: 9%; **27**: 16%; **28**: 10%; **29**: 2%; (yields are based on resin loading). The letter code below the structures refers to a common nomenclature of XG oligosaccharides.[142]

2.2.3 Automated Glycan Assembly of Cellulose Fragments with Free Reducing Ends Using a Traceless Linker

The good reactivity of BB **1** in the synthesis of cellulose oligosaccharides encouraged us to use this model synthesis for testing a recently developed photo-labile traceless linker.[143] Linker **30** is the first photo-labile traceless linker available for automated glycan synthesis and was designed in analogy to linker **11**[74]. Instead of an alkyl chain, it contains a benzyl moiety in the spacer which should be removable by hydrogenolysis[144] (Figure 13).

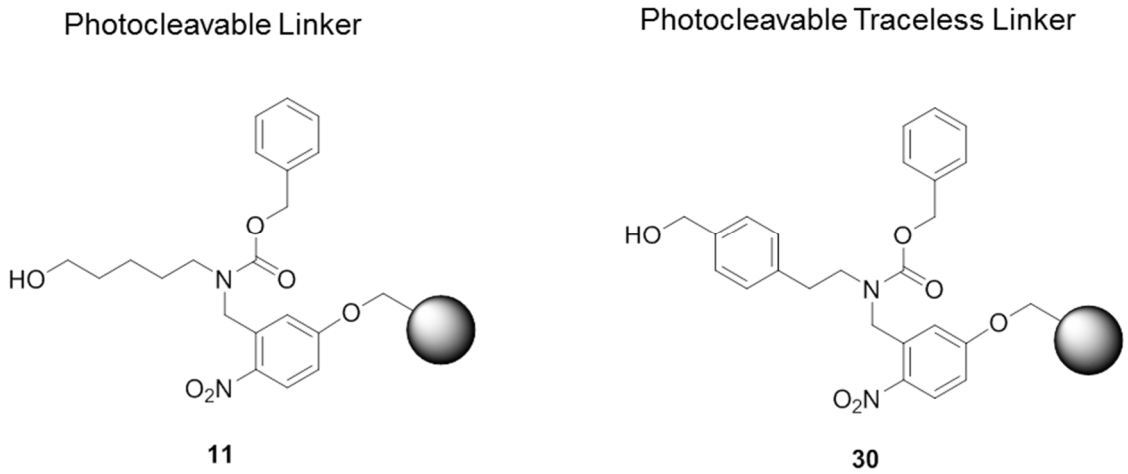

Figure 13: Photo-labile linkers for the synthesis of aminopentyl-functionalized and free-reducing end oligosaccharides respectively.

Initially, the efficiency of the glycan assembly and photocleavage using linkers **11** and **30** was compared. With this aim we decided to synthesize a cellulose tetrasaccharide using the same reaction cycles as for compound **20**. The synthesis of **31** included four iterative cycles of glycosylation and Fmoc deprotection steps employing monosaccharide building block **1**, followed by photolytic cleavage of the linker from the solid support prior to a final HPLC purification. Target molecule **31** was isolated in 67% yield and thus virtually with the same yield as aminopentyl-substituted cellulose derivative **32** that was obtained using linker **11**. Notably, the presence of an additional benzene moiety in the linker did not affect the efficiency of the glycosylation and deprotection steps in the automated assembly as well as the subsequent photolytical cleavage (Scheme 15). Bz and Bn PGs were deprotected using NaOMe and then Pd/C

and H_2 to give the fully deprotected cellulose fragment. During the removal of solvents we observed the formation of a hemiaminal ether[145] resulting from the

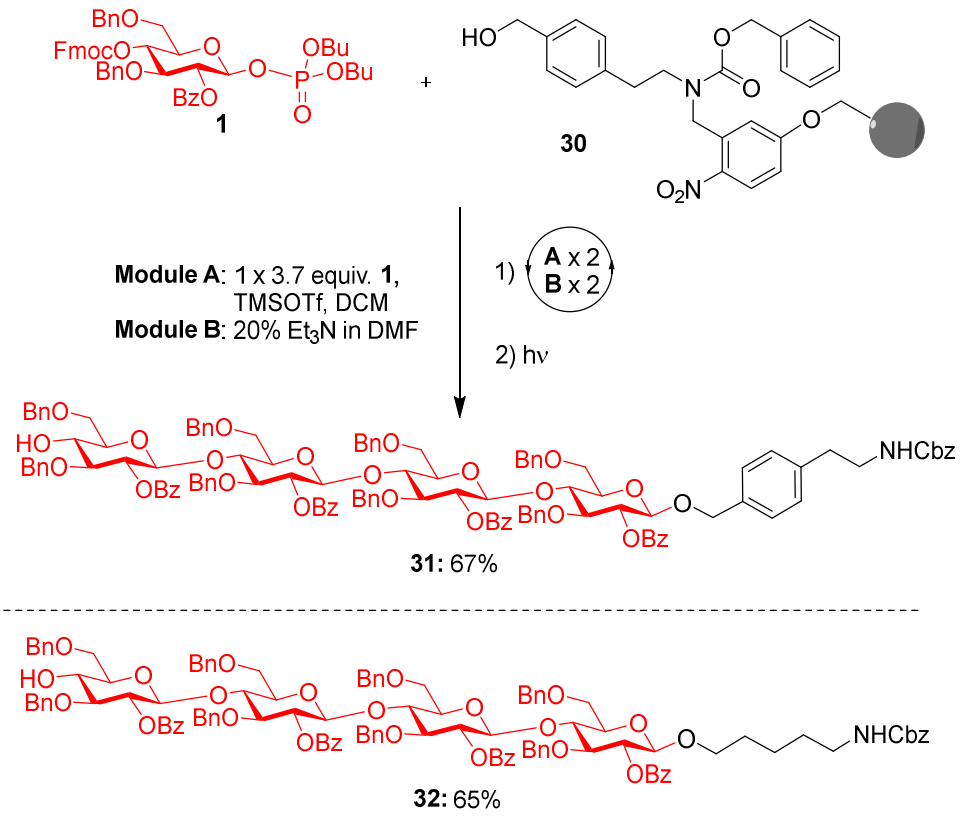

Scheme 15: Automated glycan assembly of tetrasaccharide **31**. Reagents and conditions: 1 x 3.7 equiv BB **1**, TMSOTf, CH_2Cl_2, -30 °C (5 min) → -15 °C (30 min) (Module A); 3 cycles of 20% Et_3N in DMF, 25 °C (5 min) (Module B).

reaction of the amine of the cleaved linker with the free reducing end of the oligosaccharide product. Subsequent acidic hydrolysis converted the side-product to the desired tetrasaccharide **33** that was obtained as a α/β mixture (Scheme 16). Following the same strategy, we additionally synthesized cellobiose fragment **34**.

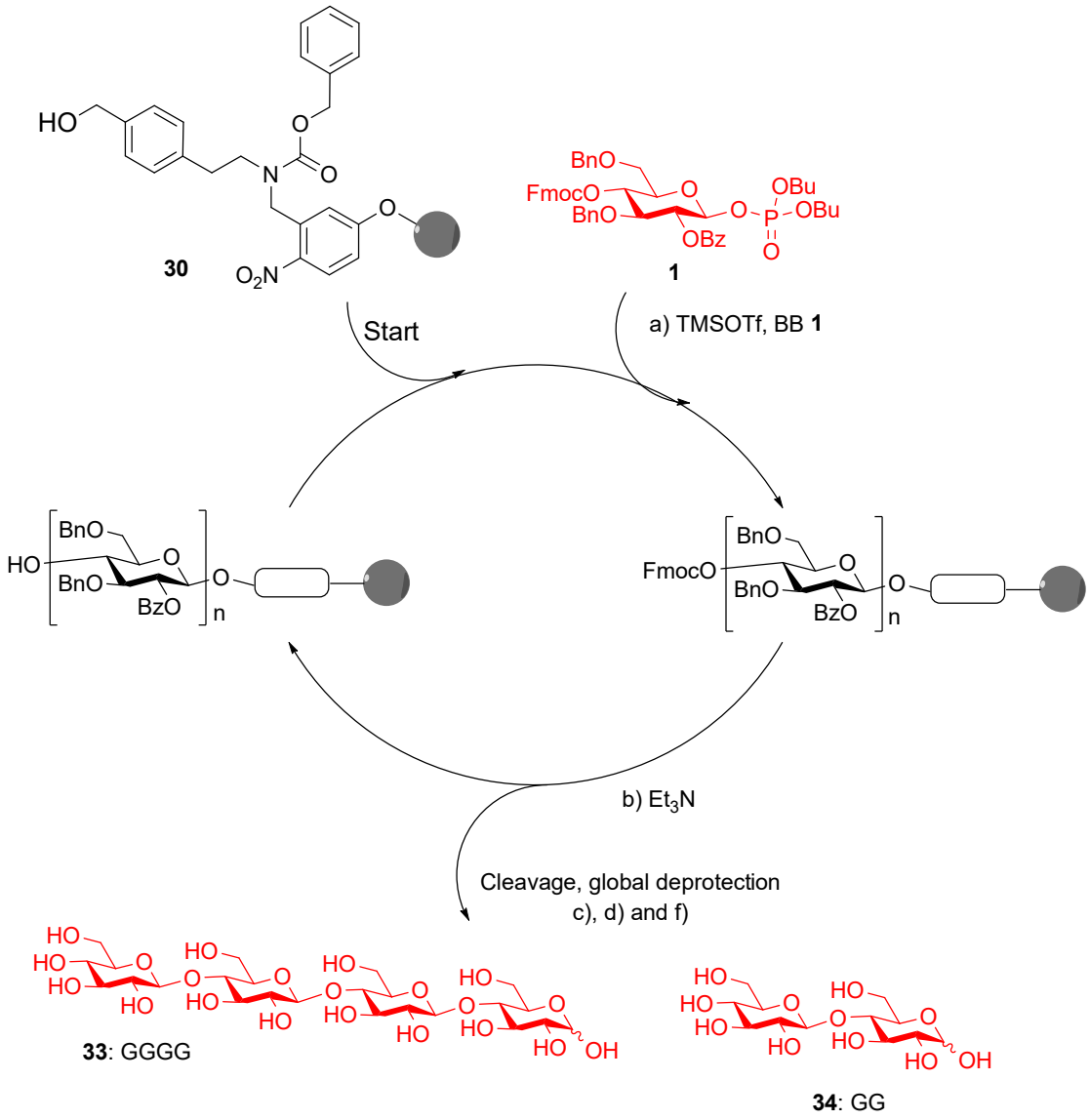

Scheme 16: Automated glycan assembly of free reducing end cellulose oligosaccharides. Reagents and conditions: a) 4 or 3.7 equiv BB **1**, TMSOTf, CH_2Cl_2, -30 °C (5 min) → -15 °C (30 min) (Module A); b) 3 cycles of 20% NEt_3 in DMF, 25 °C (5 min) (Module B); c) CH_2Cl_2, hν (305 nm); d) NaOMe, THF/MeOH, 12 h; g) H_2, Pd/C, EtOAc/MeOH/H_2O/HOAc, 12 h. **33**: 17%; **34**: 14% (yields are based on resin loading).

2.2.4 Automated Glycan Assembly of Galactosylated Xyloglucan Oligosaccharides

All of the XG oligosaccharides described in the previous section were not galactosylated. This represents a limitation for mAb screenings since no mAbs against galactosylated XG epitopes can be identified. We selected BBs **1, 13, 35** and **36** for the automated glycan assembly of galactosylated XG oligosaccharides (Figure 14). While the selection of BBs **1** and **36** as typical monosaccharide BBs

was straightforward, we decided to introduce the galactose residues using the disaccharide BB **35a/b**. Similarly to **13**, disaccharide **35a/b** was equipped with a

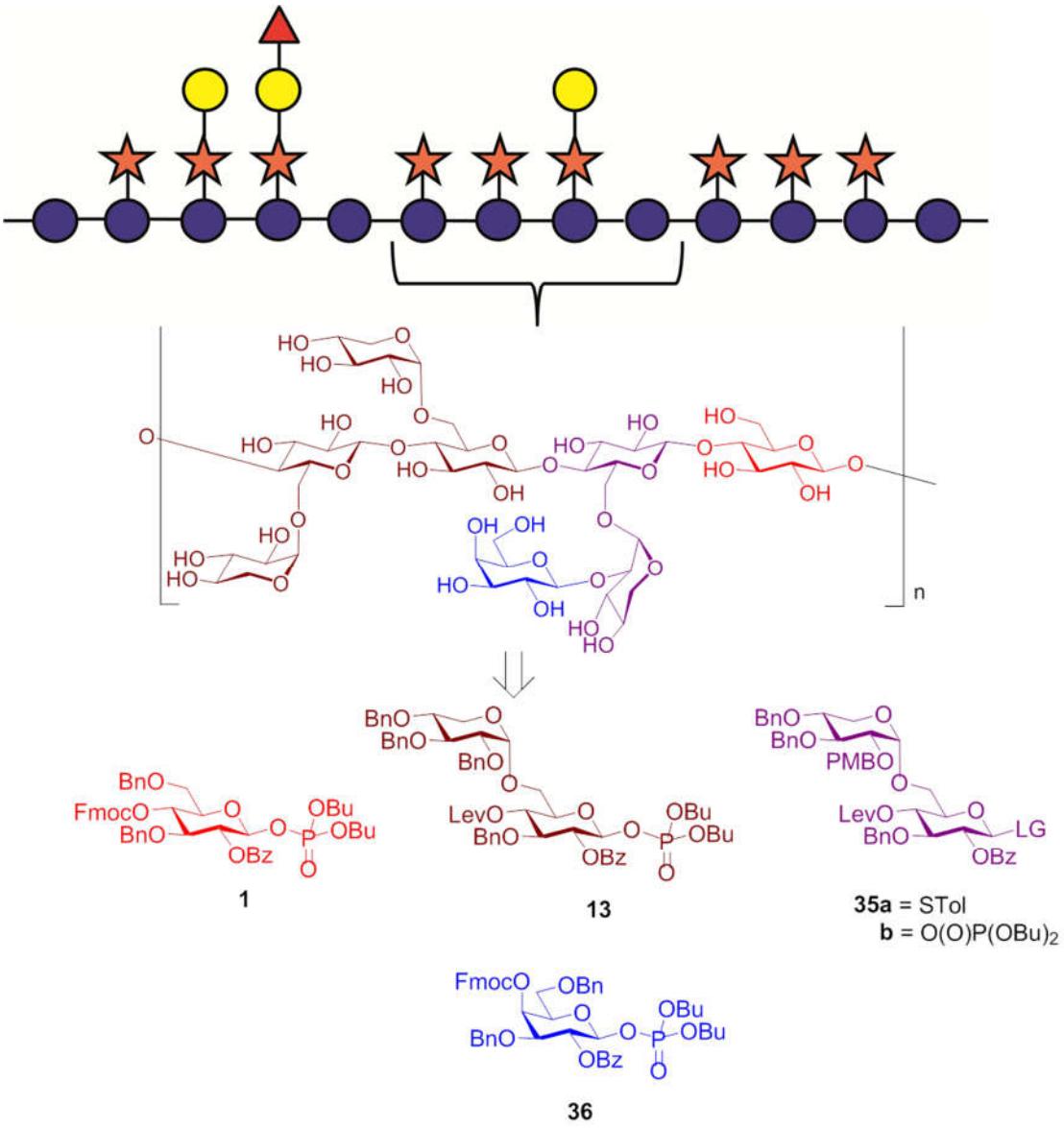

Figure 14: Retrosynthetic approach for the automated glycan assembly of galactosylated XG oligosaccharides.

temporary Lev PG for chain elongation and a Bz ester in the C2-position. An additional non-participating temporary PG was installed at the C2-position of the xylopyranose to enable the attachment of the galactose residue. Previously, Nap[110] was successfully used in the automated glycan assembly of xylan oligosaccharides. However, since we had observed occasional loss of primary Bn groups during the oxidative cleavage of NAP ethers, we here chose *p*-methoxybenzyl (PMB)[146] as a non-participating protecting group.[110] The synthesis

of BBs **35a** and **b** was accomplished in analogy to the synthesis of disaccharide BB **13** by glycosylation of diol **8** with xylose donor **43**. The synthesis of the xylose

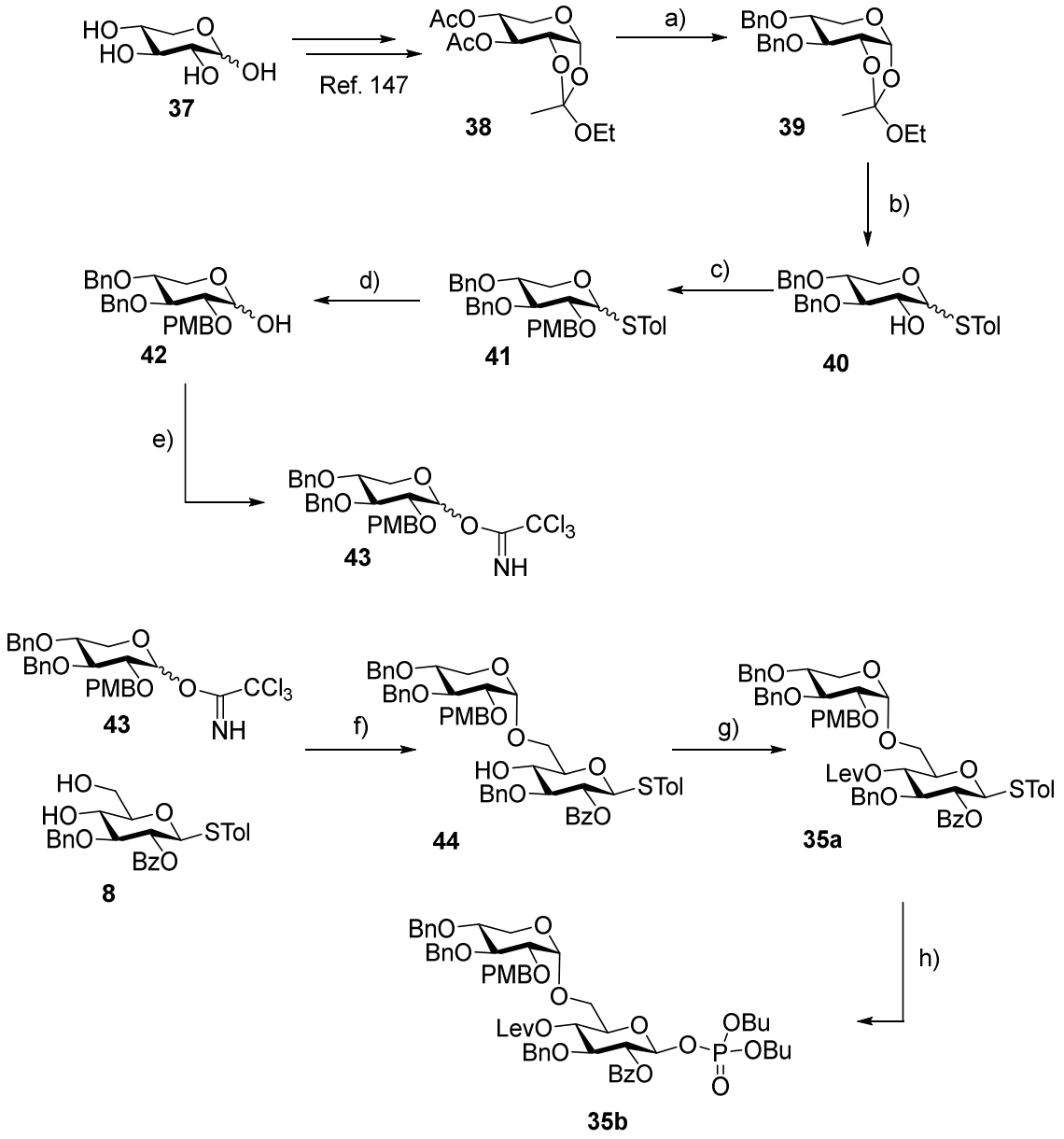

Scheme 17: Synthesis of disaccharide BBs **35a** and **35b**. Reagents and conditions: a) KOH, BnBr, toluene, reflux, 78%; b) i. $BF_3{\cdot}OEt_2$, HSTol, DCM, 0 °C; ii. NaOMe, MeOH, 74% (2 steps); c) PMBCl, NaH, DMF, 0 °C to rt, 98%; d) NIS, acetone/H_2O 9:1, 91%; e) CCl_3CN, DBU, CH_2Cl_2, 95%.f) TMSOTf, CH_2Cl_2/Et_2O 1:5, -15 °C, 50%; g) LevOH, DIC, DMAP, CH_2Cl_2, 93%; h) $HOP(O)(OBu)_2$, NIS, TMSOH, CH_2Cl_2, 0 °C, 58%.

donor started with converting xylose **37** into orthoester **38** in three steps.[147] The acetyl groups of **38** were replaced by benzyl groups by refluxing **38** in toluene with KOH and BnBr. Orthoester **39** was then opened with *p*-thiocresol and BF_3 as reported by Chayajarus *et al.*[148] Unlike previously reported, partial deacetylation

of position two was observed giving **40** together with the acetylated compound in a 1:1 ratio. Since in the next step the acetyl groups had to be removed to give compound **40**, the procedure was modified to avoid isolation of the intermediate and the crude mixture of acetylated and deacetylated compounds was directly subjected to methanolysis to yield exclusively **40**. Subsequently, the free hydroxyl was protected with PMBCl, the thioglycoside was hydrolyzed, and the xylosyl imidate **43** was formed by reaction of the anomeric hydroxyl group with trichloroacetonitrile. TMSOTf catalyzed glycosylation of the glucose diol **8** with xylose donor **43** gave **44** in 50% yield with an α/β ratio of 2:1. Next, the hydroxyl at the C4-position was protected as Lev-ester followed by the replacement of the thioether leaving group in **35a** by a phosphate to afford **35b**.

To see if BB **35a** with a thioether leaving group was sufficiently reactive in the glycosylation reactions of the automated glycan assembly process, we decided to compare its efficiency with the glycosyl phosphate **35b**. The efficiencies of the two BBs were compared (Scheme 18) using trisaccharide **46** as the target molecule. At the same time, we tested if smooth PMB-deprotection can be achieved on the solid-phase. TMSOTf-promoted glycosylation of the photo-labile linker-functionalized resin with BB **1** followed by Fmoc deprotection gave acceptor **45** which was further coupled with disaccharide BBs **35a** or **35b**. **35a** was coupled using NIS/TfOH activation while **35b** was coupled using TMSOTf. For both BBs one cycle of 3.7 equiv was used. The HPLC chromatograms of the reaction products clearly showed a superior performance of the phosphate **35b** (Scheme 18b). Using **35b**, we achieved complete conversion while, when using **35a**, a lot of monosaccharide was still present. Regarding the PMB deprotection: while six cycles of a 2,3-dichloro-5,6-dicyano-1,4-benzoquinone (DDQ) treatment are normally required to remove NAP groups on the solid phase,[110] for PMB, since it is more prone to oxidation, the number of cycles could be decreased. Initially, in the synthesis of **46** using BB **35a**, the DDQ cycles were decreased to three. However, we ultimately found that one to two cycles of DDQ-treatment are sufficient for quantitative PMB removal.

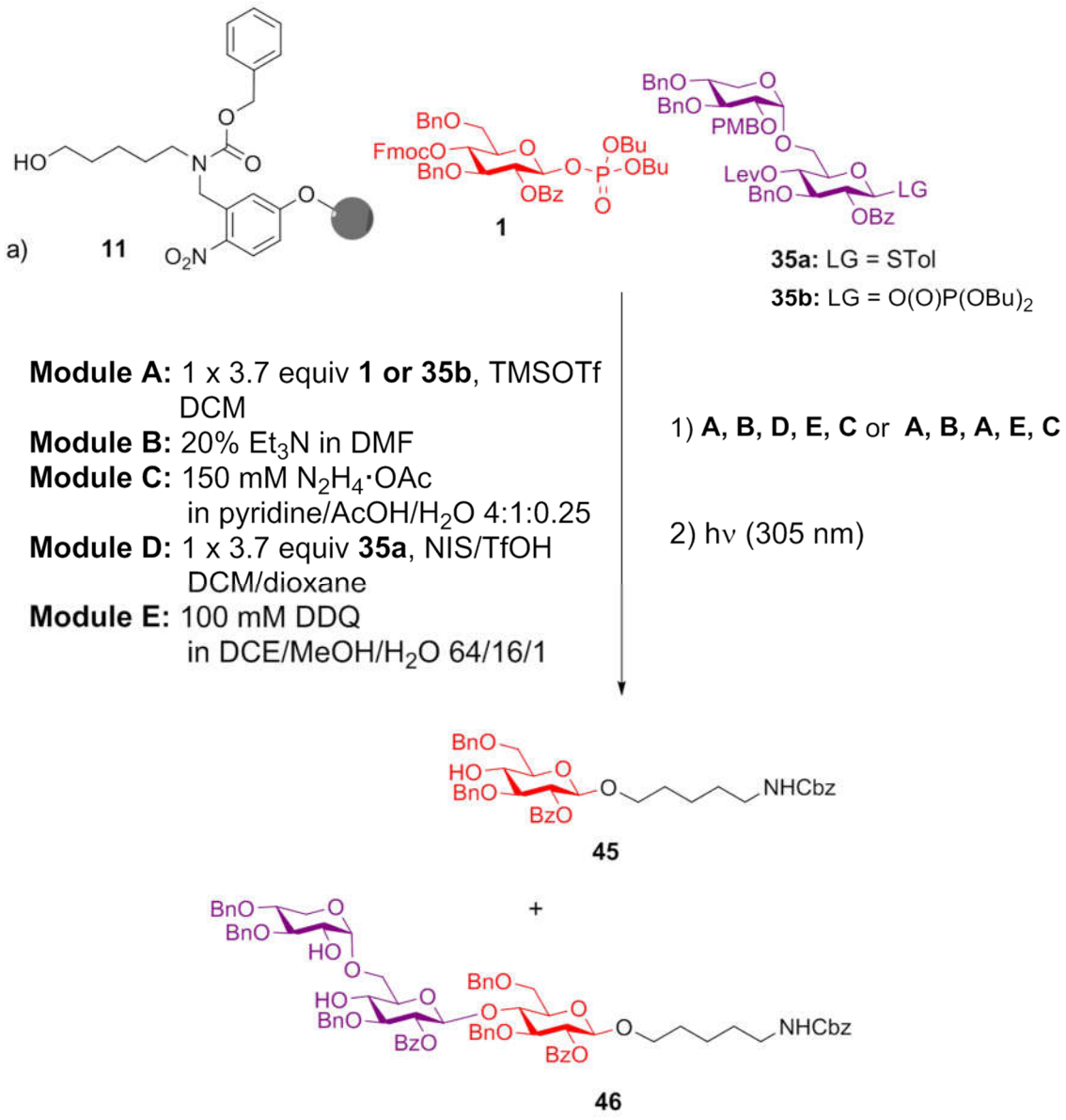

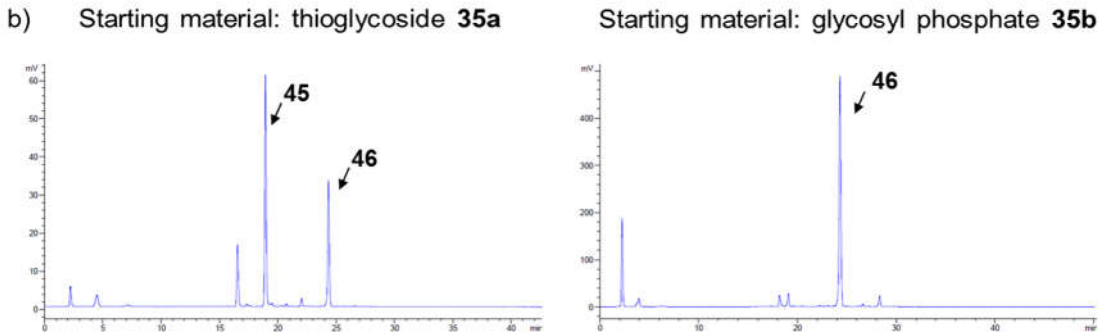

Scheme 18: a) Comparison between BBs **35a** and **35b** in the automated glycan assembly of trisaccharide **46**. Reagents and conditions: 1 × 3.7 equiv BB **1**, TMSOTf, CH_2Cl_2, −30 °C (5 min) → −15 °C (30 min) or 1 × 3.7 equiv BB **35b**, TMSOTf, CH_2Cl_2, −35 °C (5 min) → −10 °C (35 min) (Module A); 3 cycles of 20% NEt_3 in DMF, 25 °C (5 min) (Moduel B); N_2H_4·OAc (155 mM) in pyridine/AcOH/H_2O 4:1:0.25, 25 °C (30 min) (Module C); 1 × 3.7 equiv BB **35a**, NIS/TfOH, dioxane/CH_2Cl_2, −35 °C (5 min) → −20 °C (45 min) (Module D); 3 or 2 cycles DDQ (0.1 M) in DCE/MeOH/H_2O 64:16:1, 40 °C (20 min) (Module E); b) HPLC traces of the crude products after automated glycan assembly using either thioglycoside BB **35a** or glycosyl phosphate BB **35b**.

We decided to proceed with the synthesis of galactosylated oligosaccharides using BB **35b**. For the assembly of XG oligosaccharide **47**, two different reaction sequences are conceivable (Scheme 19): (i) The PMB group is cleaved immediately after glycosylation with disaccharide BB **35b** and the resulting free hydroxyl on the xylose residue is galactosylated with BB **36**. The Lev group is subsequently cleaved and a final glycosylation is performed with BB **1**. (ii) The galactose is attached to the fully assembled oligosaccharide backbone after removal of the PMB group. Initially, we tested the first approach, but we did

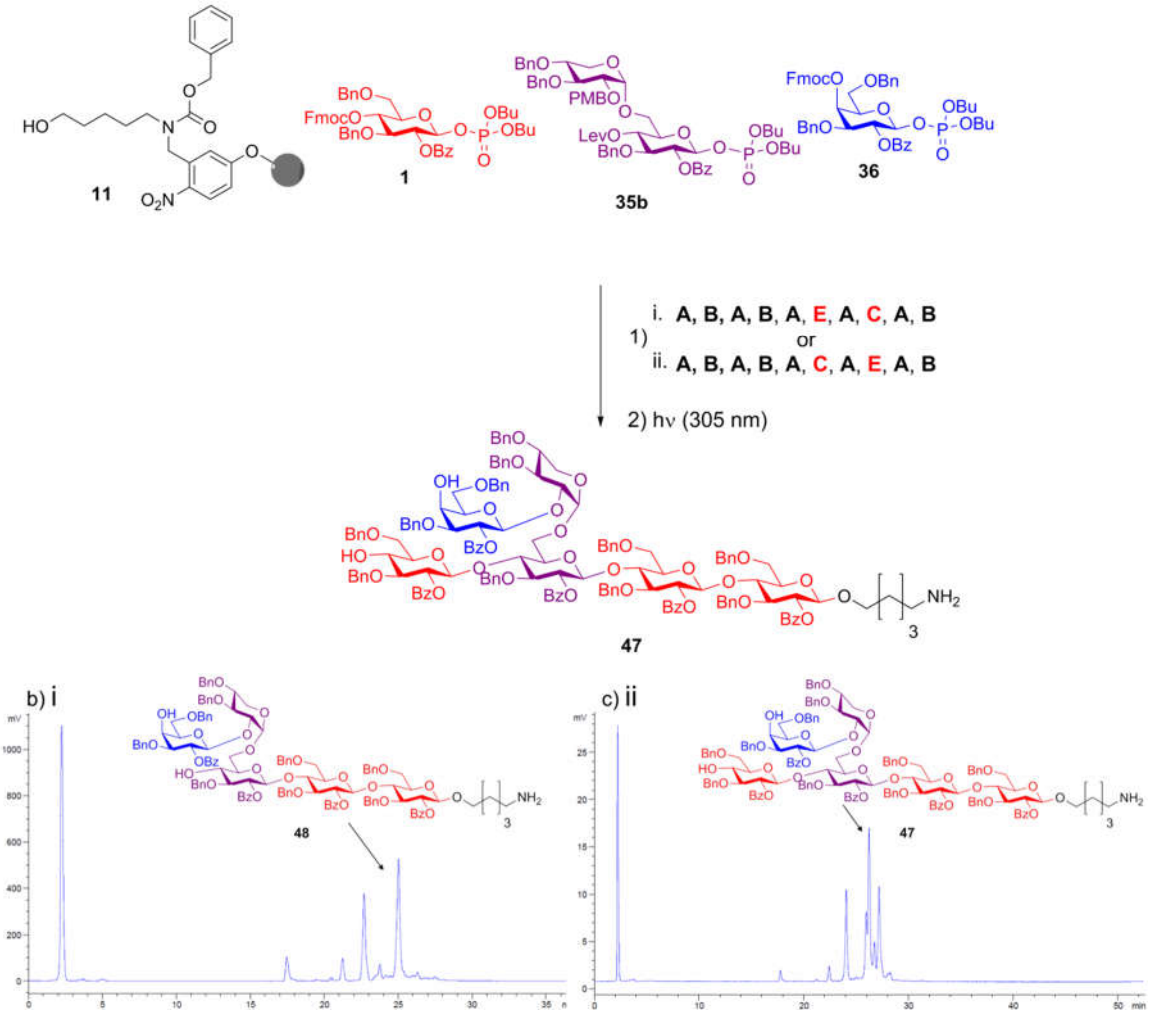

Scheme 19: a) Automated glycan assembly of heptasaccharide **47**. Reagents and conditions: 1 or 2 × 3.7 equiv BB **1**, TMSOTf, CH_2Cl_2, −30 °C (5 min) → −15 °C (30 min) or 2 × 3.7 equiv BB **35b**, TMSOTf, CH_2Cl_2, −35 °C (5 min) → −10 °C (35 min) or 2 × 3.7 equiv BB **36**, TMSOTf, CH_2Cl_2, −35 °C (5 min) → −20 °C (40 min) (Module A); 3 cycles of 20% Et_3N in DMF, 25°C (5 min) (Module B); N_2H_4·OAc (155 mM) in pyridine/AcOH/H_2O 4:1:0.25, 25°C (30 min) (Module C); 1 cycle DDQ (0.1 M) in DCE/MeOH/H_2O 64:16:1, 40 °C (20 min) (Module E); b) HPLC-chromatogram of the crude products following procedure i or c) ii.

not observe any conversion to the desired compound. Instead, we observed the formation of deletion sequences. After HPLC separation and MALDI analysis it was found that the major peak belongs to a pentasaccharide where, most likely, the terminal glucose was missing (**48**) (Scheme 19b). This might have resulted from steric hindrance by the galactose, preventing further extension of the backbone. Fortunately, when the full oligosaccharide backbone was assembled first, the desired protected XG oligosaccharide **47** was obtained. However, during

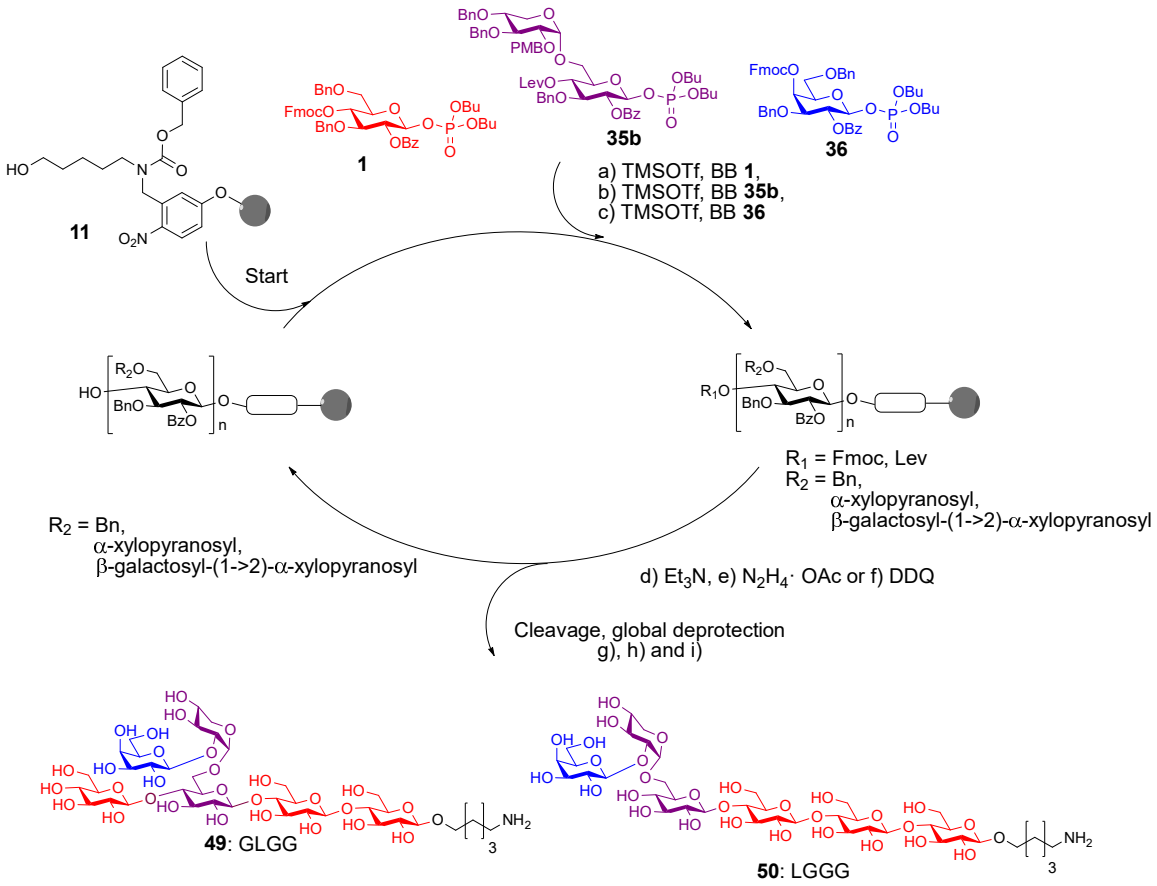

Scheme 20: Automated glycan assembly of galactosylated XG oligosaccharides. Reagents and conditions: (a) 1 or 2 × 3.7 equiv BB **1**, TMSOTf, CH_2Cl_2, −30 °C (5 min) → −15 °C (30 min); (b) 2 × 3.7 equiv BB **35b**, TMSOTf, CH_2Cl_2, −35 °C (5 min) → −10 °C (35 min); (c) 2 × 3.7 equiv BB **36**, TMSOTf, CH_2Cl_2, −35 °C (5 min) → −20 °C (40 min) (Module A); (d) 3 cycles of 20% NEt_3 in DMF, 25 °C (5 min) (Module B); (e) N_2H_4·OAc (155 mM) in pyridine/AcOH/H_2O 4:1:0.25, 25 °C (30 min) (Module C); f) 1 cycle DDQ (0.1 M) in DCE/MeOH/H_2O 64:16:1, 40 °C (20 min) (Module E); (g) CH_2Cl_2, *hv* (305 nm); (h) NaOMe, THF/MeOH, 12 h; (i) H_2, Pd/C, EtOAc/MeOH/H_2O/HOAc, 12 h. **49**: 8%; **50**: 13% (yields are based on resin loading).

the glycosylation reaction at -10°C with BB **35b**, we observed small amounts of side products that resulted from the loss of the PMB group under the acidic glycosylation conditions followed by glycosylation of the free hydroxyl with

additional equivalents of disaccharide **35b**. After global deprotection, XG oligosaccharide **49** was obtained in satisfactory yield. Following this procedure we were able to obtain an additional XG oligosaccharide **50** as well. We finally tested a lower temperature for the glycosylation with BB **35b** which indicated that at a glycosylation temperature of -15 °C no double addition with the disaccharide BB occurred.

2.2.5 Xyloglucan Oligosaccharides as Tools for Determining the Substrate Specificities of Xyloglucan Endotransglycosylases

XETs are important plant cell wall modifying enzymes which hydrolyze and recombine XGs during cell growth. To determine the substrate specificities of XETs, my colleague Dr. Ruprecht functionalized XG fragments **23**-**28** and the cellulose fragment **21** with the fluorescent dye fluorescein isothiocyanate (FITC). Small pieces of the plant Arabidopsis thaliana were incubated with the labelled oligosaccharide (Figure 15a) and then analyzed by fluorescence microscopy. If the respective oligosaccharide was incorporated into the plant cell wall, fluorescence was observed (Figure 15a). The results are summarized in Figure 15b. Compounds **24**, **25**, **26**, **27** and **28** with a xylose substituent attached to an internal glucose residue were all incorporated into the plant cell wall. In contrast, when the plant sections were incubated with the XG oligosaccharide **23** where only the terminal glucose is substituted or the cellulose fragment **21**, no fluorescence was observed. This means that the acceptor needs to be branched with at least one xylose in order to serve as an acceptor for XETs. Furthermore, this xylose unit must not be exclusively attached to the terminal non-reducing glucose. Our observation with the synthetic XG oligosaccharides thus confirmed the results of Saura-Varell *et al.*[125] who reported that xylose substitutions in positions +2 and +3 relative to the cleavage site make productive contacts with the enzymes, but lacked the required substrates to conclusively prove their hypothesis.

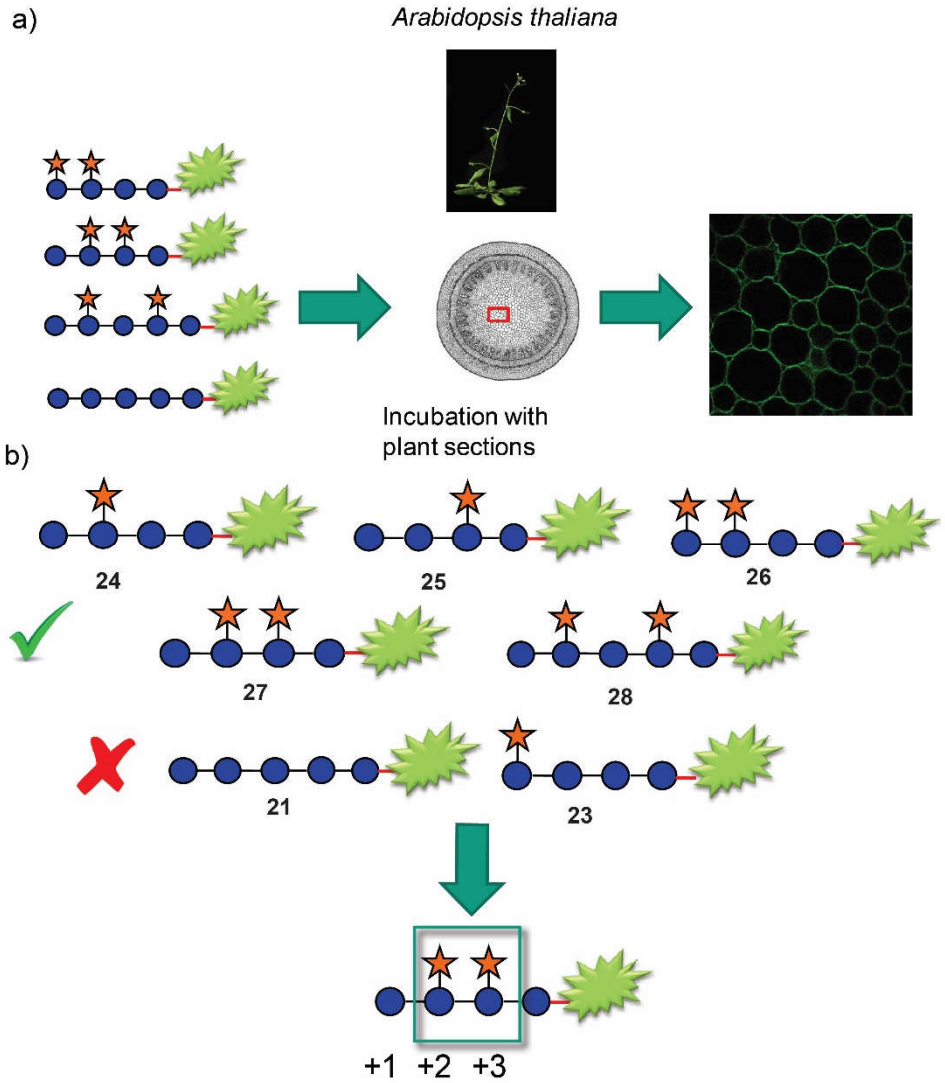

Figure 15: Experiments for determining the acceptor subsite specificity of XETs. a) Schematic representation of the experiment performed; b) Indication of which oligosaccharides did and did not get incorporated into the cell wall.

2.2.6 Characterization of Xyloglucan-directed Antibodies

mAbs are important molecular probes for *in situ* analysis of plant cell wall polysaccharides. My colleague Dr. Ruprecht printed the prepared XG oligosaccharides on microarray slides and probed the binding specificities of xyloglucan-directed mAbs. Using this approach, nine mAbs that bind to galactosylated xyloglucan oligosaccharides and five mAbs directed against unsubstituted xyloglucan (Figure 16) were identified. Strong binding of most of the antibodies recognizing galactosylated xyloglucan suggests that a single galactosyl residue β-1,2-linked to xylose is sufficient for these antibodies to bind. While the galactosyl moiety was essential for these mAbs to bind, we were able

to further characterize mAb CCRC-M87, which also displays weak binding to several XG oligosaccharides that lack galactose substitution (Figure 16).

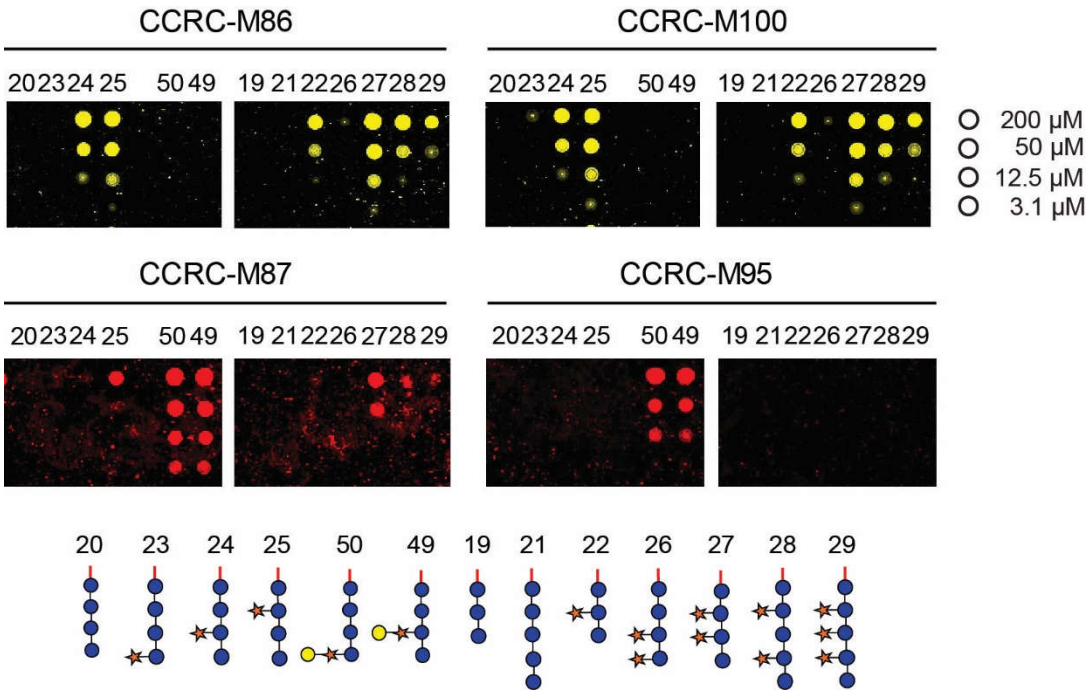

Figure 16: Plant cell wall-directed monoclonal antibodies (mAbs) bind to XG oligosaccharides. (A) Microarray scans showing binding of selected antibodies to xyloglucan oligosaccharides. Each compound was printed in four concentrations as indicated on the right. (B) Binding of mAbs specific to galactosylated xyloglucan.

2.3 Conclusions and Outlook

In conclusion, a library of eight non-galactosylated XG oligosaccharides, two galactosylated XG oligosaccharides, and three cellulose fragments were synthesized by automation glycan assembly. The first synthetic strategy relying on the use of solely monosaccharide BBs did not give satisfactory results due to low stereoselectivity in the xylosylation reactions. However, a disaccharide BB with a preinstalled α-linkage between the xylose and glucose residues enabled the synthesis of a XG oligosaccharide library. The addition of a galactose to the xylose was successfully achieved by using PMB for the first time as a temporary PG in automated glycan assembly. The synthetic XG oligosaccharides were successfully used as tools for the characterization of the XG-remodeling enzyme XET and mAbs directed against different types of XG.

Despite the fact that several antibodies against xyloglucan were characterized and the corresponding epitopes identified, many mAbs tested did not bind to any of these compounds. Probably, these antibodies require a more complex epitope for binding, including more galactose or fucose substitutions which are not included in the current xyloglucan oligosaccharide library. For the synthesis of more complex XG oligosaccharides the glycosylation conditions for disaccharide BB **35b** will need to be further optimized. This may allow the synthesis of larger oligosaccharides containing more xylose units as well as XG oligosaccharides carrying arabinose or fucose substituents. Another option to further diversify the XG oligosaccharides is enzymatic synthesis, using different glycosyltransferases such as xylosyl-, galactosyl- and fucosyltransferases.

2.4 Experimental Part

2.4.1 General information

The automated syntheses were performed on a self-built synthesizer developed in the Max Planck Institute of Colloids and Interfaces. The Resin loading was determined as described previously.[141] Solvents and reagents were used as supplied without any further purification. Anhydrous solvents were taken from a dry solvent system (JC-Meyer Solvent Systems). Column chromatography was carried out using Fluka Kieselgel 60 (230-400 mesh). NMR spectra were recorded on a Varian 400-MR (400 MHz), a Varian 600- (600 MHz), or a Bruker AVIII 700 (700 MHz) spectrometer using solutions of the respective compounds in $CDCl_3$ or D_2O. NMR chemical shifts (δ) are reported in ppm and coupling constants (*J*) in Hz. Spectra recorded in $CDCl_3$ used the solvent residual peak chemical shift as internal standard ($CDCl_3$: 7.26 ppm ^1H, 77.0 ppm ^{13}C). Spectra recorded in D_2O used the solvent residual peak chemical shift as internal standard in ^1H NMR (D_2O: 4.79 ppm ^1H) and acetic acid as internal standard in ^{13}C NMR (acetic acid in D_2O: 21.03 ppm ^{13}C). Yields of final deprotected oligosaccharides were determined after removal of residual acetic acid. Optical rotations were measured using a UniPol L1000 polarimeter (Schmidt&Haensch) with concentrations expressed as g/100 mL. IR spectra were recorded on a

Spectrum 100 FTIR spectrophotometer (Perkin-Elmer). High resolution mass spectra were obtained using a 6210 ESI-TOF mass spectrometer (Agilent) and a MALDI-TOF autoflex™ (Bruker). Analytical HPLC was performed on an Agilent 1200 series coupled to a quadrupole ESI LC/MS 6130 using a Luna 5u Silica 100A column (250 x 4.6 mm), a Phenomenex Luna C5 column (250 x 4.6 mm), a YMC-Diol-300 column (150 x 4.6 mm) or a Thermo Scientific Hypercarb column (150 x 4.6 mm). Preparative HPLC was performed on an Agilent 1200 series using a semi-preparative Luna 5u Silica 100A column, a semi-preparative Phenomenex Luna C5 column (250 x 10 mm), a preparative YMC-Diol-300 column (150 x 20 mm) or a semi-preparative Thermo Scientific Hypercarb column (150 x 10 mm).

2.4.2 Synthesizer Modules and Conditions

Synthesizer Modules and Conditions

The linker-functionalized resin **11** (16.9 µmol of hydroxyl groups) was placed in the reaction vessel of the automated oligosaccharide synthesizer and swollen for at least 30 min in DCM. Before every synthesis the resin was washed with DMF, THF, and DCM. Subsequently the glycosylation (Module **A** and **D**) and deprotection (Module **B** and **C**) steps were performed. Mixing of the components was accomplished by bubbling Argon through the reaction mixture.

Module A: Glycosylation with Glycosyl Phosphates

The resin (16.9 µmol of hydroxyl groups) was swollen in DCM (2 mL) and the temperature of the reaction vessel was adjusted to -30 °C. Prior to the glycosylation reaction the resin was washed with TMSOTf in DCM and then DCM only. For the glycosylation reaction the DCM was drained and a solution of phosphate BB (3.7 equiv in 1 mL DCM) was delivered to the reaction vessel. After the set temperature was reached, the reaction was started by the addition of TMSOTf in DCM (3.7 equiv in 1 mL DCM). The glycosylation was performed for 5 min at -30 °C or -35 °C and then at -10 °C, -15 °C or -20 °C for 30, 35 or 40 minutes. Subsequently the solution was drained and the resin was washed three times with DCM. The whole procedure was performed once, twice, or three times

depending on the conversion of the acceptor sites. Afterwards the resin was washed three times with DCM at 25 °C.

Module B: Fmoc Deprotection.

The resin was washed with DMF, swollen in 2 mL DMF, and the temperature of the reaction vessel was adjusted to 25 °C. Prior to the deprotection step, the DMF was drained and the resin was washed with DMF three times. For Fmoc deprotection, 2 mL of a solution of 20% Et_3N in DMF was delivered to the reaction vessel. After 5 min the solution was drained and the whole procedure was repeated another two times. After Fmoc deprotection was complete the resin was washed with DMF, THF, and DCM.

Module C: Lev Deprotection

Prior to the deprotection step, the resin was washed with DCM three times, swollen in 1.3 mL DCM, and the temperature of the reaction vessel was adjusted to 25 °C. For Lev deprotection, 0.8 mL of a solution of 150 mM N_2H_4·AcOH in Pyridine/AcOH/H_2O 4:1:0.25 was delivered to the reaction vessel. After 30 min, the solution was drained and the deprotection step was repeated two times. After Lev deprotection was complete the resin was washed with DCM, DMF, THF, and again DCM three times each.

Module D: Glycosylation with Thioglycosides

The resin (16.9 µmol of hydroxyl groups) was swollen in DCM (2 mL) and the temperature of the reaction vessel was adjusted to -30 °C. Prior to the glycosylation reaction the resin was washed with TMSOTf in DCM and DCM. For the glycosylation reaction, the DCM was drained and a solution of thioglycoside BB (3.7 equiv in 1 mL DCM) was delivered to the reaction vessel. After the set temperature was reached, the reaction was started by the addition of NIS (4.44 equiv) and TfOH (0.44 equiv) in DCM/dioxane (2:1). The glycosylation was performed for 5 min at -55 °C or -35 °C and then for 40 or 35 min at -30 °C or -10 °C. Subsequently the solution was drained and the resin was washed with DCM. The whole procedure was repeated once to ensure full conversion of all acceptor sites. Afterwards the resin was washed three times with DCM at 25 °C.

Module E: Nap Deprotection

The resin was washed with DCM three times and the temperature of the reaction vessel was adjusted to 40 °C. For Nap deprotection, the DCM was drained and 1.5 mL of a 0.1 M DDQ solution in DCE/MeOH/H_2O (64:16:1) was delivered to the reaction vessel. After 20 min the reaction solution was drained and the resin was washed with DMF, THF, and DCM.

Cleavage from the solid support

After assembly of the oligosaccharides, cleavage from the solid support was accomplished by modification of a previously published protocol,[149] using the Vapourtec E-Series UV-150 photoreactor Flow Chemistry System. The medium pressure metal halide lamp is filtered using the commercially available red filter. The resin, suspended in DCM, was loaded into a plastic syringe. The suspension was then pumped using a syringe pump (PHD2000, Harvard Aparatus) at 1 mL/min through a 10 mL reactor, constructed of 1/8 inch o.d. FEP tubing. The total volume within the photoreactor was 9 mL. The temperature of the photoreactor was maintained at 20 °C and the lamp power was 80%. The exiting flow was deposited in a 10 mL syringe containing a filter, with a collection flask beneath the syringe.

2.4.3 Synthesis of Building Blocks

4-Methylphenyl 2-*O*-benzoyl-3,6-*O*-dibenzyl-thio-β-D-glucopyranoside (6)

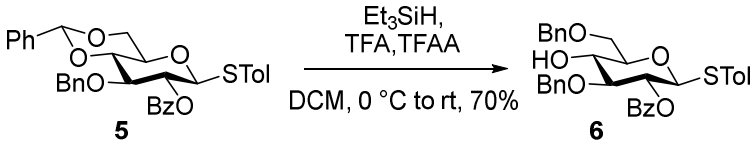

5 (15.0 g, 26.4 mmol) was dissolved in DCM (200 mL), and triethylsilane (25.3 mL, 158 mmol) was added. Then the reaction was cooled to 0 °C and TFAA (3.73 mL, 26.4 mmol) was slowly added. The reaction was stirred at 0 °C for 20 min, TFA (10.2 mL, 132 mmol) was added dropwise, and the reaction was gradually warmed to rt. After 2 h the reaction was quenched with sat. aq. $NaHCO_3$ solution (100 mL) and extracted with DCM (100 mL). The organic layer was dried over Na_2SO_4, concentrated, and purified by silica gel chromatography (Hex/EtOAc 4:1) to give compound **6** (10.5 g, 18.4 mmol, 70%) as a white solid.

^{1}H NMR (400 MHz, $CDCl_3$): δ = 8.07 (d, *J* = 7.8 Hz, 2H, Ar), 7.60 (t, *J* = 7.4 Hz, 1H, Ar), 7.51-7.44 (m, 2H, Ar), 7.40-7.29 (m, 7H, Ar), 7.17 (s, 5H, Ar), 7.02 (d, *J* = 7.7 Hz, 2H, Ar), 5.23 (t, *J* = 9.5 Hz, 1H), 4.80-4.49 (m, 5H), 3.83-3.73 (m, 3H), 3.68 (t, *J* = 8.9 Hz, 1H), 3.63-3.54 (m, 1H), 2.29 (s, 3H) ppm.

4-Methylphenyl 2-*O*-benzoyl-3,6-*O*-dibenzyl-4-*O*-fluorenylcarboxymethyl-thio-β-D-glucopyranoside (7)

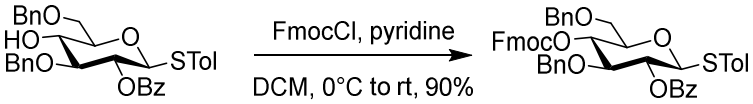

6 **7**

To a solution of **6** (2.30 g, 4.03 mmol) in DCM (30 mL) and pyridine (5 mL), FmocCl (1.34 g, 5.18 mmol) was added. After 5.5 h more pyridine (1 mL) and FmocCl (1.04 g, 4.02 mmol) were added. The reaction mixture was stirred for another 2 h and then diluted with DCM (100 mL) and washed with a 1 M HCl solution (100 mL) and brine (100 mL). The organic layer was dried over Na_2SO_4 and purified by silica gel chromatography (Tol/EtOAc 8:1) to give compound **7** (2.89 g, 3.64 mmol, 90%) as a white solid. $[\alpha]_D^{25}$ = +27.3 (*c* 1.0, $CHCl_3$). ^{1}H NMR (400 MHz, $CDCl_3$): δ = 8.09-8.03 (m, 2H, Ar), 7.76 (dd, *J* = 7.5, 3.9 Hz, 2H, Ar), 7.65-7.53 (m, 3H, Ar), 7.48 (t, *J* = 7.7 Hz, 2H, Ar), 7.44-7.27 (m, 12H, Ar), 7.11-6.99 (m, 6H, Ar), 5.30 (t, *J* = 9.5 Hz, 1H, H-2), 4.97 (t, *J* = 9.6 Hz, 1H, H-4), 4.77 (d, *J* = 10.0 Hz, 1H, H-1), 4.63-4.51 (m, 4H, C*H*$_2$Ph), 4.36 (d, *J* = 7.0 Hz, 2H, Fmoc), 4.15 (t, *J* = 6.6 Hz, 1H, Fmoc), 3.93 (t, *J* = 9.1 Hz, 1H, H-3), 3.78 (m, 1H, H-5), 3.71 (m, 2H, H-6), 2.31 (s, 3H, CH_3) ppm. ^{13}C NMR (100 MHz, $CDCl_3$): δ = 165.1, 154.3 (2C, C=O), 143.4, 143.2, 141.42, 141.39, 138.4, 138.1, 137.4, 133.4, 133.3, 130.0, 129.9, 129.8, 128.8, 128.6, 128.5, 128.3, 128.0, 127.7, 127.3, 125.2, 125.1, 120.2 (36C, Ar), 86.6 (C-1), 81.3 (C-3), 77.6 (C-5), 75.5 (C-4), 74.5 (*C*H_2Ph), 73.7 (*C*H_2Ph), 72.1 (C-2), 70.2 (Fmoc), 69.8 (C-6), 46.8 (Fmoc), 21.3 (CH_3) ppm. ESI-HRMS: m/z $[M+Na]^+$ calcd. for $C_{49}H_{44}NaO_8S$: 815.2655; found 815.2641. IR (neat) ν_{max} = 1753, 1318, 1248, 1069 cm^{-1}.

Dibutoxyphosphoryloxy 2-*O*-benzoyl-3,6-*O*-dibenzyl-4-*O*-fluorenylcarboxymethyl-β-D-glucopyranoside (1)

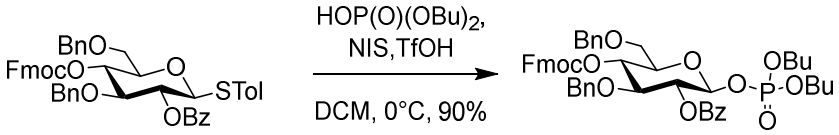

A solution of dibutyl phosphate (5.00 mL, 25.2 mmol) in DCM (15 mL) was dried over molecular sieves. After 1 h the supernatant (4.1 mL) was added to a solution of **7** (2.72 g, 3.43 mmol) in DCM (20 mL) and cooled to 0 °C. Then NIS (926 mg, 4.12 mmol) and TfOH (90.0 µL, 1.03 mmol) were added. The reaction was stirred for 2 h, quenched with an aqueous solution of $Na_2S_2O_3$/$NaHCO_3$ (1:1, 100 mL) and extracted with DCM (100 mL). The organic layer was dried over Na_2SO_4 and purified by silica gel chromatography (Hex/EtOAc 4:1) to give **1** (2.78 g, 3.16 mmol, 92%) as a yellow oil. $[\alpha]_D^{25}$ = +35.3 (*c* 1.0, $CHCl_3$). ^{1}H NMR (400 MHz, $CDCl_3$): δ = 8.04-7.99 (m, 2H, Ar), 7.78-7.72 (m, 2H, Ar), 7.62-7.51 (m, 3H, Ar), 7.47-7.35 (m, 4H, Ar), 7.33-7.18 (m, 7H, Ar), 7.10-6.99 (m, 5H, Ar), 5.44-5.33 (m, 2H, H-1, H-2), 5.10 (t, *J* = 9.6 Hz, 1H, H-4), 4.59 (d, *J* = 11.6 Hz, 1H, C*H*$_2$Ph), 4.56-4.46 (m, 3H, C*H*$_2$Ph), 4.40-4.26 (m, 2H, Fmoc), 4.12 (dd, *J* = 9.5, 4.9 Hz, 1H, Fmoc), 4.08-3.95 (m, 2H, OBu), 3.94-3.79 (m, 2H, H-5, H-3), 3.78-3.58 (m, 4H, 6-H, OBu), 1.65-1.46 (m, 2H, Bu), 1.39-1.19 (m, 4H, Bu), 0.99 (dd, *J* = 15.1, 7.5 Hz, 2H, Bu), 0.86 (t, *J* = 7.4 Hz, 3H, CH_3), 0.66 (t, *J* = 7.4 Hz, 3H, CH_3) ppm. ^{13}C NMR (125 MHz, $CDCl_3$): 164.9, 154.1 (2C, C=O), 143.2, 143.0, 141.3, 137.1, 133.4, 129.9, 128.5, 128.3, 128.2, 128.0, 127.9, 127.7, 127.6, 127.2, 125.1, 125.0, 120.0 (30C, Ar), 96.5 (C-1), 79.0 (C-3), 75.0 (C-4), 74.2 (*C*H$_2$Ph), 73.6 (2C, *C*H$_2$Ph, C-5), 72.7 (1C, C-2), 70.0 (Fmoc), 69.0 (C-6), 68.0 (OBu), 67.8 (OBu), 46.7 (Fmoc), 32.0, 31.8 (2C, Bu), 18.5, 18.2 (2C, Bu), 13.6, 13.4 (2C, CH_3) ppm. ESI-HRMS: m/z $[M+Na]^+$ calcd. for $C_{50}H_{55}NaO_{12}P$: 901.3329; found 901.3361. IR (neat) ν_{max} = 1753, 1733, 1248, 1027 cm^{-1}.

4-Methylphenyl 2-*O*-benzoyl-3-*O*-benzyl-6-*O*-levulinoyl-thio-β-D-glucopyranoside (9)

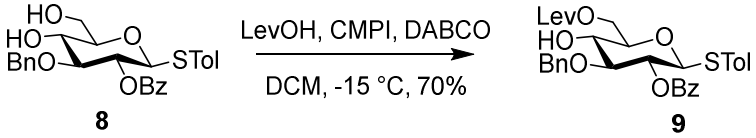

8[136] (728 mg, 1.51 mmol) was dissolved in DCM (10 mL), levulinic acid (352 mg, 3.03 mmol) and 2-chloro-1-methylpyridinium iodide (774 mg, 3.03 mmol) were added. The reaction was stirred for 15 min and then cooled to -15 °C. At this temperature DABCO (680 mg, 6.06 mmol) was added. The reaction mixture was stirred for 40 min, filtered over a plug of celite© and concentrated. The crude product was purified by silica gel chromatography (Hex/EtOAc 3:1) to yield **9** (671 mg, 1.16 mmol, 77%) as a white solid. $[a]_D^{25}$ = +5.1 (*c* 1.0, $CHCl_3$). ^{1}H NMR (400 MHz, $CDCl_3$): δ = 8.07 (d, *J* = 7.4 Hz, 2H, Ar), 7.61 (t, *J* = 7.4 Hz, 1H, Ar), 7.48 (t, *J* = 7.7 Hz, 2H, Ar), 7.35 (d, *J* = 8.0 Hz, 2H, Ar), 7.17 (s, 5H, Ar), 7.07 (d, *J* = 8.0 Hz, 2H, Ar), 5.21 (t, *J* = 9.4 Hz, 1H, H-2), 4.77-4.63 (m, 3H, H-1, C*H*$_2$Ph), 4.48 (dd, *J* = 12.1 Hz, 4.6 Hz, 1H, H-6a), 4.36 (dd, *J* = 12.1 Hz, 1.7 Hz, 1H, H-6b), 3.73-3.59 (m, 2H, H-3, H-4), 3.58-3.58 (m, 1H, H-5), 2.83-2.75 (m, 2H, Lev), 2.67-2.61 (m, 2H, Lev), 2.32 (s, 3H, CH_3), 2.20 (s, 3H, O=CCH_3) ppm. ^{13}C NMR (100 MHz, $CDCl_3$): δ = 206.8, 173.2, 165.1 (3C, *C*=O), 138.2, 137.6, 133.2, 129.8, 129.7, 129.5, 128.8, 128.4, 128.0, 127.8 (13C, Ar), 86.6 (C-1), 83.3 (C-3), 77.7 (C-5), 74.8 (*C*H_2Ph), 72.0 (C-2), 69.9 (C-4), 63.3 (C-6), 37.9 (Lev), 29.8 (O=C*C*H_3), 27.9 (Lev), 21.1 (CH_3) ppm. ESI-HRMS: m/z $[M+Na]^+$ calcd. for $C_{32}H_{34}NaO_8S$: 601.1867; found 601.1910. IR (neat) ν_{max}: 3486, 1722, 1270, 1070 cm^{-1}.

4-Methylphenyl 2-*O*-benzoyl-3-*O*-benzyl-4-*O*-fluorenylcarboxymethyl-6-*O*-levulinoyl-thio-β-D-glucopyranoside (10)

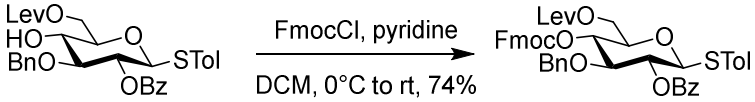

9 **10**

To a solution of **9** (671 mg, 1.16 mmol) in DCM (10 mL) and pyridine (2.3 mL), FmocCl (403 mg, 1.56 mmol) was added. The reaction mixture was stirred overnight, then diluted with DCM (100 mL) and washed with a 1 M HCl solution (100 mL) and brine (100 mL). The organic layer was dried over Na_2SO_4 and purified by silica gel chromatography (toluene/EtOAc 10:1) to give **10** (691 mg, 863 µmol, 74%) as a white solid. $[a]_D^{25}$ = +25.7 (*c* 1.0, $CHCl_3$). ^{1}H NMR (400 MHz, $CDCl_3$): δ = 8.05-8.00 (m, 2H, Ar), 7.77-7.71 (m, 2H, Ar), 7.64-7.54 (m, 3H, Ar), 7.47 (t, *J* = 7.8 Hz, 2H), 7.41-7.33 (m, 3H, Ar), 7.31-7.24 (m, 4H, Ar), 7.12-6.98

(m, 6H, Ar), 5.24 (t, *J* = 9.5 Hz, 1H, H-2), 4.93 (t, *J* = 9.6 Hz, 1H, H-4), 4.71 (d, *J* = 10 Hz, 1H, H-1), 4.56-4.44 (m, 3H, H-6a, C*H*$_2$Ph), 4.41-4.34 (m, 1H, H-6b), 4.29-4.24 (m, 2H, Fmoc), 4.19 (t, *J* = 7.1 Hz, 1H, Fmoc), 3.87 (t, *J* = 9.2 Hz, 1H, H-3), 3.77-3.70 (m, 1H, H-5), 2.84-2.71 (m, 2H, Lev), 2.68-2.58 (m, 2H, Lev), 2.33 (s, 3H, CH$_3$), 2.18 (s, 3H, CH$_3$) ppm. ^{13}C NMR (100 MHz, CDCl$_3$): δ = 206.4, 172.3, 164.8, 154.1 (4C, C=O), 143.2, 143.0, 141.3, 141.2, 138.5, 137.0, 133.5, 133.3, 129.9, 129.6, 128.4, 128.2, 128.1, 127.9, 127.8, 127.6, 127.2, 125.0, 124.9, 120.0 (30C, Ar), 86.4 (C-1), 80.9 (C-3), 75.6 (C-5), 74.4 (*C*H$_2$Ph), 74.2 (C-4), 71.8 (C-2), 70.2 (C-6), 62.6 (Fmoc), 46.7 (Fmoc), 37.8 (Lev), 29.9 (O=C*C*H$_3$), 27.9 (Lev), 21.1 (CH$_3$) ppm. ESI-HRMS: m/z [M+Na]$^+$ calcd. for C$_{47}$H$_{44}$NaO$_{10}$S: 823.2548; found 823.2588. IR (neat) ν_{max}: 1751, 1258 cm^{-1}.

Dibutoxyphosphoryloxy-2-*O*-benzoyl-3-*O*-benzyl-4-*O*-fluorenylcarboxymethyl-6-*O*-levulinoyl-thio-β-D-glucopyranoside (2)

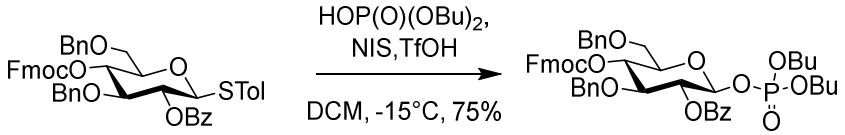

10 **2**

A solution of dibutyl phosphate (850 µL, 4.29 mmol) in DCM (12 mL) was dried over molecular sieves. After 1 h the supernatant of this mixture (1.40 mL) was added to **10** (126 mg, 157 µmol) and cooled to -15 °C. Then a solution of NIS in DCM (1 mL, 178 µmol) and TfOH (10.0 µL, 114 µmol) were added. The reaction was stirred for 2.5 h, quenched with an aqueous solution of Na$_2$S$_2$O$_3$/NaHCO$_3$ (1:1, 30 mL) and extracted with DCM (30 mL). The organic layer was dried over Na$_2$SO$_4$ and purified by silica gel chromatography (EtOAc/Hex/DCM 1:3:2 → 1:2:2) to yield compound **2** (105 mg, 118 µmol, 75%) as a yellow oil. $[\alpha]_D^{25}$ = +26.4 (*c* 1.0, CHCl$_3$). ^{1}H NMR (400 MHz, CDCl$_3$): δ = 8.00 (d, *J* = 7.3 Hz, 2H, Ar), 7.75 (t, *J* = 7.4 Hz, 2H, Ar), 7.64-7.55 (m, 3H, Ar), 7.48-7.34 (m, 4H, Ar), 7.32-7.24 (m, 3H, Ar), 7.12-6.98 (m, 4H, Ar), 5.42-5.35 (m, 2H, H-1, H-2), 5.04 (t, *J* = 9.6 Hz, 1H, H-4), 4.59-4.46 (m, 3H, H-6a, C*H*$_2$Ph), 4.44-4.37 (m, 1H, H-6b), 4.30-4.18 (m, 3H, Fmoc), 4.07-3.98 (m, 2H, OBu), 3.90-3.81 (m, 2H, H-5, H-3), 3.75-3.60 (m, 2H, OBu), 2.78-2.70 (m, 2H, Lev), 2.64-2.58 (m, 2H, Lev), 2.17 (s, 3H, Lev), 1.66-1.57 (m, 2H, Bu), 1.43-1.32 (m, 2H, Bu), 1.30-1.20 (m, 2H, Bu), 1.05-0.94 (m, 2H, Bu), 0.90 (t, *J* = 7.4 Hz, 3H, Bu), 0.66 (t, *J* =

7.4 Hz, 3H, Bu) ppm. ^{13}C NMR (100 MHz, $CDCl_3$): δ = 206.3, 172.2, 164.7, 154.0 (4C, C=O), 143.2, 142.9, 141.3, 141.2, 136.8, 133.5, 129.8, 129.0, 128.4, 128.1, 127.9, 127.9, 127.7, 127.2, 125.0, 124.8, 120.0 (24C, Ar), 96.4 (C-1), 78.8 (C-3), 74.3 (*C*H_2Ph), 73.8 (C-4), 72.7 (C-2), 72.4 (C-5), 70.2 (C-6), 68.0, 67.9 (2C, OBu), 61.86 (Fmoc), 46.6 (Fmoc), 37.8 (Lev), 31.9 , 31.6 (2C, Bu), 29.8 (O=C*C*H_3), 27.8 (Lev), 18.5, 18.1 (2C, Bu), 13.5, 13.3 (2C, CH_3) ppm. ESI-HRMS: m/z $[M+Na]^+$ calcd. for $C_{48}H_{55}NaO_{14}P$: 909.3222; found 909.3276. IR (neat) ν_{max}: 1739, 1252, 1029 cm^{-1}.

2,3,4-*O*-Tribenzyl-D-xylopyranose (14)

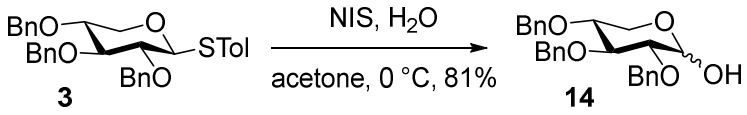

3 **14**

NIS (5.45 g, 24.2 mmol) was added to a stirred solution of **3**[150] (8.50 g, 16.1 mmol) in acetone/H_2O (9:1, 100 mL). The reaction was stirred for 5 min at rt. Then the reaction mixture was diluted with EtOAc (100 mL) and washed with an aqueous solution of $Na_2S_2O_3$ (100 mL). The crude compound was purified through a short plug of silica gel (EtOAc/Hex 1:4) to yield **14** (5.50 g, 13.1 mmol, 81% yield) as a mixture of α/β-isomers. α isomer: ^{1}H NMR (400 MHz, $CDCl_3$): δ = 7.37-7.29 (m, 15H, Ar), 5.11 (t, d, *J* = 3.2 Hz, 1H, H-1), 4.90-4.63 (m, 6H, C*H*$_2$Ph), 3.89-3.77 (m, 2H, H-3, H-5a), 3.67 (dd, *J* = 11.2 Hz, 5.3 Hz, 1H, H-5b), 3.59-3.52 (m, 1H, H-4), 3.48 (dd, *J* = 8.8 Hz, 3.5 Hz, 1H H-2), 2.88 (d, *J* = 3.0 Hz, OH) ppm. The analytical data is in agreement with literature data.[151]

***O*-Trichloroacetimidoyl 2,3,4-*O*-tribenzyl-D-xylopyranoside (15)**

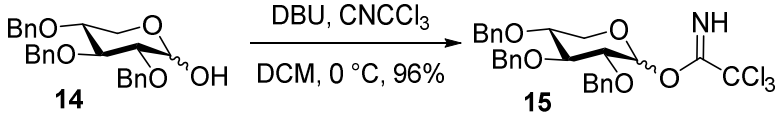

14 **15**

To a cooled (0 °C) solution of compound **14** (1.80 g, 4.28 mmol) in DCM, DBU (128 µL, 856 µmol) and trichlorocetonitrile (4.30 mL, 42.9 mmol) were added. After 3 h the solvent was evaporated and the product was purified by silica gel chromatography (EtOAc/Hex 1:5 and 5% Et_3N) to yield **15** (2.33 g, 4.12 mmol, 96%, α/β = 2:1) as a yellow oil. α isomer: ^{1}H NMR (400 MHz, $CDCl_3$) δ = 8.59 (s, 1H, NH), 7.41-7.24 (m, 15H, Ar), 6.37 (d, *J* = 3.4 Hz, 1H, H-1), 4.97-4.61

(m, 6H, C*H*$_2$Ph), 3.99 (t, *J* = 9.2 Hz, 1H), 3.84-3.62 (m, 4H) ppm. The analytical data is in agreement with literature data.[152]

4-Methylphenyl 2,3,4-*O*-tribenzyl-α-D-xylopyranosyl-(1->6)-2-*O*-benzoyl-3-*O*-benzyl-thio-β-D-glucopyranoside (16).

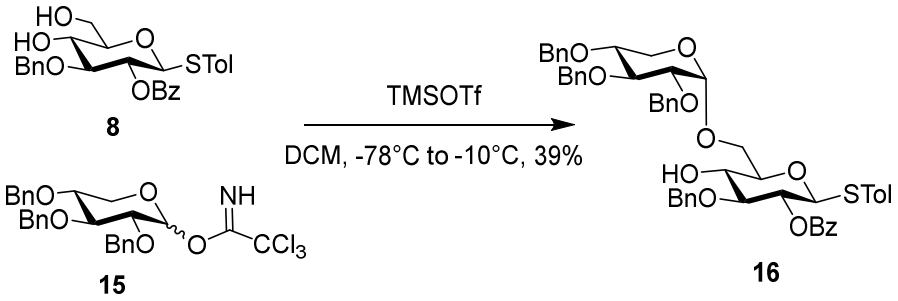

To a solution of **16** (102 mg, 181 µmol) and **8** (105 mg, 218 µmol) in DCM (1 mL) at -78 °C a TMSOTf solution in DCM (30 µL, 17.0 µmol) was added. The reaction was gradually warmed to -10 °C, then quenched with sat. aqueous solution of $NaHCO_3$ (20 mL) and extracted with EtOAc (20 mL). The crude compound was purified by silica gel chromatography (EtOAc/Hex 1:4) to give **16** (62.3 mg, 71.0 µmol, 39%) as a pale-yellow oil and the respective β isomer (31.4 mg, 36.0 µmol, 20%) as a white solid. $[a]_D^{25}$ = +35.5 (*c* 1.0, $CHCl_3$). ^{1}H NMR (400 MHz, $CDCl_3$): δ = 8.07 (d, *J* = 7.3 Hz, 2H, Ar), 7.61 (t, *J* = 7.4 Hz, 1H, Ar), 7.48 (t, *J* = 7.7 Hz, 2H, Ar), 7.40-7.20 (m, 17H, Ar), 7.16 (s, 5H, Ar), 7.06 (d, *J* = 7.9 Hz, 2H, Ar), 5.22 (t, *J* = 9.5 Hz, 1H, H-2 Glc), 4.89 (s, 2H, C*H*$_2$Ph), 4.80-4.60 (m, 8H, 3 X C*H*$_2$Ph, H-1 Xyl, H-1 Glc), 4.01 (dd, *J* = 9.4 Hz, 4.5 Hz, 1H, H-6a Glc), 3.88 (t, *J* = 8.8 Hz, 1H, H-3 Xyl), 3.76 (t, *J* = 8.7 Hz, 1H, H-4 Glc), 3.72-3.54 (m, 6H, H-3 Glc, H-4 Xyl, H-5a Xyl, H-5b Xyl, H-5 Glc, H-6b Glc), 3.47 (dd, *J* = 9.5 Hz, 3.6 Hz, 1H, H-2 Xyl), 3.24 (s, 1H, OH), 2.24 (s, 3H, CH3) ppm. ^{13}C NMR (100 MHz, $CDCl_3$): δ = 165.2 (1C, C=O), 138.7, 138.3, 138.2, 137.9, 137.8, 133.6, 133.2, 129.9, 129.6, 128.5, 128.4, 128.3, 128.1, 128.0, 127.7, 127.6 (36C, Ar), 97.8 (C-1 Xyl), 86.7 (C-1 Glc), 83.4 (C-3 Glc), 81.3 (C-3 Xyl), 79.5 (C-2 Xyl), 77.9 (C-5 Glc), 75.8, 74.7, 73.7, 73.4, (4C, *C*H_2Ph), 73.0 (C-4 Glc), 71.9 (C-2 Glc), 68.8 (C-6 Glc), 60.1 (C-5 Xyl), 21.1 (CH_3) ppm. ESI-HRMS: m/z $[M+H]^+$ calcd. for $C_{53}H_{54}NaO_{10}S$: 905.3330; found 905.3503. IR (neat) ν_{max}: 3480, 1729, 1269, 1072, 1028 cm^{-1}.

4-Methylphenyl 2,3,4-*O*-tribenzyl-α-D-xylopyranosyl-(1->6)-2-*O*-benzoyl-3-*O*-benzyl-4-*O*-levulinoyl-thio-β-D-glucopyranoside (17).

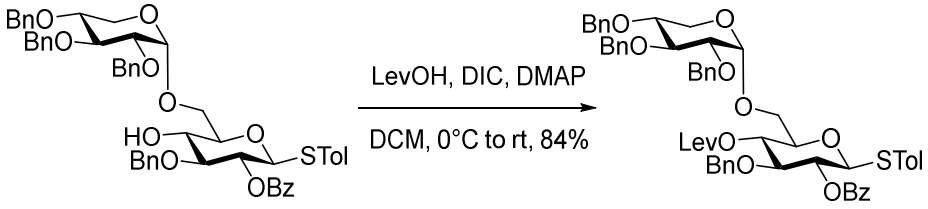

16 **17**

Compound **16** (2.00 g, 2.27 mmol) was dissolved in DCM (15 mL) and cooled to 0 °C. Then DMAP (139 µg, 1.13 mmol), DIC (420 µL, 2.72 mmol) and LevOH (527 mg, 4.54 mmol) were added. After 5 min the ice bath was removed. After the reaction was stirred for 6 h at rt, another portion of DMAP (139 µg, 1.13 mmol) was added and the reaction was left stirred overnight. The day after the reaction mixture was filtered through a plug of celite© and concentrated. The compound was purified by silica gel chromatography (Hex/EtOAc 4:1) to yield the intermediate **17** (1.87 g, 1.91 mmol, 84%) as a white solid. $[\alpha]_D^{25}$ = +26.7 (*c* 1.0, $CHCl_3$). ^{1}H NMR (400 MHz, $CDCl_3$): δ = 8.10 (d, *J* = 7.2 Hz, 2H, Ar), 7.62 (t, *J* = 7.4 Hz, 1H, Ar), 7.53-7.00 (m, 26H, Ar), 5.33 (t, *J* = 9.6 Hz, 1H, H-2 Glc), 5.06 (t, *J* = 9.3 Hz, 1H, H-4 Glc), 4.92 (s, 2H, C*H*$_2$Ph), 4.87-4.56 (m, 8H, 3 x C*H*$_2$Ph, H-1 Glc, H-1 Xyl), 4.03-3.44 (m, 9H, H-3 Glc, H-5 Glc, H-6a Glc, H-6b Glc, H-2 Xyl, H-3 Xyl, H-4 Xyl, H-5a Xyl, H-5b Xyl), 2.74-2.69 (m, 1H, Lev), 2.66-2.49 (m, 2H, Lev), 2.41-2.31 (m, 1H, Lev), 2.16 (s, 3H, CH_3), 2.13 (s, 3H, O=CCH_3) ppm. ^{13}C NMR (100 MHz, $CDCl_3$): δ = 206.0, 171.5, 164.9 (3C, C=O), 139.0, 138.3, 138.1, 137.7, 137.5, 133.7, 133.4, 133.2, 129.8, 129.7, 128.9, 128.4, 128.3, 128.2, 128.1, 128.0, 127.8, 127.7, 127.5, 125.1 (36C, Ar), 97.0, (C-1 Xyl), 87.0 (C-1 Glc), 81.4 (C-3 Glc), 81.2 (C-3 Xyl), 79.5 (C-2 Xyl), 78.2 (C-5 Glc), 77.3 (C-4 Xyl), 75.7, 74.1, 73.2, 73.0 (4C, *C*H$_2$Ph), 72.0 (C-4 Glc), 70.6 (C-2 Glc), 67.3 (C-6 Glc), 60.0 (C-5 Xyl), 37.6 (Lev), 29.6 (O=C*C*H$_3$), 27.8 (Lev), 20.9 (CH_3) ppm. ESI-HRMS: m/z $[M+Na]^+$ calcd. for $C_{58}H_{60}NaO_{12}S$: 1003.3698; found 1003.3839. IR (neat) ν_{max}: 1722, 1089, 1072, 1042, 1029 cm^{-1}.

Dibutoxyphosphoryloxy 2,3,4-*O*-tri-benzyl-α-D-xylopyranosyl-(1->6)-2-*O*-benzoyl-3-*O*-benzyl-6-*O*-levulinoyl-β-D-glucopyranoside (13).

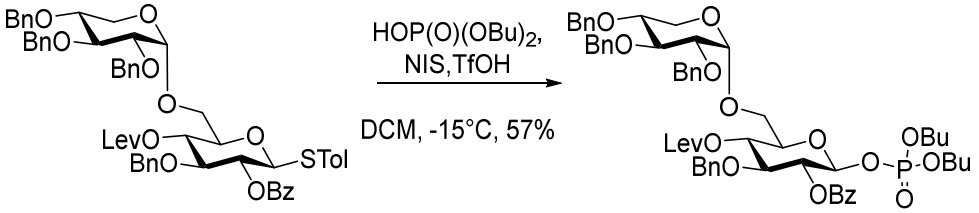

17 **13**

A solution of dibutyl phosphate (2.00 mL, 10.1 mmol) in DCM (10 mL) was dried over molecular sieves. After 1 h the supernatant of this mixture (5.40 mL) was added to **17** (1.78 g, 1.81 mmol) and cooled to 0 °C. Then NIS (490 mg, 2.18 mmol) and TfOH (50.0 µL, 563 µmol) were added. The reaction was stirred for 2 h, diluted with DCM (50 mL) and washed with an aqueous solution of $Na_2S_2O_3$/$NaHCO_3$ (1:1, 50 mL) and brine (50 mL). The organic layer was dried over Na_2SO_4 and purified by silica gel chromatography (Hex/EtOAc 4:1) to give compound **13** (1.10 g, 1.03 mmol, 57%) as a yellow oil. $[\alpha]_D^{25}$ = +41.2 (*c* 1.0, $CHCl_3$). ^{1}H NMR (400 MHz, $CDCl_3$): δ = 8.04 (d, *J* = 7.5 Hz, 2H, Ar), 7.58 (t, *J* = 7.4 Hz, 1H, Ar), 7.48-7.25 (m, 17H, Ar), 7.14 (s, 5H, Ar), 5.48-5.37 (m, 2H, H-2 Glc, H-1 Glc), 5.26 (t, *J* = 9.5 Hz, 1H, H-4 Glc), 4.96-4.83 (m, 2H, C*H*$_2$Ph), 4.76 (d, *J* = 3.4 Hz, 1H, H-1 Xyl), 4.75-4.55 (m, 6H, 3 x C*H*$_2$Ph), 4.06-3.41 (m, 13H, 4 x OBu, 6Ha Glc, 6Hb Glc, 5Ha Xyl, 5Hb Xyl, H-2 Xyl, H-3 Glc, H-4 Xyl, H-3 Xyl, H-5 Glc), 2.65-2.51 (m, 3H, Lev), 2.41 (m, 1H, Lev), 2.06 (s, 3H, Lev), 1.56-1.47 (m, 2H, Bu), 1.32-1.20 (m, 4H, Bu), 1.06-0.95 (m, 2H, Bu), 0.81 (t, 3H, *J* = 7.4 Hz, CH_3), 0.67 (t, 3H, *J* = 7.4 Hz, CH_3) ppm. ^{13}C NMR (100 MHz, CDCl3): δ = 206.2, 171.3, 164.8 (3C, C=O), 138.9, 138.4, 138.3, 137.4, 133.3, 129.9, 129.3, 128.4, 128.3, 128.2, 128.0, 127.9, 127.7, 127.5 (30C, Ar), 97.4, (C-1 Xyl), 96.3 (C-1 Glc), 81.1 (C-3), 79.6 (C-2 Xyl), 79.3 (C-3), 77.9 (C-5 Glc), 75.7 (*C*H_2Ph), 73.8 (C-4 Xyl), 73.4 (2C, *C*H_2Ph), 73 (C-2 Glc), 72.7 (*C*H_2Ph), 70.4 (C-4 Glc), 67.9, 67.7 (2C, OBu), 66.9 (C-6 Glc), 60.1 (C-5 Xyl), 37.7 (Lev), 31.9, 31.7 (2C, Bu), 29.7, 27.8 (2C, Lev), 18.5, 18.2, 13.5, 13.3 (4C, Bu) ppm. ESI-HRMS**:** m/z $[M+Na]^+$ calcd. for $C_{59}H_{71}NaO_{16}P$: 1089.4377; found 1089.4384. IR (neat) ν_{max}: 1734, 1267, 1095, 1072, 1029 cm^{-1}.

3,4-*O*-Dibenzyl-1,2-*O*-(1-ethoxyethylidene)-D-xylopyranose (39)

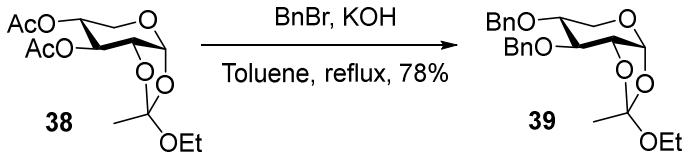

To a solution of **38**[147] (12.4 g, 40.8 mmol) in Toluene (200 mL) was added KOH (18.3 g, 327 mmol) under vigorous stirring. Then the reaction was heated until reflux and BnBr (19.4 mL 163 mmol) was added dropwise. The reaction was vigorously stirred for 3 h and then cooled to rt. The reaction mixture was then divided in two parts each one was diluted with DCM (300 mL) and washed with water (300 mL). The organic layers were combined and concentrated. The crude product was purified by silica gel chromatography (EtOAc/Hex 1:6) giving **39** (9.80 g, 24.5 mmol, 78% yield) as a yellow oil. The analytical data is in agreement with literature data.[130]

4-Methylphenyl 3,4-*O*-dibenzyl-1-thio-D-xylopyranoside (40)

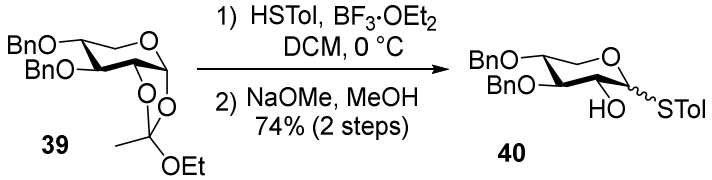

39 (12.3 g, 30.7 mmol) was dissolved in anhydrous DCM (250 mL) and 4-methylbenzenethiol (5.72 g, 46.1 mmol) was added under argon atmosphere. The reaction mixture was cooled to 0 °C and $BF_3{\cdot}OEt_2$ (5.84 mL, 46.1 mmol) was added dropwise. After 2 h the reaction was quenched with Et_3N (6.42 mL, 46.1 mmol) and washed with water (200 mL). The organic layer was concentrated in vacuum. The crude product was dissolved in MeOH (100 mL) and NaOMe (5.00 g, 93.0 mmol) was added. The reaction mixture was stirred overnight and subsequently neutralized by addition of prewashed Amberlite IR-120 resin. The resin was filtered off and the solvents were removed *in vacuo.* The crude product was purified by silica gel chromatography (Hex/EtOAc 6:1) to give **40** (9.90 g, 22.7 mmol, 74% yield, α/β = 2:5) as a white solid. $[a]_D^{25}$ = -46.5 (*c* 1.0, $CHCl_3$). ^1H NMR (400 MHz, $CDCl_3$): δ = 7.47-7.28 (m, 20H, Ar), 7.12 (d, *J* = 7.9 Hz, 4H, Ar), 5.24 (d, *J* = 2.6 Hz, 1H, H-1α), 4.87-4.74 (m, 4H, C*H*$_2$Ph-β, CH*H*Ph-α, H-1-β),

4.72-4.57 (m, 4H, C*H*$_2$Ph-β, C*H*$_2$Ph-α, C*H*HPh-α), 4.27 (dd, J = 11.9, 3.5 Hz, 1H, H-5a-β), 4.16-4.08 (m, 1H, H-5a-α), 3.95 (dd, *J* = 5.5, 2.7 Hz, 1H, H-2-α), 3.84 (dd, *J* = 12.4, 2.8 Hz, 1H, H-5b-α), 3.79 (t, *J* = 5.1 Hz, 1H, H-3-α), 3.67 (t, *J* = 6.2 Hz, 1H, H-2-β), 3.62 (t, *J* = 6.4 Hz, 1H, H-3-β), 3.59-3.44 (m, 3H, H-4-β, H-4-α, H-5b-β), 2.34 (s, 6H, C*H*$_3$-α, C*H*$_3$-β). ^{13}C NMR (101 MHz, $CDCl_3$): δ = 138.0, 137.9, 137.7, 137.5, 137.3, 137.2, 132.6, 131.6, 131.1, 129.8, 129.7, 128.5, 128.3, 128.0, 127.9, 127.8, 127.7, 127.5 (28 C, Ar), 89.1 (1C, C-1-β), 88.4 (1C, C-1-α), 79.9 (1C, C-3-β), 77.2 (1C, C-3-α), 76.0 (1C, C-4-β), 74.5 (1C, C-4-α), 74.0, 73.3, 72.4, 71.8 (4C, *C*H_2Ph), 70.8 (1C, C-2-β), 70.7 (1C, C-2-α), 64.0 (2C, C-5-β, C-5-α), 21.1 (2C, CH_3) ppm. ESI-HRMS: m/z $[M+Na]^+$ calcd. for $C_{26}H_{28}NaO_4S$: 459.1606; found 459,1604. IR (neat) ν_{max}: 3493, 2870, 1495, 1475, 1065 cm^{-1}.

4-Methylphenyl 3,4-*O*-dibenzyl-2-*O*-4-methoxybezyl-1-thio-D-xylopyranoside (41)

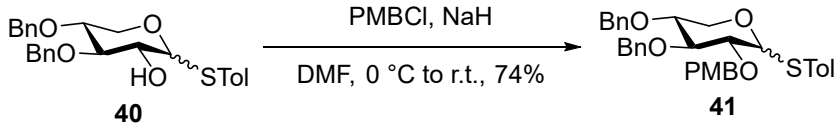

40 **41**

To a cooled (0 °C) solution of **40** (2.94 g, 6.52 mmol) in DMF (60 mL) and PMBCl (1.77 mL, 13.0 mmol) NaH (323 mg, 8.08 mmol) was added. The reaction was left warm to room temperature and stirred for 3 h. The reaction was quenched by $NHCl_4$ diluted with DCM (250 mL) and washed with $NHCl_4$ (250 mL), H_2O (250 mL) and brine (250 mL). The crude compound was purified by silica gel chromatography (EtOAc/Hex 1:6) to give **41** (3.47 g, 6.23 mmol, 96% yield) as a white solid. $[\alpha]_D^{25}$ = +29.5 (*c* 1.0, $CHCl_3$). ^{1}H NMR (400 MHz, $CDCl_3$): δ = 7.43 (d, *J* = 8.2 Hz, 2H, Ar), 7.38-7.29 (m, 26H), 7.11 (d, *J* = 7.6 Hz, 4H, Ar), 6.90-6.81 (m, 4H, Ar), 5.42 (d, *J* = 4.5 Hz, 1H, H-1α), 4.99-4.60 (m, 12H, 3xC*H*$_2$Ph-β, 3xC*H*$_2$Ph-α), 4.58 (d, *J* = 9.4 Hz, 1H, H-1β), 4.10-4.01 (m, 2H, H-5a-α, H-5a-β), 3.83-3.75 (m, 8H, OC*H*$_3$-β, OC*H*$_3$-α, H-3-α, H-2-α), 3.70-3.57 (m, 4H, H-3-β, H-5b-α, H-4-α, H-4-β), 3.40 (t, *J* = 9.0 Hz, 1H, H-2β), 3.24-3.16 (m, 1H, H-5a-β), 2.33 (s, 6H, C*H*$_3$-α, C*H*$_3$-β). ^{13}C NMR (101 MHz, $CDCl_3$): δ = 159.3, 138.7, 138.5, 138.2, 138.0, 137.8, 137.3, 132.6, 132.1, 130.2, 129.9, 129.7, 129.4, 128.5, 128.4, 128.3, 128.0, 127.9, 127.8, 127.7, 127.6, 113.8 (48 C, Ar), 88.8 (1C, C-1-β), 87.8 (1C, C-1-α), 85.5 (1C, C-3-β), 81.60 (1C, C-3-α), 80.11 (1C, C-

2-β), 79.12 (1C, C-2-α), 77.7 (1C, C-4-β), 77.6 (1C, C-4-α), 75.7, 75.1, 73.5, 73.2, 72.2 (6C, *C*H$_2$Ph), 67.5 (1C, C-5-β), 60.9 (1C, C-5-α), 55.3 (2C, O*C*H$_3$), 21.1 (2C, *C*H$_3$) ppm. ESI-HRMS: m/z [M+Na]$^+$ calcd. for $C_{34}H_{36}NaO_5S$: 579.2181; found 579.2175. IR (neat) ν_{max}: 2865, 1515, 1250, 1075 cm^{-1}.

3,4-*O*-Dibenzyl-2-*O*-4-methoxybezyl-D-xylopyranose (42)

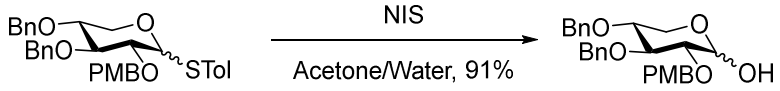

41 **42**

NIS (10.5 g, 18.7 mmol) was added to a stirred solution of **41** (6.37 g, 28.3 mmol) in acetone/H$_2$O (9:1, 140 mL). The reaction was stirred for 5 min at rt. Then the reaction mixture was diluted with EtOAc (100 mL) and washed with an aqueous solution of $Na_2S_2O_3$ (200 mL), water (200 mL) and brine (200 mL). The crude compound was purified through a short plug of silica gel (EtOAc/Hex 1:3) to yield **42** (7.70 g, 17.1 mmol, 91% yield, α/β = 2:1). $[a]_D^{25}$ = +15.4 (*c* 1.0, $CHCl_3$). ^{1}H NMR (400 MHz, $CDCl_3$): δ = 7.48-7.21 (m, 24H, Ar), 7.01-6.77 (m, 4H, Ar), 5.08 (d, *J* = 3.5 Hz, H-1-α), 4.95- 4.83 (m, 5H, C*H*$_2$Ph-α, C*H*$_2$Ph-β, CH*H*Ph-β), 4.79-4.57 (m, 8H, 2xC*H*$_2$Ph-α, C*H*$_2$Ph-β, CH*H*Ph-β,H-1-β), 3.99-3.87 (m, 2H, H-5a-β, H-3-α), 3.86-3.78 (m, 7H, H-5a-α, OC*H*$_3$-β, OC*H*$_3$-α), 3.72-3.46 (m,5H, H-3-β, H-5b-α, H-4-α, H-4-β, H-2-α), 3.34 (t, *J* = 7.9 Hz, 1H, H-2β), 3.31-3.20 (dd, *J* = 11.6, 9.6 Hz, 1H, H-5a-β). ^{13}C NMR (101 MHz, $CDCl_3$): δ = 159.3, 159.1, 138.5, 138.4, 138.1, 137.9, 130.4, 129.8, 129.7, 129.6, 128.4, 128.3, 128.2, 127.9, 127.8, 127.7, 127.7, 127.5, 113.7 (36 C, Ar), 97.7 (1C, C-1-β), 91.3 (1C, C-1-α), 83.2 (1C, C-3-β), 82.0 (1C, C-2-β), 80.4 (1C, C-3-α), 79.0 (1C, C-2-α), 77.5 (1C, C-4-β), 77.4 (1C, C-4-α), 75.4 , 75.4, 74.4, 73.2, 73.1, 72.9 (6C, *C*H$_2$Ph), 63.6 (1C, C-5-β), 60.1 (1C, C-5-α), 55.1 (2C, O*C*H$_3$) ppm. ESI-HRMS: m/z [M+Na]$^+$ calcd. for $C_{27}H_{30}NaO_6$: 473.1940; found 473.1928. IR (neat) ν_{max}: 3364, 2931, 1516, 1251, 1088, 1072, 1030 cm^{-1}.

_O_-Trichloroacetimidoyl 3,4-_O_-dibenzyl-2-_O_-4-methoxybezyl-D-xylopyranoside (43)

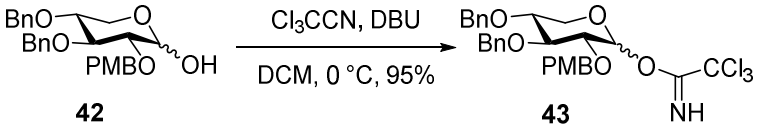

42 **43**

To a cooled (0 °C) solution of compound **42** (3.83 g, 8.50 mmol) in DCM (30 mL), DBU (127 µL, 850 µmol) and trichloroacetonitrile (3.41 mL, 34.0 mmol) were added. After 3 h the solvent was evaporated and the product was purified by silica gel chromatography (EtOAc/Hex 1:5 and 5% Et_3N) to yield **43** (4.78 g, 8.03 mmol, 95%, α/β = 2:1) as a yellow oil. $[\alpha]_D^{25}$ = +39.3 (*c* 1.0, $CHCl_3$). ^1H NMR (400 MHz, $CDCl_3$): δ = 8.71 (s, 1H, CN*H*-β), 8.58 (s, 1H, CN*H*-α), 7.40-7.29 (m, 20H), 7.28-7.21 (m, 4H, Ar), 6.88-6.80 (m, 4H, Ar), 6.32 (d, *J* = 3.5 Hz, 1H, H-1-α), 5.84-5.77 (m, 1H, H-1-β), 4.97-4.58 (m, 12H, 3xC*H*$_2$Ph-α, 3xC*H*$_2$Ph-β), 4.04-4.00 (m, 1H, H-5a-β), 3.96 (t, *J* = 9.1 Hz, 1H, H-3-α), 3.83-3.60 (m, 13H, H-5a-α, OC*H*$_3$-β, OC*H*$_3$-α, H-3-β, H-5b-α, H-4-α, H-4-β, H-2-α, H-2β), 3.49-3.42 (m, 1H, H-5b-β) ppm. ^{13}C NMR (101 MHz, $CDCl_3$): δ = 161.4, 161.1 (2C, *C*=NH), 159.2, 138.6, 138.4, 138.0, 137.9, 130.0, 129.6, 129.4, 129.2, 128.4, 128.3, 128.0, 127.9, 127.8, 127.6, 113.7 (36C, Ar), 98.8 (1C, C-1-β), 94.3 (1C, C-1-α), 91.2 (1C, *C*Cl_3-α), 90.8 (1C, *C*Cl_3-β), 83.0 (1C, C-3-β), 80.8 (1C, C-3-α), 79.7 (1C, C-2-β), 78.6 (1C, C-2-α), 77.1 (2C, C-4-β, C-4-α), 75.7, 75.4, 74.5, 73.7, 73.2, 72.6 (6C, *C*H_2Ph), 64.47 (1C, C-5-β), 62.38 (1C, C-5-α), 55.21 (2C, O*C*H_3). ESI-HRMS: m/z $[M+Na]^+$ calcd. for $C_{29}H_{30}Cl_3NNaO_6$: 616.1036; found 616.1027. IR (neat) ν_{max}: 3342, 2903, 1672, 1515, 1249, 1072, 1030 cm^{-1}.

3,4-_O_-Dibenzyl-2-_O_-4-methoxybezyl-D-xylopyranosyl-(1->6)-2-_O_-benzoyl-3-_O_-benzyl-1-thio-β-D-glucopyranoside (44).

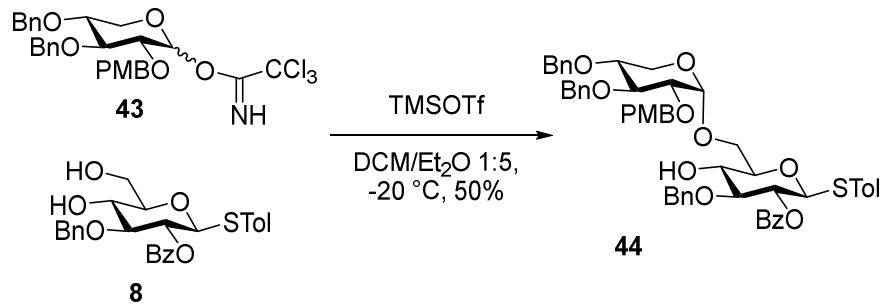

43 **8** **44**

To a solution of **43** (1.48 g, 2.49 mmol) and **8** (1.31 g, 2.74 mmol) in a solution of DCM/Et_2O 1:5 (50 mL) at -15 °C a TMSOTf solution in DCM (45 µL, 24.9 µmol) was added. After 40 minutes the reaction was diluted with DCM (50 mL) and washed with sat. aqueous solution of $NaHCO_3$ (100 mL), water (100 mL) and brine (100 mL). The crude compound was purified by silica gel chromatography (EtOAc/Hex 1:3) to give **44** (1.14 g, 1.25 mmol, 50%) as a pale-yellow oil. $[\alpha]_D^{25}$ = +47.2 (*c* 1.0, $CHCl_3$). ^{1}H NMR (400 MHz, $CDCl_3$): δ = 8.09 (d, *J* = 7.0 Hz, 2H, Ar), 7.62 (t, *J* = 7.4 Hz, 1H, Ar), 7.49 (t, *J* = 7.6 Hz, 1H, Ar), 7.42-7.23 (m, 15H, Ar), 7.22-7.14 (m, 5H, Ar), 7.07 (d, *J* = 7.9 Hz, 2H, Ar), 6.84 (d, *J* = 8.6 Hz, 2H, Ar), 5.24 (t, *J* = 9.5 Hz, 1H, H-2-Glc), 4.89 (s, 2H, C*H*$_2$Ph), 4.79-4.69 (m, 5H, H-1-Glc, 2xC*H*$_2$Ph), 4.68-4.52 (m, 3H, C*H*$_2$Ph, H-1-Xyl), 4.02 (dd, *J* = 9.9, 4.8 Hz, 1H, H-6b-Glc), 3.87 (t, *J* = 8.9 Hz, 1H, H-3-Xyl), 3.81-3.54 (m, 9H, H-4-Xyl, H-5a-Xyl, H-5b-Xyl, H-3-Glc, H-6b-Glc, H-4-Glc, OC*H*$_3$), 3.46 (dd, *J* = 9.5, 3.6 Hz, 1H, H-2-Xyl), 2.25 (s, 3H, C*H*$_3$) ppm. ^{13}C NMR (101 MHz, $CDCl_3$): δ = 165.2 (1C, *C*=O), 159.3, 138.8, 138.2, 137.9, 133.6, 133.2, 129.9, 129.9, 129.8, 129.7, 129.6, 128.5, 128.4, 128.3, 128.3, 127.9, 127.9, 127.7, 127.6, 113.8 (36C, Ar), 97.9 (1C, C-1-Xyl), 86.61 (1C, C-1-Glc), 83.4 (1C, C-3-Glc), 81.3 (1C, C-3-Xyl), 79.2 (1C, C-2-Xyl), 77.9 (1C, C-4-Xyl), 77.2 (1C, C-5-Glc), 75.8, 74.7, 73.4, 73.3 (5C, *C*H_2Ph) , 73.1 (1C, C-4-Glc), 71.9 (1C, C-2-Glc), 68.9 (1C, C-6-Glc), 60.1 (1C, C-5-Xyl), 55.2 (1C, O*C*H_3), 21.1 (1C, *C*H_3) ppm. ESI-HRMS: m/z $[M+Na]^+$ calcd. for $C_{54}H_{56}NaO_{11}S$: 935.3341; found 935.3349. IR (neat) ν_{max}: 3493, 2883, 1729, 1515, 1269, 1251, 1071, 1028 cm^{-1}.

4-Methylphenyl 2,3,4-*O*-tribenzyl-α-D-xylopyranosyl-(1->6)-2-*O*-benzoyl-3-*O*-benzyl-4-*O*-levulinoyl-1-thio-β-D-glucopyranoside (35a).

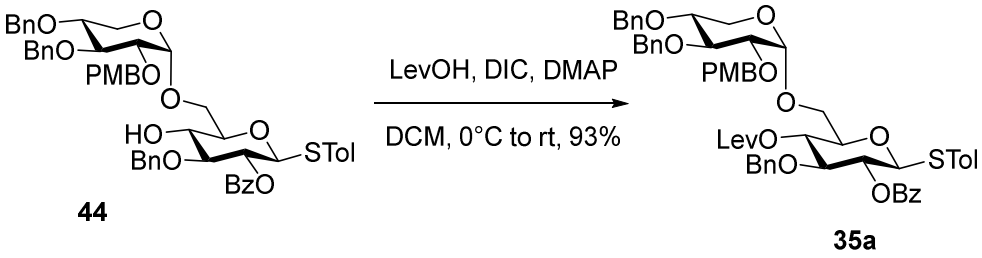

Compound **44** (1.63 g, 1.87 mmol) was dissolved in DCM (30 mL) and cooled to 0 °C. Then DMAP (218 µg, 0.02 mmol), DIC (417 µL, 2.68 mmol) and

LevOH (283 mL, 2.68 mmol) were added. After 5 min the ice bath was removed and the reaction was left stirred overnight. The day after the reaction mixture was filtered through a plug of celite© and concentrated. The compound was purified by silica gel chromatography (Hex/EtOAc 2:1) to yield **35a** (1.68 g, 1.61 mmol, 93%) as a pale-yellow oil. $[\alpha]_D^{25}$ = +30.0 (*c* 1.0, $CHCl_3$). ^1H NMR (400 MHz, $CDCl_3$): δ = 8.10-8.06 (m, 2H, Ar), 7.61 (tt, *J* = 7.4, 1.3 Hz, 1H, Ar), 7.48 (t, *J* = 7.7 Hz, 2H, Ar), 7.42-7.23 (m, 14H, Ar), 7.18-7.10 (m, 5H, Ar), 7.05 (d, *J* = 7.9 Hz, 2H, Ar), 6.84 (d, *J* = 8.6 Hz, 2H, Ar), 5.30 (dd, *J* = 10.1, 9.1 Hz, 1H, H-2-Glc), 5.03 (t, *J* = 9.5 Hz, 1H, H-4-Glc), 4.94-4.85 (d, *J* = 2.8 Hz, 2H, C*H*$_2$Ph), 4.75-4.61 (m, 6H, 2 x C*H*$_2$Ph, H-1 Glc, H-1 Xyl), 4.58 (s, 1H, C*H*$_2$Ph), 3.93-3.77 (m, 7H, H-3-Xyl, H-3-Glc, H-5-Glc, H-6a-Glc, OC*H*$_3$), 3.74 (d, *J* = 10.9 Hz, H-5a-Xyl), 3.67 (dd, *J* = 11.0, 5.6 Hz, 1H, H-5b-Xyl), 3.62-3.55 (m, 1H, H-4-Xyl), 3.50 (d, *J* = 9.2 Hz, 1H, H-6a-Glc), 3.46 (dd, *J* = 9.6, 3.5 Hz, 1H, H-2-Xyl), 2.80-2.69 (m, 1H, Lev), 2.65-2.50 (m, 2H, Lev), 2.40-2.30 (m, 1H, Lev), 2.14 (s, 3H, CH_3), 2.13 (s, 3H, O=CC*H*$_3$) ppm. ^{13}C NMR (101 MHz, $CDCl_3$): δ = 206.1, 171.6, 165.0 (3C, C=O), 159.2, 139.0, 138.4, 138.1, 137.6, 133.4, 133.2, 130.3, 129.8, 129.8, 129.7, 128.9, 128.4, 128.3, 128.2, 127.9, 127.8, 127.7, 127.6, 127.5, 113.8 (36C, Ar), 97.0 (C-1 Xyl), 87.0 (C-1 Glc), 81.5 (C-3 Glc), 81.2 (C-3 Xyl), 79.2 (C-2 Xyl), 78.2 (C-4 Xyl), 77.2 (C-5 Glc), 75.8, 74.2, 73.4, 72.7 (4C, *C*H_2Ph), 72.0 (C-2 Glc), 70.6 (C-4 Glc), 67.3 (C-6 Glc), 60.0 (C-5 Xyl), 55.2 (1C, O*C*H_3), 37.7 (1C, Lev), 29.7 (O=C*C*H_3), 27.8 (1C, Lev), 21.0 (1C, CH_3) ppm. ESI-HRMS: m/z $[M+Na]^+$ calcd. for $C_{59}H_{62}NaO_{13}S$: 1033.3809; found 1033.3807. IR (neat) ν_{max}: 2922, 1722, 1515, 1250, 1072 cm^{-1}.

Dibutoxyphosphoryloxy 2,3,4-*O*-tri-benzyl-α-D-xylopyranosyl-(1->6)-2-*O*-benzoyl-3-*O*-benzyl-6-*O*-levulinoyl-β-D-glucopyranoside (35b).

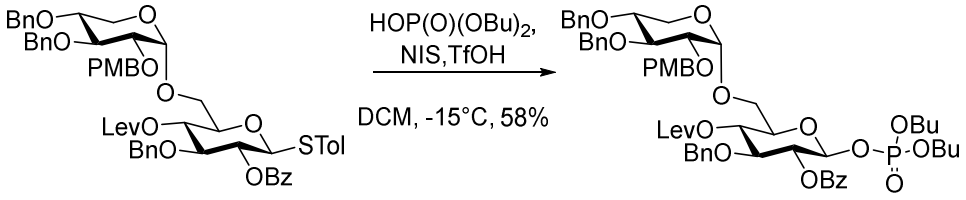

35a **35b**

A solution of dibutyl phosphate (2.00 mL, 10.1 mmol) in DCM (20 mL) was dried over molecular sieves. After 1 h the supernatant of this mixture (7.72 mL)

was added to **35a** (749 mg, 740 µmol) and cooled to 0 °C. Then NIS (200 mg, 888 µmol) and TfOH (20.0 µL, 222 µmol) were added. The reaction was stirred for 2 h, diluted with DCM (50 mL) and washed with an aqueous solution of $Na_2S_2O_3$/$NaHCO_3$ (1:1, 50 mL) and brine (50 mL). The organic layer was dried over Na_2SO_4 and purified by silica gel chromatography (Hex/EtOAc 2:1) to give compound **35b** (470 mg, 428 µmol, 58%) as a yellow oil. $[\alpha]_D^{25}$ = +40.8 (*c* 1.0, $CHCl_3$). ^{1}H NMR (400 MHz, $CDCl_3$): δ = 8.04 (d, *J* = 7.5 Hz, 2H, Ar), 7.58 (t, *J* = 7.4 Hz, 1H, Ar), 7.45 (t, *J* = 7.6 Hz, 2H, Ar), 7.41-7.24 (m, 12H, Ar), 7.14 (s, 5H, Ar), 6.87 (d, *J* = 8.2 Hz, 2H, Ar), 5.48-5.36 (m, 2H, H-2-Glc, H-1-Glc), 5.26 (t, *J* = 9.4 Hz, 1H, H-4-Glc), 4.94-4.80 (m, 2H, C*H*$_2$Ph), 4.75-4.54 (m, 7H, H-1-Xyl, 3 x C*H*$_2$Ph), 4.05-3.38 (m, 16H, OC*H*$_3$, 4 x OBu, 6Ha-Glc, 6Hb-Glc, 5Ha-Xyl, 5Hb-Xyl, H-2-Xyl, H-3-Glc, H-4 Xyl, H-3-Xyl, H-5-Glc), 2.66-2.51 (m, 3H, Lev), 2.46-2.36 (m, 1H), 2.06 (s, 3H, Lev), 1.57-1.47 (m, 2H, Bu), 1.31-1.19 (m, 4H, Bu), 1.04-0.96 (m, 2H, Bu), 0.80 (t, *J* = 7.4 Hz, 3H, C*H*$_3$), 0.66 (t, *J* = 7.4 Hz, 3H, C*H*$_3$) ppm. ^{13}C NMR (100 MHz, CDCl3): δ = 206.2, 171.3, 164.8 (3C, C=O), 159.1, 138.9, 138.3, 137.3, 133.3, 130.3, 129.8, 129.5, 129.2, 128.4, 128.3, 128.2, 127.9, 127.7, 127.6, 127.4, 113.7 (25C, Ar), 97.4 (1C, C-1-Xyl), 96.4 (1C, C-1Glc), 81.0 (1C, C-3-Xyl), 79.3 (1C, C-3-Glc), 79.2 (1C, C-2-Xyl), 77.8 (1C, C-4-Xyl), 75.7, 74.0 (2C, *C*H$_2$Ph), 73.7 (1C, C-5-Glc), 73.3 (1C, *C*H$_2$Ph), 73.0 (1C, C-2-Glc), 72.3 (1C, *C*H$_2$Ph), 70.3 (1C, C-4-Glc), 67.9, 67.7 (2C, OBu), 66.8 (1C, C-6-Glc), 60.0 (1C, C-5-Xyl), 55.1 (1C, O*C*H$_3$), 37.6 (1C, Lev), 31.8, 31.6 (2C, Bu), 29.6 (1C, O=C*C*H$_3$), 27.7 (1C, Lev), 18.5, 18.1, 13.5, 13.3 (4C, Bu). ESI-HRMS: m/z $[M+Na]^+$ calcd. for $C_{60}H_{73}NaO_{17}S$: 1119.4483; found 1119.4469. IR (neat) ν_{max}: 2963, 1734, 1267, 1091, 1072, 1030 cm^{-1}.

2.4.4 Automated Glycan Assembly

Benzyloxycarbonyl-(4-(2-aminoethyl)benzyl) 2-O-benzoyl-3-O-benzyl-6-O-[2,3,4-O-tribenzyl-α-D-xylopyranosyl]-β-D-glucopyranosyl-(1->4)-2-O-benzoyl-3,6-O-dibenzyl-β-D-glucopyranoside (12)

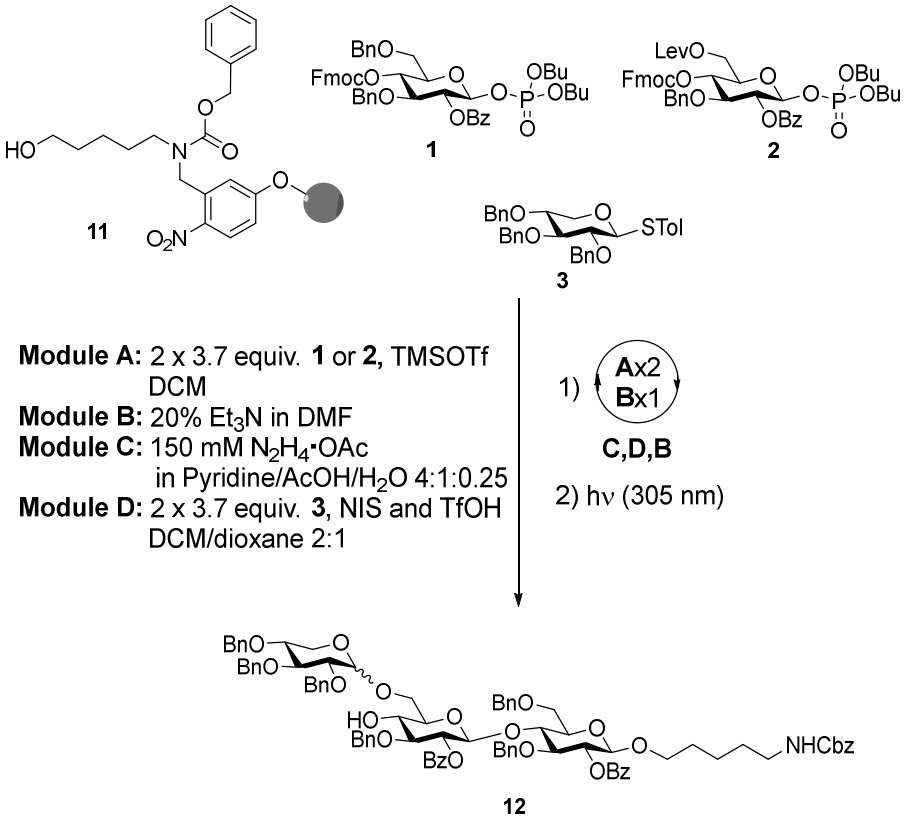

Linker-functionalized resin **11** (40 mg, 16.9 µmol) was placed in the reaction vessel of the synthesizer and synthesizer modules were applied as follows:

Module **A** (2 x 3.7 equiv **1**, TMSOTf, DCM, 2 x 35 min, -30 °C to -15 °C)

Module **B** (20% NEt_3 in DMF, 3 x 5 min, rt)

Module **A** (2x 3.7 equiv **2**, TMSOTf, DCM, 2 x 35 min, -35 °C to -15 °C)

Module **C** (150 mM N_2H_4·AcOH in pyridine/AcOH/H_2O 4:1:0.25, 3 x 30 min, rt)

Module **D** (2 x 3.7 equiv **3**, NIS and TfOH, DCM/dioxane 2:1, 2 x 35 min, -55 °C to -35 °C)

Module **B** (20% NEt_3 in DMF, 3 x 5 min, rt)

Cleavage from the resin using UV irradiation at 305 nm in a continuous flow photoreactor afforded the protected trisaccharide **12** as a mixture of α/β-isomers. The crude product was purified by normal phase HPLC using a semi-preparative Luna 5u Silica 100A column.

NP-HPLC of the crude fully protected α/β-mixture of trisaccharides **12**:

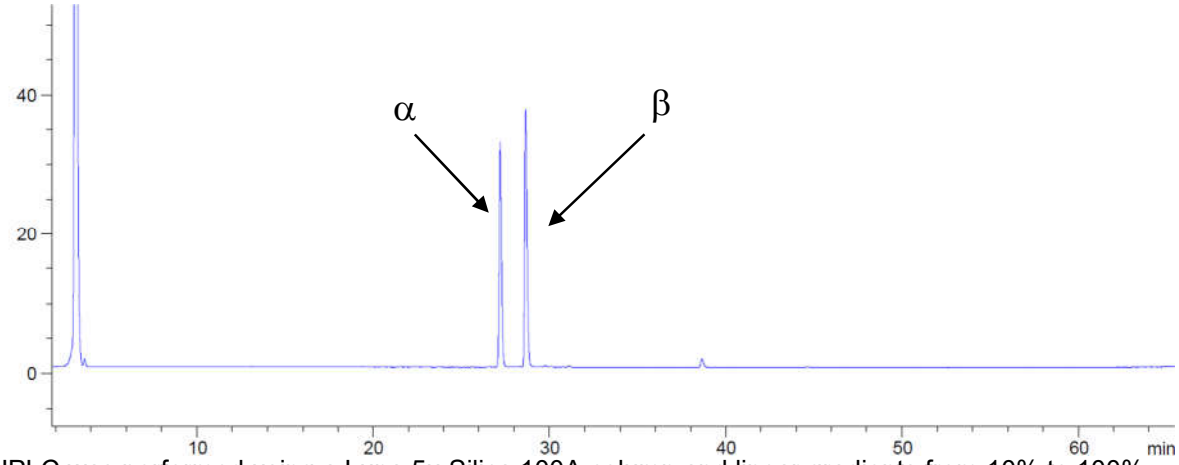

HPLC was performed using a Luna 5u Silica 100A column and linear gradients from 10% to 100% ethyl acetate in hexane (40 min, flow rate 1 mL/min).

The two isomers were separated by normal phase HPLC using a semi-preparative Luna 5u Silica 100A column affording the isomer **12α** (4.3 mg, 2.98 µmol, 18% over 7 steps, based on resin loading) and the isomer **12β** (2.8 mg, 1.94 µmol, 11% over 7 steps, based on resin loading). Isomer **12α**: ^{1}H NMR (600 MHz, $CDCl_3$): δ = 7.90 (d, *J* = 7.5 Hz, 4H), 7.59 (t, *J* = 7.4 Hz, 1H), 7.50 (t, *J* = 7.3 Hz, 1H), 7.44 (t, *J* = 7.8 Hz, 2H), 7.39-7.23 (m, 28H), 7.18-7.08 (m, 6H), 7.07-7.03 (m, 3H), 5.22-5.13 (m, 2H), 5.05 (s, 2H), 4.89-4.81 (m, 3H), 4.79-4.71 (m, 3H), 4.70-4.57 (m, 6H), 4.51 (d, *J* = 3.6 Hz, 1H), 4.37- 4.29 (m, 2H), 4.04 (t, *J* = 9.1 Hz, 1H), 3.90 (dd, *J* = 9.7, 4.2 Hz, 1H), 3.82 (t, *J* = 9.1 Hz, 1H), 3.80-3.73 (m, 2H), 3.70-3.58 (m, 3H), 3.58-3.45 (m, 4H), 3.43 (dd, *J* = 9.5, 3.7 Hz, 1H), 3.39 (td, *J* = 8.8, 4.2 Hz, 1H), 3.32-3.26 (m, 1H), 3.26-3.21 (m, 1H), 3.06 (t, *J* = 9.1 Hz, 1H), 2.90-2.83 (m, 2H), 1.49-1.04 (m, 6H) ppm. ^{13}C NMR (176 MHz, $CDCl_3$): δ = 165.0, 156.2, 138.7, 138.5, 138.2, 138.0, 137.8, 136.7, 133.1, 132.9, 130.0, 129.8, 129.7, 128.5, 128.3, 128.3, 128.2, 128.1, 128.0, 127.9, 127.8, 127.7, 127.6, 127.4, 127.1, 101.1, 100.2, 98.4, 81.4, 80.1, 79.4, 75.7, 74.7, 74.4, 74.0, 73.6, 73.4, 73.2, 72.1, 71.0, 69.4, 67.6, 66.5, 60.2, 40.8, 28.8, 23.0 ppm. MALDI-TOF**:** m/z $[M+Na]^+$ calcd. for $C_{86}H_{91}NaNO_{19}$: 1464.608; found 1464.739. Isomer **12β**: ^{1}H NMR (600 MHz, $CDCl_3$): δ = 7.92 (d, *J* = 7.2 Hz, 2H), 7.89 (d, *J* = 7.2 Hz, 2H), 7.58 (t, *J* = 7.4 Hz, 1H), 7.50 (t, *J* = 7.4 Hz, 1H), 7.43 (t, *J* = 7.8 Hz, 2H), 7.38- 7.21 (m, 28H), 7.19-7.11 (m, 6H), 7.08-7.02 (m, 3H), 5.23-5.14 (m, 2H),

5.04 (s, 2H), 4.89-4.80 (m, 4H), 4.75-4.63 (m, 4H), 4.63-4.56 (m, 3H), 4.35-4.27 (m, 3H), 4.05 (t, *J* = 9.1 Hz, 1H), 3.84 (dd, *J* = 11.7, 5.1 Hz, 1H), 3.80 (dd, *J* = 10.7, 5.5 Hz, 1H), 3.78-3.63 (m, 5H), 3.62-3.57 (m, 2H), 3.54-3.45 (m, 3H), 3.38-3.32 (m, 1H), 3.32-3.27 (m, 2H), 3.26-3.21 (m, 1H), 3.12 (dd, *J* = 11.6, 9.9 Hz, 1H), 2.89-2.81 (m, 2H), 1.49-1.04 (m, 6H) ppm. ^{13}C NMR (176 MHz, $CDCl_3$): δ = 165.0, 156.2, 138.7, 138.2, 138.1, 136.7, 133.3, 132.9, 130.1, 129.7, 129.7, 128.5, 128.3, 128.1, 127.9, 127.8, 127.5, 127.1, 103.6, 101.1, 100.4, 83.1, 81.7, 81.2, 80.5, 75.4, 74.8, 74.5, 74.4, 73.7, 73.5, 73.4, 73.3, 73.2, 73.1, 69.6, 69.2, 67.7, 66.4, 63.5, 40.8, 28.9, 23.0, 22.7 ppm. MALDI-TOF**:** m/z $[M+Na]^+$ calcd. for $C_{86}H_{91}NaNO_{19}$: 1464.608; found 1464.639.

Aminopentyl β-D-glucopyranosyl-(1->4)-β-D-glucopyranosyl-(1->4)-β-D-glucopyranoside (19)

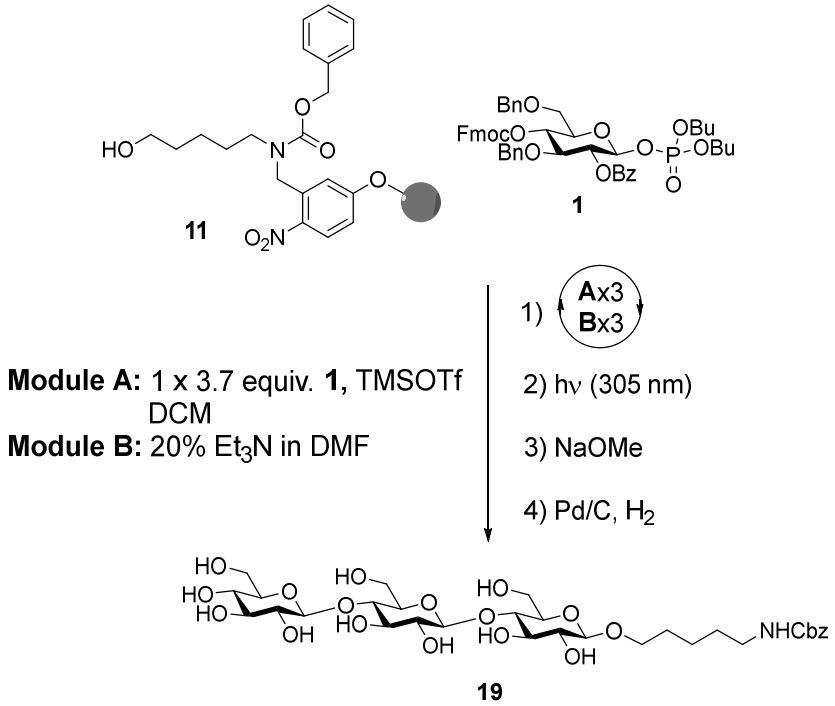

Linker-functionalized resin **11** (53 mg, 16.9 µmol) was placed in the reaction vessel of the synthesizer and synthesizer modules were applied as follows:

Module **A** (3.7 equiv **1**, TMSOTf, DCM, 35 min, -30 °C to -15 °C)

Module **B** (20% NEt_3 in DMF, 3 x 5 min, rt)

Module **A** (3.7 equiv **1**, TMSOTf, DCM, 35 min, -30 °C to -15 °C)

Module **B** (20% NEt_3 in DMF, 3 x 5 min, rt)

Module **A** (3.7 equiv **1**, TMSOTf, DCM, 35 min, -30 °C to -15 °C)
Module **B** (20% NEt_3 in DMF, 3 x 5 min, rt)

Cleavage from the resin using UV irradiation at 305 nm in a continuous flow photoreactor afforded the protected trisaccharide. The crude product was purified by normal phase HPLC using a preparative YMC-Diol-300 column.

Crude NP-HPLC of the protected trisaccharide (ELSD trace):

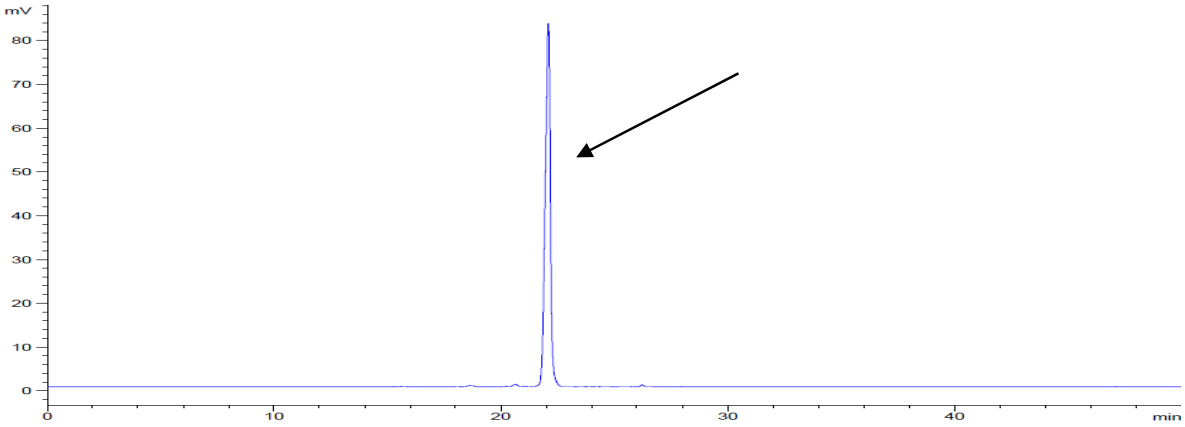

HPLC was performed using a YMC-Diol-300 column and linear gradients from 10% to 100% ethyl acetate in hexane (40 min, flow rate 1 mL/min).

The crude product was purified by normal phase HPLC using a preparative YMC-Diol-300 column affording the protected trisaccharide. The protected trisaccharide was dissolved in THF (3 mL) and NaOMe (0.5 M in MeOH, 0.5 mL) was added. The reaction mixture was stirred overnight and subsequently neutralized by addition of prewashed Amberlite IR-120 resin. The resin was filtered off and the solvents were removed *in vacuo*. The crude product was purified by reversed phase HPLC using a semi-preparative Phenomenex Luna C5 column affording the semi-protected tetrasaccharide. The product was dissolved in a mixture of EtOAc/MeOH/AcOH/H_2O (4:2:2:1, 3 mL) and the resulting solution was added to a round-bottom flask containing Pd/C (10% Pd, 10 mg). The suspension was saturated with H_2 for 30 min and stirred under an H_2-atmosphere overnight. After filtration of the reaction mixture through a syringe filter, the solvents were evaporated to provide the fully deprotected trisaccharide **19** (2.8 mg, 4.75 µmol, 28% over 9 steps, based on resin loading).

RP-HPLC of the deprotected trisaccharide **19** (ELSD trace):

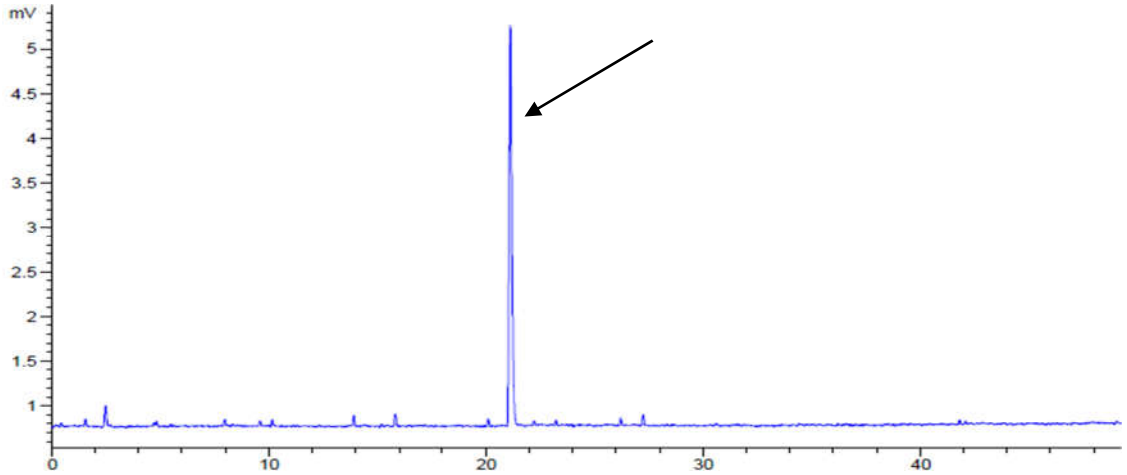

HPLC was performed using a Hypercarb column and a linear gradient from 97.5% to 30% H_2O (containing 0.1% of formic acid) in MeCN (45 min, flow rate 0.7 mL/min).

^{1}H NMR (700 MHz, D_2O): δ = 4.57-4.59 (m, 3H), 4.03-3.92 (m, 4H), 3.84 (td, *J* = 11.9, 5.0 Hz, 2H), 3.78-3.59 (m, 8H), 3.55-3.49 (m, 2H), 3.44 (t, *J* = 9.4 Hz, 1H), 3.38 (t, *J* = 8.3 Hz, 1H), 3.36-3.31 (m, 2H), 3.03 (t, *J* = 7.5 Hz, 2H), 1.75-1.67 (m, 4H), 1.51-1.45 (m, 2H) ppm. ^{13}C NMR (175 MHz, D_2O): δ = 100.6, 100.4, 100.1, 76.6, 76.5, 74.0, 73.5, 72.9, 72.8, 72.4, 72.1, 71.2, 71.0, 71.0, 68.2, 67.5, 58.6, 58.1, 58.0, 37.4, 26.2, 24.5, 20.1 ppm. ESI-HRMS**:** m/z $[M+H]^+$ calcd. for $C_{23}H_{44}NO_{16}$: 590.2655; found 590.2723.

Aminopentyl β-D-glucopyranosyl-(1->4)-β-D-glucopyranosyl-(1->4)-β-D-glucopyranosyl-(1->4)-β-D-glucopyranoside (20)

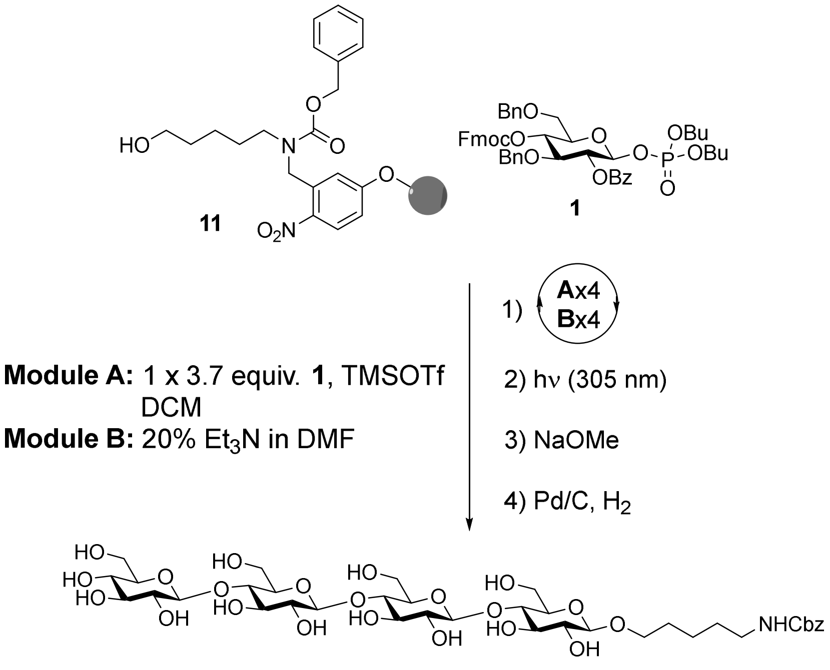

Linker-functionalized resin **11** (85 mg, 22.1 µmol) was placed in the reaction vessel of the synthesizer and synthesizer modules were applied as follows:

Module A (3.7 equiv **1**, TMSOTf, DCM, 35 min, -30 °C to -15 °C)

Module B (20% NEt_3 in DMF, 3 x 5 min, rt)

Module A (3.7 equiv **1**, TMSOTf, DCM, 35 min, -30 °C to -15 °C)

Module B (20% NEt_3 in DMF, 3 x 5 min, rt)

Module A (3.7 equiv **1**, TMSOTf, DCM, 35 min, -30 °C to -15 °C)

Module B (20% NEt_3 in DMF, 3 x 5 min, rt)

Module A (3.7 equiv **1**, TMSOTf, DCM, 35 min, -30 °C to -15 °C)

Module B (20% NEt_3 in DMF, 3 x 5 min, rt)

Cleavage from the resin using UV irradiation at 305 nm in a continuous flow photoreactor afforded the protected tetrasaccharide **32**. The crude product was purified by normal phase HPLC using a preparative YMC Diol column affording the protected tetrasaccharide **32** (22.2 mg, 11.0 µmol, 65% over 9 steps, based on resin loading).

Crude NP-HPLC of tetrasaccharide **32** (ELSD trace):

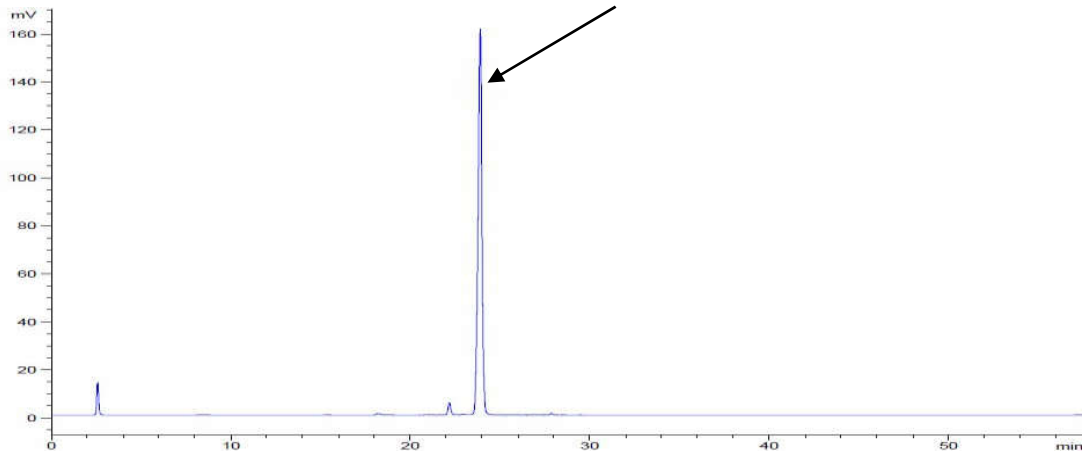

HPLC was performed using a YMC Diol column and a linear gradient from 10% to 100% ethyl acetate in hexane (40 min, flow rate 1 mL/min).

^{1}H NMR (400 MHz, $CDCl_3$): δ = 7.95-7.79 (m, 8H), 7.66-6.85 (m, 57H), 5.24 (dd, *J* = 9.6, 8.1 Hz, 1H), 5.18 (dd, J = 9.7, 8.2 Hz, 1H), 5.14-5.01 (m, 4H), 4.95-4.83 (m, 3H), 4.77-4.40 (m, 12H), 4.34 (dd, *J* = 15.2, 8.1 Hz, 2H), 4.26 (d, *J* = 8.0 Hz, 1H), 4.21-3.89 (m, 6H), 3.81 (t, *J* = 9.0 Hz, 1H), 3.76-3.69 (m, 1H), 3.65-3.29 (m, 13H), 3.28-3.20 (m, 1H), 3.15-3.09 (m, 1H), 2.92-2.79 (m, 4H), 1.47-1.01 (m, 6H) ppm. ^{13}C NMR (100 MHz, $CDCl_3$): δ = 165.0, 164.9, 164.8, 156.2, 138.7, 138.7, 138.6, 138.1, 138.0, 137.7, 137.6, 137.5, 136.7, 133.3, 133.2, 133.0, 132.8, 130.0, 129.7, 129.6, 129.5, 128.5, 128.4, 128.3, 128.2, 128.1, 128.0, 127.9, 127.8, 127.7, 127.6, 127.0, 126.9, 101.1, 100.1, 99.9, 99.7, 81.8, 80.0, 79.8, 76.4, 76.1, 75.8, 74.6, 74.5, 74.3, 74.3, 74.1, 74.0, 73.7, 73.5, 73.4, 73.3, 73.0, 71.1, 69.3, 67.4, 67.0, 66.4, 53.4, 40.7, 29.3, 28.7, 23.0 ppm. MALDI-TOF**:** m/z $[M+Na]^+$ calcd. for $C_{121}H_{123}NaNO_{27}$: 2046.252; found 2045.909.

The protected tetrasaccharide **32** was dissolved in THF (3 mL) and NaOMe (0.5 M in MeOH, 1 mL) was added. The reaction mixture was stirred overnight and subsequently neutralized by addition of prewashed Amberlite IR-120 resin. The resin was filtered off and the solvent was removed *in vacuo.* The crude product was purified by normal-phase HPLC using a preparative YMC-Diol-300 column affording the semi-protected tetrasaccharide. The product was dissolved in a mixture of EtOAc/MeOH/AcOH/H_2O (4:2:2:1, 3 mL) and the resulting solution was added to a round-bottom flask containing Pd/C (10% Pd, 11 mg). The suspension was saturated with H_2 for 30 min and stirred under an H_2-atmosphere

overnight. After filtration of the reaction mixture through a syringe filter the solvents were evaporated and the product was purified by reversed-phase HPLC using a semi-preparative hypercarb column to provide the fully deprotected tetrasaccharide 6 (2.3 mg, 3.06 µmol, 14% over 11 steps, based on resin loading).

RP-HPLC of the deprotected pentasaccharide 6 (ELSD trace):

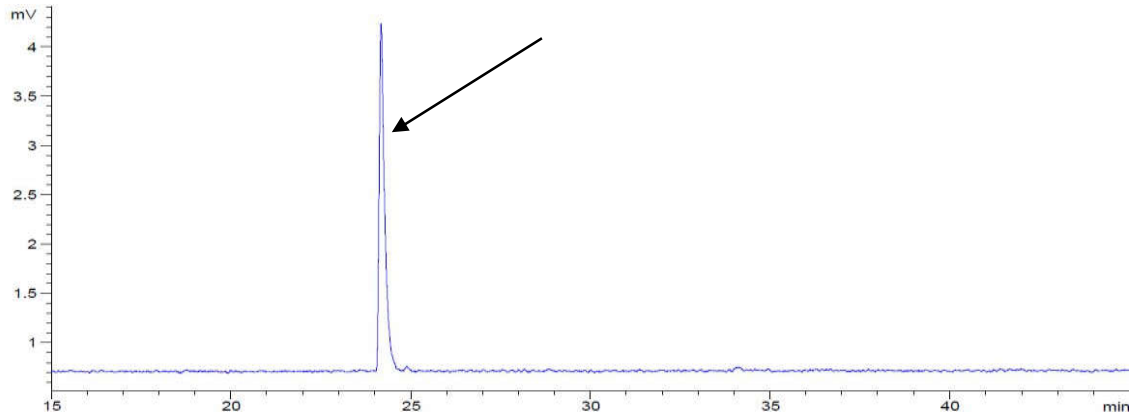

HPLC was performed using a Hypercarb column and a linear gradient from 97.5% to 30% H_2O (containing 0.1% of formic acid) in MeCN (45 min, flow rate 0.7 mL/min).

^{1}H NMR (600 MHz, D_2O): δ = 4.61-4.45 (m, 4H), 4.06-3.28 (m, 26H), 3.02 (t, *J* = 7.6 Hz, 2H), 1.76-1.64 (m, 4H), 1.51-1.44 (m, 2H) ppm.^{13}C NMR (151 MHz, D_2O): δ = 100.3, 100.1, 99.8, 76.3, 76.1, 76.0, 73.7, 73.2, 72.6, 72.5, 72.1, 71.8, 70.9, 70.7, 67.9, 67.2, 58.3, 57.8, 57.6, 37.1, 25.9, 24.2, 19.8 ppm. ESI-HRMS: m/z $[M+Na]^+$ calcd. for $C_{29}H_{53}NNaO_{21}$: 774.3008; found 774.3036.

Aminopentyl β-D-glucopyranosyl-(1->4)-β-D-glucopyranosyl-(1->4)-β-D-glucopyranosyl-(1->4)-β-D-glucopyranosyl-(1->4)-β-D-glucopyranoside (20)

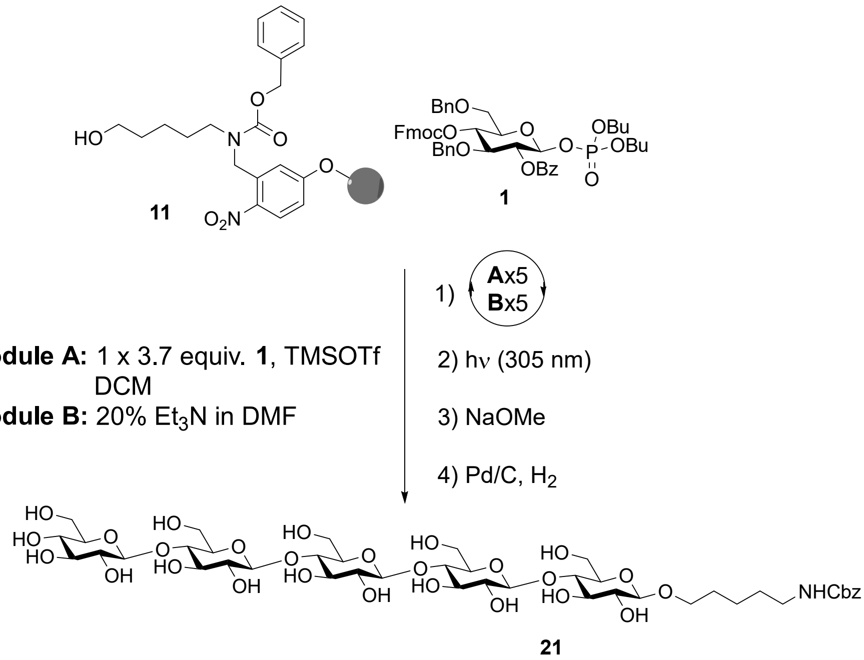

Linker-functionalized resin **11** (53 mg, 16.9 µmol) was placed in the reaction vessel of the synthesizer and synthesizer modules were applied as follows:

Module **A** (3.7 equiv **1**, TMSOTf, DCM, 35 min, -30 °C to -15 °C)

Module **B** (20% NEt_3 in DMF, 3 x 5 min, rt)

Module **A** (3.7 equiv **1**, TMSOTf, DCM, 35 min, -30 °C to -15 °C)

Module **B** (20% NEt_3 in DMF, 3 x 5 min, rt)

Module **A** (3.7 equiv **1**, TMSOTf, DCM, 35 min, -30 °C to -15 °C)

Module **B** (20% NEt_3 in DMF, 3 x 5 min, rt)

Module **A** (3.7 equiv **1**, TMSOTf, DCM, 35 min, -30 °C to -15 °C)

Module **B** (20% NEt_3 in DMF, 3 x 5 min, rt)

Module **A** (3.7 equiv **1**, TMSOTf, DCM, 35 min, -30 °C to -15 °C)

Module **B** (20% NEt_3 in DMF, 3 x 5 min, rt)

Cleavage from the resin using UV irradiation at 305 nm in a continuous flow photoreactor afforded the protected pentasaccharide. The crude product was purified by normal phase HPLC using a preparative YMC-Diol-300 column.

Crude NP-HPLC of the protected pentasaccharide (ELSD trace):

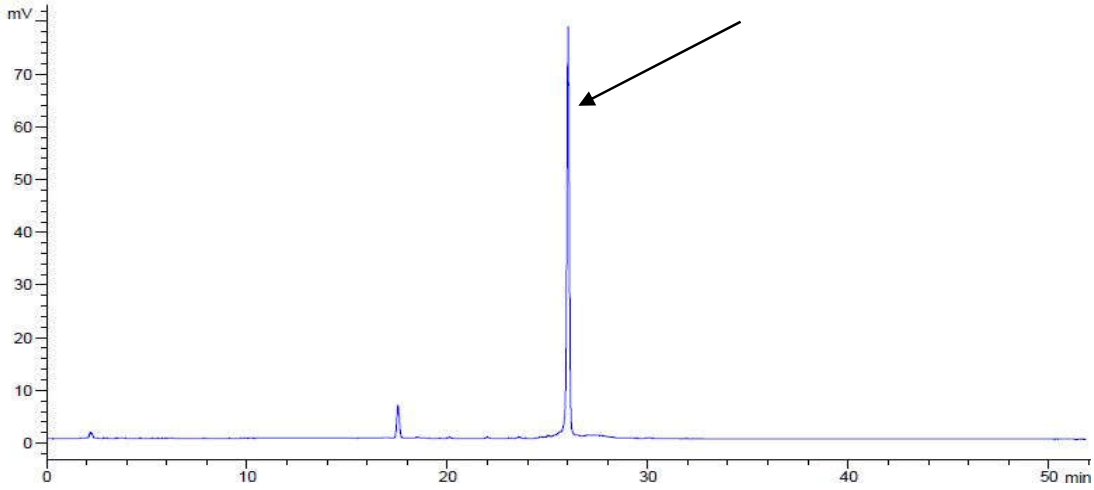

HPLC was performed using a YMC-Diol-300 column and linear gradients from 10% to 100% ethyl acetate in hexane (40 min, flow rate 1 mL/min).

The crude product was purified by normal phase HPLC using a preparative YMC-Diol-300 column affording the protected pentasaccharide. The pentasaccharide was dissolved in THF (3 mL) and NaOMe (0.5 M in MeOH, 0.5 mL) was added. The reaction mixture was stirred overnight and subsequently neutralized by addition of prewashed Amberlite IR-120 resin. The resin was filtered off and the solvent was removed *in vacuo.* The crude product was purified by normal phase HPLC using a preparative YMC-Diol-300 column affording the semi-protected pentasaccharide. The product was dissolved in a mixture of EtOAc/MeOH/AcOH/H_2O (4:2:2:1, 3 mL) and the resulting solution was added to a round-bottom flask containing Pd/C (10% Pd, 10 mg). The suspension was saturated with H_2 for 30 min and stirred under an H_2-atmosphere overnight. After filtration of the reaction mixture through a syringe filter the solvents were evaporated to provide the fully deprotected pentasaccharide **21** (3.5 mg, 3.83 µmol, 23% over 13 steps, based on resin loading).

RP-HPLC of the deprotected pentasaccharide **21** (ELSD trace):

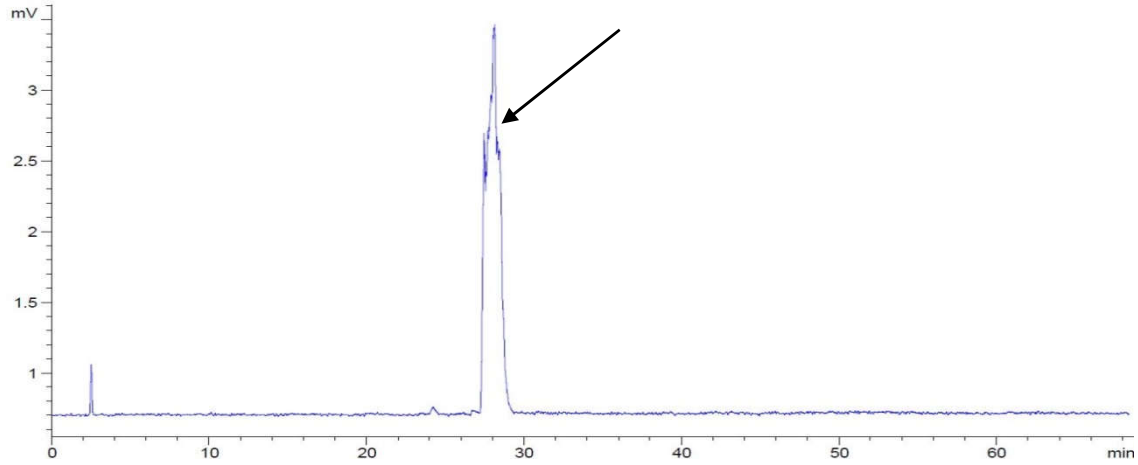

HPLC was performed using a Hypercarb column and a linear gradient from 97.5% to 30% H_2O (containing 0.1% of formic acid) in MeCN (45 min, flow rate 0.7 mL/min).

^{1}H NMR (600 MHz, D_2O): δ = 4.61-4.45 (m, 5H), 4.05-3.90 (m, 6H), 3.88-3.79 (m, 4H), 3.78-3.57 (m, 14H), 3.55-3.47 (m, 2H), 3.45-3.28 (m, 6H), 3.02 (t, *J* = 7.5 Hz, 2H), 1.75-1.65 (m, 4H), 1.53-1.44 (m, 2H) ppm. ^{13}C NMR (151 MHz, D_2O): δ = 102.8, 102.6, 102.3, 78.9, 78.7, 78.5, 76.2, 75.7, 75.1, 75.0, 74.6, 74.3, 74.3, 73.4, 73.2, 70.4, 69.7, 60.8, 60.3, 60.1, 39.6, 28.4, 26.7, 22.4 ppm. ESI-HRMS**:** m/z $[M+H]^+$ calcd. for $C_{35}H_{64}NO_{26}$: 914.3711; found 914.3747.

Aminopentyl β-D-glucopyranosyl-(1->4)-6-*O*-[α-D-xylopyranosyl]-β-D-glucopyranosyl-(1->4)-β-D-glucopyranoside (22)

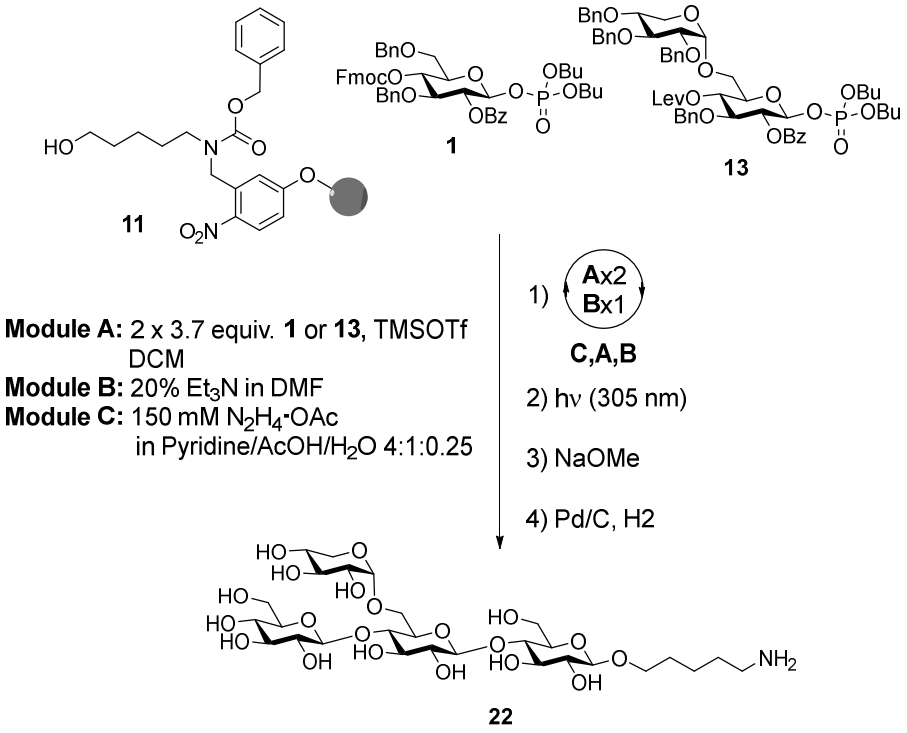

Linker-functionalized resin **11** (53 mg, 16.9 µmol) was placed in the reaction vessel of the synthesizer and synthesizer modules were applied as follows:
Module **A** (2 x 3.7 equiv **1**, TMSOTf, DCM, 2 x 35 min, -30 °C to -15 °C)
Module **B** (20% NEt_3 in DMF, 3 x 5 min, rt)
Module **A** (2 x 3.7 equiv **13**, TMSOTf, DCM, 2 x 40 min, -35 °C to -15 °C)
Module **C** (150 mM $N_2H_4 \cdot AcOH$ in pyridine/AcOH/H_2O 4:1:0.25, 3 x 30 min, rt)
Module **A** (2 x 3.7 equiv **1**, TMSOTf, DCM, 2 x 35 min, -30 °C to -15 °C)
Module **B** (20% NEt_3 in DMF, 3 x 5 min, rt)

Cleavage from the resin using UV irradiation at 305 nm in a continuous flow photoreactor afforded the protected tetrasaccharide **18**. The crude product was purified by normal phase HPLC using a preparative YMC-Diol-300 column.

Crude NP-HPLC of the protected tetrasaccharide **18** (ELSD trace):

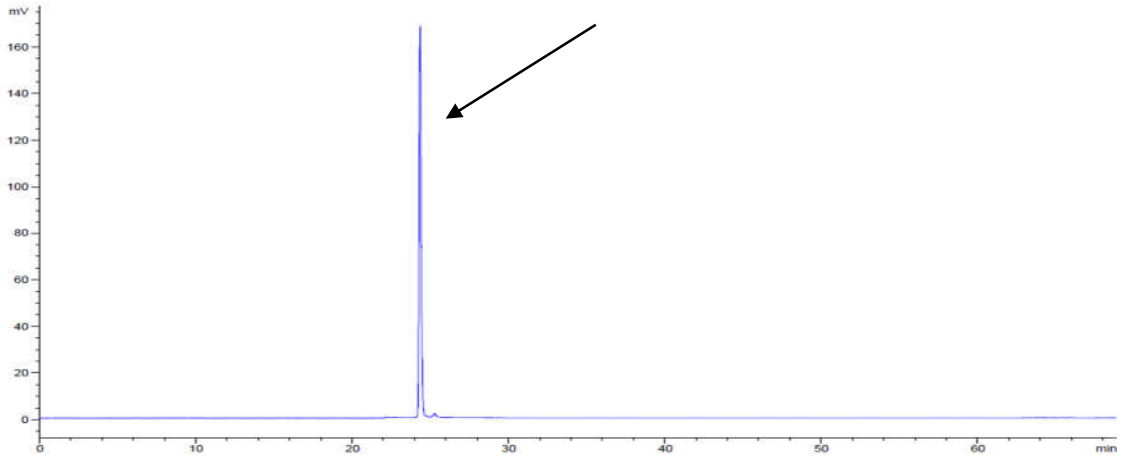

HPLC was performed using a YMC-Diol-300 column and linear gradients from 10% to 100% ethyl acetate in hexane (40 min, flow rate 1 mL/min).

The crude product was purified by normal phase HPLC using a preparative YMC-Diol-300 column affording the protected tetrasaccharide. Tetrasaccharide **18** was dissolved in THF (3 mL) and NaOMe (0.5 M in MeOH, 1 mL) was added. The reaction mixture was stirred overnight and subsequently neutralized by addition of prewashed Amberlite IR-120 resin. The resin was filtered off and the solvents were removed *in vacuo.* The crude product was purified by normal phase HPLC using a preparative YMC-Diol-300 column affording the semi-protected tetrasaccharide. The product was dissolved in a mixture of EtOAc/MeOH/AcOH/H_2O (4:2:2:1, 3 mL) and the resulting solution was added to a round-bottom flask containing Pd/C (10% Pd, 13 mg). The suspension was saturated with H_2 for 30 min and stirred under an H_2-atmosphere overnight. After filtration of the reaction mixture through a syringe filter the solvents were evaporated to provide the fully deprotected pentasaccharide **22** (1.8 mg, 2.49 µmol, 15% over 9 steps, based on resin loading).

RP-HPLC of the deprotected tetrasaccharide **22** (ELSD trace):

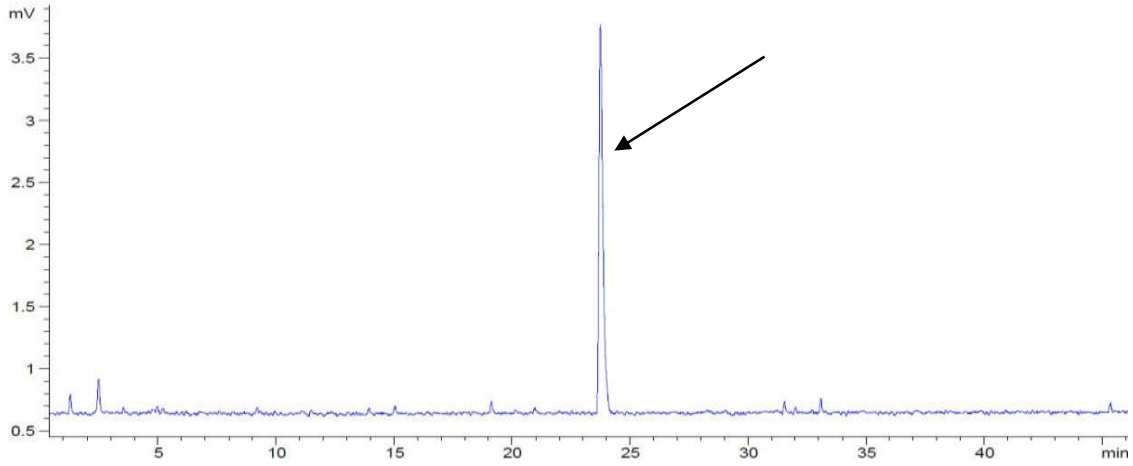

HPLC was performed using a Hypercarb column and a linear gradient from 97.5% to 30% H_2O (containing 0.1% of formic acid) in MeCN (45 min, flow rate 0.7 mL/min).

^{1}H NMR (600 MHz, D_2O): δ = 4.97 (d, *J* = 3.6 Hz, 1H), 4.57 (d, *J* = 8.0 Hz, 1H), 4.54 (d, *J* = 7.9 Hz, 1H), 4.50 (d, *J* = 8.0 Hz, 1H), 4.05-3.90 (m, 5H), 3.86-3.81 (m, 2H), 3.78-3.48 (m, 14H), 3.45-3.38 (m, 2H), 3.36-3.31 (m, 2H), 3.02 (t, *J* = 7.5 Hz 2H), 1.75-1.66 (m, 4H), 1.51-1.44 (m, 2H) ppm.^{13}C NMR (151 MHz, D_2O): δ = 100.4, 100.3, 99.7, 96.6, 77.0, 76.5, 73.8, 73.2, 72.4, 72.2, 71.8, 71.2, 70.8, 70.8, 70.6, 70.6, 69.2, 67.8, 67.2, 63.9, 59.3, 58.3, 57.8, 37.1, 25.9, 24.2, 19.8 ppm. ESI-HRMS**:** m/z $[M+H]^+$ calcd. for $C_{28}H_{52}NO_{20}$: 722.3078; found 722.3108.

Aminopentyl 6-*O*-[α-D-xylopyranosyl]-β-D-glucopyranosyl-(1->4)-β-D-glucopyranosyl-(1->4)-β-D-glucopyranosyl-(1->4)-β-D-glucopyranoside (23)

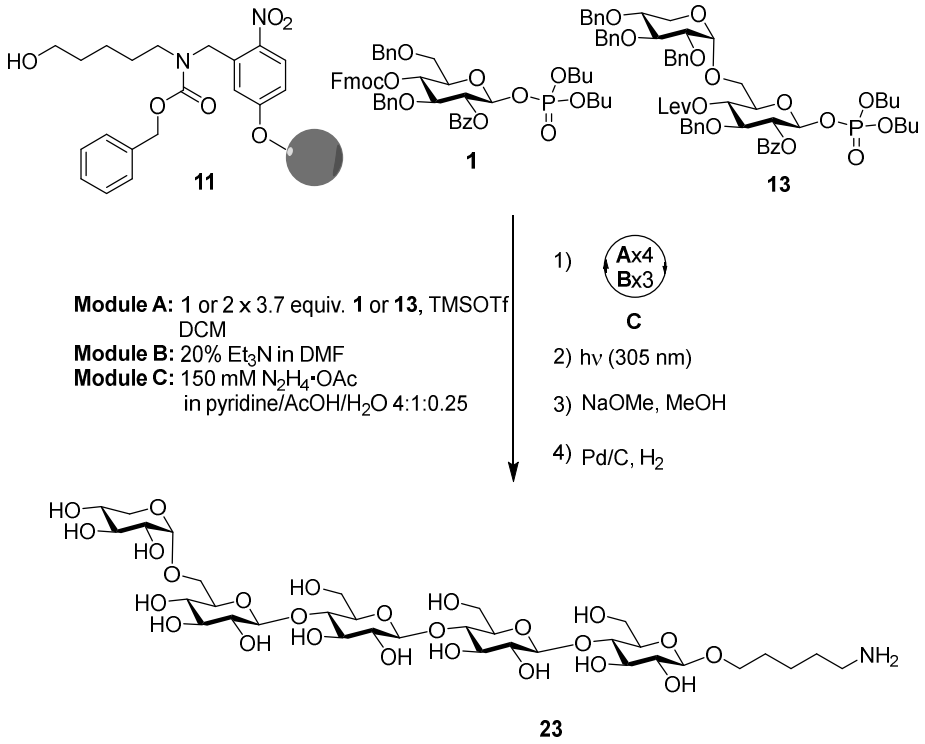

Linker-functionalized resin **11** (52 mg, 16.9 µmol) was placed in the reaction vessel of the synthesizer and synthesizer modules were applied as follows:

Module **A** (1 x 3.7 equiv **1**, TMSOTf, DCM, 2 x 35 min, -30 °C to -15 °C)

Module **B** (20% NEt_3 in DMF, 3 x 5 min, rt)

Module **A** (1 x 3.7 equiv **1**, TMSOTf, DCM, 2 x 35 min, -30 °C to -15 °C)

Module **B** (20% NEt_3 in DMF, 3 x 5 min, rt)

Module **A** (1 x 3.7 equiv **1**, TMSOTf, DCM, 2 x 35 min, -30 °C to -15 °C)

Module **B** (20% NEt_3 in DMF, 3 x 5 min, rt)

Module **A** (2 x 3.7 equiv **13**, TMSOTf, DCM, 2 x 40 min, -35 °C to -15 °C)

Module **C** (150 mM N_2H_4·AcOH in pyridine/AcOH/H_2O 4:1:0.25, 3 x 30 min, rt)

Cleavage from the resin using UV irradiation at 305 nm in a continuous flow photoreactor afforded the protected pentasaccharide. The crude product was purified by normal-phase HPLC using a preparative YMC-Diol-300 column.

Crude NP-HPLC of the protected pentasaccharide (ELSD trace):

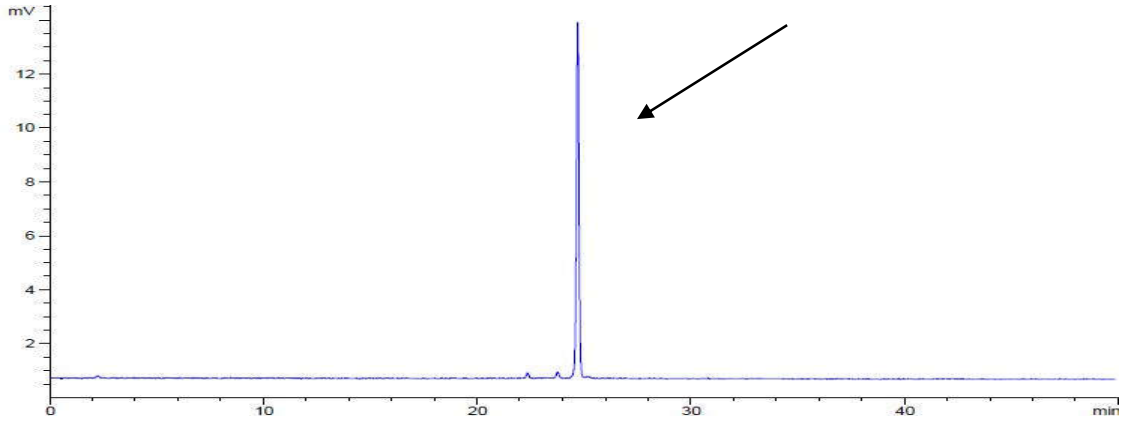

HPLC was performed using a YMC-Diol-300 column and linear gradients from 10% to 100% ethyl acetate in hexane (40 min, flow rate 1 mL/min).

The crude product was purified by normal-phase HPLC using a preparative YMC-Diol-300 column affording the protected pentasaccharide. The protected pentasaccharide was dissolved in THF (3 mL) and NaOMe (0.5 M in MeOH, 1 mL) was added. The reaction mixture was stirred overnight and subsequently neutralized by addition of prewashed Amberlite IR-120 resin. The resin was filtered off and the solvent was removed *in vacuo.* The crude product was purified by normal-phase HPLC using a preparative YMC-Diol-300 column affording the semi-protected pentasaccharide. The product was dissolved in a mixture of EtOAc/MeOH/AcOH/H2O (4:2:2:1, 3 mL) and the resulting solution was added to a round-bottom flask containing Pd/C (10% Pd, 11 mg). The suspension was saturated with H_2 for 30 min and stirred under an H_2-atmosphere overnight. After filtration of the reaction mixture through a syringe filter the solvents were evaporated and the pentasaccharide was purified by reversed-phase HPLC using a semi-preparative hypercarb column to provide the fully deprotected pentasaccharide **23** (1.5 mg, 1.70 µmol, 10% over 11 steps, based on resin loading).

RP-HPLC of the deprotected pentasaccharide **23**(ELSD trace):

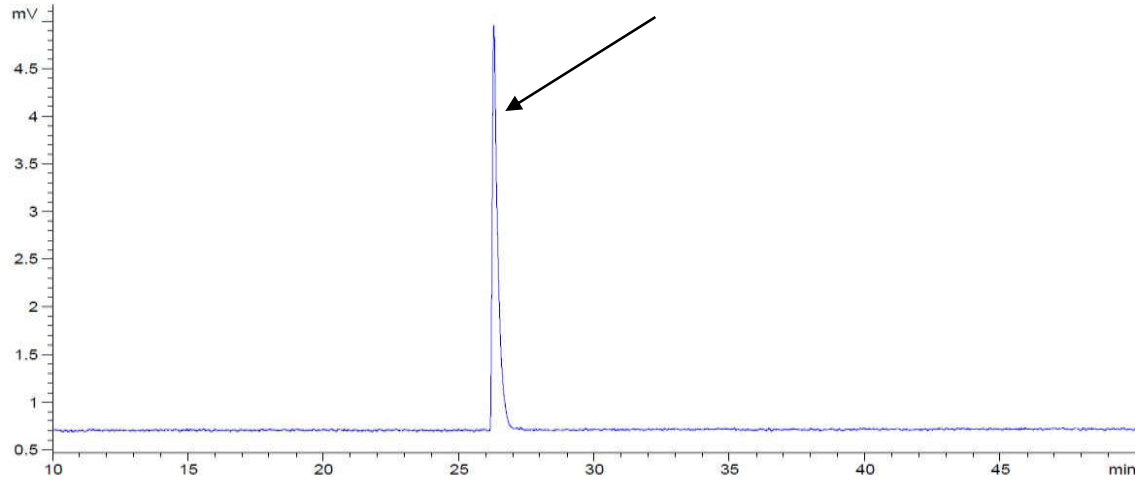

HPLC was performed using a Hypercarb column and a linear gradient from 97.5% to 30% H_2O (containing 0.1% of formic acid) in MeCN (45 min, flow rate 0.7 mL/min).

^{1}H NMR (700 MHz, D_2O): δ = 4.95 (d, *J* = 3.7 Hz, 1H), 4.59-4.45 (m, 4H), 4.01-3.26 (m, 31H), 3.02 (t, *J* = 7.6 Hz, 2H), 1.73-1.62 (m, 4H), 1.49-1.43 (m, 2H) ppm. ^{13}C NMR (176 MHz, D_2O): δ = 103.1, 102.6, 102.3, 98.5, 78.8, 75.9, 75.1, 75.0, 74.6, 74.5, 74.4, 74.3, 73.2, 73.1, 71.8, 70.4, 69.7, 61.5, 60.3, 60.2, 60.1, 39.6, 28.4, 26.7, 22.3. ppm. ESI-HRMS**:** m/z $[M+H]^+$ calcd. for $C_{34}H_{62}NO_{25}$: 884.3611; found 884.3640.

Aminopentyl β-D-glucopyranosyl-(1->4)-6-*O*-[α-D-xylopyranosyl]-β-D-glucopyranosyl-(1->4)-β-D-glucopyranosyl-(1->4)-β-D-glucopyranoside (24)

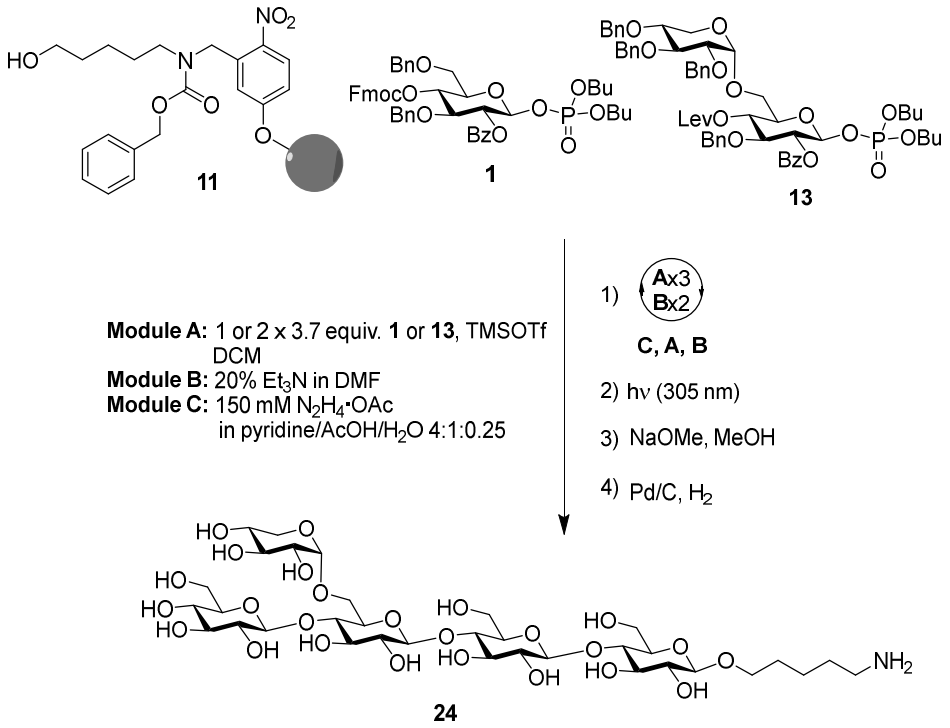

Linker-functionalized resin **11** (52 mg, 16.9 µmol) was placed in the reaction vessel of the synthesizer and synthesizer modules were applied as follows:

Module **A** (1 x 3.7 equiv **1**, TMSOTf, DCM, 2 x 35 min, -30 °C to -15 °C)

Module **B** (20% NEt_3 in DMF, 3 x 5 min, rt)

Module **A** (1 x 3.7 equiv **1**, TMSOTf, DCM, 2 x 35 min, -30 °C to -15 °C)

Module **B** (20% NEt_3 in DMF, 3 x 5 min, rt)

Module **A** (2 x 3.7 equiv **13**, TMSOTf, DCM, 2 x 40 min, -35 °C to -15 °C)

Module **C** (150 mM N_2H_4·AcOH in pyridine/AcOH/H_2O 4:1:0.25, 3 x 30 min, rt)

Module **A** (2 x 3.7 equiv **1**, TMSOTf, DCM, 2 x 35 min, -30 °C to -15 °C)

Module **B** (20% NEt_3 in DMF, 3 x 5 min, rt)

Cleavage from the resin using UV irradiation at 305 nm in a continuous flow photoreactor afforded the protected pentasaccharide. The crude product was purified by normal-phase HPLC using a preparative YMC-Diol-300 column.

Crude NP-HPLC of the protected pentasaccharide (ELSD trace):

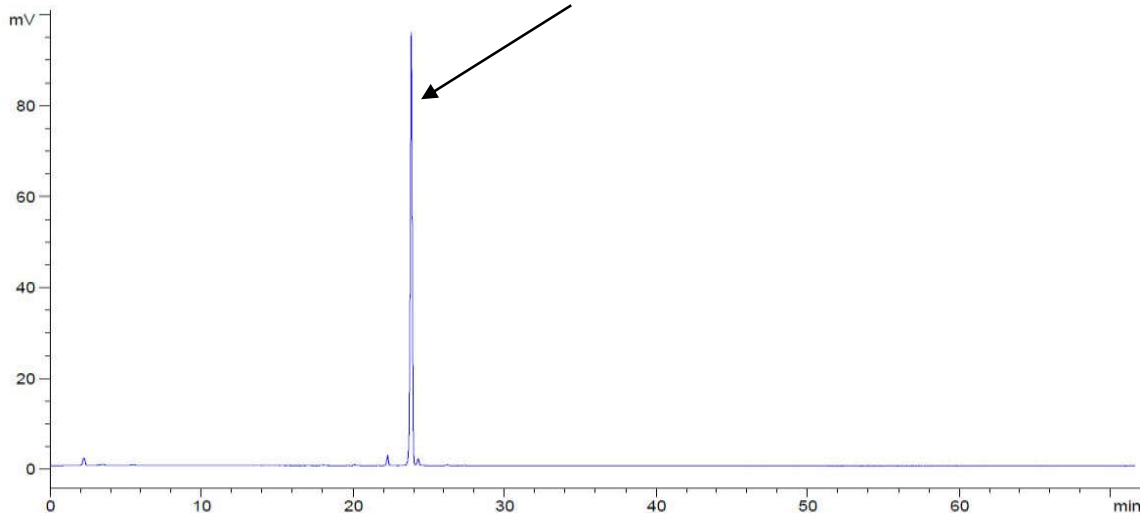

HPLC was performed using a YMC-Diol-300 column and linear gradients from 10% to 100% ethyl acetate in hexane (40 min, flow rate 1 mL/min).

The crude product was purified by normal-phase HPLC using a preparative YMC-Diol-300 column affording the protected pentasaccharide. The protected pentasaccharide was dissolved in THF (3 mL) and NaOMe (0.5 M in MeOH, 1 mL) was added. The reaction mixture was stirred overnight and subsequently neutralized by addition of prewashed Amberlite IR-120 resin. The resin was filtered off and the solvent was removed *in vacuo.* The crude product was purified by normal-phase HPLC using a preparative YMC-Diol-300 column affording the semi-protected pentasaccharide. The product was dissolved in a mixture of EtOAc/MeOH/AcOH/H2O (4:2:2:1, 3 mL) and the resulting solution was added to a round-bottom flask containing Pd/C (10% Pd, 11 mg). The suspension was saturated with H_2 for 30 min and stirred under an H_2-atmosphere overnight. After filtration of the reaction mixture through a syringe filter the solvents were evaporated to provide the fully deprotected pentasaccharide **24** (5.3 mg, 6.00 µmol, 36% over 11 steps, based on resin loading).

RP-HPLC of the deprotected pentasaccharide **24** (ELSD trace):

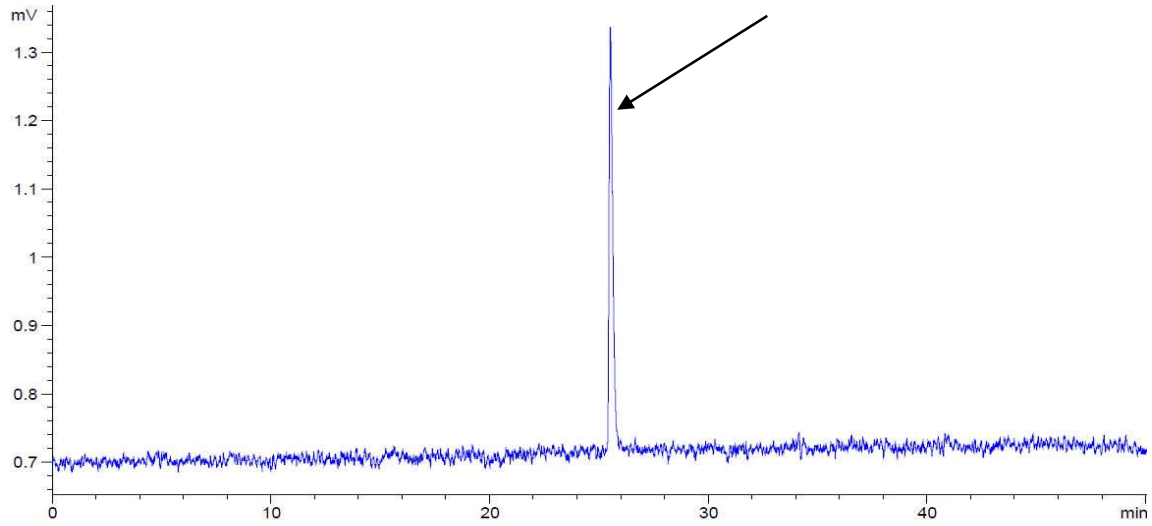

HPLC was performed using a Hypercarb column and a linear gradient from 97.5% to 30% H_2O (containing 0.1% of formic acid) in MeCN (45 min, flow rate 0.7 mL/min).

^{1}H NMR (600 MHz, D_2O): δ = 4.98 (d, *J* = 3.2 Hz, 1H), 4.60-4.46 (m, 4H), 4.05-3.28 (m, 31H), 3.05-3.00 (m, 2H), 1.76-1.62 (m, 4H), 1.56-1.42 (m, 2H).ppm. ^{13}C NMR (151 MHz, D_2O): δ = 100.4, 100.2, 100.1, 99.8, 96.6, 76.6, 76.5, 76.4, 73.8, 73.2, 72.5, 72.1, 71.8, 71.2, 70.8, 70.7, 70.5, 69.2, 67.9, 67.2, 63.9, 59.3, 58.3, 57.8, 57.6, 37.1, 25.9, 24.2, 19.8. ppm. ESI-HRMS**:** m/z $[M+H]^+$ calcd. for $C_{34}H_{62}NO_{25}$: 884,3647; found 884.3611.

Aminopentyl β-D-glucopyranosyl-(1->4)-β-D-glucopyranosyl-(1->4)-6-*O*-[α-D-xylopyranosyl]-β-D-glucopyranosyl-(1->4)-β-D-glucopyranoside (25)

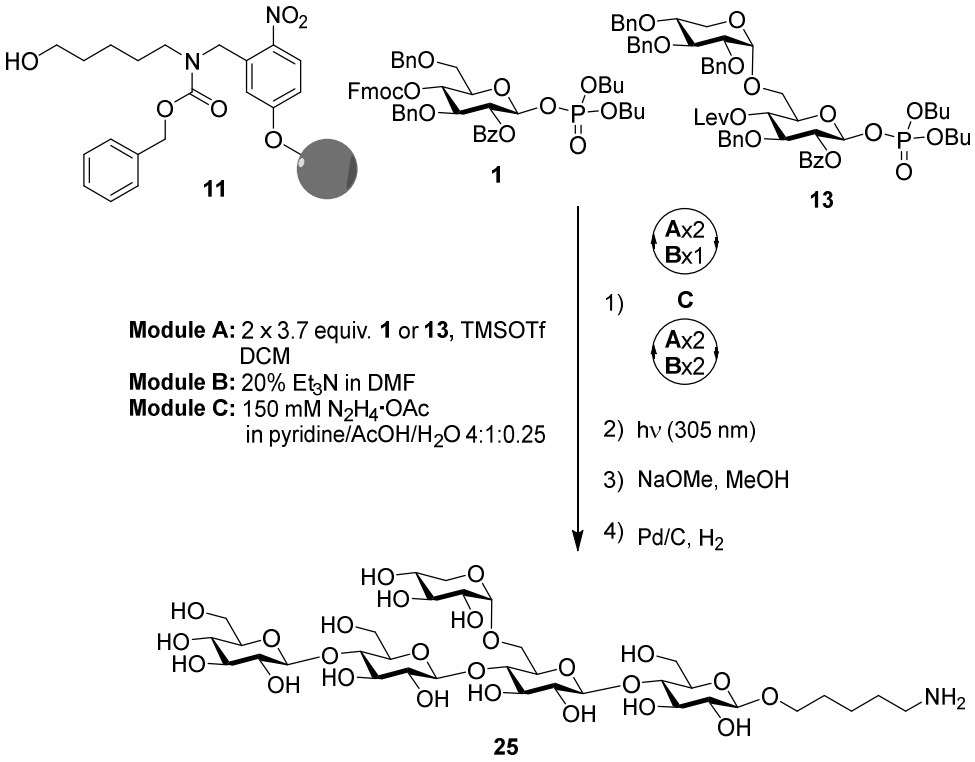

Linker-functionalized resin **11** (52 mg, 16.9 µmol) was placed in the reaction vessel of the synthesizer and synthesizer modules were applied as follows:

Module **A** (1 x 3.7 equiv **1**, TMSOTf, DCM, 2 x 35 min, -30 °C to -15 °C)

Module **B** (20% NEt_3 in DMF, 3 x 5 min, rt)

Module **A** (2 x 3.7 equiv **13**, TMSOTf, DCM, 2 x 40 min, -35 °C to -15 °C)

Module **C** (150 mM N_2H_4·AcOH in pyridine/AcOH/H_2O 4:1:0.25, 3 x 30 min, rt)

Module **A** (2 x 3.7 equiv **1**, TMSOTf, DCM, 2 x 35 min, -30 °C to -15 °C)

Module **B** (20% NEt_3 in DMF, 3 x 5 min, rt)

Module **A** (2 x 3.7 equiv **1**, TMSOTf, DCM, 2 x 35 min, -30 °C to -15 °C)

Module **B** (20% NEt_3 in DMF, 3 x 5 min, rt)

Cleavage from the resin using UV irradiation at 305 nm in a continuous flow photoreactor afforded the protected pentasaccharide. The crude product was purified by normal-phase HPLC using a preparative YMC-Diol-300 column.

Crude NP-HPLC of the protected pentasaccharide (ELSD trace):

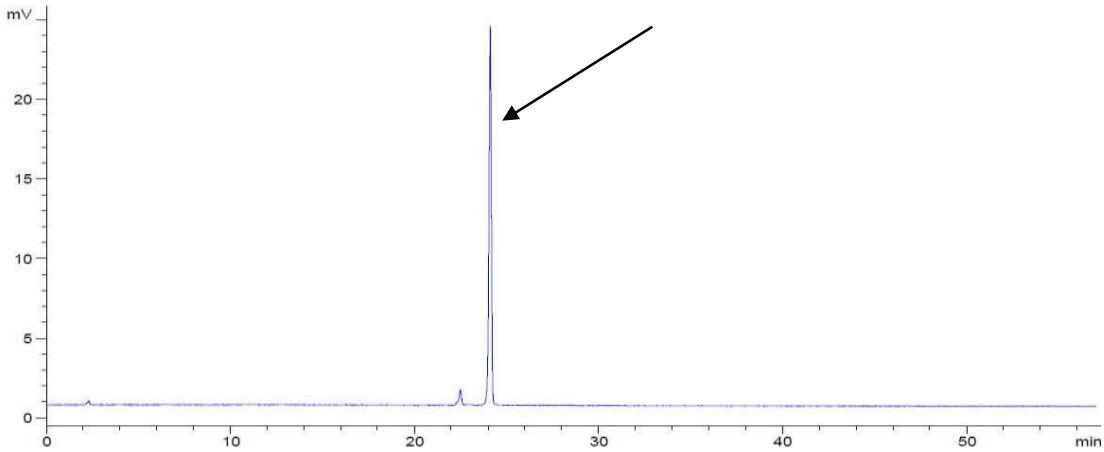

HPLC was performed using a YMC-Diol-300 column and linear gradients from 10% to 100% ethyl acetate in hexane (40 min, flow rate 1 mL/min).

The crude product was purified by normal-phase HPLC using a preparative YMC-Diol-300 column affording the protected pentasaccharide. Th protected pentasaccharide was dissolved in THF (3 mL) and NaOMe (0.5 M in MeOH, 1 mL) was added. The reaction mixture was stirred overnight and subsequently neutralized by addition of prewashed Amberlite IR-120 resin. The resin was filtered off and the solvent was removed *in vacuo.* The crude product was purified by normal-phase HPLC using a preparative YMC-Diol-300 column affording the semi-protected pentasaccharide. The product was dissolved in a mixture of EtOAc/MeOH/AcOH/H2O (4:2:2:1, 3 mL) and the resulting solution was added to a round-bottom flask containing Pd/C (10% Pd, 14 mg). The suspension was saturated with H_2 for 30 min and stirred under an H_2-atmosphere overnight. After filtration of the reaction mixture through a syringe filter the solvents were evaporated to provide the fully deprotected pentasaccharide **25** (6.3 mg, 7.13 µmol, 42% over 11 steps, based on resin loading).

RP-HPLC of the deprotected pentasaccharide **25** (ELSD trace):

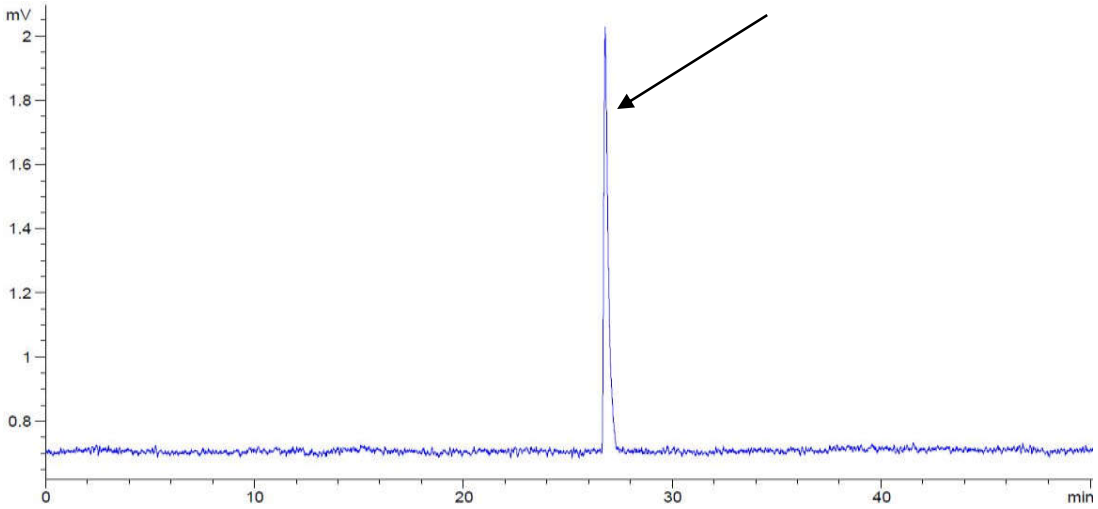

HPLC was performed using a Hypercarb column and a linear gradient from 97.5% to 30% H_2O (containing 0.1% of formic acid) in MeCN (45 min, flow rate 0.7 mL/min).

^{1}H NMR (600 MHz, D_2O): δ = 4.91 (d, *J* = 3.7 Hz, 1H), 4.53-4.40 (m, 4H), 4.01-3.22 (m, 31H), 2.93 (t, *J* = 7.6 Hz, 2H), 1.68-1.58 (m, 4H), 1.45-1.36 (m, 2H) ppm. ^{13}C NMR (101 MHz, D_2O): δ = 100.4, 100.2, 99.7, 96.7, 76.9, 76.4, 76.2, 73.8, 73.2, 72.7, 72.5, 72.2, 71.8, 71.7, 71.2, 70.6, 69.3, 67.9, 67.2, 63.8, 59.3, 58.3, 57.8, 57.7, 37.1, 25.9, 24.2, 19.9 ppm. ESI-HRMS**:** m/z $[M+H]^+$ calcd. for $C_{34}H_{62}NO_{25}$: 884,3647; found 884.3641.

Aminopentyl 6-*O*-[α-D-xylopyranosyl]-β-D-glucopyranosyl-(1->4)-6-*O*-[α-D-xylopyranosyl]-β-D-glucopyranosyl-(1->4)-β-D-glucopyranosyl-(1->4)-β-D-glucopyranoside (26)

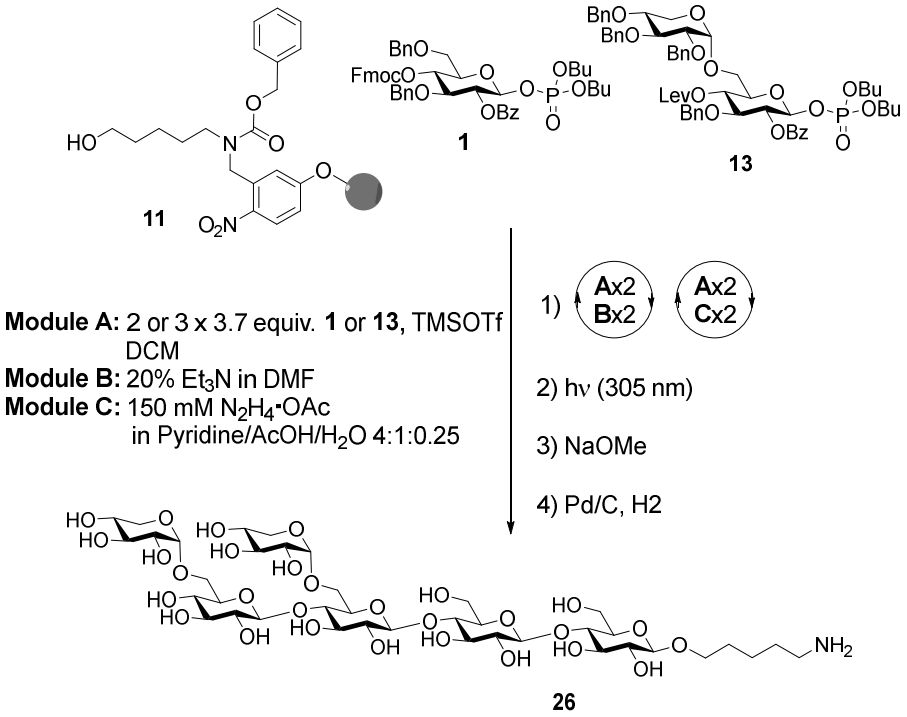

Linker-functionalized resin **11** (53 mg, 16.9 µmol) was placed in the reaction vessel of the synthesizer and synthesizer modules were applied as follows:

Module **A** (2 x 3.7 equiv **1**, TMSOTf, DCM, 2 x 35 min, -30 °C to -15 °C)

Module **B** (20% NEt_3 in DMF, 3 x 5 min, rt)

Module **A** (2 x 3.7 equiv **1**, TMSOTf, DCM, 2 x 35 min, -30 °C to -15 °C)

Module **B** (20% NEt_3 in DMF, 3 x 5 min, rt)

Module **A** (2 x 3.7 equiv **13**, TMSOTf, DCM, 2 x 40 min, -35 °C to -15 °C)

Module **C** (150 mM N_2H_4·AcOH in pyridine/AcOH/H_2O 4:1:0.25, 3 x 30 min, rt)

Module **A** (3 x 3.7 equiv **13**, TMSOTf, DCM, 3 x 40 min, -35 °C to -15 °C)

Module **C** (150 mM N_2H_4·AcOH in pyridine/AcOH/H_2O 4:1:0.25, 3 x 30 min, rt)

Cleavage from the resin using UV irradiation at 305 nm in a continuous flow photoreactor afforded the protected hexasaccharide. The crude product was purified by normal phase HPLC using a preparative YMC-Diol-300 column.

Crude NP-HPLC of the protected hexasaccharide (ELSD trace):

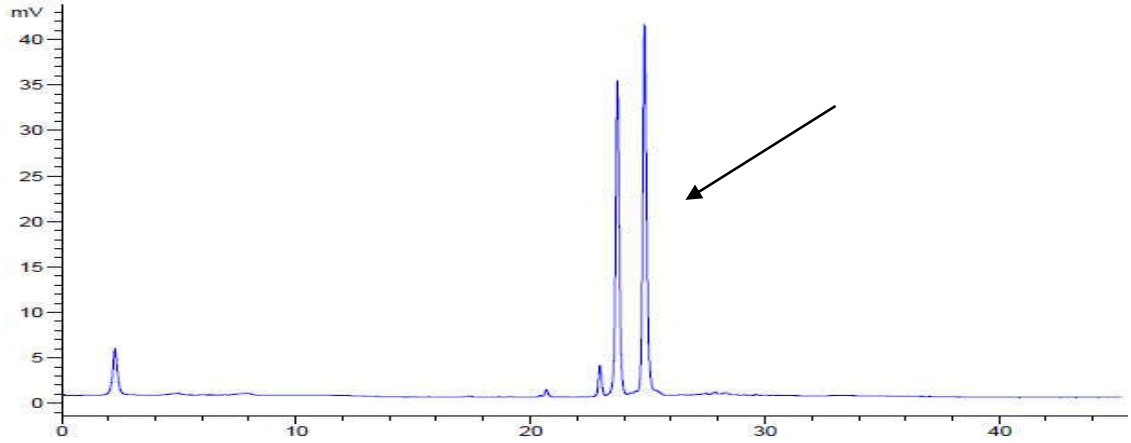

HPLC was performed using an YMC-Diol-300 column and linear gradients from 10% to 100% ethyl acetate in hexane (40 min, flow rate 1 mL/min).

The crude product was purified by normal phase HPLC using a preparative YMC-Diol-300 column affording the protected hexasaccharide. The protected hexasaccharide was dissolved in THF (3 mL) and NaOMe (0.5 M in MeOH, 0.5 mL) was added. The reaction mixture was stirred overnight and subsequently neutralized by addition of prewashed Amberlite IR-120 resin. The resin was filtered off and the solvents were removed *in vacuo.* The crude product was purified by normal phase HPLC using a preparative YMC-Diol-300 column affording the semi-protected hexasaccharide. The product was dissolved in a mixture of EtOAc/MeOH/AcOH/H_2O (4:2:2:1, 3 mL) and the resulting solution was added to a round-bottom flask containing Pd/C (10% Pd, 10 mg). The suspension was saturated with H_2 for 30 min and stirred under an H_2-atmosphere overnight. After filtration of the reaction mixture through a syringe filter the solvents were evaporated to provide the fully deprotected hexasaccharide **26** (1.5 mg, 1.48 µmol, 9% over 11 steps).

RP-HPLC of the deprotected hexasaccharide **26** (ELSD trace):

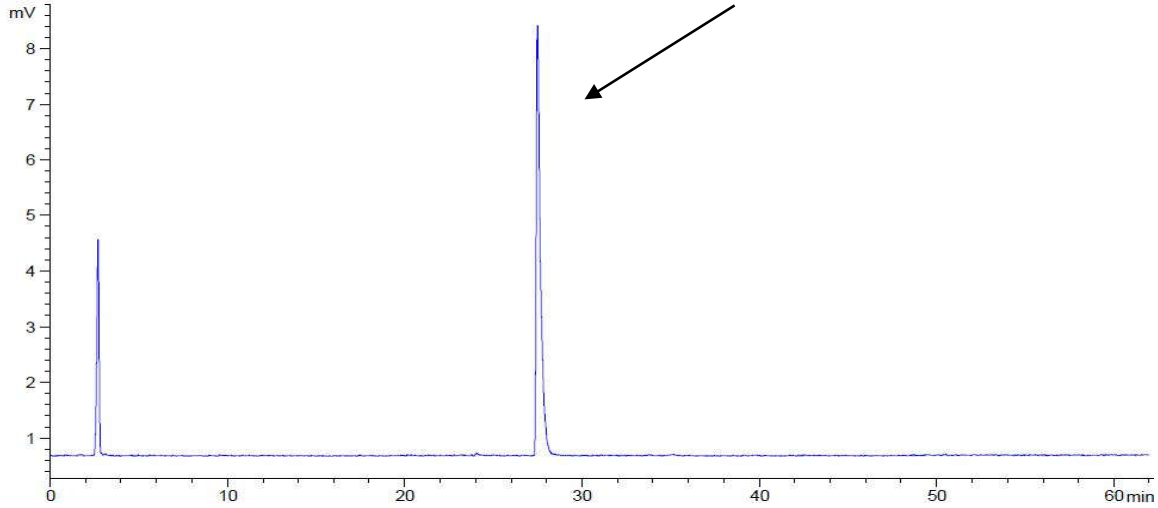

HPLC was performed using a Hypercarb column and a linear gradient from 97.5% to 30% H_2O (containing 0.1% of formic acid) in MeCN (45 min, flow rate 0.7 mL/min).

^{1}H NMR (700 MHz, D_2O): δ = 5.01-4.94 (m, 2H), 4.59-4.54 (m, 3H), 4.50 (d, *J* = 8.4 Hz, 1H), 4.05-3.91 (m, 6H), 3.87-3.52 (m, 26H), 3.44-3.31 (m, 4H), 3.06-3.01 (m, 2H), 1.74-1.66 (m, 4H), 1.52-1.44 (m, 2H) ppm. ^{13}C NMR (176 MHz, D_2O): δ = 178.5, 178.4, 101.5, 101.1, 101.0, 100.7, 97.5, 96.9, 77.9, 77.5, 77.3, 74.2, 73.4, 73.0, 73.0, 72.8, 72.7, 72.0, 71.7, 71.6, 71.6, 71.4, 70.1, 68.8, 68.2, 68.1, 64.7, 64.6, 60.2, 59.9, 58.7, 58.5, 38.0, 26.8, 25.1, 20.7 ppm. ESI-HRMS**:** m/z $[M+H]^+$ calcd. for $C_{39}H_{70}NO_{29}$: 1016.4029; found 1016.4093.

Aminopentyl β-D-glucopyranosyl-(1->4)-6-*O*-[α-D-xylopyranosyl]-β-D-glucopyranosyl-(1->4)-6-*O*-[α-D-xylopyranosyl]-β-D-glucopyranosyl-(1->4)-β-D-glucopyranoside (27)

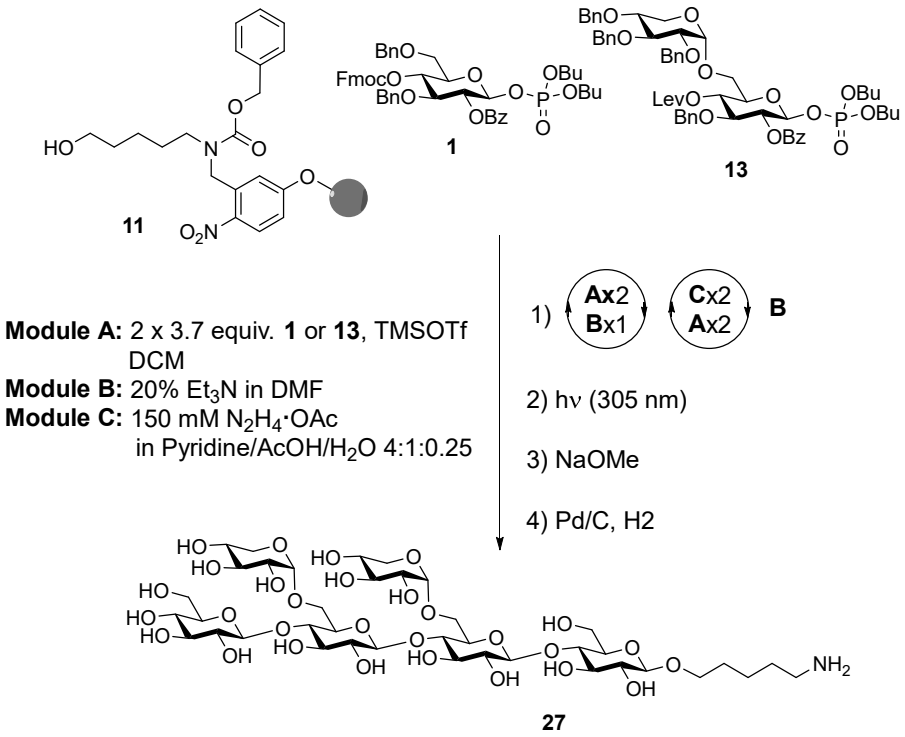

Linker-functionalized resin **11** (53 mg, 16.9 µmol) was placed in the reaction vessel of the synthesizer and synthesizer modules were applied as follows:
Module **A** (2 x 3.7 equiv **1**, TMSOTf, DCM, 2 x 35 min, -30 °C to -15 °C)
Module **B** (20% NEt_3 in DMF, 3 x 5 min, rt)
Module **A** (2 x 3.7 equiv **13**, TMSOTf, DCM, 2 x 40 min, -35 °C to -15 °C)
Module **C** (150 mM N_2H_4·AcOH in pyridine/AcOH/H_2O 4:1:0.25, 3 x 30 min, rt)
Module **A** (2 x 3.7 equiv **13**, TMSOTf, DCM, 2 x 40 min, -35 °C to -15 °C)
Module **C** (150 mM N_2H_4·AcOH in pyridine/AcOH/H_2O 4:1:0.25, 3 x 30 min, rt)
Module **A** (2 x 3.7 equiv **1**, TMSOTf, DCM, 2 x 35 min, -30 °C to -15 °C)
Module **B** (20% NEt_3 in DMF, 3 x 5 min, rt)

Cleavage from the resin using UV irradiation at 305 nm in a continuous flow photoreactor afforded the protected tetrasaccharide. The crude product was purified by normal phase HPLC using a preparative YMC-Diol-300 column.

Crude NP-HPLC of the protected hexasaccharide (ELSD trace):

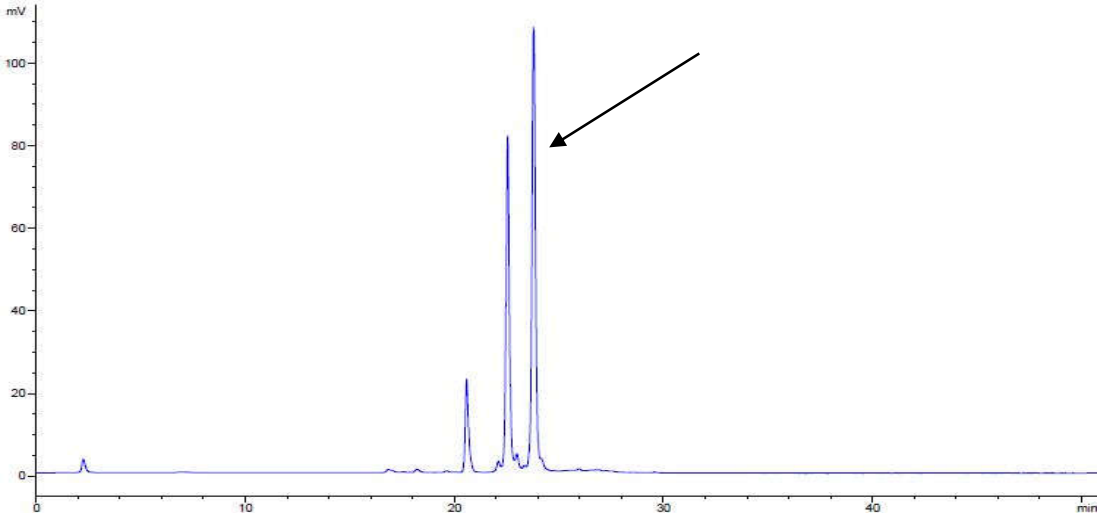

HPLC was performed using an YMC-Diol-300 column and linear gradients from 10% to 100% ethyl acetate in hexane (40 min, flow rate 1 mL/min).

The crude product was purified by normal phase HPLC using a preparative YMC-Diol-300 column affording the protected hexasaccharide (13.9 mg, 5.25 µmol, 31% over 9 steps, based on resin loading). The protected hexasaccharide from two different batches were combined (26.8 mg, 10.1 µmol), dissolved in THF (3 mL) and NaOMe (0.5 M in MeOH, 1 mL) was added. The reaction mixture was stirred overnight and subsequently neutralized by addition of prewashed Amberlite IR-120 resin. The resin was filtered off and the solvents were removed *in vacuo*. The crude product was purified by normal phase HPLC using a preparative YMC-Diol-300 column affording the semi-protected hexasaccharide. The product was dissolved in a mixture of EtOAc/MeOH/AcOH/H_2O (4:2:2:1, 3 mL) and the resulting solution was added to a round-bottom flask containing Pd/C (10% Pd, 20 mg). The suspension was saturated with H_2 for 30 min and stirred under an H_2-atmosphere overnight. After filtration of the reaction mixture through a syringe filter the solvents were evaporated to provide the fully deprotected hexasaccharide **27** (5.6 mg, 5.51 µmol, 55% over 2 steps).

RP-HPLC of the deprotected hexasaccharide **27** (ELSD trace):

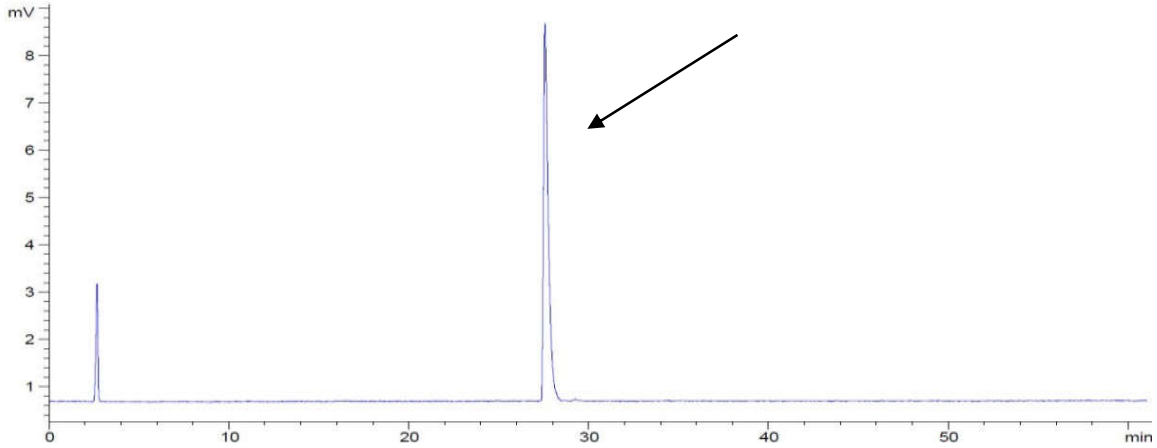

HPLC was performed using a Hypercarb column and a linear gradient from 97.5% to 30% H_2O (containing 0.1% of formic acid) in MeCN (45 min, flow rate 0.7 mL/min).

^{1}H NMR (600 MHz, D_2O): δ = 4.97 (s, 2H), 4.58 (t, *J* = 7.2 Hz, 2H), 4.53 (d, *J* = 7.9 Hz, 1H), 4.50 (d, *J* = 8.0 Hz, 1H), 4.06-3.29 (m, 36H), 3.02 (t, *J* = 7.3 Hz, 2H), 1.73-1.66 (m, 4H), 1.52-1.43 (m, 2H) ppm. ^{13}C NMR (151 MHz, D_2O): δ = 100.4, 100.2, 99.7, 96.6, 96.6, 77.0, 76.9, 76.5, 73.8, 73.2, 72.4, 72.2, 71.8, 71.7, 71.2, 71.0, 70.8, 70.8, 70.8, 70.6, 70.5, 70.5, 69.2, 67.8, 67.2, 63.9, 59.3, 58.3, 57.8, 37.1, 25.9, 24.2, 19.8 ppm. ESI-HRMS**:** m/z $[M+H]^+$ calcd. for $C_{39}H_{70}NO_{29}$: 1016.4029; found 1016.4116.

Aminopentyl β-D-glucopyranosyl-(1->4)-6-*O*-[α-D-xylopyranosyl]-β-D-glucopyranosyl-(1->4)-β-D-glucopyranosyl-(1->4)-6-*O*-[α-D-xylopyranosyl]-β-D-glucopyranosyl-(1->4)-β-D-glucopyranoside (28)

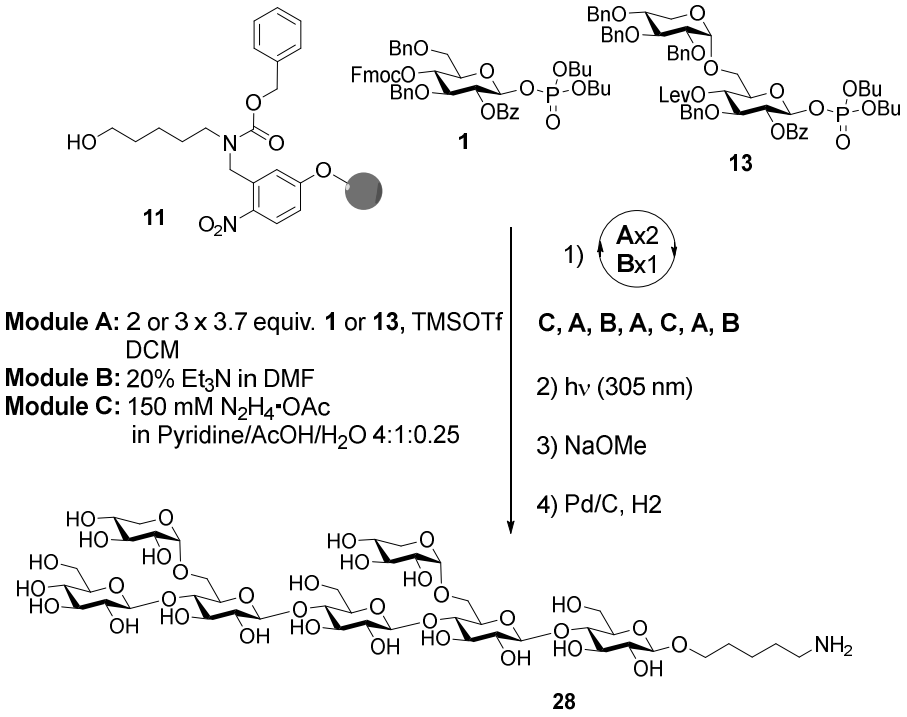

Linker-functionalized resin **11** (53 mg, 16.9 µmol) was placed in the reaction vessel of the synthesizer and synthesizer modules were applied as follows:
Module **A** (2 x 3.7 equiv **1**, TMSOTf, DCM, 2 x 35 min, -30 °C to -15 °C)
Module **B** (20% NEt_3 in DMF, 3 x 5 min, rt)
Module **A** (2 x 3.7 equiv **13**, TMSOTf, DCM, 3 x 40 min, -35 °C to -15 °C)
Module **C** (150 mM N_2H_4·AcOH in pyridine/AcOH/H_2O 4:1:0.25, 3 x 30 min, rt)
Module **A** (2 x 3.7 equiv **1**, TMSOTf, DCM, 2 x 35 min, -30 °C to -15 °C)
Module **B** (20% NEt_3 in DMF, 3 x 5 min, rt)
Module **A** (3 x 3.7 equiv **13**, TMSOTf, DCM, 3 x 40 min, -35 °C to -15 °C)
Module **C** (150 mM N_2H_4·AcOH in pyridine/AcOH/H_2O 4:1:0.25, 3 x 30 min, rt)
Module **A** (2 x 3.7 equiv **1**, TMSOTf, DCM, 2 x 35 min, -30 °C to -15 °C)
Module **B** (20% NEt_3 in DMF, 3 x 5 min, rt)

Cleavage from the resin using UV irradiation at 305 nm in a continuous flow photoreactor afforded the protected heptasaccharide. The crude product was purified by normal phase HPLC using a preparative YMC-Diol-300 column.

Crude NP-HPLC of the protected heptasaccharide (ELSD trace):

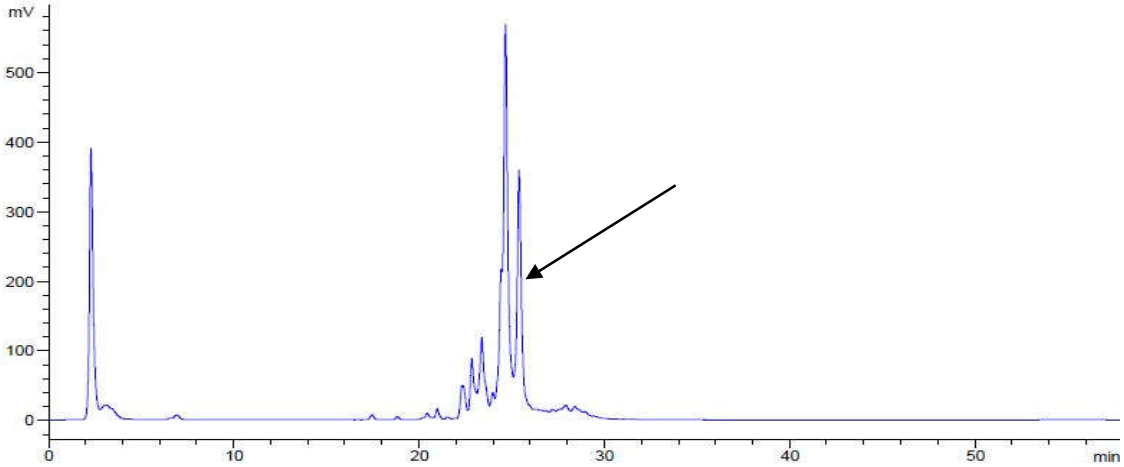

HPLC was performed using an YMC-Diol-300 column and linear gradients from 10% to 100% ethyl acetate in hexane (40 min, flow rate 1 mL/min).

The crude product was purified by normal phase HPLC using a preparative YMC-Diol-300 column affording the protected heptasaccharide. The protected heptasaccharide was dissolved in THF (3 mL) and NaOMe (0.5 M in MeOH, 0.5 mL) was added. The reaction mixture was stirred overnight and subsequently neutralized by addition of prewashed Amberlite IR-120 resin. The resin was filtered off and the solvents were removed *in vacuo.* The crude product was purified by normal phase HPLC using a preparative YMC-Diol-300 column affording the semi-protected heptasaccharide. The product was dissolved in a mixture of EtOAc/MeOH/AcOH/H_2O (4:2:2:1, 3 mL) and the resulting solution was added to a round-bottom flask containing Pd/C (10% Pd, 10 mg). The suspension was saturated with H_2 for 30 min and stirred under an H_2-atmosphere overnight. After filtration of the reaction mixture through a syringe filter the solvents were evaporated to provide the fully deprotected heptasaccharide **28** (2.0 mg, 1.7 µmol, 10% over 13 steps).

RP-HPLC of the deprotected heptasaccharide **28** (ELSD trace):

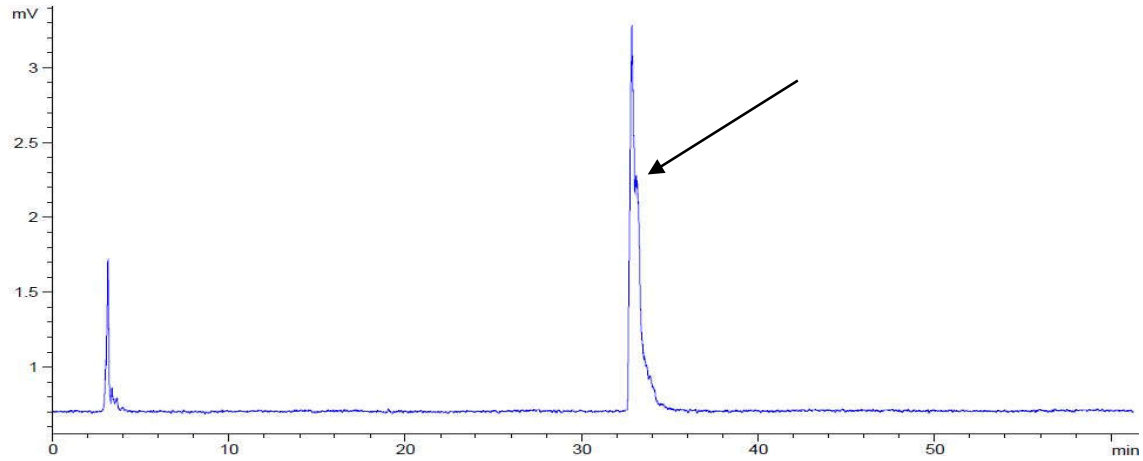

HPLC was performed using a Hypercarb column and a linear gradient from 97.5% to 30% H_2O (containing 0.1% of formic acid) in MeCN (45 min, flow rate 0.7 mL/min).

^{1}H NMR (700 MHz, D_2O): δ = 4.98 (s, 2H), 4.57 (d, *J* = 7.8 Hz, 3H), 4.54 (d, *J* = 8.0 Hz, 1H), 4.51 (d, *J* = 7.9 Hz, 1H), 4.05-3.31 (m, 42H), 3.03 (t, *J* = 7.3 Hz, 2H), 1.75-1.65 (m, 4H), 1.52-1.44 (m, 2H) ppm. ^{13}C NMR (176 MHz, D_2O): δ = 100.9, 100.8, 100.6, 100.2, 97.1, 77.4, 77.1, 77.0, 76.9, 74.3, 73.7, 73.0, 72.9, 72.7, 72.3, 71.7, 71.3, 71.3, 71.1, 71.1, 71.0, 69.7, 68.3, 67.7, 64.4, 60.5, 59.8, 59.5, 58.8, 58.5, 58.3, 58.2, 57.6, 37.6, 26.4, 24.7, 20.3 ppm. ESI-HRMS**:** m/z $[M+H]^+$ calcd. for $C_{45}H_{80}NO_{34}$: 1178.4557; found 1178.4575.

Aminopentyl β-D-glucopyranosyl-(1->4)-6-*O*-[α-D-xylopyranosyl]-β-D-glucopyranosyl-(1->4)-6-*O*-[α-D-xylopyranosyl]-β-D-glucopyranosyl-(1->4)-6-*O*-[α-D-xylopyranosyl]-β-D-glucopyranosyl-(1->4)-β-D-glucopyranoside (29)

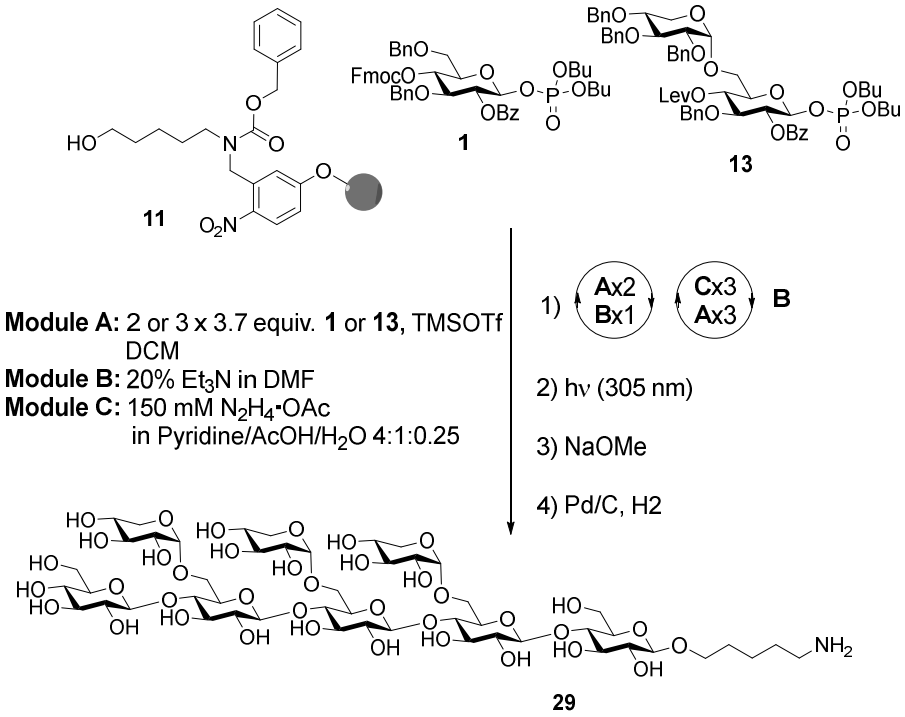

Linker-functionalized resin **11** (53 mg, 16.9 µmol) was placed in the reaction vessel of the synthesizer and synthesizer modules were applied as follows:
Module **A** (2 x 3.7 equiv **1**, TMSOTf, DCM, 2 x 35 min, -30 °C to -15 °C)
Module **B** (20% NEt_3 in DMF, 3 x 5 min, rt)
Module **A** (2 x 3.7 equiv **13**, TMSOTf, DCM, 2 x 40 min, -35 °C to -15 °C)
Module **C** (150 mM N_2H_4·AcOH in pyridine/AcOH/H_2O 4:1:0.25, 3 x 30 min, rt)
Module **A** (3 x 3.7 equiv **13**, TMSOTf, DCM, 3 x 40 min, -35 °C to -15 °C)
Module **C** (150 mM N_2H_4·AcOH in pyridine/AcOH/H_2O 4:1:0.25, 3 x 30 min, rt)
Module **A** (3 x 3.7 equiv **13**, TMSOTf, DCM, 3 x 40 min, -35 °C to -15 °C)
Module **C** (150 mM N_2H_4·AcOH in pyridine/AcOH/H_2O 4:1:0.25, 3 x 30 min, rt)
Module **A** (2 x 3.7 equiv **1**, TMSOTf, DCM, 2 x 35 min, -30 °C to -15 °C)
Module **B** (20% NEt_3 in DMF, 3 x 5 min, rt)

Cleavage from the resin using UV irradiation at 305 nm in a continuous flow photoreactor afforded the protected octasaccharide. The crude product was purified by normal phase HPLC using a preparative YMC-Diol-300 column.

Crude NP-HPLC of the protected octasaccharide (ELSD trace):

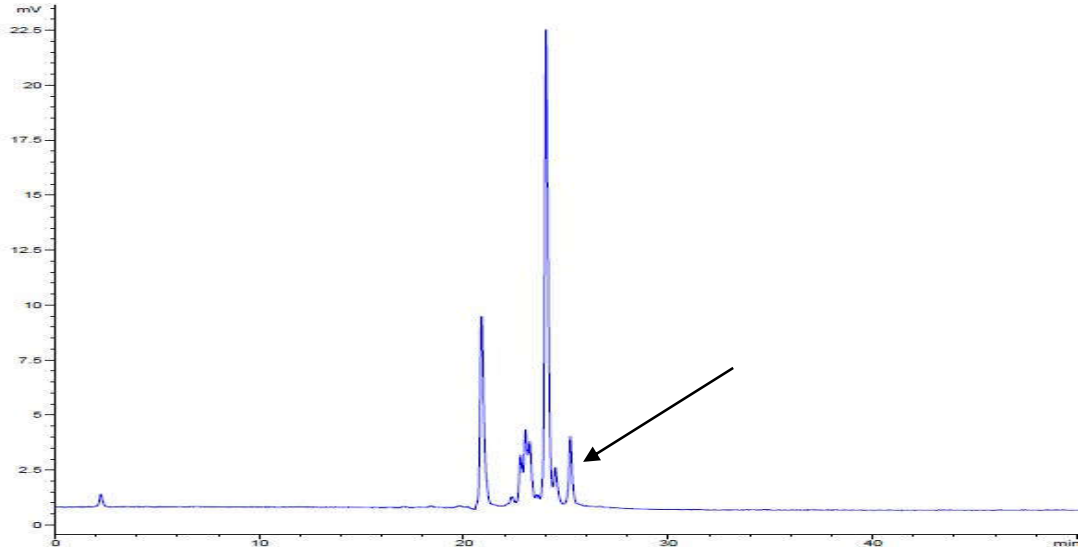

HPLC was performed using an YMC-Diol-300 column and linear gradients from 10% to 100% ethyl acetate in hexane (40 min, flow rate 1 mL/min).

The crude product was purified by normal phase HPLC using a preparative YMC-Diol-300 column affording the protected octasaccharide. The protected octasaccharide was dissolved in THF (3 mL) and NaOMe (0.5 M in MeOH, 0.5 mL) was added. The reaction mixture was stirred overnight and subsequently neutralized by addition of prewashed Amberlite IR-120 resin. The resin was filtered off and the solvents were removed *in vacuo.* The crude product was purified by normal phase HPLC using a preparative YMC-Diol-300 column affording the semi-protected octasaccharide. The product was dissolved in a mixture of EtOAc/MeOH/AcOH/H_2O (4:2:2:1, 3 mL) and the resulting solution was added to a round-bottom flask containing Pd/C (10% Pd, 10 mg). The suspension was saturated with H_2 for 30 min and stirred under an H_2-atmosphere overnight. After filtration of the reaction mixture through a syringe filter the solvents were evaporated to provide the fully deprotected octasaccharide **29** (0.5 mg, 0.38 µmol, 2% over 13 steps).

RP-HPLC of the deprotected octasaccharide **29** (ELSD trace):

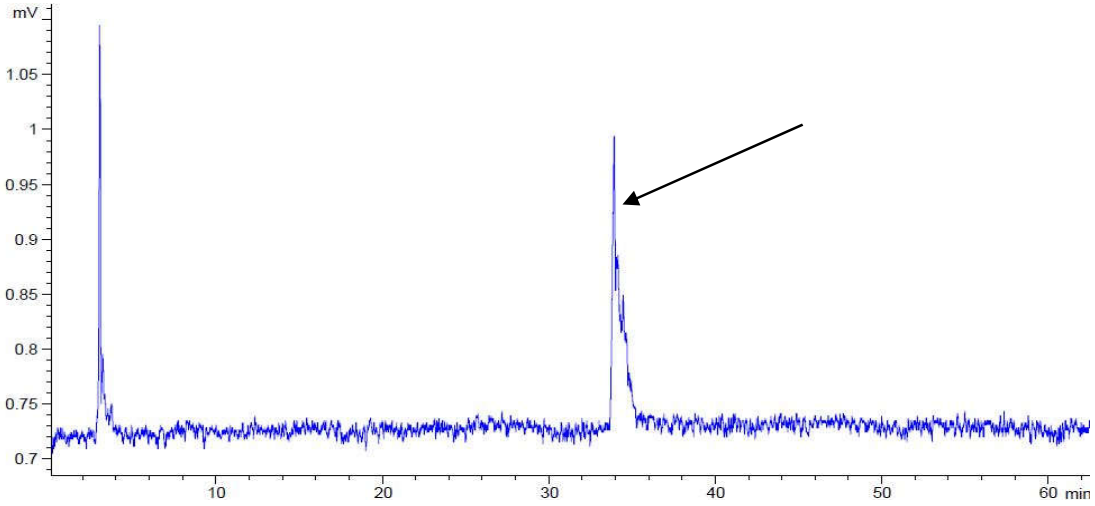

HPLC was performed using a Hypercarb column and a linear gradient from 97.5% to 30% H_2O (containing 0.1% of formic acid) in MeCN (45 min, flow rate 0.7 mL/min).

^{1}H NMR (700 MHz, D_2O): δ = 4.98 (m, 3H), 4.62-4.56 (m, 3H), 4.54 (d, *J* = 7.9 Hz, 1H), 4.51 (d, *J* = 8.1 Hz, 1H), 4.06-3.49 (m, 44H), 3.47-3.40 (m, 3H), 3.03 (t, *J* = 7.5 Hz, 2H), 1.75-1.67 (m, 4H), 1.51-1.46 (m, 2H) ppm. ^{13}C NMR (176 MHz, D_2O): δ = 100.4, 100.3, 99.7, 96.6, 77.0, 73.8, 73.2, 72.4, 72.2, 71.8, 70.8, 69.3, 67.9, 67.2, 63.8, 59.3, 37.1, 25.9, 24.2, 19.9 ppm. ESI-HRMS**:** m/z $[M+Na]^+$ calcd. for $C_{50}H_{87}NaNO_{38}$: 1332.4799; found 1333.4848.

Benzyloxycarbonyl-(4-(2-aminoethyl)benzyl) 2-*O*-benzoyl-3,6-*O*-dibenzyl-β-D-glucopyranosyl-(1->4)-2-*O*-benzoyl-3,6-*O*-dibenzyl-β-D-glucopyranosyl-(1->4)-2-*O*-benzoyl-3,6-*O*-dibenzyl-β-D-glucopyranosyl-(1->4)-2-*O*-benzoyl-3,6-*O*-dibenzyl-β-D-glucopyranoside (31)

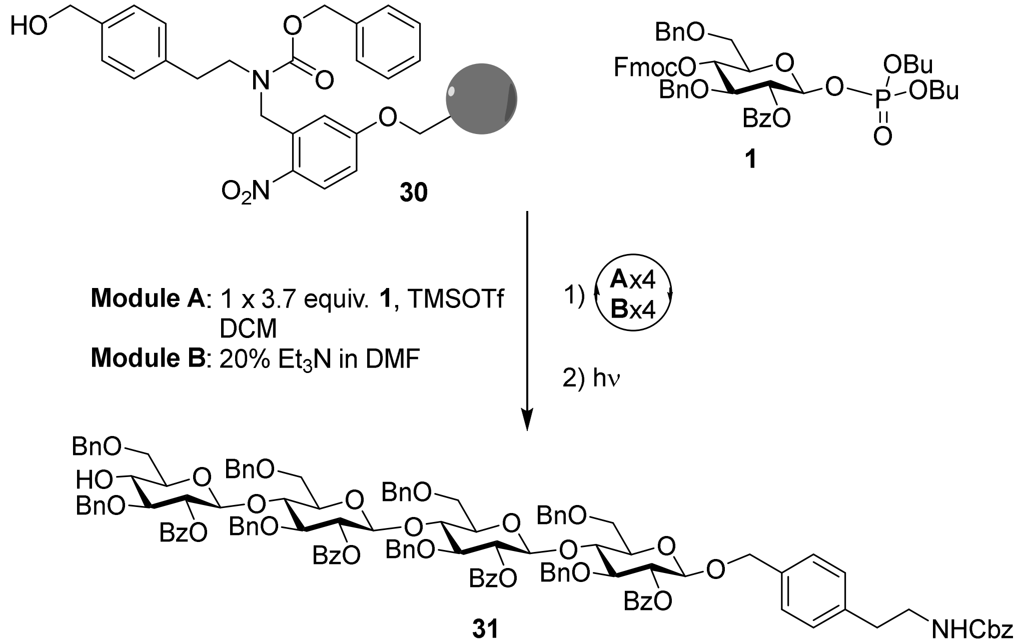

Linker functionalized resin **31** (85 mg, 22.1 µmol) was placed in the reaction vessel of the synthesizer and synthesizer modules were applied as follows:

Module **A** (3.7 equiv **1**, TMSOTf, DCM, 35 min, -30 °C to -15 °C)
Module **C** (20% NEt_3 in DMF, 3 x 5 min, rt)
Module **A** (3.7 equiv **1**, TMSOTf, DCM, 35 min, -30 °C to -15 °C)
Module **C** (20% NEt_3 in DMF, 3 x 5 min, rt)
Module **A** (3.7 equiv **1**, TMSOTf, DCM, 35 min, -30 °C to -15 °C)
Module **C** (20% NEt_3 in DMF, 3 x 5 min, rt)
Module **A** (3.7 equiv **1**, TMSOTf, DCM, 35 min, -30 °C to -15 °C)
Module **C** (20% NEt_3 in DMF, 3 x 5 min, rt)

Cleavage from the resin using UV irradiation at 305 nm in a continuous flow photoreactor afforded the protected tetrasaccharide. The crude product was purified by normal phase HPLC using a preparative YMC Diol column affording the protected tetrasaccharide **31** (30.7 mg, 14.8 µmol, 67% over 9 steps, based on resin loading).

Crude NP-HPLC of tetrasaccharide **31** (ELSD trace):

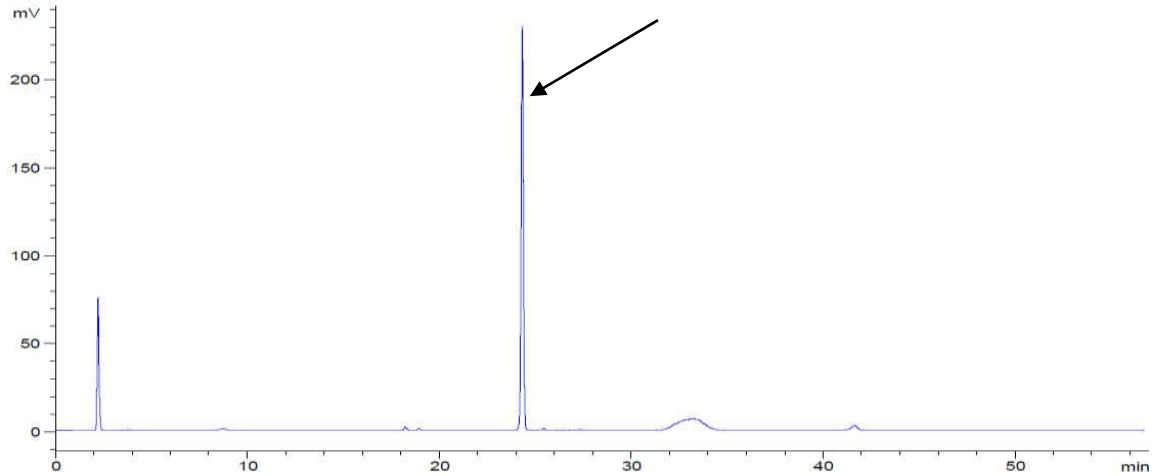

HPLC was performed using an YMC Diol column and a linear gradient from 10% to 100% ethyl acetate in hexane (40 min, flow rate 1 mL/min).

^{1}H NMR (400 MHz, $CDCl_3$): δ = 7.88-7.69 (m, 8H), 7.61-6.71 (m, 61H), 5.21-5.07 (m, 3H), 5.06-4.98 (m, 3H), 4.88-4.74 (m, 3H), 4.70-4.21 (m, 17H), 4.17-3.86 (m, 6H), 3.74 (t, *J* = 9.0 Hz, 1H), 3.58-3.22 (m, 15H), 3.03 (dt, *J* = 9.8, 2.6 Hz, 1H), 2.79 (ddt, *J* = 24.5, 9.8, 2.2 Hz, 1H), 2.62 (t, *J* = 6.9 Hz, 1H) ppm. ^{13}C NMR (100 MHz, $CDCl_3$): δ = 165.0, 164.9, 164.8, 164.7, 156.2, 138.7, 138.7, 138.6, 138.1, 138.0, 137.7, 137.6, 137.5, 136.5, 135.3, 133.3, 133.2, 133.0, 132.8, 130.0, 129.8, 129.7, 129.6, 129.5, 129.0, 128.9, 128.5, 128.3, 128.2, 128.1, 128.0, 127.9, 127.8, 127.7, 127.6, 127.6, 127.0, 126.9, 125.3, 100.0, 99.9, 99.8, 99.3, 81.8, 80.0, 79.8, 76.3, 76.1, 75.8, 74.6, 74.5, 74.3, 74.2, 74.0, 73.7, 73.5, 73.4, 73.0, 72.8, 71.1, 70.0, 67.3, 67.0, 66.6, 42.0, 35.6, 29.7, 21.4 ppm. MALDI-TOF**:** m/z $[M+Na]^+$ calcd. for $C_{125}H_{123}NaNO_{27}$: 2094.294; found 2093.544.

β-D-Glucopyranosyl-(1->4)-β-D-glucopyranosyl-(1->4)-β-D-glucopyranosyl-(1->4)-D-glucopyranose (33)

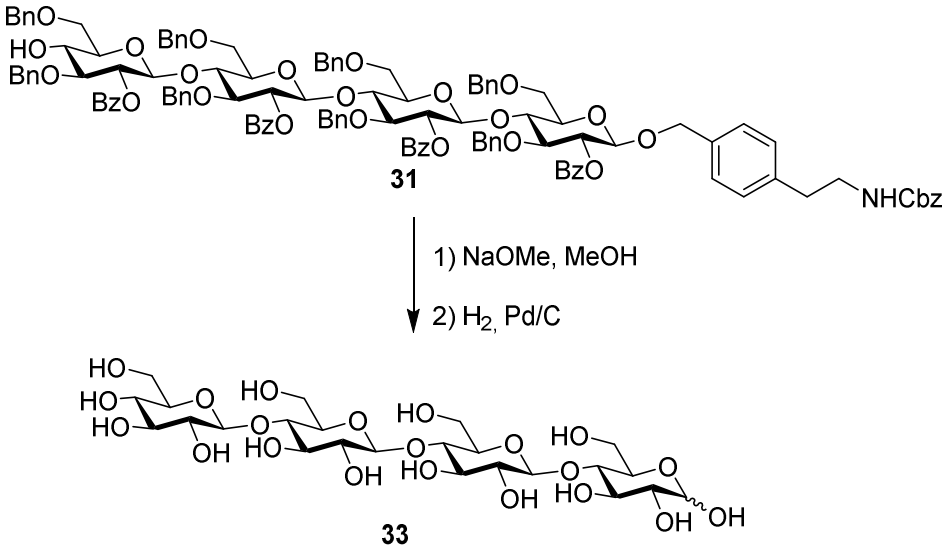

Tetrasaccharide **31** was dissolved in THF (3 mL) and NaOMe (0.5 M in MeOH, 0.5 mL) was added. The reaction mixture was stirred overnight and subsequently neutralized by addition of H^+-Amberlite resin. The resin was filtered off and the solvents were removed *in vacuo.* The crude product was purified by reversed phase HPLC using a preparative YMC Diol column affording the semi-protected disaccharide. The product was dissolved in a mixture of EtOAc/MeOH/AcOH/H_2O (4:2:2:1, 3 mL) and the resulting solution was added to a round-bottom flask containing Pd/C (10% Pd, 20 mg). The suspension was saturated with H_2 for 30 min and stirred under an H_2-atmosphere overnight. After filtration of the reaction mixture through a syringe filter, the solvents were evaporated. The fully deprotected tetrasaccharide **33** was re-dissolved in 0.5 mL water and stirred with a spatula tip of H^+-Amberlite resin to hydrolyze a side product that has formed by condensation of the oligosaccharide with the cleaved linker. Without removal of the water the fully deprotected tetrasaccharide **33** was directly purified by reversed phase HPLC using a semi-preparative Hypercarb column to provide an α/β mixture of the tetrasaccharide **33** (2.0 mg, 3.00 µmol, 20% over 2 steps).

RP-HPLC of the deprotected disaccharide **33** (ELSD trace):

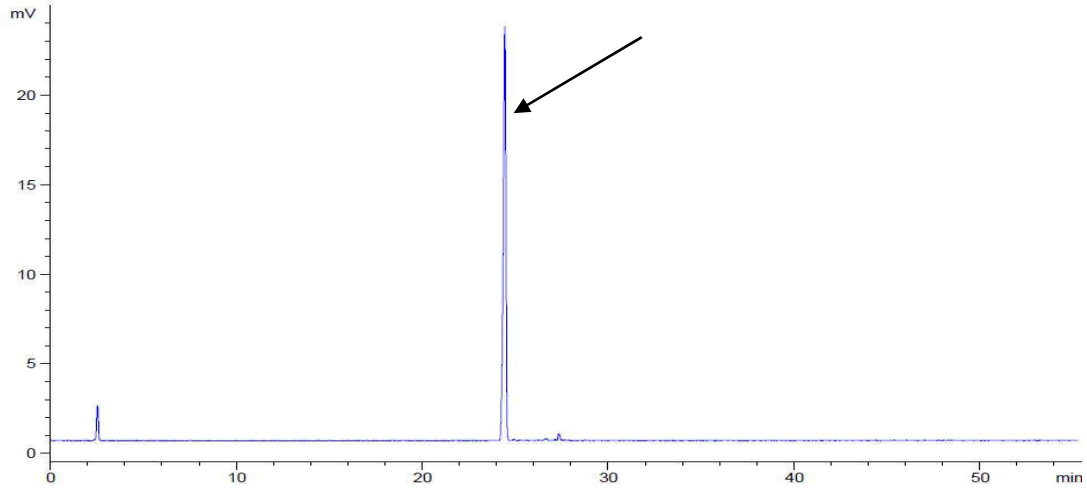

HPLC was performed using a Hypercarb column and a linear gradient from 97.5% to 62.5% H_2O (containing 0.1% of formic acid) in MeCN (26 min, flow rate 0.7 mL/min).

^{1}H NMR (400 MHz, D_2O): δ = 5.17 (d, *J* = 3.7 Hz, 1H), 4.61 (d, *J* = 8.0 Hz, 1H), 4.50-4.43 (m, 3H), 4.00-3.15 (m, 48H) ppm. ^{13}C NMR (151 MHz, D_2O): δ = 168.4, 105.1, 104.9, 98.3, 94.4, 81.2, 81.1, 81.0, 80.8, 78.6, 78.1, 77.4, 76.8, 76.6, 76.5, 75.7, 75.5, 73.9, 73.8, 72.7, 72.0, 63.2, 62.6, 62.5. ppm. ESI-HRMS: m/z = $[M+Na]^+$ calcd. for $C_{24}H_{42}NaO_{21}$:689.2116; found 689.2130.

β-D-Glucopyranosyl-(1->4)-D-glucopyranose (34)

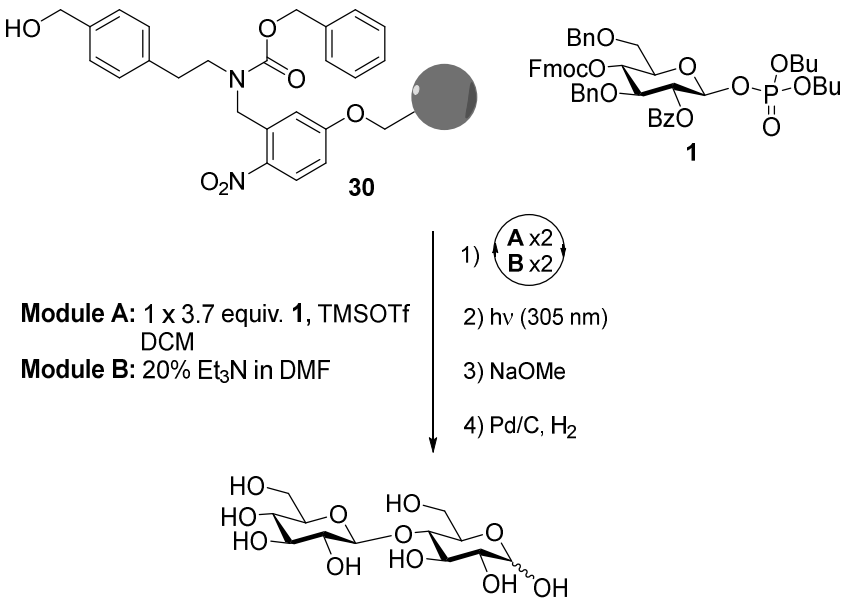

34

Linker functionalized resin **34** (60 mg, 15.1 µmol) was placed in the reaction vessel of the synthesizer and synthesizer modules were applied as follows:
Module **A** (4 equiv. **1**, TMSOTf, DCM, 35 min, -30 °C to -15 °C)
Module **C** (20% NEt_3 in DMF, 3 x 5 min, rt)
Module **A** (4 equiv. **1**, TMSOTf, DCM, 35 min, -30 °C to -15 °C)
Module **C** (20% NEt_3 in DMF, 3 x 5 min, rt)

Cleavage from the resin using UV irradiation at 305 nm in a continuous flow photoreactor afforded the protected disaccharide. The crude product was purified by normal phase HPLC using a preparative YMC Diol column.

Crude NP-HPLC of the protected disaccharide (ELSD trace):

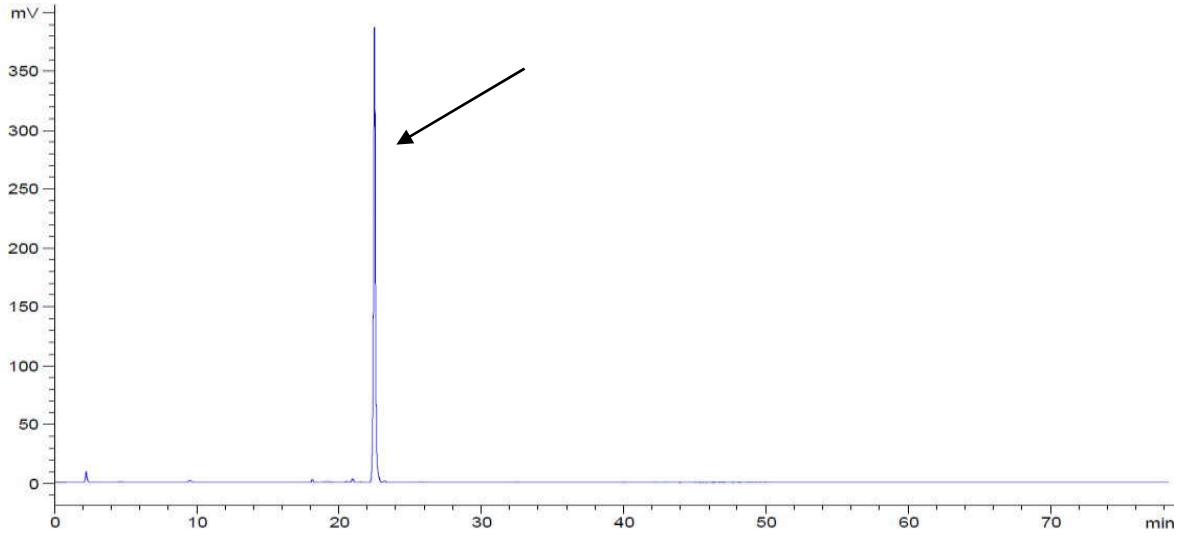

HPLC was performed using a YMC Diol column and a linear gradient from 10% to 100% ethyl acetate in hexane (40 min, flow rate 1 mL/min).

The protected disaccharide was dissolved in THF (3 mL) and NaOMe (0.5 M in MeOH, 0.5 mL) was added. The reaction mixture was stirred overnight and subsequently neutralized by addition of H^+-Amberlite resin. The resin was filtered off and the solvents were removed *in vacuo.* The crude product was purified by reversed phase HPLC using a semi-preparative C5 column affording the semi-protected disaccharide. The product was dissolved in a mixture of EtOAc/MeOH/AcOH/H_2O (4:2:2:1, 3 mL) and the resulting solution was added to a round-bottom flask containing Pd/C (10% Pd, 20 mg). The suspension was saturated with H_2 for 30 min and stirred under an H_2-atmosphere overnight. After

filtration of the reaction mixture through a syringe filter, the solvents were evaporated. The fully deprotected disaccharide **34** was re-dissolved in 0.5 mL water and stirred with a spatula tip of H^+-Amberlite resin to hydrolyze a side product that has formed by condensation of the oligosaccharide with the cleaved linker. Without removal of the water the fully deprotected disaccharide **34** was directly purified by reversed phase HPLC using a semi-preparative Hypercarb column to provide an α/β mixture of the disaccharide **34** (0.8 mg, 2.34 µmol, 15% over 9 steps, based on resin loading).

RP-HPLC of the deprotected disaccharide **34** (ELSD trace):

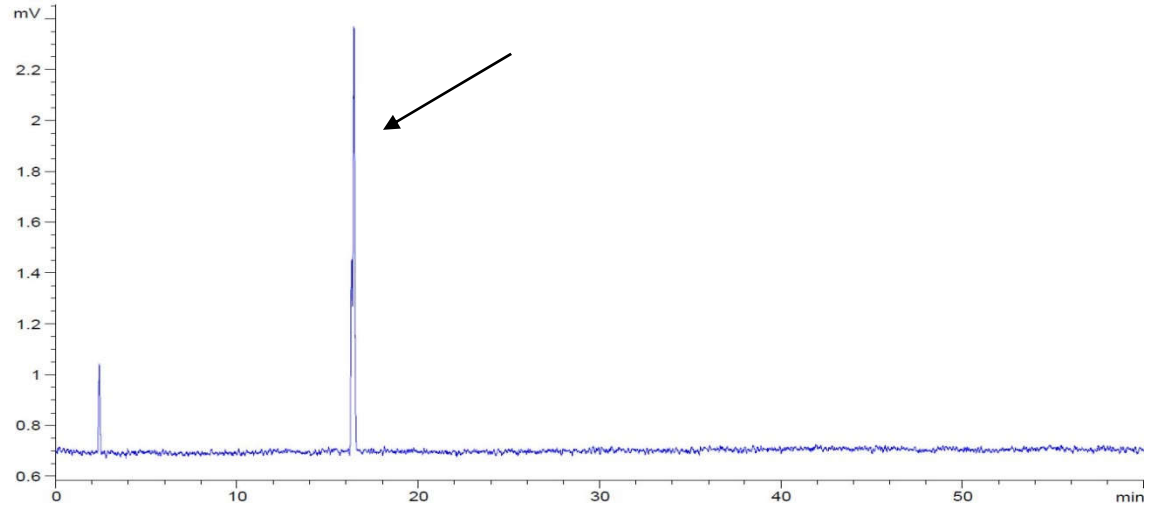

HPLC was performed using a Hypercarb column and a linear gradient from 97.5% to 30% H_2O (containing 0.1% of formic acid) in MeCN (45 min, flow rate 0.7 mL/min).

^{1}H NMR (400 MHz, D_2O): δ = 5.11 (d, *J* = 3.8 Hz, 1H), 4.55 (d, *J* = 8.0 Hz, 1H), 4.40 (d, *J* = 7.9 Hz, 2H), 3.88-3.13 (m, 24H) ppm. ^{13}C NMR (100 MHz, D_2O): δ = 102.5, 95.7, 91.7, 78.6, 78.5, 75.9, 75.4, 74.7, 74.2, 73.8, 73.1, 71.3, 71.1, 70.0, 69.4, 60.5, 60.0, 59.8 ppm. ESI-HRMS: m/z = $[M+Na]^+$ calcd. for $C_{12}H_{22}NaO_{11}^+$: 365.2862; found 365.1012.

Aminopentyl β-D-glucopyranosyl-(1->4)-6-*O*-[2-*O*-[β-D-galactocopyranosyl]-α-D-xylopyranosyl]-β-D-glucopyranosyl-(1->4)-β-D-glucopyranosyl-(1->4)-β-D-glucopyranoside (49)

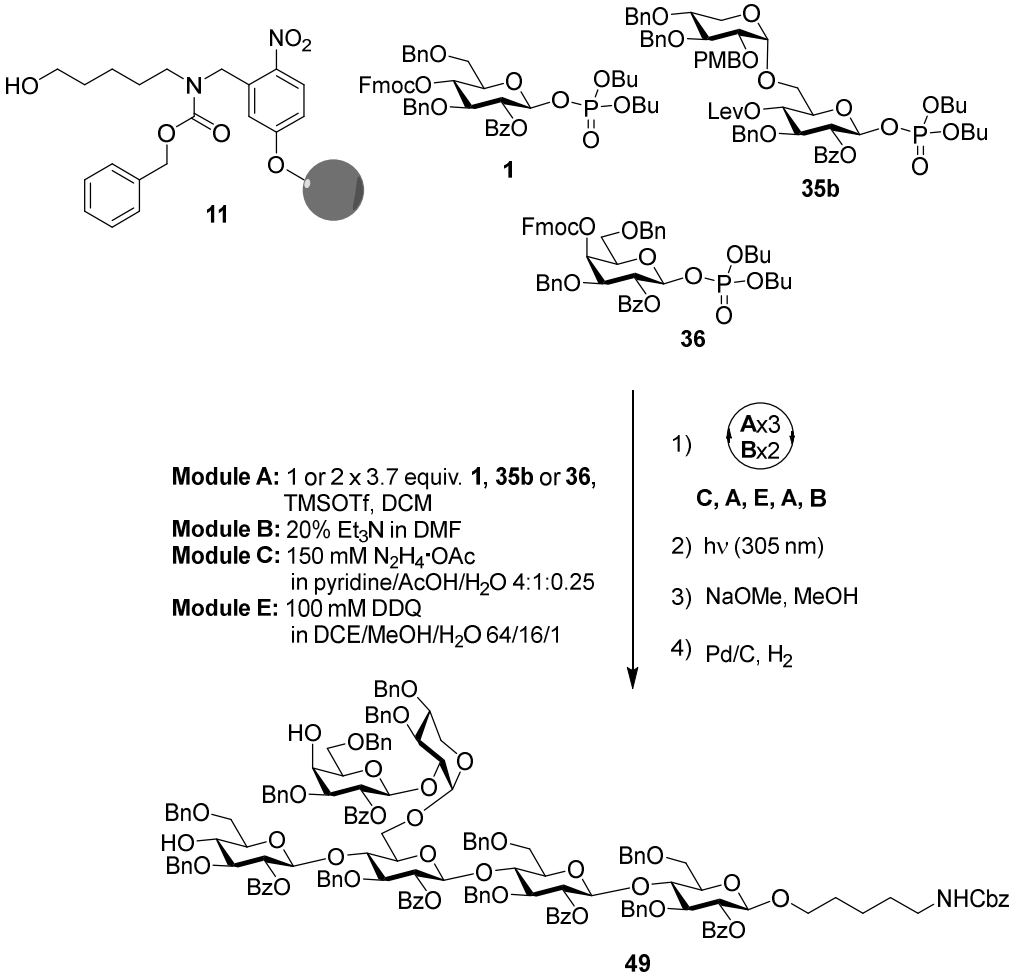

Linker-functionalized resin **11** (52 mg, 16.9 µmol) was placed in the reaction vessel of the synthesizer and synthesizer modules were applied as follows:

Module **A** (1 x 3.7 equiv **1**, TMSOTf, DCM, 2 x 35 min, -30 °C to -15 °C)

Module **B** (20% NEt_3 in DMF, 3 x 5 min, rt)

Module **A** (1 x 3.7 equiv **1**, TMSOTf, DCM, 2 x 35 min, -30 °C to -15 °C)

Module **B** (20% NEt_3 in DMF, 3 x 5 min, rt)

Module **A** (2 x 3.7 equiv **35b**, TMSOTf, DCM, 2 x 40 min, -35 °C to -10 °C)

Module **C** (150 mM N_2H_4·AcOH in pyridine/AcOH/H_2O 4:1:0.25, 3 x 30 min, rt)

Module **A** (2 x 3.7 equiv **1**, TMSOTf, DCM, 2 x 35 min, -30 °C to -15 °C)

Module **D** (100 mM DDQ in DCE/MeOH/H_2O 64:16:1, 1 x 20 min, 40 °C)

Module **A** (2 x 3.7 equiv **36**, TMSOTf, DCM, 2 x 45 min, -35 °C to -20 °C)

Module **B** (20% NEt_3 in DMF, 3 x 5 min, rt)

Cleavage from the resin using UV irradiation at 305 nm in a continuous flow photoreactor afforded the protected hexasaccharide. The crude product was purified by normal-phase HPLC using a preparative YMC-Diol-300 column. The crude product was purified by normal-phase HPLC using a preparative YMC-Diol-300 column affording the protected hexasaccharide.

Crude NP-HPLC of the protected hexasaccharide (ELSD trace):

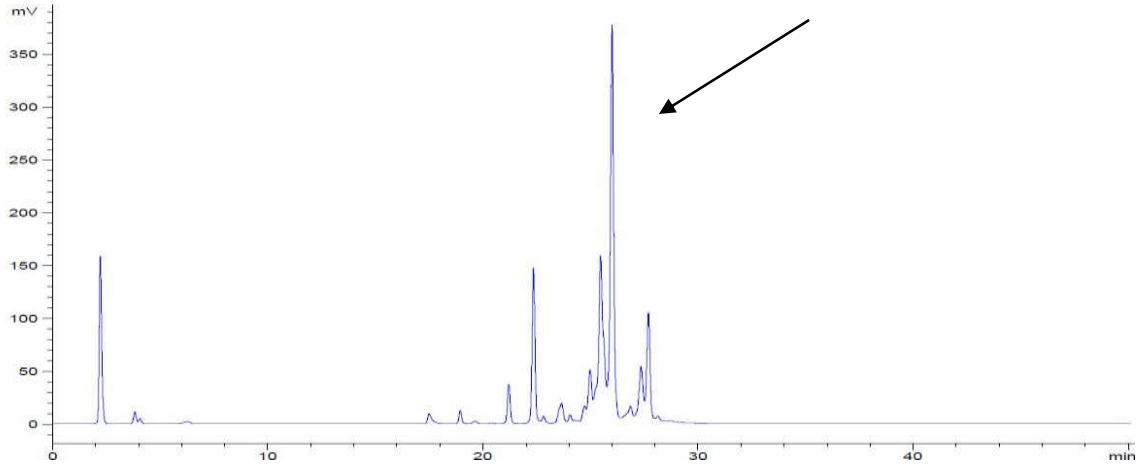

HPLC was performed using a YMC-Diol-300 column and linear gradients from 10% to 100% ethyl acetate in hexane (40 min, flow rate 1 mL/min).

The protected hexasaccharide was dissolved in THF (3 mL) and NaOMe (0.5 M in MeOH, 0.5 mL) was added. The reaction mixture was stirred overnight and then other NaOMe (0.5 M in MeOH, 0.5 mL). The reaction was stirred other 48 h and then NaOMe (0.5 M in MeOH, 1 mL) was added. The reaction mixture was stirred overnight and subsequently neutralized by addition of prewashed Amberlite IR-120 resin. The resin was filtered off and the solvent was removed *in vacuo.* The crude product was purified by normal-phase HPLC using a preparative YMC-Diol-300 column affording the semi-protected hexasaccharide. The product was dissolved in a mixture of EtOAc/MeOH/AcOH/H2O (4:2:2:1, 3 mL) and the resulting solution was added to a round-bottom flask containing Pd/C (10% Pd, 11 mg). The suspension was saturated with H_2 for 30 min and stirred under an H_2-atmosphere overnight. After filtration of the reaction mixture through a syringe filter the solvents were evaporated to provide the fully deprotected hexasaccharide **49** (1.2 mg, 1.15 µmol, 7% over 13 steps, based on resin loading).

RP-HPLC of the deprotected hexasaccharide **49**(ELSD trace):

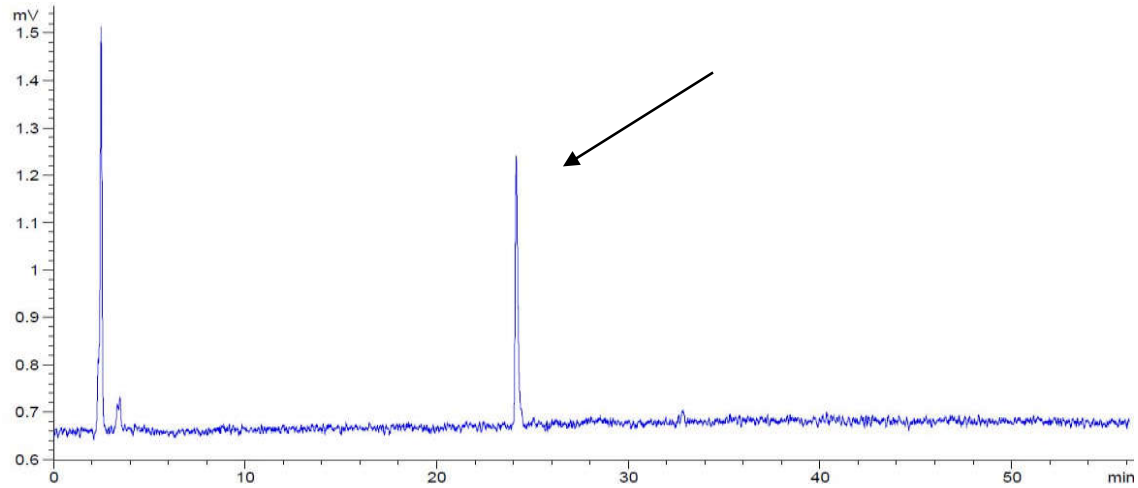

HPLC was performed using a Hypercarb column and a linear gradient from 97.5% to 30% H_2O (containing 0.1% of formic acid) in MeCN (45 min, flow rate 0.7 mL/min).

^{1}H NMR (600 MHz, D_2O): δ = 5.19 (d, *J* = 3.6 Hz, 1H), 4.63 (d, *J* = 7.8 Hz, 1H), 4.55 (d, *J* = 7.9 Hz, 2H), 4.49 (d, *J* = 8.0 Hz, 1H), 4.48 (d, *J* = 7.8 Hz, 1H), 4.12-3.27 (m, 37H), 3.02 (t, *J* = 7.5 Hz, 2H), 1.74-1.65 (m, 4H), 1.51-1.44(m, 2H) ppm. ^{13}C NMR (151 MHz, D_2O): δ = 101.6, 100.8, 100.1, 99.8, 96.3, 77.8, 76.6, 76.4, 73.8, 73.5, 73.2, 72.5, 72.1, 71.8, 71.5, 71.1, 70.7, 70.5, 70.2, 69.7, 68.7, 67.9, 67.4, 67.1, 66.3, 64.1, 58.8, 58.6, 37.1, 25.9, 24.2, 19.8 ppm. ESI-HRMS**:** m/z $[M+H]^+$ calcd. for $C_{40}H_{72}NO_{30}$: 1046.4139; found 1046.4188.

Aminopentyl 6-*O*-[2-*O*-[β-D-galactocopyranosyl]-α-D-xylopyranosyl]-β-D-glucopyranosyl-(1->4)-β-D-glucopyranosyl-(1->4)-β-D-glucopyranosyl-(1->4)-β-D-glucopyranoside (50)

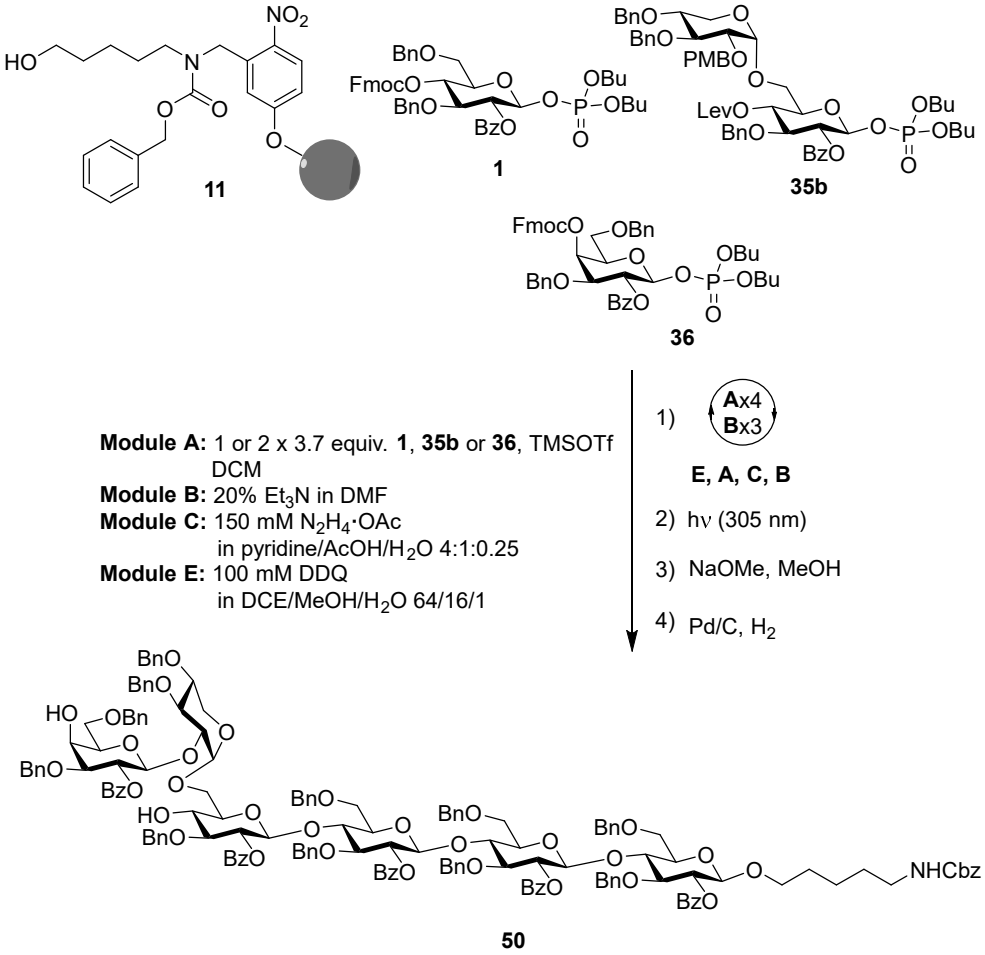

Linker-functionalized resin **11** (52 mg, 16.9 µmol) was placed in the reaction vessel of the synthesizer and synthesizer modules were applied as follows:

Module **A** (1 x 3.7 equiv **1**, TMSOTf, DCM, 2 x 35 min, -30 °C to -15 °C)

Module **B** (20% NEt_3 in DMF, 3 x 5 min, rt)

Module **A** (1 x 3.7 equiv **1**, TMSOTf, DCM, 2 x 35 min, -30 °C to -15 °C)

Module **B** (20% NEt_3 in DMF, 3 x 5 min, rt)

Module **A** (1 x 3.7 equiv **1**, TMSOTf, DCM, 2 x 35 min, -30 °C to -15 °C)

Module **B** (20% NEt_3 in DMF, 3 x 5 min, rt)

Module **A** (2 x 3.7 equiv **35b**, TMSOTf, DCM, 2 x 40 min, -35 °C to -10 °C)

Module **D** (100 mM DDQ in DCE/MeOH/H_2O 64:16:1, 1 x 20 min, 40 °C)

Module **A** (2 x 3.7 equiv **36**, TMSOTf, DCM, 2 x 45 min, -35 °C to -20 °C)

Module **C** (150 mM N_2H_4·AcOH in pyridine/AcOH/H_2O 4:1:0.25, 3 x 30 min, rt)

Module **B** (20% NEt_3 in DMF, 3 x 5 min, rt)

Cleavage from the resin using UV irradiation at 305 nm in a continuous flow photoreactor afforded the protected hexaccharide. The crude product was purified by normal-phase HPLC using a preparative YMC-Diol-300 column.

Crude NP-HPLC of the protected hexasaccharide (ELSD trace):

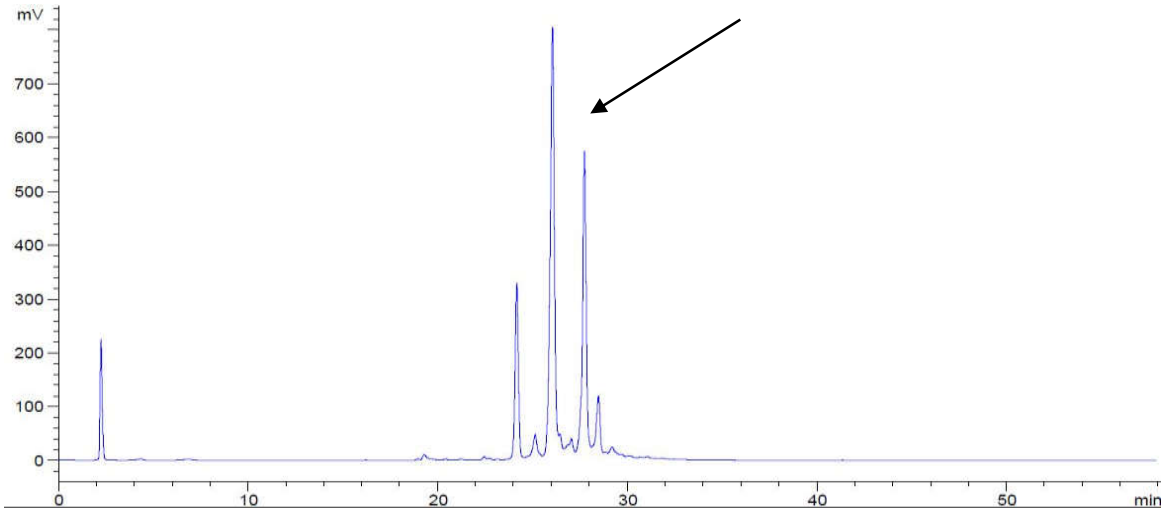

HPLC was performed using a YMC-Diol-300 column and linear gradients from 10% to 100% ethyl acetate in hexane (40 min, flow rate 1 mL/min).

The crude product was purified by normal-phase HPLC using a preparative YMC-Diol-300 column affording the protected hexasaccharide. The protected hexasaccharide was dissolved in THF (3 mL) and NaOMe (0.5 M in MeOH, 0.5 mL) was added. The reaction mixture was stirred for 24 h and then other NaOMe (0.5 M in MeOH, 0.5 mL). The reaction was stirred other 24 h and then NaOMe (0.5 M in MeOH, 1 mL) was added. The reaction mixture was stirred 6 h and subsequently neutralized by addition of prewashed Amberlite IR-120 resin. The resin was filtered off and the solvent was removed *in vacuo.* The crude product was purified by normal-phase HPLC using a preparative YMC-Diol-300 column affording the semi-protected hexasaccharide. The product was dissolved in a mixture of EtOAc/MeOH/AcOH/H2O (4:2:2:1, 3 mL) and the resulting solution was added to a round-bottom flask containing Pd/C (10% Pd, 6 mg). The suspension was saturated with H_2 for 30 min and stirred under an H_2-atmosphere overnight. After filtration of the reaction mixture through a syringe filter the solvents were evaporated to provide the fully deprotected hexasaccharide **50** (2.3 mg, 2.20 µmol, 13% over 13 steps, based on resin loading).

RP-HPLC of the deprotected hexasaccharide **50** (ELSD trace):

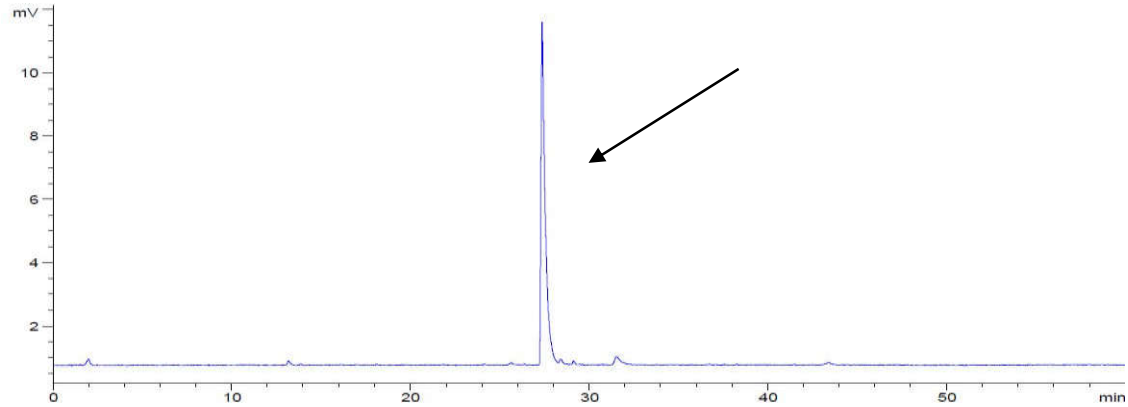

HPLC was performed using a Hypercarb column and a linear gradient from 97.5% to 30% H_2O (containing 0.1% of formic acid) in MeCN (45 min, flow rate 0.7 mL/min).

^{1}H NMR (700 MHz, D_2O): δ = 5.18 (s, 1H), 4.59 (d, *J* = 7.6 Hz, 1H), 4.56 (d, *J* = 7.5 Hz, 3H), 4.51 (d, *J* = 8.0 Hz, 1H), 4.03-3.30 (m, 37H), 3.03 (t, *J* = 7.7 Hz, 2H), 1.76-1.65 (m, 4H), 1.53-1.45 (m, 2H) ppm.^{13}C NMR (176 MHz, D_2O): δ = 102.1, 100.4, 100.1, 99.8, 95.9, 77.9, 76.6, 76.4, 76.1, 73.3, 72.8, 72.6, 72.5, 72.2, 72.1, 71.9, 71.8, 70.8, 70.7, 70.4, 69.7, 68.7, 67.9, 67.6, 67.1, 66.4, 64.5, 58.8, 58.7, 57.8, 57.7, 57.6, 37.1, 25.9, 24.2, 19.8 ppm. ESI-HRMS**:** m/z $[M+H]^+$ calcd. for $C_{40}H_{72}NO_{30}$: 1046.4139; found 1046.4166.

3 Mixed-Linkage Glucan Oligosaccharides Produced by Automated Glycan Assembly Serve as Tools to Determine the Substrate Specificity of Lichenase

This chapter has been modified in part from the following article:

P. Dallabernardina, F. Schumacher, P. H. Seeberger, F. Pfrengle, *Chem. Eur. J.,* **2017**, *23*, 3191-3196. Mixed-linkage glucan oligosaccharides produced by automated glycan assembly serve as tools to determine the substrate specificity of lichenase. DOI: http://dx.doi.org/10.1002/chem.201605479

3.1.1 Mixed-Linkage Glucans

MLG is a hemicellulosic polysaccharide mainly present in the cell wall of grasses and cereals.[153] MLGs are thought to play a structural role and/or are used for energy storage. As an important component of dietary fiber, MLG exhibits beneficial effects on human health, including reduction of colorectal cancer risk,[154] lowering of blood cholesterol, and regulation of blood glucose levels for diabetes management.[155] MLGs are considered as attractive additives for the manufacturing of low-fat food.[156] The structure of MLG is represented by an unbranched glucan chain composed of short stretches of β-1,4-linked oligosaccharides connected through β-1,3-linkages.[157,158] These cello-oligosaccharide sequences typically consist of three (cellotriosyl) to four (cellotetraosyl) residues. However, shorter and longer stretches also may be found.[159] The ratio of β-1,3-linkages versus β-1,4-linkages together with the order and the occurrence of the different cellulose subunits strongly affects the physicochemical properties of the polymer. The β-1,3-linkages in the β-1,4-linked glucan chain form molecular kinks that prevent an intermolecular alignment with microfibrils as observed in the case of cellulose. Instead, the limited intermolecular interactions result in the formation of a gel-like material which not

only provides the cell wall with strength, but also flexibility and other important characteristics of cellular function.[160]

3.1.2 Lichenase

Besides holding enormous potential as biocatalysts that allow the brewery and animal feed industries to produce high quality brews and more digestible feed,[161] MLG-degrading enzymes are essential tools for the structural characterization of MLGs.[162] The MLG-hydrolase lichenase cleaves every β-1,4-linkage following a β-1,3-linkage in a mixed-linkage glucan backbone (Figure 1).[127] The resulting oligosaccharide fragments are usually represented as MLGX, with X describing the number of glucose units contained (Figure 17b).

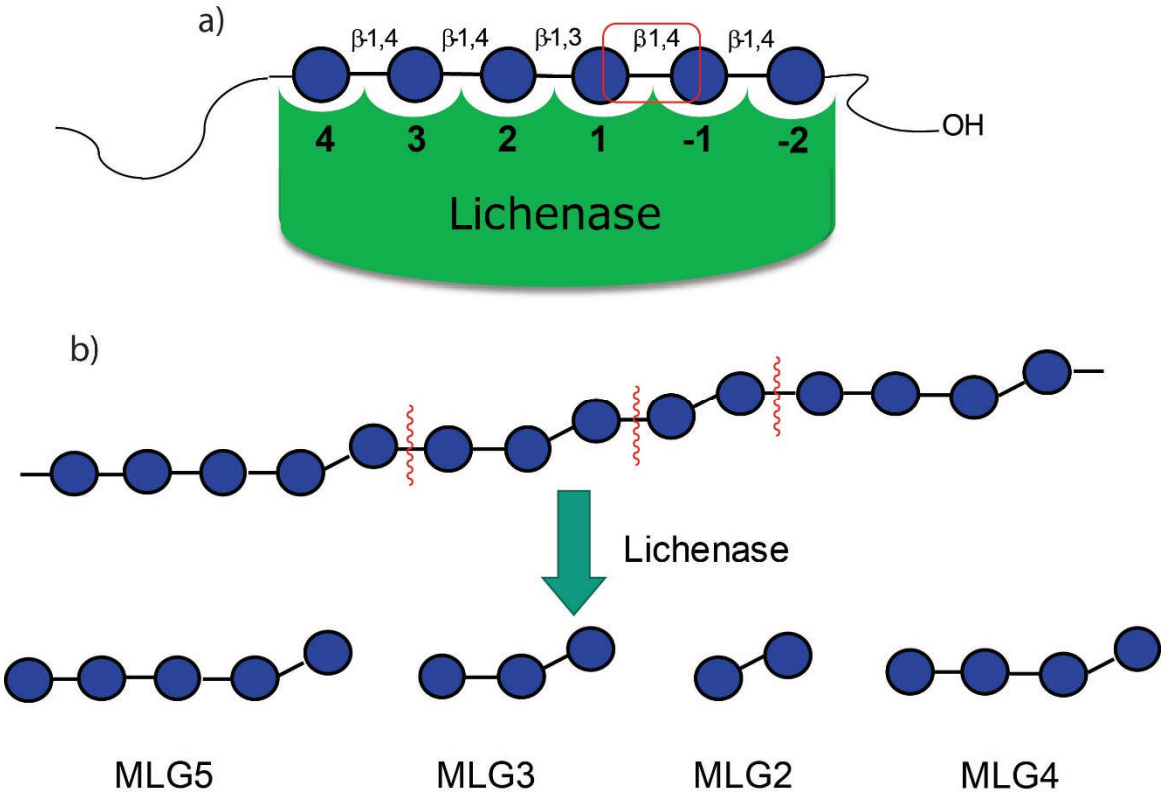

Figure 17: a) Schematic representation of the catalytc site of lichenase. b) Schematic representation of a mixed-linkage glucan polysaccharide and the oligosaccharide fragments obtained after lichenase treatment.

Recently, the strict specificity of lichenase was questioned when an intact hexasaccharide composed of a MLG2 and a MLG4 fragment was obtained after digestion of MLG with lichenase.[159] Simmons *et al.* were able to identify this new fragment by combining different analytical techniques. They suggest that

lichenase cannot hydrolyze this oligosaccharide because position -3 of the catalytic subsites must be occupied by a glucose residue for cleavage (Figure 17a). The MLG2-MLG4 fragment which lacks a residue in this position cannot be recognized and is not hydrolyzed. This discovery has implications for the reported structure of MLGs, as their subunit distribution is mostly derived from the analysis of lichenase digestion products.

3.2 Results and Discussion

3.2.1 Automated Glycan assembly of Mixed-Linkage Glucan Oligosaccharides

Synthetic MLG-oligosaccharides of varying connectivity would permit a simple LC-MS analysis of their digestion products after hydrolysis, providing a toolkit for the determination of the substrate specificities of lichenase and other MLG endoglucanases. To produce these MLG oligosaccharides by automated glycan assembly, glucose BBs **1** and **51** were chosen since they already provided good results in the automated glycan assembly of β-1,3-[112] and β-1,4-linked glucan oligosaccharides previously (Figure 18).

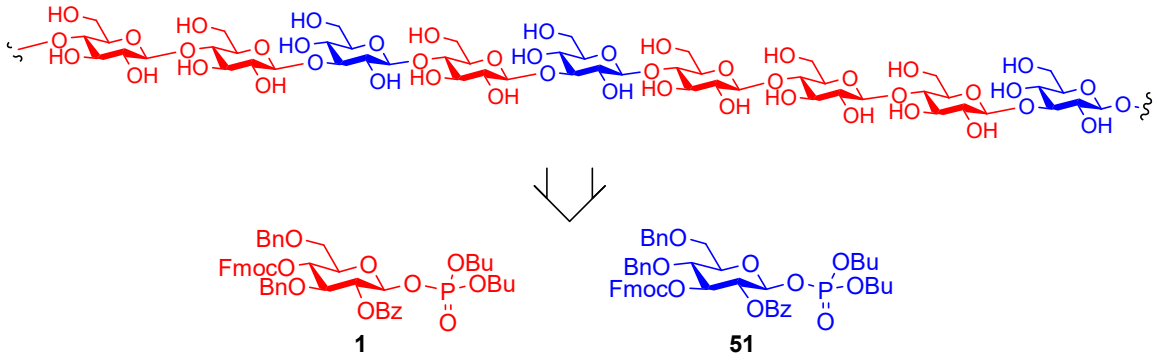

Figure 18: Retrosynthetic approach for the synthesis of MLG oligosacharides.

Fmoc was chosen as a temporary protecting group for chain elongation. Permanent protection was realized with Bz esters in the C2-position to ensure β-selectivity in the glycosylation reactions, and Bn ethers were installed in all other positions. Phosphate served as the leaving group since glycosyl phosphates previously provided the best efficiencies in similar glycosylation reactions.[112]

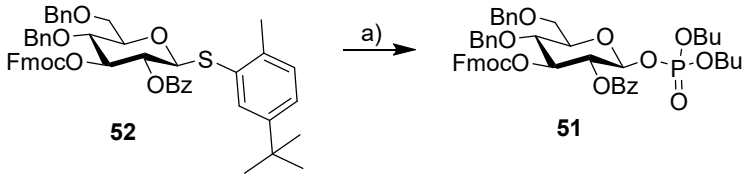

Scheme 21: Synthesis of phosphate BB **51**. Reagents and conditions: a) $HOP(O)(OBu)_2$, NIS, TMSOH, CH_2Cl_2, 0 °C, 79%.

Glycosyl phosphate **51** was synthesized from **52**[112] by replacing the thioether leaving group using NIS and catalytic amounts of TfOH**.** To determine the amount of **1** and **51** required for the individual glycosylation steps in the automated glycan assembly of MLG oligosaccharides, trisaccharide **53** was chosen as a simple test substrate (Figure 19a). After TMSOTf-promoted glycosylation of linker-functionalized resin **11** using one cycle of 3.7 equivalents of **1**, the Fmoc group was cleaved using Et_3N, and the resulting free 4-OH was glycosylated with 3.7 equivalents of **51**. Fmoc was cleaved and another glycosylation with 3.7 equivalents of **1** was performed. After removal of the terminal Fmoc group, the reaction products were cleaved from the resin in a continuous flow photoreactor and analyzed by HPLC. Besides the desired product **53**, a side product was formed that was identified as a disaccharide deletion sequence. From the HPLC analysis, it was not possible to deduce which glycosylation reaction did not go to completion (Figure 19b). Since we knew from previous studies that one cycle of 3.7 equivalents glycosyl donor is sufficient for the synthesis of cello-oligosaccharides using BB **1**, two possible reasons for the incomplete reaction remained: either BB **51** is less reactive than BB **1** and the second glycosylation was inefficient, or the C-3 hydroxyl group in the third glycosylation reaction exhibits reduced nucleophilicity compared to the C-4 hydroxyl in the second glycosylation. To test the first option we repeated the synthesis, but used two cycles of 3.7 equivalents BB **51**. However, HPLC analysis of the products revealed the same amount of deletion sequence as before (Figure 19b). Only when we used two cycles of 3.7 equivalents BB **1** in the third glycosylation, were we able to obtain full conversion. Thus, we performed

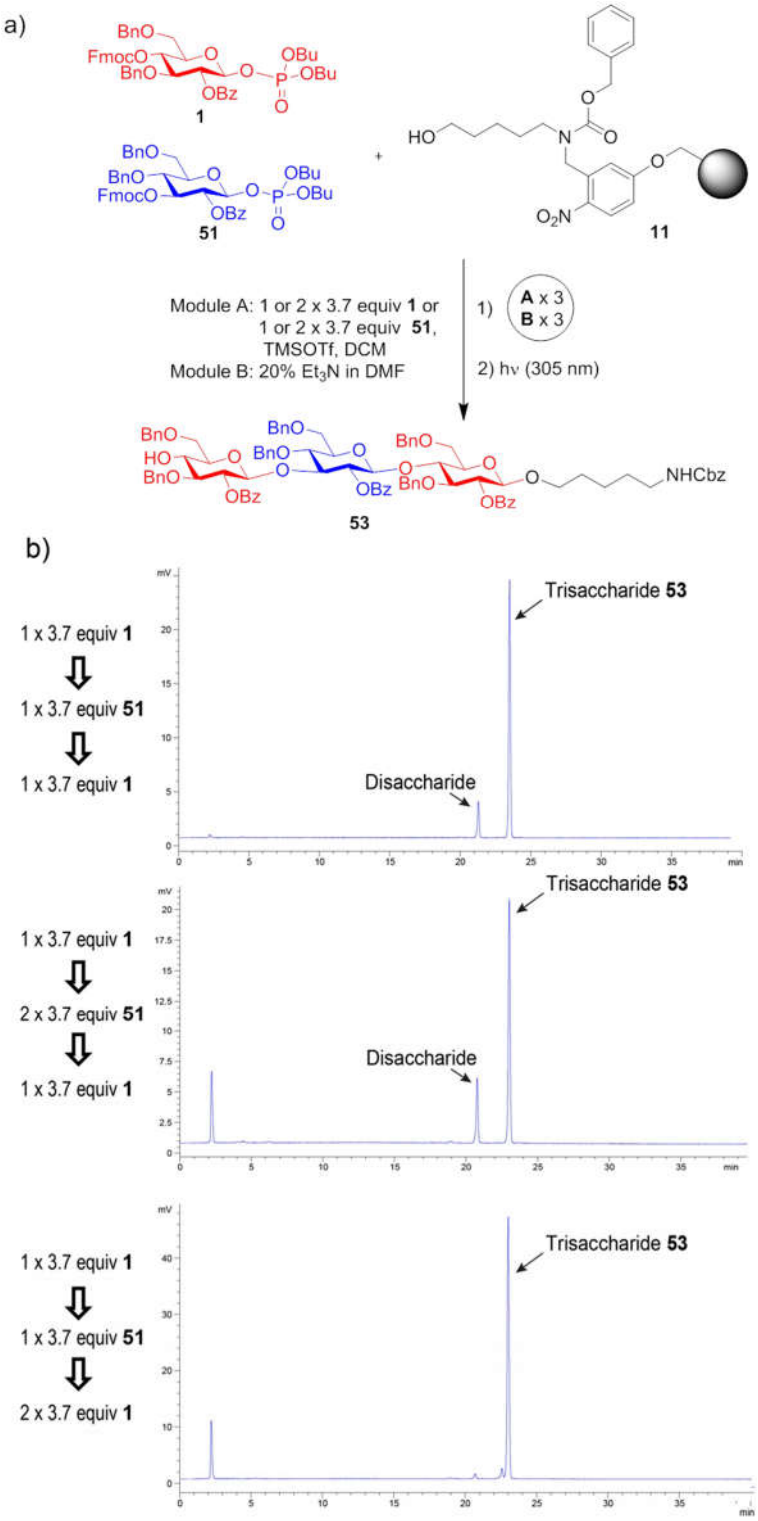

Figure 19: Optimization of the automated glycan assembly process towards MLG oligosaccharides. a) Automated glycan assembly of trisaccharide **48**. Reagents and conditions: 1 or 2 × 3.7 equiv. BB **1** or **46**, TMSOTf, CH_2Cl_2, −30 °C (5 min) → −15 °C (30 min) (Module A); 3 cycles of 20% NEt_3 in DMF, 25 °C (5 min) (Module B). b) HPLC analysis (ELSD trace) of the crude products after the different automated assembly processes.

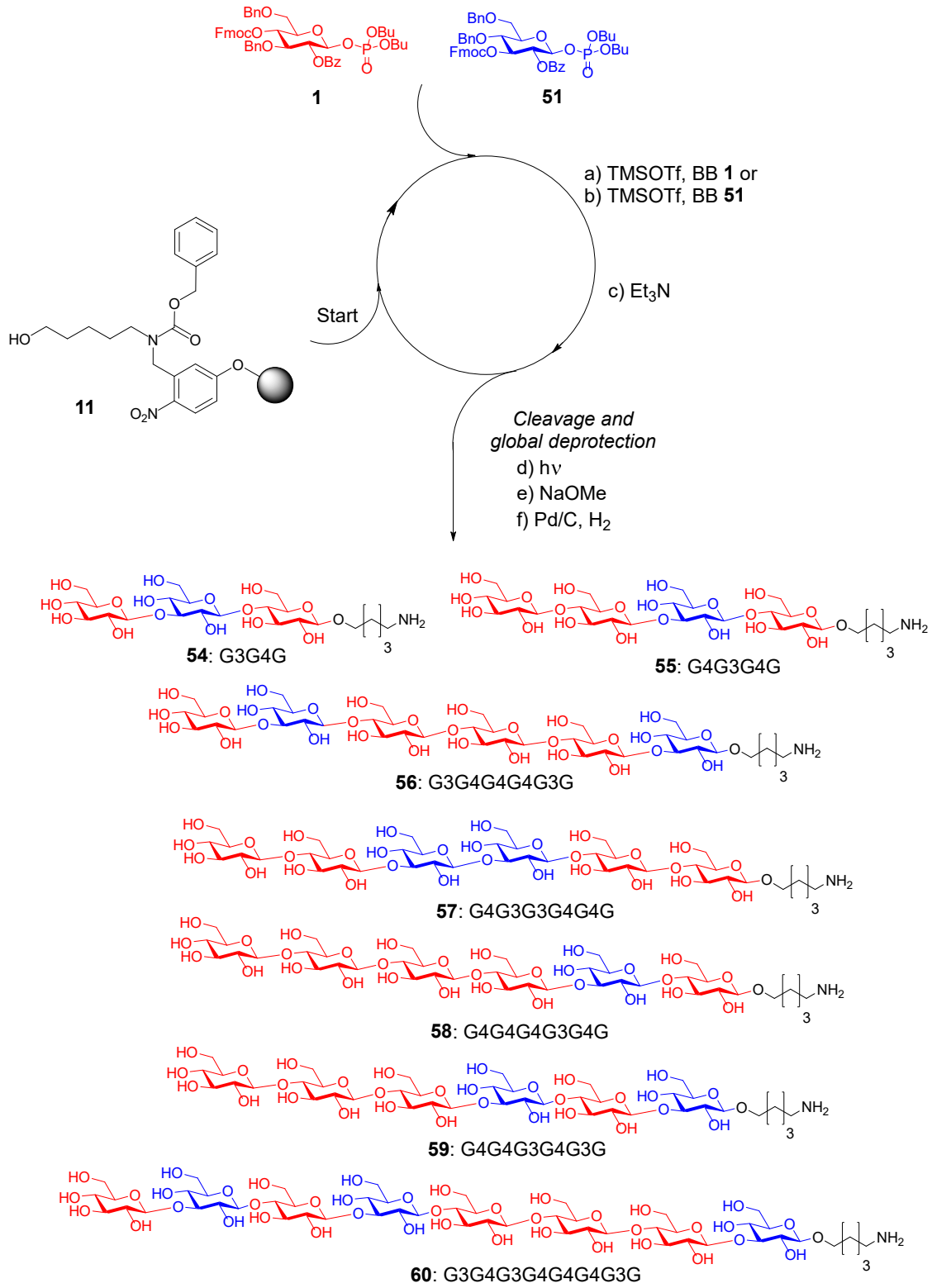

Scheme 22: Automated glycan assembly of MLG oligosaccharides: 1 or 2 × 3.7 equiv BB **1**, TMSOTf, CH_2Cl_2, −30 °C (5 min) → −15 °C (30 min) (Module A); b) 1 or 2 × 3.7 equiv BB **51**, TMSOTf, CH_2Cl_2, −30 °C (5 min) → −15 °C (30 min) (Module A); (c) 3 cycles of 20% NEt_3 in DMF, 25 °C (5 min) (Module B); (d) CH_2Cl_2, hν (305 nm); (e) NaOMe, THF/MeOH, 12 h; (f) H_2, Pd/C, EtOAc/MeOH/H_2O/HOAc, 12 h. **54**: 13%; **55**: 26%; **56**: 12%; **57**: 12%; **58**: 34%; **59**: 18%; **60**: 23% (yields are based on resin loading). The letter code below the structures refers to a common nomenclature of MLG oligosaccharides.[159]

one glycosylation cycle for the formation of β-1,4-linkages and two cycles for β-1,3-linkages in all later syntheses. Using the optimized glycosylation conditions, we synthesized a series of MLG oligosaccharides and obtained after global deprotection MLG oligosaccharides **54-60** in 12–34% yield based on resin loading (Scheme 22). Intrigued by the good results and knowing that unlike cellulose even longer structures of unprotected MLG polymers have good solubility in water, the synthesis of a 20mer oligosaccharide was attempted (Figure 20). For the synthesis of this oligosaccharide, a capping step was introduced after reaching the size of an octamer, to cap potential deletion sequences and facilitate purification. Despite this precaution, the automated glycan assembly of the 20mer gave a complex mixture of products as determined

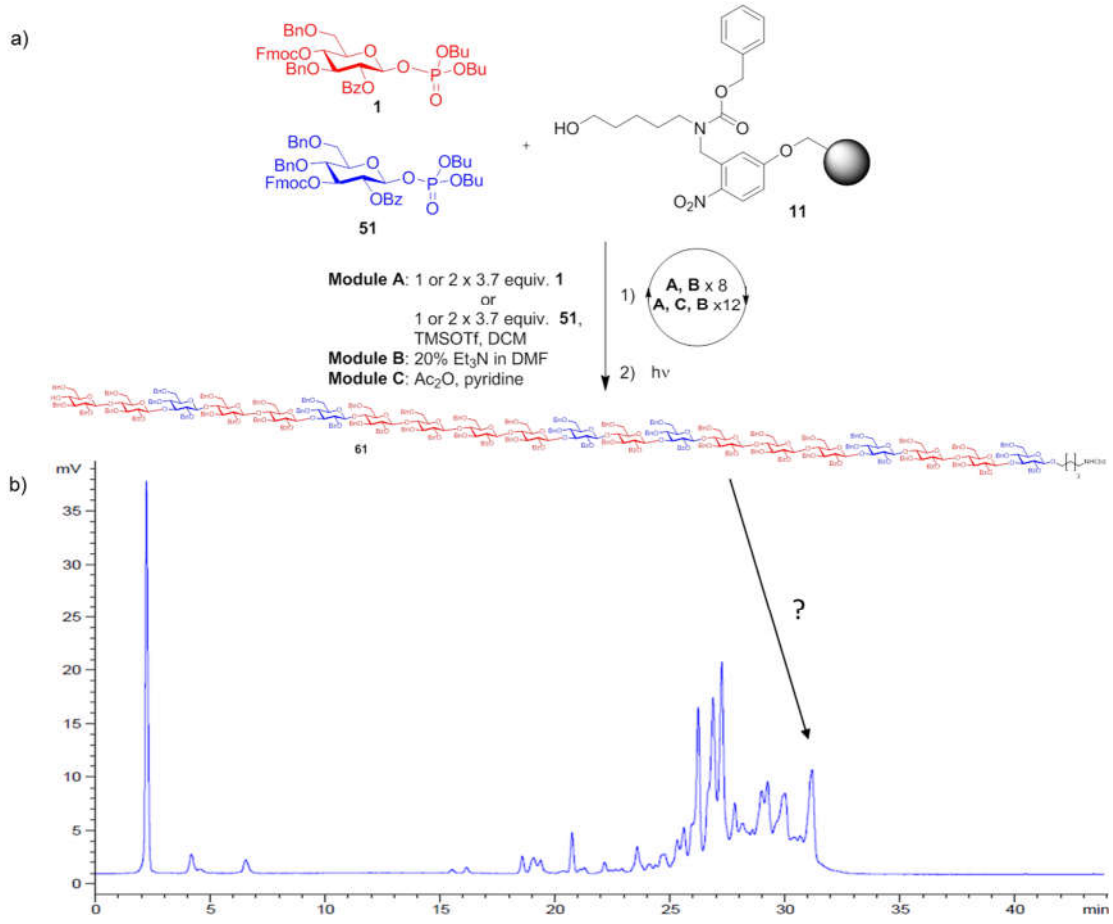

Figure 20: Synthesis of an MLG 20mer. a) Automated glycan assembly of 20mer **56**. Reagents and conditions: 1 or 2 × 3.7 equiv. BB **1** or **51**, TMSOTf, CH_2Cl_2, −30 °C (5 min) → −15 °C (30 min) (Module A); 3 cycles of 20% NEt_3 in DMF, 25 °C (5 min) (Module B); 3 cycles of Ac_2O, pyridine, 25 °C (30 min) (Module C). b) HPLC analysis (ELSD trace) of the crude product after the automated assembly process.

by HPLC analysis (Figure 21). The crude mixture was purified by preparative HPLC and the different fractions were analyzed by MALDI-MS. The results confirmed the presence of several deletion sequences ranging from the 11mer to the desired 20mer.

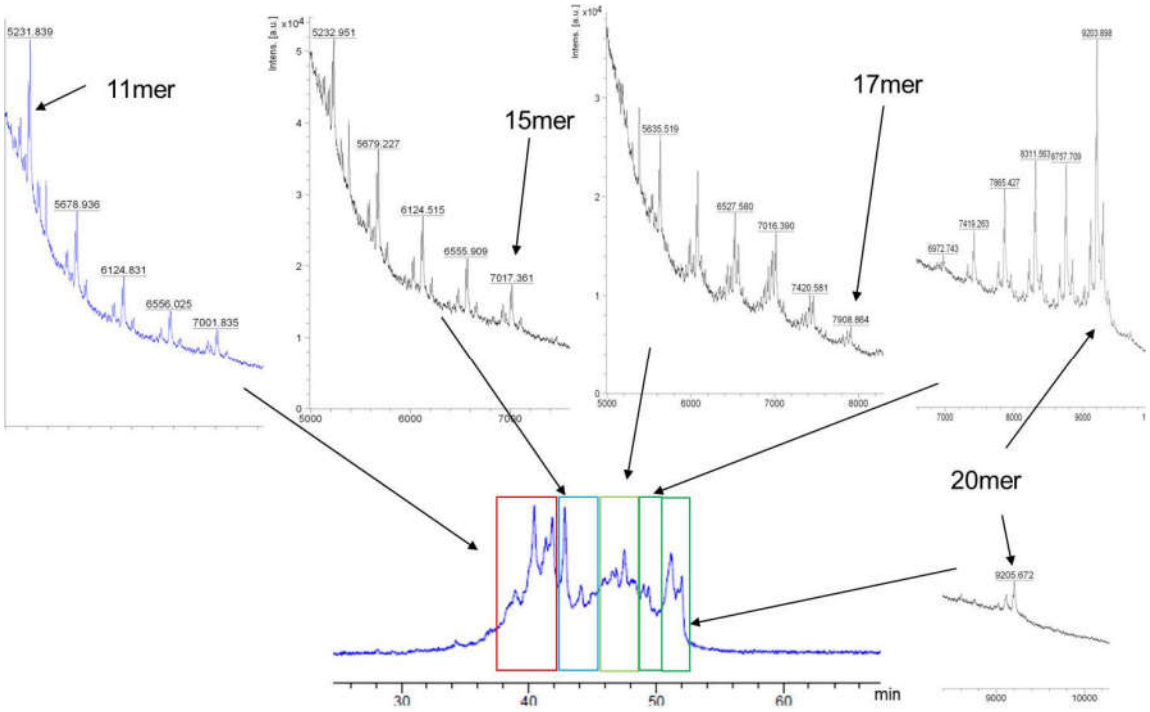

Figure 21: Purification of **61** by preparative HPLC and MALDI analysis of the resulting fractions.

3.2.2 Characterization of Lichenase Specificity

To enable a comprehensive investigation of the substrate specificity of lichenase, the oligosaccharides were designed to cover different distances between the 1,3-linkages and different numbers of 1,4-linked glucose residues at the non-reducing end. The collection of MLG oligosaccharides was incubated with lichenase from Bacillus subtilis (GH family 16), and after three hours the resulting digestion products were analyzed by HPLC coupled to a mass spectrometer and an evaporative light scattering detector (ELSD) (Figure 22). Compounds **55**, **58**, and **59** were hydrolyzed according to the general observation that lichenase cleaves every β-1,4-linkage following a β-1,3-linkage (Figure 3). However, hexasaccharide **56**, which represents the "lichenase-resistent" structure reported by Simmons et al.,[159] was not hydrolyzed. Similarly, for octasaccharide **60**, only one of the two glycosidic bonds following a β-1,3-linkage was hydrolyzed. The fact that the MLG2 moiety at the non-reducing end of **60**

was not cleaved confirms the hypothesis that lichenase is not able to release MLG2 fragments from the non-reducing end of MLG oligo- or polysaccharides.[159] The unnatural structure **57,** containing two consecutive β-1,3-linkages, was only partially hydrolyzed.

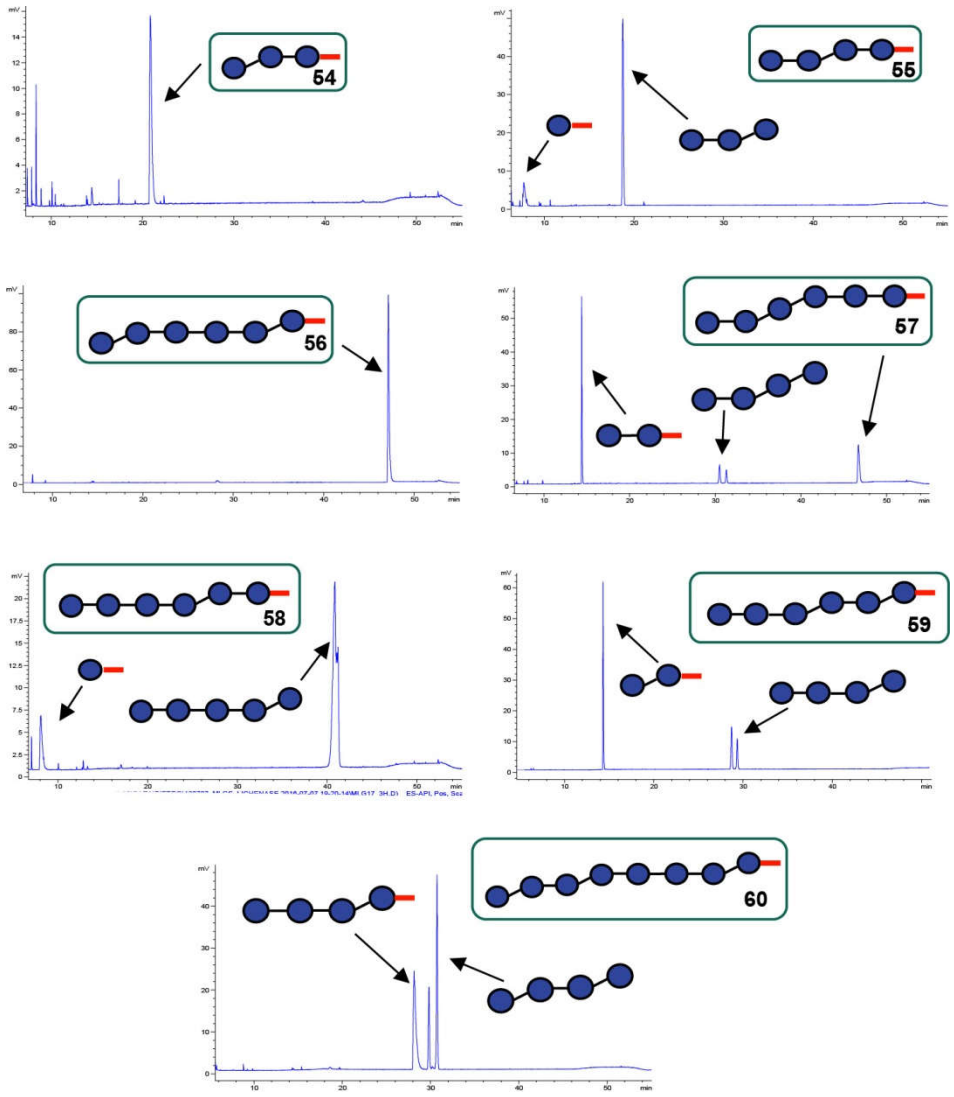

Figure 22: Digestion of synthetic MLG oligosaccharides with lichenase and HPLC-MS analysis of the reaction products. Peaks are annotated with MLG fragments with aminopentenyl linker or free reducing end (with or without red bar, respectively). Note that the α-and β-forms of the fragments with free-reducing end usually elute as separate peaks.

To investigate the importance of the -3 subsite relative to the site of hydrolysis for substrate recognition, we qualitatively determined the relative rate differences between the hydrolysis of compounds **56**, **57**, and **58** in a time-course experiment. No significant hydrolysis was observed after incubating compound **56** with lichenase for 24 hours (Figure 23a). In contrast, **57**, which contains a β-

1,3-linked glucose residue in the -3 subsite, was slowly hydrolyzed, demonstrating positive interactions of the glucose residue with the enzyme. When the -3 subsite was occupied with a β-1,4-linked glucose residue such as in **58**, hydrolysis was completed within 30 minutes. Thus, occupation and correct linkage-type of the -3 subsite is key for efficient digestion (Figure 23b), confirming the observation that no MLG2 fragments are released from the non-reducing end of MLG oligo- and polysaccharides.

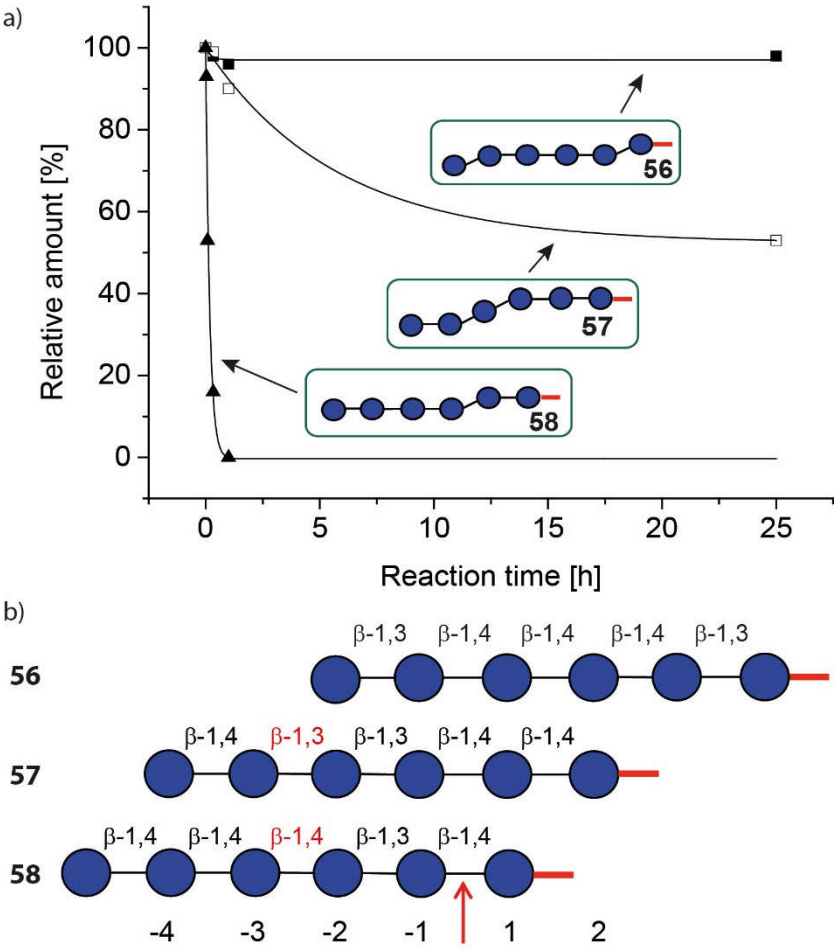

Figure 23: Comparison of the lichenase cleavage rates between oligosaccharides **56**, **57**, and **58**. a) Timecourse experiment following the digestion of the substrates over a period of 24 h. The structure of the substrates is indicated by boxes. b) Schematic representation of oligosaccharides **56**-**58** and the subsites occupied during hydrolysis. The linker is indicated by a red bar and the cleavage site is denoted by a red arrow.

3.3 Conclusion

Two differentially protected glucose BBs are sufficient for the automated glycan assembly of a set of tailor-made natural and unnatural MLG

oligosaccharides. These synthetic oligosaccharides were key to determining the substrate specificity of the MLG-degrading enzyme lichenase. Incubation of the glycans with lichenase resulted in digestion products that were analyzed by HPLC-MS. Simple end-point measurements confirmed recent reconsiderations[159] concerning the substrate specificity of lichenase. As a consequence, structural analyses of MLG polysaccharides have to be reconsidered. The fact that lichenase does not release disaccharides from the non-reducing end of MLG oligo- and polysaccharides highlights the importance of the -3 subsite relative to the site of hydrolysis for substrate recognition. Further information on the binding requirements in the -3 subsite were obtained by comparing the hydrolysis rates of three MLG oligosaccharides containing either no, a β-1,3-linked, or a β-1,4-linked glucose residue in the -3 subsite. The MLG oligosaccharides we describe provide a convenient means for determining the substrate specificities of newly discovered mixed-linkage β-glucanases.[163]

3.4 Experimental Part

3.4.1 General information

The automated syntheses were performed on a self-built synthesizer developed in the Max Planck Institute of Colloids and Interfaces. Resin loading was determined as described previously.[141] Solvents and reagents were used as supplied without any further purification. Anhydrous solvents were taken from a dry solvent system (JC-Meyer Solvent Systems). Column chromatography was carried out using Fluka Kieselgel 60 (230-400 mesh). NMR spectra were recorded on a Varian 400-MR (400 MHz), a Varian 600 (600 MHz) spectrometer using solutions of the respective compound in $CDCl_3$ or D_2O. NMR chemical shifts (δ) are reported in ppm and coupling constants (*J*) in Hz. Spectra recorded in $CDCl_3$ used the solvent residual peak chemical shift as a reference ($CDCl_3$: 7.26 ppm ^1H, 77.0 ppm ^{13}C). Spectra recorded in D_2O used the solvent residual peak chemical shift as a reference in ^1H NMR (D_2O: 4.79 ppm ^1H) and the residual acetic acid (D_2O: 21.0 ppm ^{13}C) or formic acid (D_2O: 166.3 ppm ^{13}C) as a reference in ^{13}C NMR. Yields of final deprotected oligosaccharides were

determined after removal of residual acetic acid. Optical rotations were measured using a UniPol L1000 polarimeter (Schmidt&Haensch) with concentrations expressed as g/100 mL. IR spectra were recorded on a Spectrum 100 FTIR spectrophotometer (Perkin-Elmer). High resolution mass spectra were obtained using a 6210 ESI-TOF mass spectrometer (Agilent). Analytical HPLC was performed on an Agilent 1200 series coupled to a quadrupole ESI LC/MS 6130 using a Phenomenex Luna C5 column (250 x 4.6 mm), a YMC-Diol-300 column (150 x 4.6 mm), a Phenomenex Synergi Hydro-RP18 (250 x 4.6 mm) or a Thermo Scientific Hypercarb column (150 x 4.6 mm). Preparative HPLC was performed on an Agilent 1200 series using a semi-preparative Phenomenex Luna C5 column (250 x 10 mm), a preparative YMC-Diol-300 column (150 x 20 mm) or a semi-preperative Thermo Scientific Hypercarb column (150 x 4.6 mm).

3.4.2 Synthesizer Modules and Conditions

Linker-functionalized resin **11** (16.6-17.9 µmol of hydroxyl groups) was placed in the reaction vessel and swollen for at least 30 min in DCM. Before every synthesis the resin was washed with DMF, THF and DCM. Subsequently the glycosylation (Module **A**) and deprotection (Module **B**) steps were performed. Mixing of the components was accomplished by bubbling argon through the reaction mixture.

Module A: Glycosylation with Glycosyl Phosphates

The resin (16.6-17.9 µmol of hydroxyl groups) was swollen in DCM (2 mL) and the temperature of the reaction vessel was adjusted to -30 °C. Prior to the glycosylation reaction the resin was washed with TMSOTf in DCM and then DCM only. For the glycosylation reaction the DCM was drained and a solution of phosphate BB (3.7 equiv in 1 mL DCM) was delivered to the reaction vessel. After the set temperature was reached, the reaction was started by the addition of TMSOTf in DCM (3.7 equiv in 1 mL DCM). The glycosylation was performed for 5 min at -30 °C and then at -15 °C for 30 minutes. Subsequently the solution was drained and the resin was washed three times with DCM. The whole procedure was performed once or twice to improve conversion of the acceptor sites. Afterwards the resin was washed three times with DCM at 25 °C.

Module B: Fmoc Deprotection.

The resin was washed with DMF, swollen in 2 mL DMF and the temperature of the reaction vessel was adjusted to 25 °C. Prior to the deprotection step the DMF was drained and the resin was washed with DMF three times. For Fmoc deprotection 2 mL of a solution of 20% Et_3N in DMF was delivered to the reaction vessel. After 5 min the solution was drained and the whole procedure was repeated another two times. After Fmoc deprotection was complete the resin was washed with DMF, THF and DCM.

Cleavage from the Solid Support

After assembly of the oligosaccharides, cleavage from the solid support was accomplished by modification of a previously published protocol,[149] using the Vapourtec E-Series UV-150 photoreactor Flow Chemistry System. The medium pressure metal halide lamp is filtered using the commercially available red filter. The resin, suspended in DCM, was loaded into a plastic syringe. The suspension was then pumped using a syringe pump (PHD2000, Harvard Aparatus) at 1 mL/min through a 10 mL reactor, constructed of 1/8 inch o.d. FEP tubing. The total volume within the photoreactor was 9 mL. The temperature of the photoreactor was maintained at 20 °C and the lamp power was 80%. The exiting flow was deposited in a 10 mL syringe containing a filter, with a collection flask beneath the syringe.

3.4.3 Synthesis Building Block

Dibutoxyphosphoryloxy 2-*O*-benzoyl-4,6-*O*-dibenzy-3-*O*-fluorenylcarboxymethyl-β-D-glucopyranoside (51)

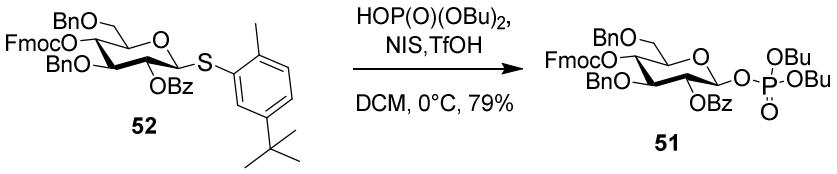

A solution of dibutyl phosphate (10.0 mL, 50.4 mmol) in DCM (20 mL) was dried over molecular sieves. After 30 min the supernatant (5 mL) was added to a solution of **52** (3.29 g, 3.87 mmol) in DCM (20 mL) and cooled to 0 °C. Then, NIS (1.05 g, 4.67 mmol) and TfOH (30 µL, 0.34 mmol) were added. The reaction was stirred for 1 h, quenched with an aqueous solution of $Na_2S_2O_3$/$NaHCO_3$ (1:1, 100

mL), and extracted with DCM (100 mL). The organic layer was dried over Na_2SO_4 and concentrated. The residue was purified by silica gel chromatography (Hex/EtOAc 3:1) to give **51** (2.70 g, 3.07 mmol, 79%) as a yellow oil. $[\alpha]_D^{25}$ = +32.7 (*c* 1.0, $CHCl_3$). ^{1}H NMR (400 MHz, $CDCl_3$): δ = 8.02 (dd, *J* = 8.2, 1.4 Hz, 2H, Ar), 7.70 (dd, *J* = 7.6, 3.9 Hz, 2H, Ar), 7.53-7.12 (m, 19H), 5.49-5.40 (m, 2H, H-1, H-2), 5.28 (t, *J* = 9.4 Hz, 1H, H-3), 4.71-4.47 (m, 4H, C*H*$_2$Ph), 4.28 (dd, *J* = 10.4, 7.0 Hz, 1H, H-6a), 4.15-3.96 (m, 5H, H-6, H-4, Fmoc, OBu), 3.86-3.66 (m, 5H, Fmoc, H-5, OBu), 1.65-1.57 (m, 2H, Bu), 1.42-1.24 (m, 4H, Bu), 1.04 (m, 2H, Bu), 0.89 (t, *J* = 7.4 Hz, 3H), 0.69 (t, *J* = 7.4 Hz, 3H) ppm. ^{13}C NMR (101 MHz, $CDCl_3$): δ = 165.0, 154.4 (2C, C=O), 143.3, 142.9, 141.1, 141.0, 137.8, 137.4, 133.4, 129.9, 128.4, 128.3, 127.9, 127.8, 127.7, 127.1, 125.2, 124.9, 119.8 (25C, Ar), 96.4 (C-1), 79.0 (C-3), 75.5 (C-3), 75.3 (C-4), 74.9 (*C*H$_2$Ph), 73.6 (*C*H$_2$Ph), 72.0 (C-2), 70.3 (C-6), 67.9 (3C, Fmoc, OBu), 46.4 (Fmoc), 32.0, 31.8, 18.5, 18.2 (4C, Bu) 13.53, 13.32 (2C, CH_3) ppm. ESI-HRMS m/z $[M+Na]^+$ calcd for $C_{50}H_{55}O_{12}PNa$ 901.3329, found 901.3347. IR (neat): ν_{max} = 2962, 1753, 1733, 1453 cm^{-1}.

3.4.4 Automated Glycan Assembly

Aminopentyl β-D-glucopyranosyl-(1->3)-β-D-glucopyranosyl-(1->4)-β-D-glucopyranose (54)

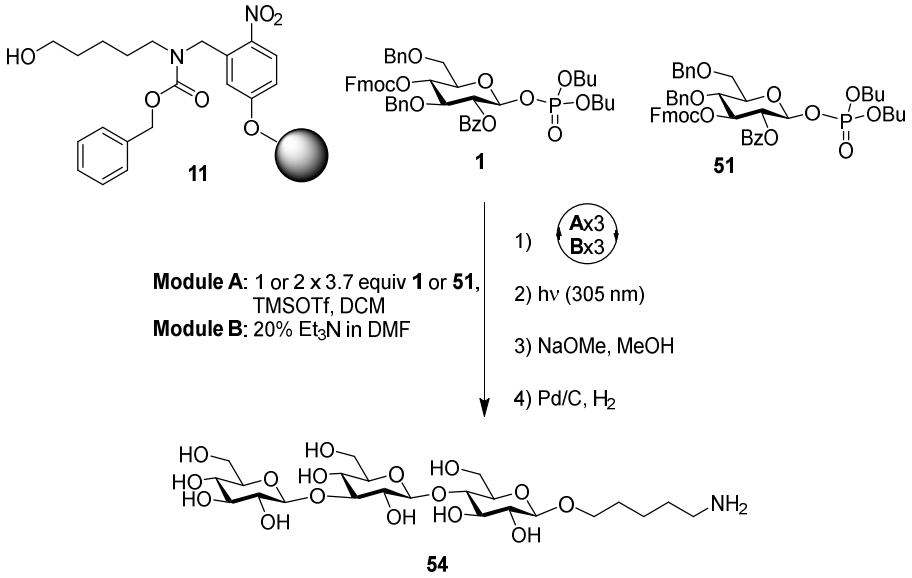

Linker-functionalized resin **11** (54 mg, 17.5 µmol) was placed in the reaction vessel of the synthesizer and synthesizer modules were applied as follows:

Module **A** (3.7 equiv. **1**, TMSOTf, DCM, 35 min, -30 °C to -15 °C)
Module **B** (20% NEt_3 in DMF, 3 x 5 min, rt)
Module **A** (2 x 3.7 equiv. **51**, TMSOTf, DCM, 35 min, -30 °C to -15 °C)
Module **B** (20% NEt_3 in DMF, 3 x 5 min, rt)
Module **A** (3.7 equiv. **1**, TMSOTf, DCM, 35 min, -30 °C to -15 °C)
Module **B** (20% NEt_3 in DMF, 3 x 5 min, rt)

Cleavage from the resin using UV irradiation at 305 nm in a continuous flow photoreactor afforded the protected trisaccharide. The crude product was purified by normal phase HPLC using a preparative YMC Diol column.

Crude NP-HPLC of the protected trisaccharide **53** (ELSD trace):

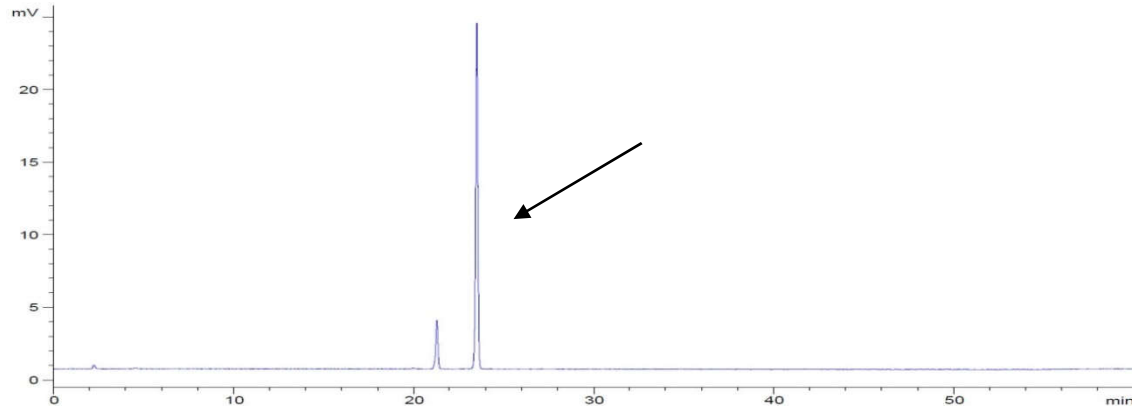

HPLC was performed using a YMC Diol column and a linear gradient from 10% to 100% ethyl acetate in hexane (40 min, flow rate 1 mL/min).

The protected trisaccharide **53** was dissolved in THF (3 mL) and NaOMe (0.5 M in MeOH, 0.5 mL) was added. The reaction mixture was stirred overnight and subsequently neutralized by addition of H^+-Amberlite resin. The resin was filtered off and the solvents were removed *in vacuo.* The crude product was purified by reverse phase HPLC using a preparative C5 column affording the semi-protected trisaccharide. The product was dissolved in a mixture of EtOAc/MeOH/AcOH/H_2O (4:2:2:1, 3 mL) and the resulting solution was added to a round-bottom flask containing Pd/C (10% Pd, 18 mg). The suspension was saturated with H_2 for 30 min and stirred under an H_2-atmosphere overnight. After filtration of the reaction mixture through a syringe filter, the solvents were evaporated to provide trisaccharide **54** (1.3 mg, 2.21 µmol, 13% over 9 steps, based on resin loading).

RP-HPLC of the deprotected trisaccharide **54** (ELSD trace):

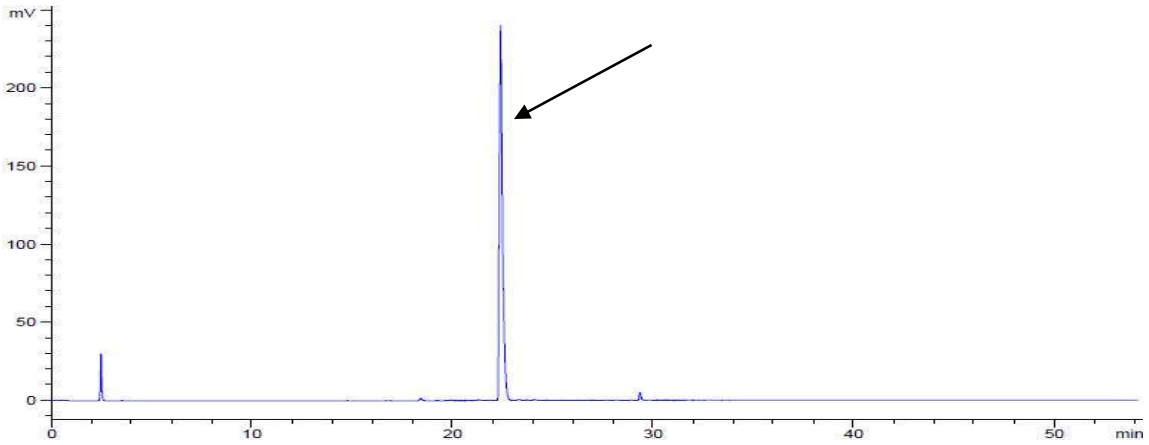

HPLC was performed using a Hypercarb column and a linear gradient from 97.5% to 30% H_2O (containing 0.1% of formic acid) in MeCN (45 min, flow rate 0.7 mL/min).

^{1}H NMR (600 MHz, D_2O): δ 4.76 (d, *J* = 7.9 Hz, 1H), 4.56 (d, *J* = 8.0 Hz, 1H), 4.50 (d, *J* = 8.0 Hz, 1H), 4.08-3.26 (m, 20H), 2.98 (t, *J* = 7.6 Hz, 2H), 1.72-1.64 (m, 4H), 1.50-1.43 (m, 2H) ppm. ^{13}C NMR (151 MHz, D_2O): δ 100.2, 99.8, 99.5, 81.5, 76.1, 73.5, 73.0, 72.2, 71.9, 70.9, 70.4, 67.6, 67.0, 65.5, 58.0, 57.5, 36.9, 25.7, 19.6 ppm. ESI-HRMS: m/z $[M+H]^+$ calcd. for $C_{23}H_{44}NO_{16}$: 590.2660; found 590.2661.

Aminopentyl β-D-glucopyranosyl-(1->4)-β-D-glucopyranosyl-(1->3)-β-D-glucopyranosyl-(1->4)-β-D-glucopyranose (55)

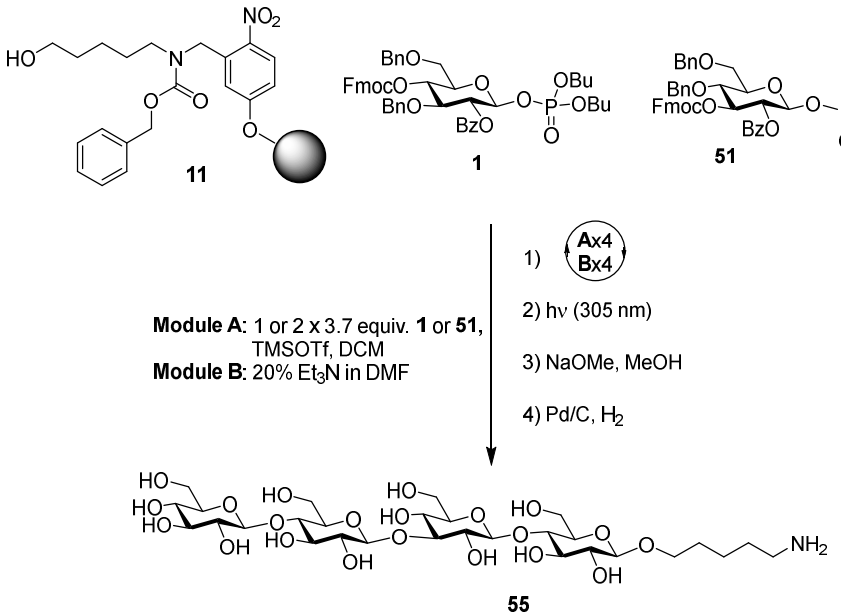

Linker-functionalized resin **11** (54 mg, 17.5 µmol) was placed in the reaction vessel of the synthesizer and synthesizer modules were applied as follows:
Module **A** (3.7 equiv. **1**, TMSOTf, DCM, 35 min, -30 °C to -15 °C)
Module **B** (20% NEt_3 in DMF, 3 x 5 min, rt)
Module **A** (3.7 equiv. **51**, TMSOTf, DCM, 35 min, -30 °C to -15 °C)
Module **B** (20% NEt_3 in DMF, 3 x 5 min, rt)
Module **A** (2 x 3.7 equiv. **1**, TMSOTf, DCM, 35 min, -30 °C to -15 °C)
Module **B** (20% NEt_3 in DMF, 3 x 5 min, rt)
Module **A** (3.7 equiv. **1**, TMSOTf, DCM, 35 min, -30 °C to -15 °C)
Module **B** (20% NEt_3 in DMF, 3 x 5 min, rt)

Cleavage from the resin using UV irradiation at 305 nm in a continuous flow photoreactor afforded the protected tetrasaccharide. The crude product was purified by normal phase HPLC using a preparative YMC Diol column.

Crude NP-HPLC of the protected tetrasaccharide (ELSD trace):

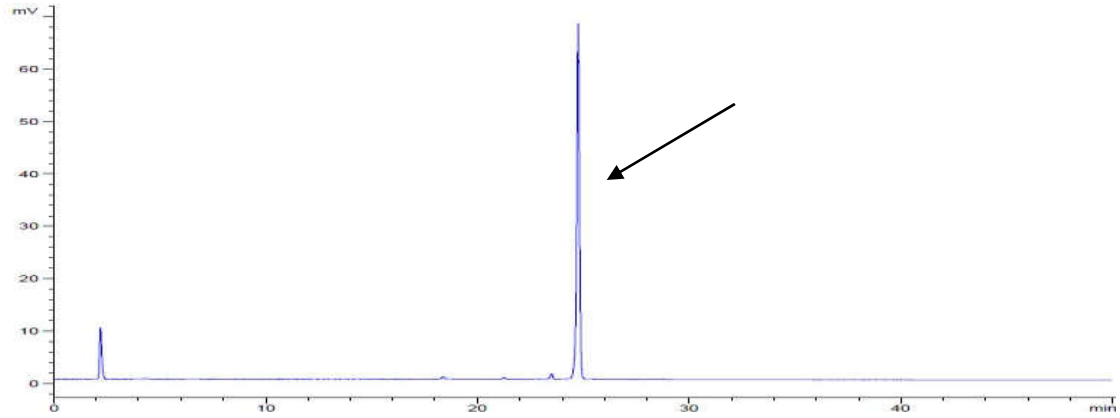

HPLC was performed using a YMC Diol column and a linear gradient from 10% to 100% ethyl acetate in hexane (40 min, flow rate 1 mL/min).

The protected tetrasaccharide was dissolved in THF (3 mL) and NaOMe (0.5 M in MeOH, 56.0 µL) was added. The reaction mixture was stirred overnight and subsequently neutralized by addition of H^+-Amberlite resin. The resin was filtered off and the solvents were removed *in vacuo.* The crude product was purified by normal phase HPLC using a preparative YMC Diol column affording the semi-protected tetrasaccharide. The product was dissolved in a mixture of EtOAc/MeOH/AcOH/H_2O (4:2:2:1, 3 mL) and the resulting solution was added to a round-bottom flask containing Pd/C (10% Pd, 9 mg). The suspension was

saturated with H_2 for 30 min and stirred under an H_2-atmosphere 40 h. After filtration of the reaction mixture through a syringe filter, the solvents were evaporated to provide the tetrasaccharide **55** (3.4 mg, 4.52 µmol, 26% over 11 steps, based on resin loading).

RP-HPLC of the deprotected tetrasaccharide **55** (ELSD trace):

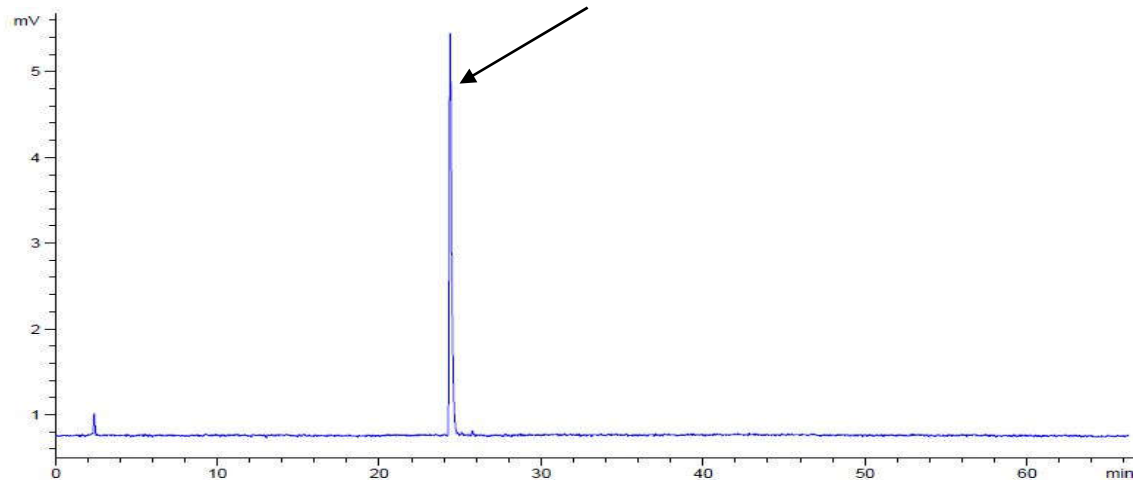

HPLC was performed using a Hypercarb column and a linear gradient from 97.5% to 30% H_2O (containing 0.1% of formic acid) in MeCN (45 min, flow rate 0.7 mL/min).

^{1}H NMR (600 MHz, D_2O): δ 4.72 (d, *J* = 7.9 Hz, 1H), 4.49-4.39 (m, 3H), 3.97-3.21 (m, 26H), 2.94 (t, *J* = 7.5 Hz, 2H), 1.68-1.55 (m, 4H), 1.45-1.34 (m, 2H) ppm. ^{13}C NMR (151 MHz, D_2O): δ 100.8, 100.6, 100.3, 82.1, 76.8, 74.2, 73.7, 73.0, 72.6, 72.4, 71.4, 71.3, 71.2, 68.3, 67.7, 66.2, 58.8, 58.3, 37.6, 26.4, 24.7, 20.3 ppm. ESI-HRMS: m/z $[M+H]^+$ calcd. for $C_{29}H_{54}NO_{21}$: 752.3188; found 752.3181.

Aminopentyl β-D-glucopyranosyl-(1->3)-β-D-glucopyranosyl-(1->4)-β-D-glucopyranosyl-(1->4)-β-D-glucopyranosyl-(1->4)-β-D-glucopyranosyl-(1->3)-β-D-glucopyranoside (56)

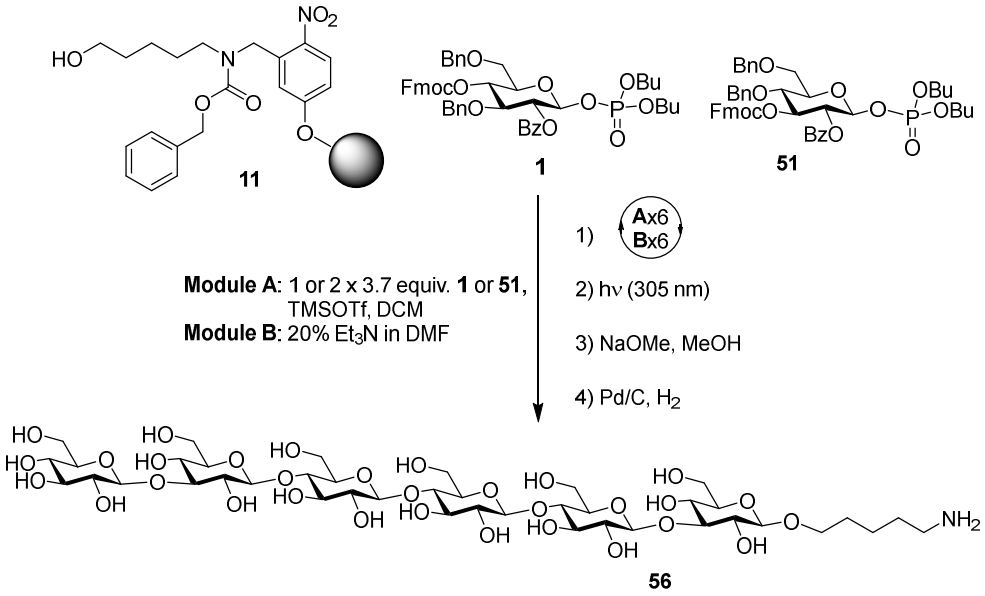

Linker functionalized resin **11** (51 mg, 16.6 µmol) was placed in the reaction vessel of the synthesizer and synthesizer modules were applied as follows:

Module **A** (3.7 equiv. **51**, TMSOTf, DCM, 35 min, -30 °C to -15 °C)

Module **B** (20% NEt_3 in DMF, 3 x 5 min, rt)

Module **A** (2 x 3.7 equiv. **1**, TMSOTf, DCM, 35 min, -30 °C to -15 °C)

Module **B** (20% NEt_3 in DMF, 3 x 5 min, rt)

Module **A** (3.7 equiv. **1**, TMSOTf, DCM, 35 min, -30 °C to -15 °C)

Module **B** (20% NEt_3 in DMF, 3 x 5 min, rt)

Module **A** (3.7 equiv. **1**, TMSOTf, DCM, 35 min, -30 °C to -15 °C)

Module **B** (20% NEt_3 in DMF, 3 x 5 min, rt)

Module **A** (3.7 equiv. **51**, TMSOTf, DCM, 35 min, -30 °C to -15 °C)

Module **B** (20% NEt_3 in DMF, 3 x 5 min, rt)

Module **A** (2 x 3.7 equiv. **1**, TMSOTf, DCM, 35 min, -30 °C to -15 °C)

Module **B** (20% NEt_3 in DMF, 3 x 5 min, rt)

Cleavage from the resin using UV irradiation at 305 nm in a continuous flow photoreactor afforded the protected hexasaccharide. The crude product was purified by normal phase HPLC using a preparative YMC Diol column.

Crude NP-HPLC of protected hexasaccharide (ELSD trace):

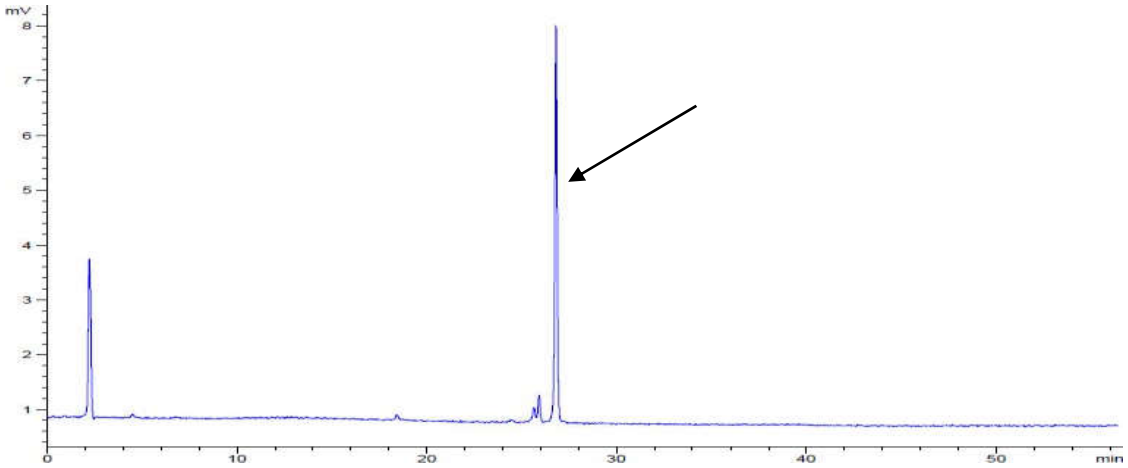

HPLC was performed using a YMC Diol column and a linear gradient from 10% to 100% ethyl acetate in hexane (40 min, flow rate 1 mL/min).

The protected hexasaccharide was dissolved in THF (3 mL) and NaOMe (0.5 M in MeOH, 74.0 μL) was added. The reaction mixture was stirred overnight and subsequently neutralized by addition of a drop of AcOH and the solvents were removed *in vacuo.* The crude product was purified by normal phase HPLC using a preparative YMC Diol column affording the semi-protected hexasaccharide. The product was dissolved in a mixture of EtOAc/MeOH/AcOH/H_2O (4:2:2:1, 3 mL) and the resulting solution was added to a round-bottom flask containing Pd/C (10% Pd, 9 mg). The suspension was saturated with H_2 for 30 min and stirred under an H_2-atmosphere 40 h. After filtration of the reaction mixture through a syringe filter, the solvents were evaporated. The crude product was purified by reverse phase HPLC using a semi-preparative Hypercarb column affording the hexasaccharide **56** (2.1 mg, 1.95 μmol, 12% over 15 steps, based on resin loading).

RP-HPLC of the deprotected hexasaccharide **56** (ELSD trace):

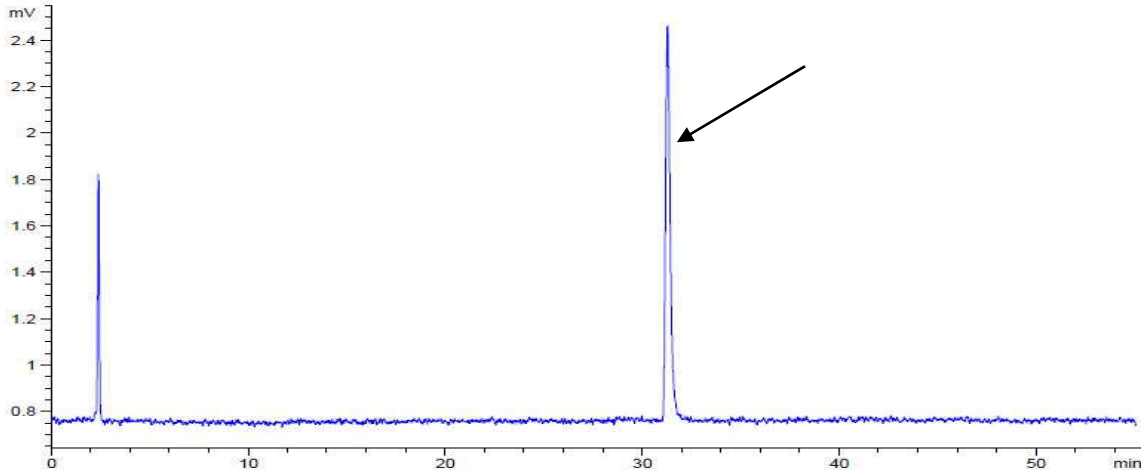

HPLC was performed using a Hypercarb column and a linear gradient from 97.5% to 30% H_2O (containing 0.1% of formic acid) in MeCN (45 min, flow rate 0.7 mL/min).

^{1}H NMR (700 MHz, D_2O): δ 4.78-4.74 (m, 2H), 4.57-4.53 (m, 3H), 4.50 (d, *J* = 8.1 Hz, 1H), 4.03-3.34 (m, 38H), 3.02-2.98 (m, 2H), 1.73-1.65 (m, 4H), 1.50-1.43 (m, 2H) ppm. ^{13}C NMR (176 MHz, D_2O): δ 98.0, 97.6, 97.2, 79.8, 79.2, 73.6, 71.3, 70.8, 70.1, 69.3, 68.7, 68.5, 68.2, 68.1, 65.4, 64.9, 63.4, 63.3, 56.0, 34.7, 23.4, 21.9, 17.4 ppm. ESI-HRMS: m/z $[M+H]^+$ calcd. for $C_{29}H_{54}NO_{21}$: 1076.4245; found 1076.4249.

Aminopentyl β-D-glucopyranosyl-(1->4)-β-D-glucopyranosyl-(1->3)-β-D-glucopyranosyl-(1->3)-β-D-glucopyranosyl-(1->4)-β-D-glucopyranosyl-(1->4)-β-D-glucopyranoside (57)

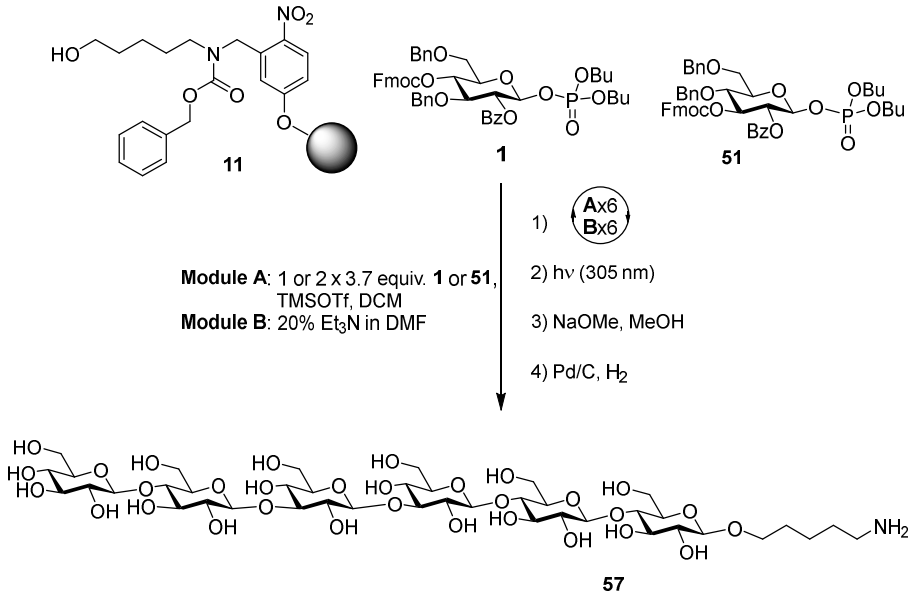

Linker-functionalized resin **11** (54 mg, 17.5 µmol) was placed in the reaction vessel of the synthesizer and synthesizer modules were applied as follows:

Module **A** (3.7 equiv. **1**, TMSOTf, DCM, 35 min, -30 °C to -15 °C)

Module **B** (20% NEt_3 in DMF, 3 x 5 min, rt)

Module **A** (3.7 equiv. **1**, TMSOTf, DCM, 35 min, -30 °C to -15 °C)

Module **B** (20% NEt_3 in DMF, 3 x 5 min, rt)

Module **A** (3.7 equiv. **51**, TMSOTf, DCM, 35 min, -30 °C to -15 °C)

Module **B** (20% NEt_3 in DMF, 3 x 5 min, rt)

Module **A** (2 x 3.7 equiv. **51**, TMSOTf, DCM, 35 min, -30 °C to -15 °C)

Module **B** (20% NEt_3 in DMF, 3 x 5 min, rt)

Module **A** (2 x 3.7 equiv. **1**, TMSOTf, DCM, 35 min, -30 °C to -15 °C)

Module **B** (20% NEt_3 in DMF, 3 x 5 min, rt)

Module **A** (3.7 equiv. **1**, TMSOTf, DCM, 35 min, -30 °C to -15 °C)

Module **B** (20% NEt_3 in DMF, 3 x 5 min, rt)

Cleavage from the resin using UV irradiation at 305 nm in a continuous flow photoreactor afforded the protected hexasaccharide. The crude product was purified by normal phase HPLC using a preparative YMC Diol column.

Crude NP-HPLC of the protected hexasaccharide (ELSD trace):

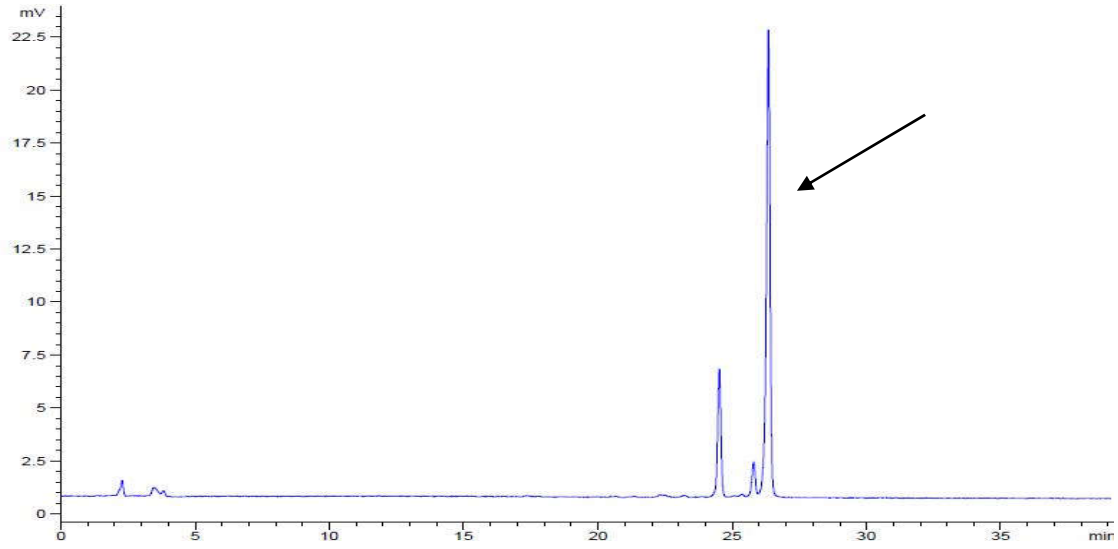

HPLC was performed using a YMC Diol column and a linear gradient from 10% to 75% ethyl acetate in hexane (30 min, flow rate 1 mL/min).

The protected hexasaccharide was dissolved in THF (3 mL) and NaOMe (0.5 M in MeOH, 51.0 µL) was added. The reaction mixture was stirred overnight

and subsequently neutralized by addition of H^+-Amberlite resin. The resin was filtered off and the solvents were removed *in vacuo.* The crude product was purified by normal phase HPLC using a preparative YMC Diol column affording the semi-protected hexasaccharide. The product was dissolved in a mixture of EtOAc/MeOH/AcOH/H_2O (4:2:2:1, 3 mL) and the resulting solution was added to a round-bottom flask containing Pd/C (10% Pd, 8 mg). The suspension was saturated with H_2 for 30 min and stirred under an H_2-atmosphere 40 h. After filtration of the reaction mixture through a syringe filter, the solvents were evaporated to provide the hexasaccharide **57** (2.2 mg, 2.05 µmol, 12% over 15 steps, based on resin loading).

RP-HPLC of the deprotected hexasaccharide **57** (ELSD trace):

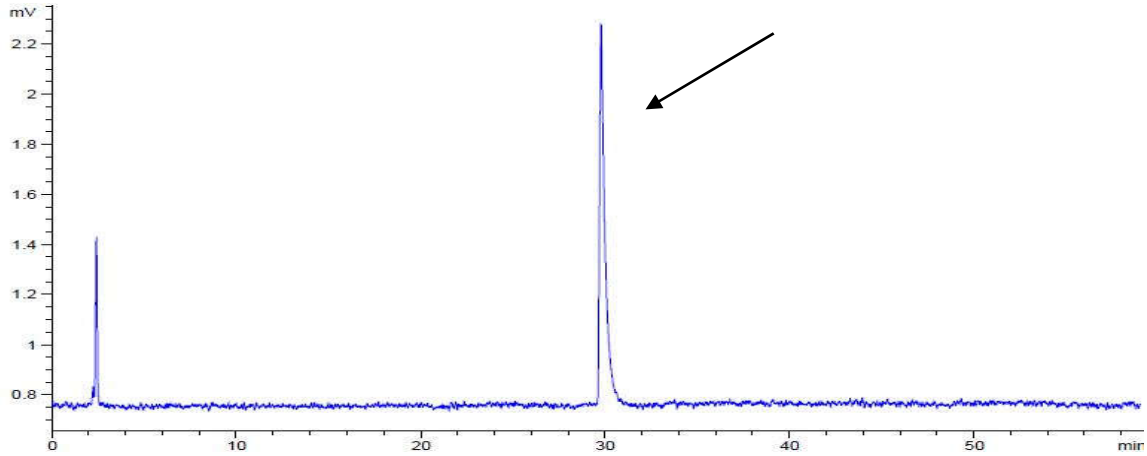

HPLC was performed using a Hypercarb column and a linear gradient from 97.5% to 30% H_2O (containing 0.1% of formic acid) in MeCN (45 min, flow rate 0.7 mL/min).

^{1}H NMR (400 MHz, D_2O): δ 4.72 (d, *J* = 8.0 Hz, 2H), 4.53-4.36 (m, 4H), 4.02-3.18 (m, 38H), 3.01-2.83 (m, 2H), 1.66-1.57 (m, 4H), 1.44-1.34 (q, 2H) ppm. ^{13}C NMR (101 MHz, D_2O): δ 100.4, 100.1, 99.8, 81.7, 81.4, 76.3, 76.1, 73.8, 73.4, 73.2, 72.6, 72.1, 71.9, 71.1, 70.9, 70.7, 67.9, 67.2, 65.8, 65.7, 58.3, 57.7, 37.1, 26.0, 24.2, 19.9. ESI-HRMS: m/z $[M+H]^+$ calcd. for $C_{41}H_{74}NO_{31}$: 1076.4245; found 1076.4240.

Aminopentyl β-D-glucopyranosyl-(1->4)-β-D-glucopyranosyl-(1->4)-β-D-glucopyranosyl-(1->4)-β-D-glucopyranosyl-(1->3)-β-D-glucopyranosyl-(1->4)-β-D-glucopyranoside (58)

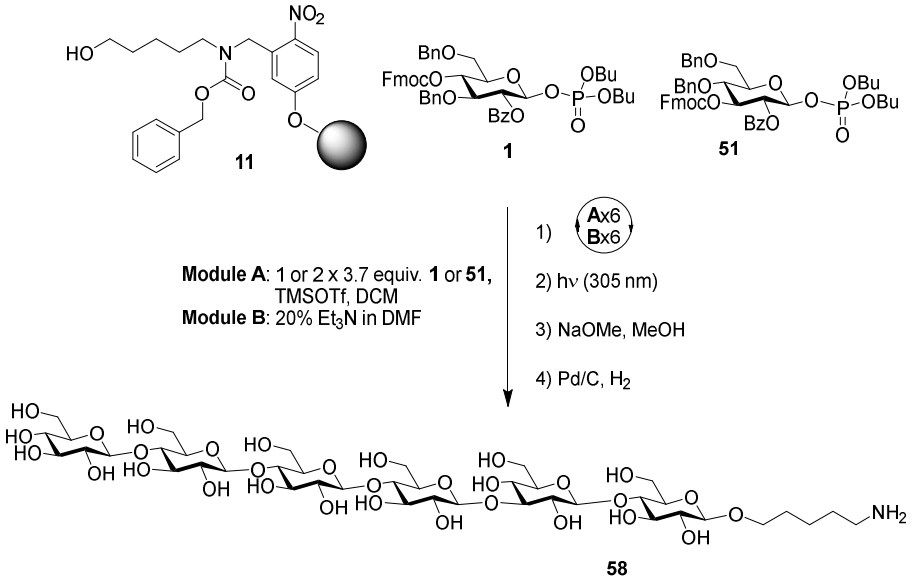

Linker functionalized resin **11** (55 mg, 17.9 µmol) was placed in the reaction vessel of the synthesizer and synthesizer modules were applied as follows:

Module **A** (3.7 equiv. **1**, TMSOTf, DCM, 35 min, -30 °C to -15 °C)

Module **B** (20% NEt_3 in DMF, 3 x 5 min, rt)

Module **A** (3.7 equiv. **51**, TMSOTf, DCM, 35 min, -30 °C to -15 °C)

Module **B** (20% NEt_3 in DMF, 3 x 5 min, rt)

Module **A** (2 x 3.7 equiv. **1**, TMSOTf, DCM, 35 min, -30 °C to -15 °C)

Module **B** (20% NEt_3 in DMF, 3 x 5 min, rt)

Module **A** (3.7 equiv. **1**, TMSOTf, DCM, 35 min, -30 °C to -15 °C)

Module **B** (20% NEt_3 in DMF, 3 x 5 min, rt)

Module **A** (3.7 equiv. **1**, TMSOTf, DCM, 35 min, -30 °C to -15 °C)

Module **B** (20% NEt_3 in DMF, 3 x 5 min, rt)

Module **A** (3.7 equiv. **1**, TMSOTf, DCM, 35 min, -30 °C to -15 °C)

Module **B** (20% NEt_3 in DMF, 3 x 5 min, rt)

Cleavage from the resin using UV irradiation at 305 nm in a continuous flow photoreactor afforded the protected hexasaccharide. The crude product was purified by normal phase HPLC using a preparative YMC Diol column.

Crude NP-HPLC of the protected hexasaccharide (ELSD trace):

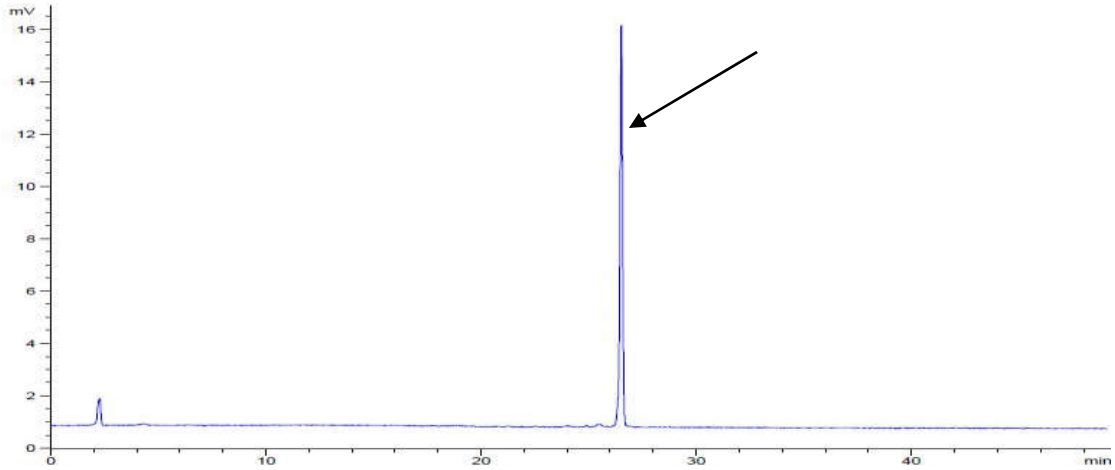

HPLC was performed using a YMC Diol column and a linear gradient from 10% to 100% ethyl acetate in hexane (40 min, flow rate 1 mL/min).

The protected hexasaccharide was dissolved in THF (3 mL) and NaOMe (0.5 M in MeOH, 131 μL) was added. The reaction mixture was stirred overnight and subsequently neutralized by addition of H^+-Amberlite resin. The resin was filtered off and the solvents were removed *in vacuo.* The crude product was purified by normal phase HPLC using a preparative YMC Diol column affording the semi-protected hexasaccharide. The product was dissolved in a mixture of EtOAc/MeOH/AcOH/H_2O (4:2:2:1, 3 mL) and the resulting solution was added to a round-bottom flask containing Pd/C (10% Pd, 15 mg). The suspension was saturated with H_2 for 30 min and stirred under an H_2-atmosphere 40 h. After filtration of the reaction mixture through a syringe filter, the solvents were evaporated to provide the hexasaccharide **58** (6.5 mg, 6.04 μmol, 34% over 15 steps, based on resin loading).

RP-HPLC of the deprotected hexasaccharide **58** (ELSD trace):

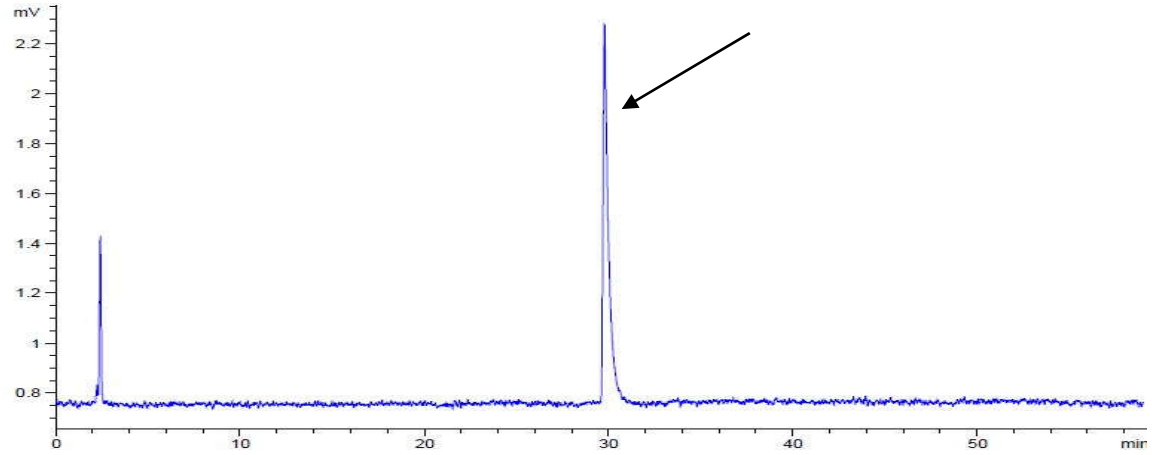

HPLC was performed using a Hypercarb column and a linear gradient from 97.5% to 30% H_2O (containing 0.1% of formic acid) in MeCN (45 min, flow rate 0.7 mL/min).

^{1}H NMR (400 MHz, D_2O): δ 4.70 (d, *J* = 7.9 Hz, 1H), 4.52-4.38 (m, 5H), 3.98-3.16 (m, 38H), 3.01-2.86 (m, 2H), 1.68-1.54 (m, 4H), 1.46-1.31 (m, 2H) ppm. ^{13}C NMR (101 MHz, D_2O): δ 13C NMR (101 MHz, D2O) δ 100.3, 100.1, 99.8, 81.4, 76.37, 76.2, 76.1, 76.0, 73.8, 73.4, 73.2, 72.6, 72.1, 71.8, 71.7, 71.0, 70.9, 70.8, 70.7, 67.9, 67.2, 65.7, 58.3, 57.6, 37.1, 26.0, 24.2, 19.9 ppm. ESI-HRMS: m/z $[M+H]^+$ calcd. for $C_{41}H_{74}NO_{31}$: 1076.4245; found 1076.4250.

Aminopentyl β-D-glucopyranosyl-(1->4)-β-D-glucopyranosyl-(1->4)-β-D-glucopyranosyl-(1->3)-β-D-glucopyranosyl-(1->4)-β-D-glucopyranosyl-(1→3)-β-D-glucopyranoside (59)

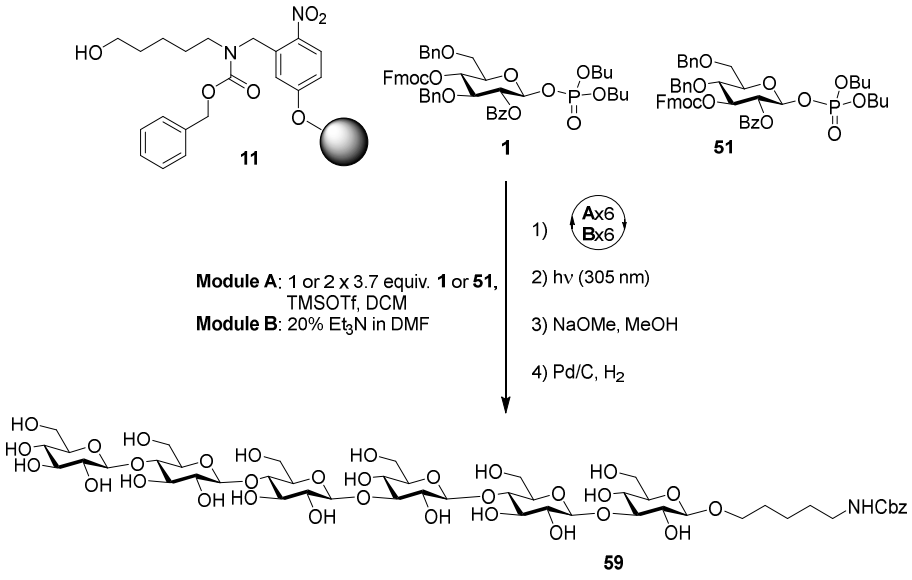

Linker functionalized resin **11** (55 mg, 17.9 µmol) was placed in the reaction vessel of the synthesizer and synthesizer modules were applied as follows:
Module **A** (3.7 equiv. **51**, TMSOTf, DCM, 35 min, -30 °C to -15 °C)
Module **B** (20% NEt_3 in DMF, 3 x 5 min, rt)
Module **A** (2 x 3.7 equiv. **1**, TMSOTf, DCM, 35 min, -30 °C to -15 °C)
Module **B** (20% NEt_3 in DMF, 3 x 5 min, rt)
Module **A** (3.7 equiv. **51**, TMSOTf, DCM, 35 min, -30 °C to -15 °C)
Module **B** (20% NEt_3 in DMF, 3 x 5 min, rt)
Module **A** (2 x 3.7 equiv. **1**, TMSOTf, DCM, 35 min, -30 °C to -15 °C)
Module **B** (20% NEt_3 in DMF, 3 x 5 min, rt)
Module **A** (3.7 equiv. **1**, TMSOTf, DCM, 35 min, -30 °C to -15 °C)
Module **B** (20% NEt_3 in DMF, 3 x 5 min, rt)
Module **A** (3.7 equiv. **1**, TMSOTf, DCM, 35 min, -30 °C to -15 °C)
Module **B** (20% NEt_3 in DMF, 3 x 5 min, rt)

Cleavage from the resin using UV irradiation at 305 nm in a continuous flow photoreactor afforded the protected hexasaccharide. The crude product was purified by normal phase HPLC using a preparative YMC Diol column.

Crude NP-HPLC of the protected hexasaccharide (ELSD trace):

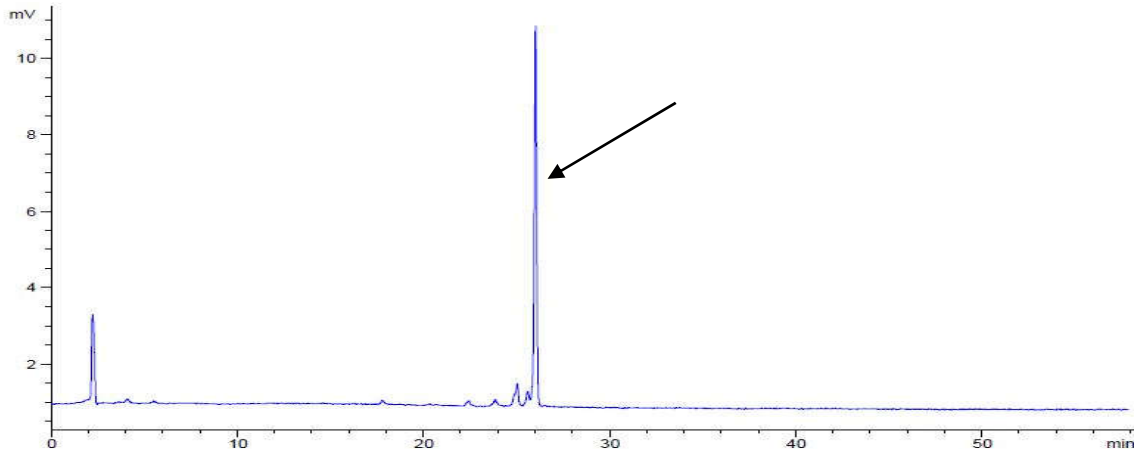

HPLC was performed using a YMC Diol column and a linear gradient from 10% to 100% ethyl acetate in hexane (40 min, flow rate 1 mL/min).

The protected hexasaccharide was dissolved in THF (3 mL) and NaOMe (0.5 M in MeOH, 74.5 µL) was added. The reaction mixture was stirred overnight and subsequently neutralized by addition of H^+-Amberlite resin. The resin was

filtered off and the solvents were removed *in vacuo.* The crude product was purified by normal phase HPLC using a preparative YMC Diol column affording the semi-protected hexasaccharide. The product was dissolved in a mixture of EtOAc/MeOH/AcOH/H_2O (4:2:2:1, 3 mL) and the resulting solution was added to a round-bottom flask containing Pd/C (10% Pd, 16 mg). The suspension was saturated with H_2 for 30 min and stirred under an H_2-atmosphere overnight. After filtration of the reaction mixture through a syringe filter, the solvents were evaporated to provide the hexasaccharide **59** (3.5 mg, 3.25 µmol, 18% over 15 steps, based on resin loading).

RP-HPLC of the deprotected hexasaccharide **59** (ELSD trace):

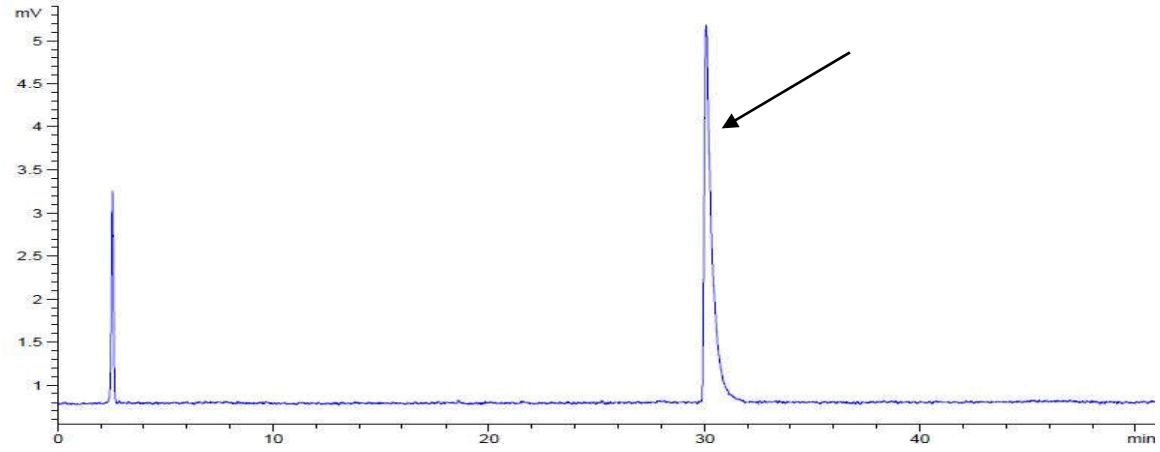

HPLC was performed using a Hypercarb column and a linear gradient from 97.5% to 30% H_2O (containing 0.1% of formic acid) in MeCN (45 min, flow rate 0.7 mL/min).

^{1}H NMR (600 MHz, D_2O): δ 4.59-4.45 (m, 4H), 4.05-3.26 (m, 38H), 3.02 (t, *J* = 7.6 Hz, 2H), 1.75-1.63 (m, 4H), 1.51-1.43 (m, 2H) ppm. ^{13}C NMR (151 MHz, D_2O): δ 100.4, 100.2, 99.8, 82.3, 81.6, 76.4, 76.3, 76.2, 73.8, 73.4, 73.3, 72.7, 71.9, 71.1, 71.0, 70.9, 70.8, 70.7, 67.9, 67.3, 66.0, 65.8, 58.6, 58.4, 57.8, 37.2, 26.0, 24.3, 19.9 ppm. ESI-HRMS: m/z $[M+H]^+$ calcd. for $C_{41}H_{74}NO_{31}$: 1076.4245; found 1076.4213.

Aminopentyl β-D-glucopyranosyl-(1->3)-β-D-glucopyranosyl-(1->4)-β-D-glucopyranosyl-(1->3)-β-D-glucopyranosyl-(1->4)-β-D-glucopyranosyl-(1->4)-β-D-glucopyranosyl-(1->3)-β-D-glucopyranoside (60)

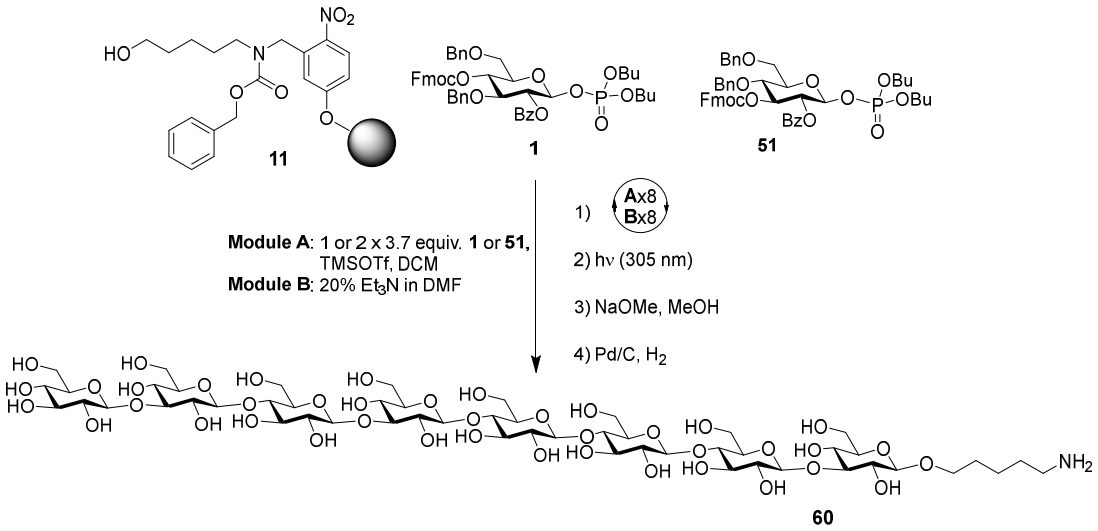

Linker functionalized resin **11** (53 mg, 17.2 µmol) was placed in the reaction vessel of the synthesizer and synthesizer modules were applied as follows:

Module **A** (3.7 equiv. **51**, TMSOTf, DCM, 35 min, -30 °C to -15 °C)

Module **B** (20% NEt_3 in DMF, 3 x 5 min, rt)

Module **A** (2 x 3.7 equiv. **1**, TMSOTf, DCM, 35 min, -30 °C to -15 °C)

Module **B** (20% NEt_3 in DMF, 3 x 5 min, rt)

Module **A** (3.7 equiv. **1**, TMSOTf, DCM, 35 min, -30 °C to -15 °C)

Module **B** (20% NEt_3 in DMF, 3 x 5 min, rt)

Module **A** (3.7 equiv. **1**, TMSOTf, DCM, 35 min, -30 °C to -15 °C)

Module **B** (20% NEt_3 in DMF, 3 x 5 min, rt)

Module **A** (3.7 equiv. **51**, TMSOTf, DCM, 35 min, -30 °C to -15 °C)

Module **B** (20% NEt_3 in DMF, 3 x 5 min, rt)

Module **A** (2 x 3.7 equiv. **1**, TMSOTf, DCM, 35 min, -30 °C to -15 °C)

Module **B** (20% NEt_3 in DMF, 3 x 5 min, rt)

Module **A** (3.7 equiv. **51**, TMSOTf, DCM, 35 min, -30 °C to -15 °C)

Module **B** (20% NEt_3 in DMF, 3 x 5 min, rt)

Module **A** (2 x 3.7 equiv. **1**, TMSOTf, DCM, 35 min, -30 °C to -15 °C)

Module **B** (20% NEt_3 in DMF, 3 x 5 min, rt)

Cleavage from the resin using UV irradiation at 305 nm in a continuous flow photoreactor afforded the protected octasaccharide. The crude product was purified by normal phase HPLC using a preparative YMC Diol column.

Crude NP-HPLC of the protected octasaccharide (ELSD trace):

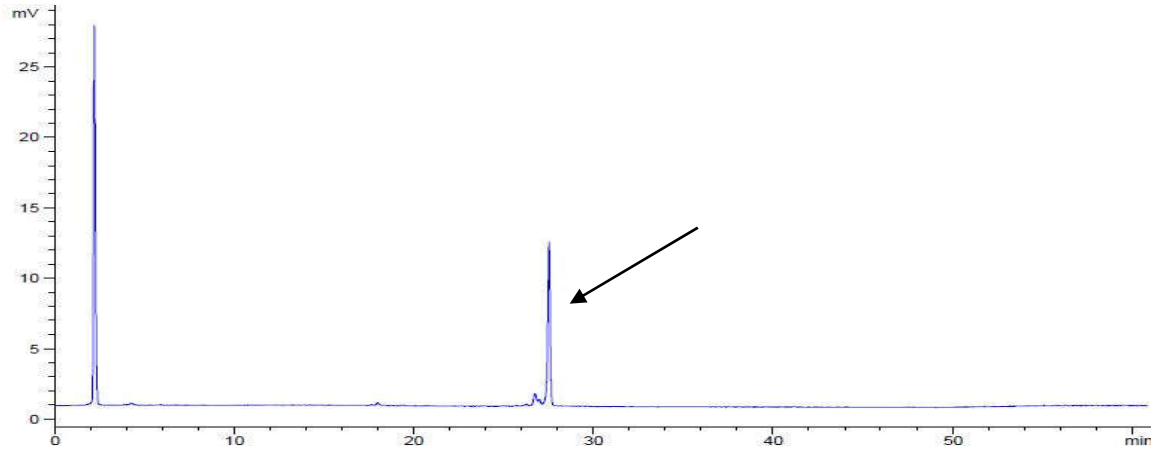

HPLC was performed using a YMC Diol column and a linear gradient from 10% to 100% ethyl acetate in hexane (40 min, flow rate 1 mL/min).

The protected octasaccharide was dissolved in THF (3 mL) and NaOMe (0.5 M in MeOH, 126 μL) was added. The reaction mixture was stirred overnight and subsequently neutralized by addition of H^+-Amberlite resin. The resin was filtered off and the solvents were removed *in vacuo.* The crude product was purified by normal phase HPLC using a preparative YMC Diol column affording the semi-protected octasaccharide. The product was dissolved in a mixture of EtOAc/MeOH/AcOH/H_2O (4:2:2:1, 3 mL) and the resulting solution was added to a round-bottom flask containing Pd/C (10% Pd, 20 mg). The suspension was saturated with H_2 for 30 min and stirred under an H_2-atmosphere overnight. After filtration of the reaction mixture through a syringe filter, the solvents were evaporated to provide the octasaccharide **60** (5.6 mg, 4.00 μmol, 23% over 19 steps, based on resin loading).

RP-HPLC of the deprotected octasaccharide **60** (ELSD trace):

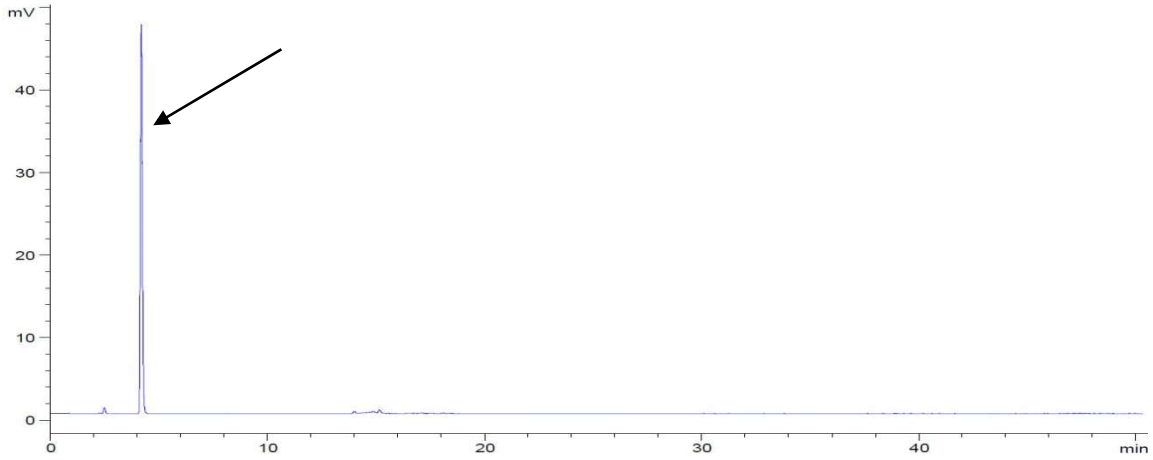

HPLC was performed using a Phenomenex Synergi Hydro-RP18 column and a linear gradient from 100% to 0% H_2O (containing 0.1% of formic acid) in MeCN (45 min, flow rate 1 mL/min).

^{1}H NMR (600 MHz, D_2O): δ 4.59-4.52 (m, 4H), 4.50 (d, *J* = 8.1 Hz, 1H), 4.07-3.26 (m, 53H), 3.02 (t, *J* = 7.6 Hz, 2H), 1.75-1.65 (m, 4H), 1.50-1.44 (m, 2H) ppm. ^{13}C NMR (151 MHz, D_2O): δ 100.8, 100.6, 100.5, 100.4, 99.9, 82.5, 82.0, 81.8, 76.6, 76.5, 76.4, 76.3, 74.0, 73.6, 73.6, 72.9, 72.8, 72.1, 71.4, 71.2, 71.0, 70.9, 70.9, 68.1, 67.6, 66.2, 66.0, 58.7, 58.6, 58.0, 57.9, 37.4, 26.2, 24.4, 20.1 ppm. ESI-HRMS: m/z $[M+H]^+$ calcd. for $C_{41}H_{74}NO_{31}$: 1400.5310; found 1400.5301.

3.4.5 Analysis of Glycosyl Hydrolase Substrate Specificities

Lichenase (endo-1,3:1,4-β-D-Glucanase) from *Bacillus subtilis* (GH16) was purchased from Megazyme (Bray, Ireland) and used in the following buffer that was suggested by the manufacturer: 100 mM $NaPO_4$, pH 6.5. The enzyme was used at a concentration of 1 U/mL for the end-point measurements and at 0.33 U/ml for the time-course experiments. The oligosaccharides were used at a concentration of 1 mM. All reactions were carried out at 40°C and terminated by incubation at 80°C for 5 min. The reactions were analyzed on an Agilent 1200 Series HPLC equipped with an Agilent 6130 quadrupole MS and an Agilent 1200 ELSD. For the end point experiment the oligosaccharides were separated on a Hypercarb column (150 x 4.6 mm, Thermo Scientific) using a water (including 0.1% formic acid)-ACN gradient at a flow-rate of 0.7 mL/min starting at 2.5% ACN for 5 min, ramping up to 15% ACN at 8 min, followed by a slow increase of ACN to 30% at 40 min, a steep ramp to 100% ACN at 43.5 min, a decline back to 2.5%

ACN from 46 min to 47min, and equilibration until 55 min at 2.5% ACN. For the time-course experiment the oligosaccharides were separated on a Synergi column (150 x 4.6 mm, Phenomenex) using a water (including 0.1% formic acid)-ACN gradient at a flow-rate of 1.0 ml/min starting at 0% ACN for 5 min, ramping up to 20% ACN at 20 min, a steep ramp to 100% ACN at 25 min, flush of the column with 100% ACN for 5 min, a decline back to 0% ACN from 30 min to 35min, and equilibration until 45 min at 0% ACN. The peaks in the ELSD traces were assigned based on their retention time and the corresponding masses in the MS.

Bibliography

1. S. C. Fry, *New Phytol.* , 2004, **161**, 641-675.
2. L. Teiz and E. Zeiger, in *Plant Physiology 5th edition*, Editon edn., **2010**.
3. A. Bacic, A. J. Harris and B. A. Stone, ed. J. Preiss, Ed. Academic Press: New York, Editon edn., 1988, pp. 52-108.
4. M. John, H. Röhring, J. Schmidt, R. Walden and J. Schell, *Trends Plant Sci.* , 1997, **2**, 111-115.
5. G. De Lorenzo and S. Ferrari, *Curr. Opin. Plant Biol*, 2002, **5**, 295-299.
6. W. Van den Ende, B. De Conick and A. Van Laere, *Trends Plant Sci.* , 2004, **9**, 523-528.
7. K. J. Lee, S. E. Marcus and J. P. Knox, *Mol. Plant.*, 2011, **4**, 212-219.
8. M. Pauly and K. Keegstra, *Curr. Opin. Plant Biol.*, 2010, **13**, 305-312.
9. J. W. DeVries, *Proc. Nutr. Soc.*, 2003, **62**, 37-43.
10. P. J. Harris and B. G. Smith, *Int. J. Food Sci. Tech*, 2012, **24**, 64-73.
11. A. O. Tzianabos, *Clin. Microbiol. Rev.*, 2000, **13**, 523-533.
12. S. P. Wasser, *Appl. Microbiol. Biotechnol.*, 2002, **60**, 258–274.
13. I. A. Schepetkin and M. T. Quinn, *Int. Immunopharmacol.*, 2006, 317-333.
14. A. V. Sergeev, E. S. Revazova, S. I. Denisova, O. V. Kalatskaia and A. N. Rytenko, *Bull. Exp. Biol. Med.*, 1985, **100**, 741–743.
15. A. Brogniart, A. B. Pelonze and R. Dumas, *Comptes Rendus*, 1839, **8**, 51-53.
16. A. Payen, *C. R. Hebd. Seances Acad. Sci.*, 1838, **7**, 1052.
17. D. Klemm, B. Heublein, H.-P. Fink and A. Bohn, *Angew. Chem. Int. Ed.*, 2005, **44**, 3358-3393.
18. D. Klemm, H.-P. Schmauder and T. Heinze, in *Biopolymers*, eds. E. Vandamme, S. D. Beats and A. Steinbüchel, Wiley-VCH, Weinheim, Editon edn., 2002, vol. 6, pp. 290-292.
19. D. L. Kaplan, in *Biopolymers from Renewable Resources*, ed. D. L. Kaplan, Springer, Berlin, Editon edn., 1998, pp. 1-29.
20. R. M. Brown Jr, I. M. Saxena and K. Kudlicka, *Trends Plant Sci.* , 1996, **1**, 149-155.
21. R. J. Moon, A. Martini, J. Nairn, J. Simonsen and J. Youngblood, *Chem. Soc. Rev.*, 2011, **40**, 3941-3994.
22. Y. Nishiyama, *J. Wood Sci.*, 2009, **55**, 241-249.
23. O. Lerouxel, D. M. Cavalier, A. H. Liepman and K. Keegstra, *Curr. Opin. Plant Biol.*, 2006, **9**, 621-630.
24. E. Schulze, *Ber. Dtsch. Chem. Ges.*, 1891, **24**, 2277.
25. A. Ebringerova, Z. Hromadkova and T. Heinze, *Adv. Polym. Sci.*, 2005, **186**, 1–67.
26. H. V. Scheller and P. Ulvskov, *Annu. Rev. Plant. Biol.*, 2010, **61**, 263-289.
27. K. S. Dhugga, R. Barreiro, B. Whitten, J. Hazebroek, G. S. Randhawa, M. Dolan, A. J. Kinney, D. Tomes, S. Nichols and P. Anderson, *Science*, 2004, **16**, 363-366.
28. A. H. Liepman, C. G. Wilkerson and K. Keegstra, *PNAS*, 2005, **102**, 2221-2226.
29. R. A. Burton, S. M. Wilson, M. Hrmova, A. J. Harvey, N. J. Shirley, A. Medhurst, B. S. Stone, E. J. Newbigin, A. Bacic and G. B. Fincher, *Science*, 2006, **311**, 1940-1942.

30. J.-C. Cocuron, O. Lerouxel, G. Drakakaki, A. P. Alonso, A. H. Liepman, K. Keegstra, N. Raikhel and C. G. Wilkerson, *PNAS*, 2007, **104**, 8550-8555.
31. H. Braconnot, *Annales de chimie et de physique*, 1825, **2**, 173-178.
32. J.-P. Joseleau and S. Perez, *The Plant Cell Walls*.
33. I. Braccini, R. P. Grasso and S. Perez, *Carbohyd. Res.*, 1999, **317**, 119-130.
34. F. Micheli, *Trends Plant Sci.*, 2001, **6**, 414-419.
35. P. Albersheim, D. J. Nevis, P. D. English and A. Karr, *Carbohyd. Res.*, 1967, **5**, 340-345.
36. A. D. Blakeney, P. J. Harris, R. J. Henry and B. A. Stone, *Carbohyd. Res.*, 1983, **113**, 291-299.
37. F. A. Pettolino, C. Walsh, G. B. Fincher and A. Bacic, *Nat. Protoc.*, 2012, **7**, 1590-1607.
38. S. D. Mansfield, H. Kim, F. Lu and J. Ralph, *Nat. Protoc.*, 2012, **9**, 1579-1589.
39. J. P. Knox, *Curr. Opin. Plant Biol.*, 2008, **11**, 308–313.
40. S. Pattathil, U. Avci, D. Baldwin, A. G. Swennes, J. A. McGill, Z. Popper, T. Bootten, A. Albert, R. H. Davis, C. Chennareddy, R. Dong, B. O'Shea, R. Rossi, C. Leoff, G. Freshour, R. Narra, M. O'Neil, W. S. York and M. G. Hahn, *Plant Physiol.*, 2010, **153**, 514-525.
41. I. Moller, S. E. Marcus, A. Haeger, Y. Verhertbruggen, R. Verhoef, H. Schols, P. Ulvskov, J. D. Mikkelsen, J. P. Knox and W. G. T. Willats, *Glycoconj. J.*, 2008, **25**, 37-48.
42. G. Kohler and C. Milstein, *Nature*, 1975, **256**, 495-497.
43. H. L. Pedersen, J. U. Fangel, B. McCleary, C. Ruzanski, M. G. Rydahl, M. C. Ralet, V. Farkas, L. von Schantz, S. E. Marcus, M. C. F. Andersen, R. Field, M. Ohlin, J. P. Knox, M. H. Clausen and W. G. T. Willats, *J. Biol. Chem.*, 2012, **287**, 39429-39438.
44. E. Paramithiotis, M. Pinard, T. Lawton, S. LaBoissiere, V. L. Leathers, W.-Q. Zou, L. A. Estey, J. Lamontagne, M. T. Lehto, L. H. Kondejewski, G. P. Francoeur, M. Papadopoulos, A. Haghighat, S. J. Spatz, M. Head, R. Will, J. Ironside, K. O'Rourke, Q. Tonelli, H. C. Ledebur, A. Chakrabartty and N. R. Cashman, *Nat. Med.*, 2003, **9**, 893-899.
45. F. Fazio, M. C. Bryan, O. Blixt, J. C. Paulson and C-H. Wong, *J. Am. Chem. Soc.*, 2002, **124**, 14397-14402.
46. S. Fukui, T. Feizi, C. Galustin, A. M. Lawson and W. Chai, *Nat. Biotechnol.*, 2002, **20**, 1011-1017.
47. B. T. Houseman and M. Mrkisch, *Chem. Biol.*, 2002, **9**, 443-454.
48. S. Park and I. Shin, *Angew. Chem. Int. Ed.*, 2002, **6**, 692-702.
49. D. Wang, S. Liu, B. J. Trummer, C. Deng and A. Wang, *Nat. Biotechnol.*, 2002, **20**, 275-281.
50. W. G. T. Willats, S. E. Rasmussen, T. Kristensen, J. D. Mikkelsen and J. P. Knox, *Proteomics*, 2002, **2**, 1666-1671.
51. D. Schmidt, F. Schumacher, A. Geissner, P. H. Seeberger and F. Pfrengle, *Chem. Eur. J.*, 2015, **21**, 5709-5713.
52. T. J. Boltje, T. Buskas and G.-J. Boons, *Nat. Chem.*, 2009, **1**, 611-622.
53. P. H. Seeberger, *Chem. Soc. Rev.*, 2008, **37**, 19-28.
54. Y. Wu, D.-C. Xiong, S.-C. Chen, Y.-S. Wang and X-S. Ye, *Nat. Commun.*, 2017, **8**, 14851.

55. Y. Matsuzaki, Y. Ito, Y. Nakahara and T. Ogawa, *Tetrahedron Lett.*, 1993, **34**, 1061-1064.
56. V. Pozsgay, *Tetrahedron: Asymmetry*, 2000, **11**, 151-172.
57. B. Fraser-Reid, J. Lu, K. N. Jayaprakash and J. C. Lopez, *Tetrahedron: Asymmetry*, 2006, **17**, 2449-2463.
58. H.-S. Cheon, Y. Lian and Y. Kishi, *Org. Lett.*, 2007, **9**, 3323-3326.
59. M. Joe, Y. Bai, R. C. Nacario and T. L. Lowary, *J. Am. Chem. Soc.*, 2007, **129**, 9985-9901.
60. Y. Ishiwata and Y. Ito, *J. Am. Chem. Soc.*, 2011, **133**, 2275-2291.
61. O. Calin, S. Eller and P. H. Seeberger, *Angew. Chem., Int. Ed.*, 2013, **52**, 5862−5865.
62. S. U. Hansen, G. J. Miller, M. J. Cliff, G. C. Jayson and J. M. Gardiner, *Chem. Sci.*, 2015, **6**, 6158-6164.
63. K. Naresh, F. Schumacher, H. S. Hahm and P. H. Seeberger, *Chem. Commun.*, 2017, **53**, 9085-9088.
64. S. S. Nigudkar and A. V. Demchenko, *Chem. Sci.*, 2015, **6**, 2687-2704.
65. E. Fischer, *Ber. Dtsch. Chem. Ges.*, 1893, **26**.
66. W. Koenigs and E. Knorr, *Ber. Dtsch. Chem. Ges.*, 1901, **34**, 957-981.
67. R. R. Schmidt and J. Michel, *Angew. Chem. Int. Ed.*, 1980, **19**, 731-733.
68. , Wiley-VCH Verlag GmbH & Co. KGaA, Weinheim, 2008.
69. J. D. C. Codée, R. E. J. N. Litjens, R. den Heeten, H. S. Overkleeft, J. H. van Boom and G. A. van der Marel, *Org. Lett.*, 2003, **5**, 1519-1522.
70. J. D. C. Codée, L. J. van den Bos, R. E. J. N. Litjens, H. S. Overkleeft, C. A. A. van Boeckel, J. H. van Boom and G. A. van der Marel, *Tetrahedron*, 2004, **60**, 1057-1064.
71. G. H. Veeneman, S. H. van Leeuwen and J. H. van Boom, *tetrahedron Lett.*, 1990, **31**, 1331-1334.
72. P. Konradsson, U. E. Udodong and B. Fraser-Reid, *tetrahedron Lett.*, 1990, **31**, 4313-4316.
73. J. D. C. Codée, R. E. J. N. Litjens, L. J. van den Bos, H. S. Overkleeft and G. A. van der Marel, *Chem. Soc. Rev.*, 2005, **34**, 769-782.
74. S. Eller, M. Collot, J. Yin, H. S. Hahm and P. H. Seeberger, *Angew. Chem. Int. Ed.*, 2013, **52**, 5858–5861.
75. O. J. Plante, R. B. Andrade and P. H. Seeberger, *Org. Lett.*, 1999, **1**, 211-214.
76. L. K. Mydock and A. V. Demchenko, *Org. Biom. Chem.*, 2009, **8**, 497-510.
77. T. Hosoya, T. Takano, P. Kosma and T. Rosenau, *J. Org. Chem.*, 2014, **79**, 7889-7894.
78. S. van der Vorm, T. Hansen, H. S. Overkleeft, G. A. van der Marel and J. D. C. Codée, *Chem. Sci.*, 2017, **8**.
79. A. Ishiwata, Y. Munemura and Y. Ito, *Tetrahedron*, 2008, **64**, 92-102.
80. C. S. Chao, C. Y. Lin, S. Mulani, W. C. Hung and K. K. Mong, *Chem. Eur. J.*, 2011, **17**, 12193-12202.
81. G. Wulff and G. Röhle, *Angew. Chem. Int. Ed.*, 1974, **13**, 157-216.
82. A. V. Demchenko, T. Stauch and G. J. Boons, *Synlett*, 1997, 818-820.
83. J.-H. Kim, H. Yang and G.-J. Boons, *Angew. Chem., Int. Ed.*, 2005, **44**, 947-949.
84. J.-H. Kim, H. Yang, J. Park and G.-J. Boons, *J. Am. Chem. Soc.*, 2005, **127**, 12090-12097.

85. D. J. Cox and A. J. Fairbanks, *Tetrahedron: Asymmetry*, 2009, **20**, 773-780.
86. G. P. Singh, A. J. A. Watson and A. J. Fairbanks, *Org. Lett.*, 2015, **17**.
87. M. A. Fascione, S. J. Adshead, S. A. Stalford, C. A. Kilner, A. G. Leach and W. B. Turnbull, *Chem. Commun.*, 2009, 5841-5843.
88. B. S. Komarova, Y. E. Tsvetkov and N. E. Nifantiev, *Chem. Rec.*, 2016, **16**, 488-506.
89. J. Y. Baek, Y.-J. Shin, H. B. Jeon and K. S. Kim, *Tetrahedron Lett.*, 2005, **46**, 5143–5147.
90. J. Y. Baek, B.-Y. Lee, M. G. Jo and K. S. Kim, *J. Am. Chem. Soc.*, 2009, **131**, 17705-17713.
91. H. S. Hahm, M. Hurevich and P. H. Seeberger, *Nat. Commun.*, 2016, **7**, 12482.
92. J. P. Yasomanee and A. V. Demchenko, *Angew. Chem. Int. Ed.* , 2014, **53**, 10453-10456.
93. J. P. Yasomanee and A. V. Demchenko, *J. Am. Chem. Soc.*, 2012, **134**, 20097-20102.
94. D. Crich, *Acc. Chem. Res.*, 2010, **43**, 1144-1153.
95. D. Crich and W. Cai, *J. Org. Chem.*, 1999, **64**, 4926-4930.
96. M. G. Beaver and K. A. Woerpel, *J. Org. Chem.*, 2010, **75**, 1107-1118.
97. R. B. Merrifield, *J. Am. Chem. Soc.*, 1963, **85**, 2149-2154.
98. R. B. Merrifield, *Angew. Chem. Int. Ed.*, 1985, **24**, 799-810.
99. M. H. Caruthers, *Science*, 1985, **230**, 281-285.
100. R. B. Merrifield, *Science* 1965, **150**, 178-185.
101. C. Schuerch and J. M. Frechet, *J. Am. Chem. Soc.* , 1971, **93**, 492-496.
102. O. J. Plante, E. R. Palmacci and P. H. Seeberger, *Science*, 2001, **291**, 1523-1527.
103. S.-L. Tang, L. B. Linz, B. C. Bonning and N. L. B. Pohl, *J. Org. Chem.*, 2015, **80**, 10482-10489.
104. S. G. Pistorio, S. S. Nigudkar, K. J. Stine and A. V. Demchenko, *J. Org. Chem.*, 2016, **81**, 8796-8805.
105. T. Nokami, R. Hayashi, Y. Saigusa, A. Shimizu, C.-Y. Liu, K.-K. T. Mong and J. Yoshida, *Org. Lett.*, 2013, **15**, 4520-4523.
106. J. Kandasamy, M. Hurevich and P. H. Seeberger, *Chem. Commun.*, 2013, **49**, 4453-4455.
107. M. W. Weishaupt, S. Matthies and P. H. Seeberger, *Chem. Eur. J.* , 2013, **19**, 12497–12503.
108. P. H. Seeberger and D. B. Werz, *Nat. Rev. Drug. Discover.* , 2005, **4**, 751-763.
109. L. Kröck, D. Esposito, B. Castagner, C. C. Wang, P. Bindschädler and P. H. Seeberger, *Chem. Sci.*, 2012, **3**, 1617–1622.
110. D. Senf, C. Ruprecht, G. H. M. de Kruijf, S. O. Simonetti, F. Schumacher, P. H. Seeberger and F. Pfrengle, *Chem. Eur. J.*, 2017, **23**, 3197-3205.
111. M. Collot S. Eller, J. Yin, H.-S. Hahm, P. H. Seeberger, *Angew. Chem. Int. Ed.*, **2013**, ***52***, 5858–5861.
112. M. W. Weishaupt, H. S. Hahm, A. Geissner and P. H. Seeberger, *Chem. Commun.*, 2017, **53**, 3591-3594.
113. M. Pauly and K. Keegstra, *Annu. Rev. Plant. Biol.*, 2016, **67**, 235-259.
114. A. Schultink, L. Liu, L. Zhu and M. Pauly, *Plants*, 2014, **3**, 526-542.

115. W. D. Bauer, K. W. Talmadge, K. Keegstra and P. Albersheim, *Plant Physiol.*, 1973, **51**, 174–187.
116. K. H. Caffall and D. Mohnen, *Carbohyd. Res.*, 2009, **344**, 1879-1900.
117. M. Pauly, P. Albersheim, A. Darvill and W. S. York, *Plant J.*, 1999, **20**, 629-639.
118. T. Hayashi, *Annu. Rev. Plant. Biol.*, 1989, **40**, 139-168.
119. M. S. Buckeridge, H. P. dos Santos and M. A. S. Tine, *Plant Physiol. Biochem.*, 2000, **38**, 141-156.
120. N. C. Carpita and D. M. Gibesut, *Plant J.* , 1993, **3**, 1-30.
121. K. Nishitani, *J. Plant Res.*, 1998, **111**, 159-166.
122. K. Nishitani and R. Tominaga, *J. Biol. Chem.*, 1992, **282**, 21058-21064.
123. J. E. Thompson, R. C. Smith and S. C. Fry, *Biochem. J.*, 1997, **327**, 699-708.
124. E. P. Lorences and S. C. Fry, *Physiol. Plant.*, 1993, **88**, 105-112.
125. M. Saura-Valls, R. Fauré, H. Brumer, T. T. Teeri, S. Cottaz, H. Driguez and A. Planas, *J. Biol. Chem.*, 2008, **283**, 21853-21863.
126. B. Henrissat and G. Davies, *Curr. Opin. Struct. Biol.*, 1997, **7**, 637-644.
127. A. Planas, *BBA-Protein Struct. M.*, 2000, **1543**, 361-382.
128. G. J. Davies, V. M. A. Ducros, A. Varrot and D. L. Zechel, *Biochem. Soc. Trans.*, 2003, **31**, 523-527.
129. P. Johansson, H. Brumer, M. J. Baumann, Å. M. Kallas, H. Henriksson, S. E. Denman, T. T. Teeri and T. A. Jones, *Plant Cell*, 2004, **16**, 874-886.
130. A. Wotowic and J.-C. Jacquinet, *Carbohyd. Res.*, 1990, **205**, 235-245.
131. K. Sakai, Y. Nakahara and T. Ogawa, *Tetrahedron Lett.*, 1990, **31**, 3035-3038.
132. D. K. Watt, D. J. Brasch, D. S. Larsen, L. D. Melton and J. Simpson, *Carbohyd. Res.*, 2000, **325**, 300-312.
133. D. K. Watt, D. J. Brasch, D. S. Larsen, L. D. Melton and J. Simpson, *Carbohyd. Res.*, 1996, **286**, 1-15.
134. R. Faurè, M. Saura-Valls, H. Brumer, A. Planas, S. Cottaz and H. Driguez, *J. Org. Chem.*, 2006, **71**, 5151-5161.
135. S. David, A. Malleron and C. Dini, *Carbohyd. Res.*, 1989, **188**, 193-200.
136. T. Polat and C.-H. Wong, *J. Am. Chem. Soc.* , 2007, **129**, 12795-12800.
137. M. P. DeNinno, J. B. Etienne and K. C. Duplantier, *Tetrahedron Lett.*, 1995, **36**, 669–672.
138. H. J. Koeners, J. Verhoeven and J. H. Van Boom, *Reel. Trav. Chim. Pays-Bus.*, 1981, **100**, 65-72.
139. K. Saigo, M. H. Usui, K. Kikuchi, E. Shimada and T. Mukaiyama, *Bull. Chem. Soc. Jpn.*, 1977, **50**, 1863-1866.
140. B. Lüning, T. Norberg and J. Tejbrant, *J. Carbohydr. Chem.* , 1992, **11**, 933-943.
141. M. P. Bartetzko, F. Schumacher, H. S. Hahm, P. H. Seeberger and F. Pfrengle, *Org. Lett.*, 2015, **17**, 4344-4347.
142. S. C. Fry, W. S. York, P. Albersheim, A. Darvill, T. Hayashi, J.-P. Joseleau, Y. Kato, E. P. Lorences, G. A. Maclachlan, M. McNeil, A. J. Mort, J. S. G. Reid, H. U. Seitz, R. R. Selvendran, A. G. J. Voragen and A. R. White, *Physiol. Plant.*, 1993, **89**, 1-3.
143. M. Wilsdorf, D. Schmidt, M. P. Bartetzko, P. Dallabernardina, F. Schumacher, P. H. Seeberger and F. Pfrengle, *Chem. Commun.*, 2016, **52**, 10187-10189.

144. X. Wu, M. Grathwohl and R. R. Schmidt, *Angew. Chem. Int. Ed.*, 2002, **41**, 4489-4493.
145. W. Pigman, E. A. Cleveland, D. H. Couch and J. H. Cleveland, *J. Am. Chem. Soc.*, 1951, **73**, 1976-1979.
146. H. Takaku and K. Kamaike, *Chem. Lett.*, 1982, **11**, 189-192.
147. J. B. Son, M.-H. Hwang, W. Lee and D.-H. Lee, *Org. Lett.*, 2007, **9**, 3897-3900.
148. K. Chayajarus, D. J. Chambers, M. J. Chugthai and A. J. Fairbanks, *Org. Lett.*, 2004, **6**, 3797-3800.
149. S. Eller, M. Collot, J. Yin, H. S. Hahm and P. H. Seeberger, *Angewandte Chemie*, 2013, **52**, 5858-5861.
150. B. Lüning, T. Norberg and J. Tejbrant, *J. Carbohydr. Chem.* , 1992, **11**, 933-943.
151. S.-H Choi, S. Mansoorabadi, Y.-N. Liu, T.-C. Chien and H.-W. Liu, *J. Am. Chem. Soc.*, 2012, **134**, 13946-13949.
152. K. Deng, M. M. Adams, P. Damani, P. O. Livingston, G. Ragupathi and D. Y. Gin, *Angew. Chem. Int. Ed.*, 2008, **47**, 6395-6398.
153. R. A. Burton and G. B. Fincher, *Molecular Plant*, 2009, **2**, 873-882.
154. M. J. Hill, *Europ. J. Cancer Prev.*, 1997, **6**, 219-225.
155. G. Frost, A. A. Leeds, C. J. Doré, S. Madeiros, S. Brading and A. Dornhorst, *Lancet*, 1999, **353**, 1045-1048.
156. C. S. Brennan and L. J. Cleary, *J. Cereal Sci.*, 2005, **42**, 1-13.
157. S. Peat, W. J. Whelan and J. G. Roberts, *J. Chem. Soc.*, 1957, 3916-3924.
158. F. W. Parrish, A. S. Perlin and E. T. Reese, *Can. J. Chem.*, 1960, 2094-2104.
159. T. J. Simmons, D. Uhrin, T. Gregson, L. Murray, I. H. Sadler and S. C. Fry, *Phytochemistry*, 2013, **95**, 322-332.
160. G. B. Fincher, *Curr. Opin. Plant Biol.*, 2009, **12**, 140-147.
161. F. E. Elgharbi, A. Hmida-Sayari, M. Sahnoun, R.Kammoun, L. Jlaeil, H. Hassiri and S. Bejar, *Carbohyd. Pol.*, 2013, **98**, 967-975.
162. X. Xue and S. C. Fry, *Ann. Bot.*, 2012, **109**, 873-886.
163. N. M. McGregor, M. Morar, T. H. Fenger, P. Stogios, N. Lenfant, V. Yin, X. Xu, E. Evdokimova, H. Chui, B. Henrissat, A. Savchenko and H. Brumer, *J. Biol. Chem.*, 2016, **291**, 1175-1197.